Evasion of Cell Death in Burkitt's Lymphoma and Pancreatic Cancer Cells

Author

Wilkie, Alexander David

Published

2016

Thesis Type

Thesis (PhD Doctorate)

School

School of Natural Sciences

DOI

10.25904/1912/399

Evasion of Cell Death in Burkitt's Lymphoma and Pancreatic Cancer Cells

Alexander David Wilkie

B. Biotech (Hons)

School of Natural Sciences

Eskitis Institute for Drug Discovery

Griffith University

Submitted in fulfilment of the requirements of the degree of Doctor of Philosophy

November 2015

Abstract

This thesis examined exploitation of cell death to combat cancer from two angles: investigating cell death signalling pathways to find new targets for treatment, and using the novel anti-austerity approach to combat the tolerance of cancer cells to nutrient deprivation.

Cancers often display high levels of genetic diversity, even within cancers of a particular organ. These genetic differences often make treatments which work with a particular cancer ineffective on another - even from the same origin, and lead to differences in outcomes to selective pressures such as nutrient deprivation. Current treatments are aimed at killing rapidly proliferating cells and often have severe side effects. Their efficacy is highly dependent on early diagnosis and many cancers are resistant to chemotherapeutic drugs. In addition, cancer cells on the inside of tumours have the ability to survive under adverse conditions such as nutrient deprivation due to intermittent blood supply, Therefore, alternative treatment strategies must be explored.

Defects in cell death play a large contributing factor to cancer progression and tumour growth and the evasion of cell death by cancers presents a major problem in its treatment Conventional cancer treatment relies on the activation of cell death in fast growing cancer cells while attempting to leave normal cells undamaged. Therefore, selective triggering of cell death in a cancer cell would be extremely useful. In order to achieve this goal a thorough understanding of the cell death response of a particular cell type to a particular stimulus must be known. Moreover, any novel or unusual cell death signalling pathways would provide more opportunities and targets for attempting to trigger selective cell death in cancers.

Two main signalling pathways lead to the activation of caspases which are the proteins responsible for apoptosis: the extrinsic pathway initiated by activation of death receptors on the cell surface and activation of caspase-8, and the intrinsic (mitochondrial) pathway which is activated by internal stimuli, including DNA damage resulting in activation of caspase-9. Recently however, several additional apoptosis activating platforms have been identified including the RIPoptosome – a cell death

signalling platform which can trigger both apoptosis and necroptosis. The pathways of apoptosis signalling in the Burkitt's lymphoma cell lines BL30A (apoptosis sensitive) and BL30K (resistant) were examined following DNA damage. It was found that in the BL30A cell line caspase-8 is required following DNA damage and there was no evidence of involvement of cell surface death receptor activation. Inhibition of caspase-9 in the intrinsic pathway was ineffective at preventing apoptosis. However, inhibition of cytoplasmic p53 activity effectively inhibited apoptosis. Additionally, caspase-8 appears to associate with FADD in a high molecular weight complex in response to DNA damage. The BL30K cell line is resistant to cell death by this pathway, manifesting in a delay in cell death. Our preliminary findings point to HSP7C as a possible regulatory protein in this apoptosis pathway. Elucidation of this apoptosis pathway may help in understanding of other apoptotic pathways and may lead to the discovery of new targets for treatment of cancer by induction of apoptosis. Another strategy to bypass resistance of cancers to cell death is by using drugs that target the tolerance of cancers to lack of nutrients.

Targeting cancers tolerance to lack of nutrients is emerging as a promising field of study and has been termed anti-austerity. Several compounds which possess anti-austerity properties have been identified, including angelmarin. Among cancers, pancreatic cancers show extremely high tolerance to lack of nutrients. This tolerance to lack of nutrients makes it ideal for the study of anti-austerity compounds. Pancreatic cancers are some of the most severe cancers, with extremely poor prognoses and high mortality rates. Current treatments for pancreatic cancers are largely ineffective, highlighting the need to pursue alternative treatments.

The anti-austerity compound angelmarin is explored here for its potential as a pancreatic cancer treatment. Angelmarin was shown to selectively induce PANC-1 death in nutrient deprived conditions, particularly glucose, but had no effect on cells grown under normal conditions. The data obtained indicates a lack of caspase activation and a lack of nuclear fragmentation providing evidence that apoptosis is not the cell death type activated by angelmarin. Evidence is provided that autophagy is not the primary cell death type as LC3b staining did not account for the amount of cell death observed and Beclin-1 expression was down-regulated in response to

angelmarin in PANC-1 cells. Finally evidence is provided that necroptosis may be involved in the response to angelmarin, as inhibition of RIP1 prevented cell death, and mitochondria lost membrane integrity.

This thesis has explored an unusual pathway of apoptosis induction in Burkitt's lymphoma in the hopes of eventually triggering this pathway in other cancers, and examined the potential of the anti-cancer agent angelmarin for its ability to overcome the tolerance of pancreatic cancer to lack of nutrients. Both approaches for using cell death as a tool for developing better treatments have the same goal - counteracting the evasion of cell death of cancer.

Statement of Originality

This work, entitled **Evasion of Cell Death in Burkitt's Lymphoma and Pancreatic Cancer Cells,** has not been previously submitted for a degree or diploma in any university. The research described in this thesis was completed in the School of Biomolecular and Physical Sciences and Eskitis Institute for Drug Discovery, at Griffith University, under the supervision of Associate Professor Dianne Watters. To the best of my knowledge and belief, this thesis contains no material previously published or written by another person except where due reference is made in the thesis itself.

Alexander D. Wilkie.

November 30th, 2015

Table of Contents

List of Figures

Chapter 1

Chapter 3

List of Tables

Chapter 1

Chapter 2

Chapter 4

List of Abbreviations

Abbreviation	Meaning	Other names
4eBP1	eIF4e Binding Protein 1	
AFC	7-amino-4-trifluoromethyl coumarin	
AIF	Apoptosis Inducing Factor	
AMBRA-1	autophagy/Beclin-1 regulator 1	
AMP	Adenosine Mono-Phosphate	
AMPK	Adenosine Mono-Phosphate Kinase	
APS	Ammonium Persulphate	
ASC	Apoptosis -associated Speck-like protein containing a CARD	
ATG	AuTophagy related Genes	
ATG13	AuTophagy related Gene protein 13	Rubicon, KIAA0226
ATM	Ataxia Telangiectasia Mutated	
ATP	Adenosine Tri-Phosphate	
ATR	Ataxia Telangiectasia Rad-3 related protein	
Bcl	B Cell Lymphoma	
Beclin-1		ATG6, vps30
BH	Bcl-2 homology domain	
Bim	Bcl2 interacting mediator of cell death / Bcl like protein 11	BCL2L11
BimEL	Bim Extra Long	
BimL	Bim Long	
BimS	Bim Short	
BL	Burkitt's Lymphoma	
BNIP3	Bcl-2/adenovirus E1B 19 kDa protein-interacting protein 3	
CAD	Caspase Activated DNAse	
CARD	Caspase Activation and Recruitment Domain	
Caspase	Cysteinyl ASPartate proteASE	
CDK-2	Cyclin Dependent Kinase 2	
CED	CEll Death abnormal	
c-FLIP	FLICE-like Inhibitory Protein	
cIAP	Inhibitor of Apoptotic Protein	BIRC2
CICD	Caspase Independent Cell Death	
DAPI	di-amidino phenylindole	
DAPK	Death Associated Protein Kinase	
DED	Death Effector Domain	
DEPTOR	DEP containing mTOR interacting protein	
DEVD	Aspartate-Glutamate-Valine-Aspartate	

DISC	Death Inducing Signalling Complex	
DMEM	Dulbecco's Modified Eagle Medium	
DMSO	dimethyl sulfoxide	
DRAM	damage regulated autophagic modulator	
DSB	Double Stranded Breaks	
DYNLL1	Dynein light chain 1, cytoplasmic	
E2F	Transcription factor E2F	
EBV	Epstein Barr Virus	
EDTA	Ethylene Diamine Tetraacetic Acid	
EGL-1	Egg Laying abnormal-1	
EGTA	Ethylene Glycol Tetraacetic Acid	
eIF4e	Eukaryotic translation Initiation Factor 4E	
ER	Endoplasmic Reticulum	
ERK	Extracellular signal-Regulated Kinase	
FADD	Fas Associated Death Domain	
FBS	Foetal Bovine Serum	
FIP200	RB1-inducible coiled-coil protein 1	RB1CC1
FITC	Fluorescein isothiocyanate	
FLICE	FADD-Like Interleukin-1 ß Converting Enzyme	
GDP	Guanine Di-Phosphate	
GEF	Guanine nucleotide Exchange Factor	
GRP78	Glucose Regulated Protein 78	BiP, HSPA5
GTP	Guanine Tri-Phosphate	
HIF1 α	Hypoxia-inducible factor 1-alpha	
HMGB1	High Motility Group Box 1	
HPDE	Human Pancreatic Duct Epithelial	
HRP	HorseRadish Peroxidase	
HSP	Heat Shock Protein	
HSP7C	Heat Shock Cognate 71 kDa protein	HSPA8, HSC70, HSP73
Htr2a	5-Alphahydroxytryptamine receptor 2A	Omi
iCAD	Inhibitor of Caspase Activated DNAse	
ICE	Interleukin-1 ß Converting Enzyme	
iDISC	Intracellular Death Inducing Signalling Complex	
IETD	Isoleucine-Glutamate-Threonine-Aspartate	
IP3R	Inositol 1,4,5-Trisphosphate Receptor	
JNK	c-Jun N-terminal Kinase	MAPK8
LC3	microtubule associated Long Chain 3	
LEHD	Leucine-Glutamate-Histidine-Aspartate	
LUBAC	Linear UBiquitin Assembly Complex	

MAPK	Mitogen Activated Protein Kinase	
Mdm2	Murine Double Minute 2	
MEF	Mouse Embryonic Fibroblast	
MLST8	Mammalian Lethal with SEC13 protein 8	
MOMP	Mitochondrial Outer Membrane Permeabilisation	
mTOR	Mammalian Target Of Rapamycin	
mTORC	Mammalian Target Of Rapamycin Complex	
NAC	N-Acetyl Cysteine	
NAD+	Nicotinamide Adenine Dinucleotide (oxidised)	
NADPH	Nicotinamide Adenine Dinucleotide Phosphate	
NDM	Nutrient Deprivation Medium	
NF- $\varkappa$B	nuclear factor $\varkappa$-light-chain-enhancer of activated B cells	
NMR	Nuclear Magnetic Resonance	
Nox-1	NADPH oxidase 1	
NP-40	Nonidet p40	
nPIST	neuronal PDZ domain protein interacting specifically with TC10	
p90RSK	p90 Ribosomal S6 Kinase	
PAGE	Poly-Acrylamide Gel Electrophoresis	
PARP	Poly (ADP-Ribose) Polymerase	
PBS	Phosphate-Buffered Saline	
PCD	Programmed Cell Death	
PDK1	Phosphoinositide Dependent Kinase 1	
PFA	Para-formaldehyde	
PI3K	Phosphatidylinositol 3-Kinase	
PI3P	Phosphatidylinositol-3-Phosphate	
PIDD	p53 Induced protein with a Death Domain	
Pifithrin	P-FIfty THree INhibitor	
Pifithrin-μ	2-Phenylethynesulfonamide	PES
PINK	PTEN INduced putative Kinase	
PKB	Protein Kinase B	
PMSF	PhenylMethaneSulfonyl Fluoride	
PPP	Pentose Phosphate Pathway	
PRAS40	Proline Rich Akt Substrate of 40 kDa	
PUMA	P53 Upregulated Modulator of Apoptosis	
PVDF	PolyVinyliDene Fluoride	
RAIDD	RIP-1 associated protein with a death domain	CRADD
RalB	Ras-related protein Ral-B	
RAPTOR	Regulatory-Associated Protein of mTOR	
Ras	RAt Sarcoma (name derived)	
RB1CC1	RetinoBlastoma 1-inducible coiled-coil-1	FIP200
RHIM	RIP Homotypic Interaction Motif	

RIP1	Receptor (TNFR) interacting protein (serine/threonine) kinase	RIPK1
RNS	Reactive Nitrogen Species	
ROS	Reactive Oxygen Species	
RPMI	Roswell Park Memorial Institute (name)	
S6K	Ribosomal protein S6 kinase ß-1	
S6RP	S6 Ribosomal Protein	
SDS	Sodium Dodecyl Sulfate	
SH3GLB1	SH3 domain containing GRb2-like protein B 1	
SLAM	Signalling Lymphocyte Activation Molecule	
SMAC	Second Mitochondria-derived Activator of Caspases	
SQSTM1	SEeQueSTosoMe-1	
tBid	truncated Bid	
TCA	TriCarboxylic Acid	
TEMED	N,N,N,N-Tetramethyl-Ethylenediamine	
Tid-1	Heat shock protein 40	HSP40
TNF	Tumour Necrosis Factor	
TNFR1	TNF Receptor 1	
TNFR2	TNF Receptor 2	
TRADD	TNFR1 Associated Death Domain protein	
TRAF	TNFR- Associated Factor	
TRAIL	TNF Related Apoptosis Inducing Ligand	
TRAIL-R1	TRAIL receptor 1	
TRAIL-R2	TRAIL receptor 2	
TRITC	Tetramethylrhodamine	
TSC	Tuberous SClerosis	
ULK-1	UNC-51 Like Kinase	
UVRAG	UV Radiation Associated Gene protein	
VMP1	Vacuolar Membrane Protein 1	
Vps	Vacuolar Protein Sorting	
XIAP	X-linked Inhibitor of Apoptosis Proteins	

Acknowledgements

I would like to thank my supervisor Dr. Dianne Watters for her support, guidance and encouragement throughout my PhD. Her assistance was invaluable in helping me complete this endeavour, and my gratitude to Dianne is difficult to express. I would also like to thank my associate supervisor Denis Crane and Mark Coster for providing the angelmarin for use in this study.

Special thanks are due to Judith Newman for her help in the laboratory. Your experience and helpful advice were incredibly useful, and I will always consider you a friend. Additionally, I would like to thank my friends in the lab, sharing in the struggles of research – Nikki Rumball, Amy Pan, Melanie Eden, Melody Christie, Ben Matthews and Mitch Wright.

Most of all I would like to thank Mikaela Cornwell, without her love and support I would not have been able to make it this far.

Finally I would like to thank my family – my parents Christel and Ken Wilkie and my brother Ben Wilkie for putting up with me and encouraging me over the duration of this thesis. I would like to dedicate this thesis to my grandparents, all of whom have passed on but will never be forgotten. Thank you all so much.

List of publications and presentations

Conference proceedings:

Wilkie, A.D. & Watters, D. (2011). DNA damage induced apoptosis in the BL30A Burkitt's lymphoma cell line requires caspase-8 and mitochondrial p53 activity. *The first Australian workshop on cell death*. Whitsunday Islands, Australia. **August 21st-25th, 2011.**

Wilkie, A.D. (2013). Apoptosis pathway of the BL30A Burkitt's lymphoma cell line following DNA damage. *Griffith University – Eskitis Institute*. Nathan, Australia. **April 11th-12th, 2013.**

Wilkie, A.D. (2014). The anti-austerity agent angelmarin in pancreatic cancer. *Griffith University – Eskitis Institute*. Nathan, Australia. **March 27th-28th, 2014.**

Chapter 1

Introduction

1.1 Cell Death

1.1.1 General Introduction

There are several hallmarks which define cancer including sustained proliferative signalling, evasion of growth suppressors, resisting cell death, enabling of replicative immortality, induction of angiogenesis and the activation of invasion and metastasis [reviewed by](Hanahan and Weinberg 2011). Arguably the most prominent feature is the evasion of cell death.

Defects in cell death play a large contributing factor to cancer progression and tumour growth. Cell death is vitally important for organismal health and development (Conradt and Horvitz 1998). The purpose of cell death in multi-cellular organisms are too numerous to list, and differ between the cell death types. The balance between death and survival of a cell is perhaps the most important function in a process called homeostasis. Cancers are the result of defects in signalling or execution of cell death. Many research groups have shown the significance of cell death in organismal health by studies in which animals do not survive long without functional cell death pathways [reviewed by] (Kaufmann and Hengartner 2001; Kreuzaler and Watson 2012). In general, cancer is caused by one of two cell death related events: cells are not being destroyed upon receiving the appropriate signals, or cells are replicating too quickly for the normal amount of cell death to counter the replication. The type of cell death involved is dependent on many variables including the severity of the stimulus.

One of the major causes of cell death is the induction of damage to DNA. DNA is the most vulnerable component of the cell as it cannot be simply replaced. It is required to be replicated with near perfect accuracy. Because of this many mechanisms exist to protect the DNA from damage and repair mistakes in the replication of DNA. However, when this damage is too severe or irreparable the cell commits to cell death via one of several methods, usually apoptosis [reviewed by](Roos and Kaina 2006).

Current cancer treatments are focused on either the inhibition of proliferation - targeting fast growing cells, or oncogene addiction. 'Oncogene addition' is a term coined by Bernard Weinstein which describes the phenomenon that cancer cells develop dependence on certain oncogenic pathways for survival and proliferation (Weinstein 2000). Dependence on these specific pathways often means that alternative pathways active in normal cells are inactivated and unusable in cancers. Thus targeting the path the cancer is using will be detrimental to the cancer, but not in normal cells where alternative pathways are used (Weinstein 2000; Weinstein and Joe 2006; Blum and Kloog 2014). Conventional cancer treatment relies on the activation of cell death in cancer cells while attempting to leave normal cells undamaged. Therefore, selective triggering of cell death in a cancer cell line would be extremely useful. In order to achieve this goal a thorough understanding of the cell death response of a particular cell type to a particular stimulus must be known. Moreover, any novel or unusual cell death signalling pathways would provide more opportunities and targets for attempting to trigger selective cell death in cancers. There are numerous cell death types which will be examined and the signalling pathways explored.

1.1.2 Types of cell death

Programmed cell death (PCD) is any form of cell death mediated by an intracellular program. It was first proposed when it was observed in the timed breakdown of cells in moth pupae development (Lockshin and Williams 1965). Cell death types are divided according to morphological features, enzymological criteria, functional aspects or immunological criteria [reviewed by] (Lockshin and Zakeri 2004; Duprez, Wirawan et al. 2009). The morphological classes of cell death are apoptosis, macroautophagy (hereafter referred to as Autophagy), necrosis and cell death associated with mitotic catastrophe. Cell death is then further classified based on enzymological criteria, functional aspects and immunological criteria into signalling pathways including necroptosis, pyroptosis, pyronecrosis, paraptosis and CICD (caspase independent cell death) among many others (Galluzzi, Maiuri et al. 2007; Kroemer, Galluzzi et al. 2009).

The major cell death types will briefly be summarised here. Apoptosis is a type of cell death which is a highly ordered and organised process (Kerr, Wyllie et al. 1972). It does not cause damage to the surrounding cells and components of the cell destroyed are reused by the surrounding cells. Autophagy is another highly ordered process which is generally activated in response to a lack of cellular resources and cells recycle components of themselves in an effort to remain viable. This recycling continues to a point where the cell can no longer remain viable at which point it is termed autophagic cell death. Necrosis on the other hand is what seems like an unordered process of cell death. In necrosis the cells swell until osmotic pressure causes them to burst, damaging all surrounding cells and often causing an inflammatory reaction. This being said, there are signalling pathways in place to selectively activate necrosis [Reviewed by] (Klionsky and Emr 2000; Krysko, Vanden Berghe et al. 2008; Duprez, Wirawan et al. 2009). Although these pathways are the most common many other pathways of cell death exist.

Many of the minor cell death types are variations of the above processes. Changes in the signalling events or execution strategies have lead to them not being able to be classified as the above processes but branch into new subcategories. This is why many of the names are simply variations of apoptosis or necrosis, such as paraptosis, or necroptosis (Kroemer, Galluzzi et al. 2009). The list of cell death types to date is quite numerous.

1.2 Apoptosis

1.2.1 Introduction

Apoptosis is a form of programmed cell death. It is the counterpart to mitosis as it balances cell proliferation by mitosis with cell death by apoptosis. Apoptosis was first described in 1972 by Kerr, Wyllie and Currie as a genetically programmed pathway of cell death, however some of the components have been previously described. It was morphologically distinct from necrosis, the cell death pathway in response to severe stimulus. It was originally termed shrinkage necrosis but later adopted the term apoptosis, from the Greek meaning literally "to fall away from". This referred to the falling or dropping off of petals from a flower or leaves from a tree in autumn, owing to the morphology of the process during death. It has been observed in many multi-cellular organisms, including mammals, *Drosophila* and nematodes. It also has important functions in the development of organisms as well as responses to cellular disease or damage. It is a highly organised process that requires the use of energy in the form of ATP. Because it is an organised process the death process generally does not damage surrounding cells nor produces an inflammatory reaction. This makes apoptosis very useful for an organism in the elimination of unwanted cells.

1.2.2 Function of apoptosis

Under normal conditions apoptosis levels are in tune with mitosis levels to maintain the correct numbers of cells. This continuing balance between cell proliferation and cell death is called homeostasis (King and Cidlowski 1998; Fulda 2009). It was estimated that approximately 10 billion cells are produced each day in a human adult to balance the number of cells dying from apoptosis (Renehan, Booth et al. 2001). This estimate has since been revised to approximately 50-70 billion cells per day in a normal human adult (Reed 2006).

Apoptosis is also vital to the elimination of damaged or diseased cells. This includes cells damaged by chemical or mechanical stresses, cells not receiving survival signals and immune system activation of apoptosis of cells infected by pathogens. Apoptosis is also vital to wound healing. Damaged cells must be eliminated to allow healthy cells to replace them in order to avoid excessive scarring.

A further role of apoptosis is in development. Some cells are genetically programmed to die as a normal part of the developmental process. Several examples of this include the removal of webbing between fingers and toes in several animals including humans; in nervous system development; and in immune system development. In the nervous system development large numbers of excess nerve cells are made, but those which fail to produce a functional synaptic connection are destroyed via apoptosis (Oppenheim 1981). In immune system development cells producing self interactive antigens are eliminated via apoptosis (Spinozzi, Nicoletti et al. 1995; Tsujimoto, Lisukov et al. 1996). This last example, while most prevalent in development, is an ongoing process that occurs in the normal function of the immune system. A non-human example of developmental apoptosis is the destruction of tadpoles' tail in frogs (Kerr, Harmon et al. 1974). However when apoptosis does not happen as intended, problems arise.

Disruptions in the normal function or levels of apoptosis lead to many diseases and disorders. These can arise from either an excess of apoptosis or insufficient apoptosis. Diseases from excess apoptosis include several degenerative diseases including Parkinson's disease and Alzheimer's disease, as well as autoimmune diseases such as rheumatoid arthritis. Cancer is the best example of disease caused by insufficient apoptosis. Evasion of apoptosis is perhaps the most well known hallmark of cancer (Caro-Maldonado and Muñoz-Pinedo 2011).

Cancer is generally described as an excess of cell proliferation or a deficiency in cell death (Lowe and Lin 2000). However, there are several cancer types that do not follow this model as some cancers are slow replicating, but the cells are extremely long lived. Many different cancer types have been found with differing resistances to growth and death factors, and even the evasion of the limits on cellular proliferation provided by

telomeres (Blasco 2005). The involvement of apoptosis in cancer highlights the importance of its discovery.

1.2.3 History

The initial discovery of apoptosis was made in a *Caenorhabditis elegans* nematode worm model where it was found that certain cells were genetically programmed to die at specific points in development. Of the 1090 somatic cells, 131 cells were destroyed via apoptosis, and this number, nor the locations of the cells programmed to die, did not change significantly between different worms, showing that the process is both highly specific and selective. Genetic studies in *C. elegans* revealed the existence of several genes encoding important proteins in nematode apoptosis as described by Horvitz et al in 2003. Four main proteins were identified: EGL-1 (egg laying abnormal), CED-9 (cell death abnormal), CED-4 and CED-3. The nematode apoptotic process is quite simple and is shown in Figure 1.1 (Kerr, Wyllie et al. 1972). All of these nematode proteins have mammalian homologues which will be discussed later, both of which lead to the ordered cell death phenotype observed.

Figure 1.1: Major proteins involved in the *C. elegans* apoptotic pathway. EGL-1 (**eg**g **l**aying abnormal -1), CED (**ce**ll **d**eath abnormal) -9, -4 and -3.

Apoptosis is defined by several features. In the early stages of apoptosis the nuclear chromatin condenses and is often seen as a crescent shaped nucleus (Chowdhury, Tharakan et al. 2006; Taatjes, Sobel et al. 2008). Following chromatin condensation the nucleus breaks into pieces (Kerr, Wyllie et al. 1972; Hacker 2000; Kroemer, Galluzzi et al. 2009). Throughout the apoptotic process the cellular organelles, including the mitochondria, remain intact. The cell membrane of apoptotic cells shows a characteristic blebbing (cell surface appears bumpy or bubbly), and then buds of the

cell membrane containing various cellular components fall away from the cell to be engulfed by macrophages or surrounding cells (Hacker 2000; Elmore 2007). Figure 1.2 shows a basic overview of the apoptotic process. This provides a useful way for recycling cellular components (Savill and Fadok 2000). This budding morphology was the reason for naming of the death process as apoptosis. Despite this membrane blebbing the cell membrane does not lose integrity until late in the apoptotic process. The DNA laddering observed in apoptosis upon Southern blotting is caused by the fragmentation of DNA. This laddering is due to cleavage of DNA by CAD, an endonuclease that cleaves DNA in the linker regions between histones on which DNA is wrapped. Each histone holds approximately 180-200bp of DNA and this is why the laddering occurs (as multiples of ~200bp) (Bortner, Oldenburg et al. 1995).

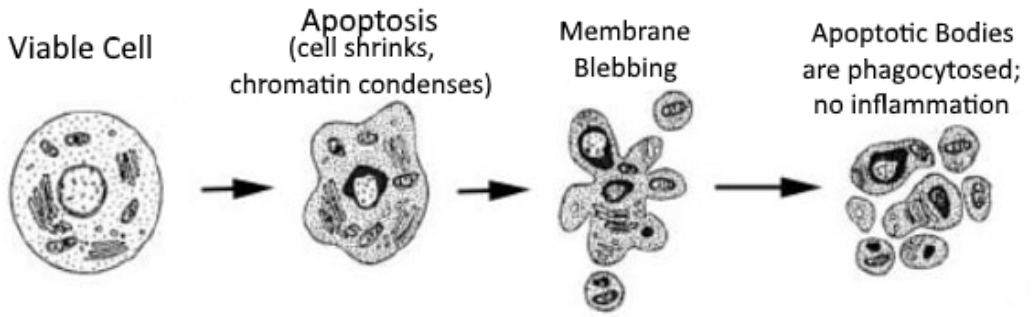

Figure 1.2: Overview of the apoptotic process. Adapted from (Van Cruchten and Van Den Broeck 2002), used with permission 2016.

1.2.4 The major players in apoptosis – caspases

The morphological features mentioned above are brought about by the activity of caspases. Caspases is the name derived for a group of proteins from their function as Cysteinyl aspartate proteases. 18 caspase encoding gene sequences have been identified in mammals (Eckhart, Ballaun et al. 2008), however only 12 caspase proteins exist in humans. Caspases play roles in apoptosis, inflammation signalling, immune cell proliferation, epidermal barrier formation as well as several other processes (Eckhart, Ballaun et al. 2005; Eckhart, Ballaun et al. 2008). Caspases are divided into several classes according to their function. Initiator caspases, caspase-2, -8, -9 and -10 start the apoptotic signalling process. It should be noted that while caspase-2 is generally

classed as an initiator caspase, it contains components of both initiator and effector caspases. Effector caspases, caspase-3, -6 and -7 carry the apoptotic signal to the execution of the cell. Caspases-1, -4 and -5 are involved in inflammation. Caspase-14 has a role in terminal differentiation of epidermal keratinocytes (Eckhart, Ballaun et al. 2008). As this research is focused on apoptosis induction, only caspases involved in apoptosis will be discussed. Caspases are made as inactive zymogens which require cleavage to become fully activated (Riedl and Shi 2004). However, the pro-caspase forms have been shown to possess limited activity. Initiator caspases act on effector caspases as the starting step in apoptosis induction. Initiator caspases are often auto-catalytic, meaning that once in proximity to each other each caspase will cleave and activate another identical caspase protein. For this activation to occur two proteins must dimerise (Muzio, Stockwell et al. 1998; Chen, Orozco et al. 2002), and a protein complex containing initiator caspases generally facilitates this, such as the DISC (Kischkel, Hellbardt et al. 1995) or apoptosome (Salvesen and Dixit 1999). Other less well known caspase activating platforms include the PIDDosome and RIPoptosome (Tinel and Tschopp 2004; Feoktistova, Geserick et al. 2011; Tenev, Bianchi et al. 2011). An example of autocatalytic activation is where caspase-8 activates another caspase-8 protein once brought together in DISC formation. Figure 1.3 shows an outline of the caspase activation process. Once activated, initiator caspases cleave effector caspases activating them, and these effector caspases cleave many substrates ultimately leading to the morphology of apoptosis generally described. Although the mammalian caspases are classed as either initiator or effector, the *C. elegans* nematode worm model, central to initial apoptotic research, contains only one caspase - CED-3. This plays the role of both initiator and effector caspases and is the only caspase-homolog protein in nematodes (Horvitz 2003).

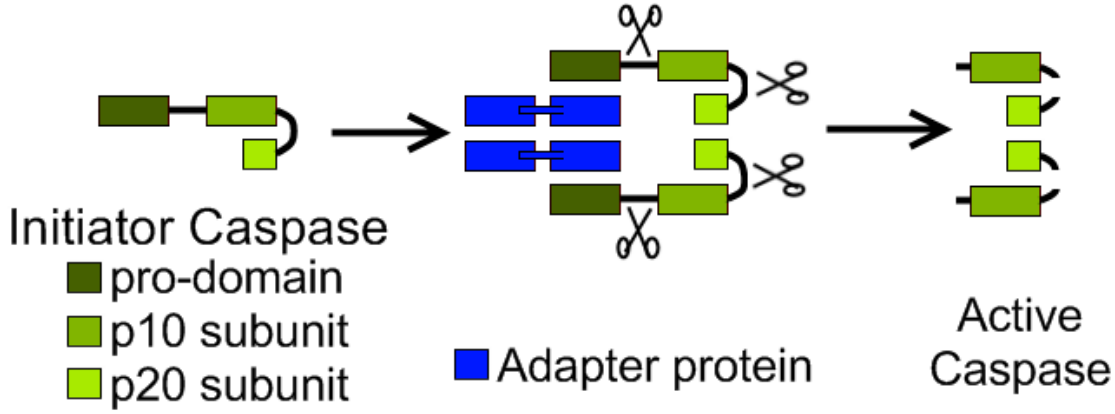

Figure 1.3: Simplification of initiator caspase auto-activation. Once the initiator caspase is brought into proximity of another caspase by a signalling complex the caspases cleave one another at the sites indicated with scissors to form the active caspase. Adapted from (Tait and Green 2010), used with permission 2015.

1.2.4.1 Nomenclature

Inconsistent and multiple names for various apoptotic related proteins were becoming a problem in the mid-1990's. To rectify this Alnemri and colleagues published a letter in 1996 in which the formation of a committee to provide a consistent nomenclature for naming of these proteins was announced. "Caspase" was selected as the name for these proteins, with the "c" representing the cysteine protease mechanism, and the "aspase" signifying that they cleave after an aspartic acid residue. Numbers of the caspases were assigned according to the publication dates (Alnemri, Livingston et al. 1996). This naming convention was accepted by the scientific community and is still used to date.

1.2.4.2 Structure

There are two structural domains often seen in caspases: Death Effector Domains (DED) and Caspase Activation and Recruitment Domains (CARD). All caspases contain at least one of either the CARD or DED domains (Shi 2002). All caspases also contain a peptidase C14 domain. For example, initiator caspases -8 and -10 contain a DED domain, whereas initiator caspases -2 and -9 contain a CARD domain. While the amino acid sequence similarity of caspases is low, the three-dimensional structures are very

similar within these domains. This structure contains 6 anti-parallel α-helicies in a Greek key configuration.

As stated earlier, caspases are formed as inactive zymogens. The full length form of many caspases has been shown to have limited catalytic activity and consists of a single peptide, usually approximately 50 kDa. Initiator caspases are characterised by extended N terminal pro-domains greater than 90 amino acids whereas effector caspases generally contain a pro-domain of 20-30 amino acids (Shi 2002). Once cleaved and activated the protein takes the form of a protein dimer which shows greatly increased catalytic activity. Donepudi and colleagues demonstrated that caspase-8 is expressed as a monomer but upon activation dimerises (Donepudi, Mac Sweeney et al. 2003). The two parts of the active dimer are generally approximately 10-12 kDa and 17-20 kDa in length (Shi 2002; Fuentes-Prior and Salvesen 2004).

1.2.4.3 Substrates

All caspases have specificity for a short sequence of amino acids ending in an aspartate residue, which they cleave after. The general sequence structure is ZEXD, where E is glutamic acid, X is any amino acid (depending on the caspase) and D is aspartate. It should be noted that the ending aspartate is invariable as a substrate requirement however the glutamine is not essential for all caspase substrates. Z is either a hydrophobic amino acid (group I) an aspartate residue (group II) or an aliphatic amino acid (group III). In this classing system of caspases group I contains caspases-1, 4, 5 and 13; group II contains caspases-2, 3 and 7; and group III contains caspases-6, 8, 9 and 10 (Nicholson 1999). The specific sequences recognised by caspases as listed in table 1.1 are the optimal sequences for the caspases, but caspase cleavage is not entirely specific to these sequences (Pop, Salvesen et al. 2008; Benkova, Lozanov et al. 2009). In order for caspases to cleave substrates ATP is required (Ferrari, Stepczynska et al. 1998).

The number of caspase substrates is too numerous to list here, however several examples of important substrates will be examined. A database of caspase substrates called the CASBAH was created to provide a comprehensive list of caspase substrates in an online search engine (Luthi and Martin 2007). Two examples of caspase substrates important to apoptosis are PARP-1 and ICAD. Proteins involved in the apoptotic pathway are cleaved and activated, and other proteins are cleaved to be destroyed. A key caspase-3 substrate is PARP-1 (poly (ADP-ribose) polymerase) which once cleaved and inactivated stops the use of energy for DNA repair, reserving it for use in the apoptotic process (Danial and Korsmeyer 2004; Jin and El-Deiry 2005). ICAD (inhibitor of caspase activated DNase) which once cleaved and activated releases CAD enabling it to degrade chromosomal DNA into nucleosomal size fragments giving the DNA ladder characteristic of apoptosis (Fischer, Janicke et al. 2003).

1.2.4.4 Caspase-8

Caspase-8 was originally discovered in 1996 by Muzio et al. They termed the newly discovered protein FLICE meaning FADD-like ICE, ICE being Interleukin 1ß converting enzyme (later to be termed caspase-1). In this paper they provided evidence that caspase-8 (FLICE) was vital to Fas mediated apoptosis via the formation of a signalling complex. Some of this evidence included the precipitation of FLICE using His-6-tagged FADD as well as His-6-tagged FADD missing the death effector domain. They found that FLICE bound His6-FADD but not His6-FADD without the DED. Additionally they found that over-expression of FLICE induced apoptosis in MCF7 cells, which was blocked by ICE family inhibitors (Muzio, Chinnaiyan et al. 1996). It should also be noted that caspase-8 has been demonstrated to be activated independently of Fas (Bantel, Engels et al. 1999).

Table 1.1: Functions of caspases and their optimal cleavage sequences. * Caspases 15, 16, 17, 18 have genes only, no proteins for these caspases have been found.

Caspase	Species	Function	Substrate preference
1	Human	processing of pro-forms of interleukin-1ß and interleukin-18, two pro-inflammatory cytokines (Cerretti, Kozlosky et al. 1992; Thornberry, Rano et al. 1997)	WEHD
2	Human	Apoptosis Init & Effect (Thornberry, Rano et al. 1997)	DEHD
3	Human	Apoptosis Effector (Thornberry, Rano et al. 1997)	DEVD
4	Human	processing of pro-forms of interleukin-1ß and interleukin-18, two pro-inflammatory cytokines (Thornberry, Rano et al. 1997)	(W/L)EHD
5	Human	processing of pro-forms of interleukin-1ß and interleukin-18, two pro-inflammatory cytokines (Thornberry, Rano et al. 1997)	(W/L)EHD
6	Human	Apoptosis Effector (Thornberry, Rano et al. 1997)	VEHD
7	Human	Apoptosis Effector (Thornberry, Rano et al. 1997)	DEVD
8	Human	Apoptosis Initiator (Thornberry, Rano et al. 1997)	IETD
9	Human	Apoptosis Initiator (Thornberry, Rano et al. 1997)	LEHD
10	Human	Apoptosis Initiator (Nicholson 1999)	
11	Murine (Mouse)	processing of pro-forms of interleukin-1ß and interleukin-18, two pro-inflammatory cytokines (Koenig, Eckhart et al. 2001)	
12	Human	Apoptosis Initiator (ER stress induced) (Nakagawa, Zhu et al. 2000)	
13	Bovine	Homolog of caspase-4 (Koenig, Eckhart et al. 2001)	WEHD
14	Human	Differentiation activated in epidermal keratinocyte differentiation (Eckhart, Declercq et al. 2000)	
15	Mammalian (including pig, dog, cattle)	Pro-apoptotic (Eckhart, Ballaun et al. 2005)	
16		Similar to 14 (Eckhart, Ballaun et al. 2008)	

17	platypus, non mammalian vertebrates	Similar to 3 (Eckhart, Ballaun et al. 2008)	
18	platypus, chicken, opossum	Similar to 8 (Eckhart, Ballaun et al. 2008)	
CED-3	Nematodes	Similar to all apoptotic caspases	DSVD

1.2.4.5 Caspase-8 is activated on the cell surface by death receptors

The extrinsic pathway of apoptosis generally proceeds following binding of a death ligand to a death receptor on the surface of the cell. These receptors include Fas (Trauth, Klas et al. 1989; Yonehara, Ishii et al. 1989), TRAIL-R1 (TNF related apoptosis inducing ligand) receptor 1 and TRAIL-R2. TRAIL-R1 is also called DR-4 (Death Receptor 4) and TRAIL-R2 is also called DR-5. TNFR (tumour necrosis factor receptor) is another such receptor protein. Once the appropriate ligand has bound to its receptor, a protein complex involving FADD (in the case of Fas) or TRADD (TNFR associated death domain protein) (in the case of TRAIL and TNFR) causes the cleavage and activation of caspase-8 or -10 respectively. The death domain of FADD interacts with the death domain of Fas (Chinnaiyan, O'Rourke et al. 1995). The complex formed from the binding of FADD to Fas, followed by the recruitment of caspase-8 is called the DISC (Death Inducing Signalling Complex). It is currently thought that the DISC is comprised of 3 Fas proteins, attracting 2 FADD proteins, which recruit 2 procaspase-8 proteins. The two procaspase-8 proteins once in proximity to each other cleave one another to their active form. Active caspase-8 then cleaves and activates caspase-3 and other caspases and degrades several proteins leading to cell death via apoptosis. Figure 1.4 shows a brief overview of the extrinsic apoptotic pathway.

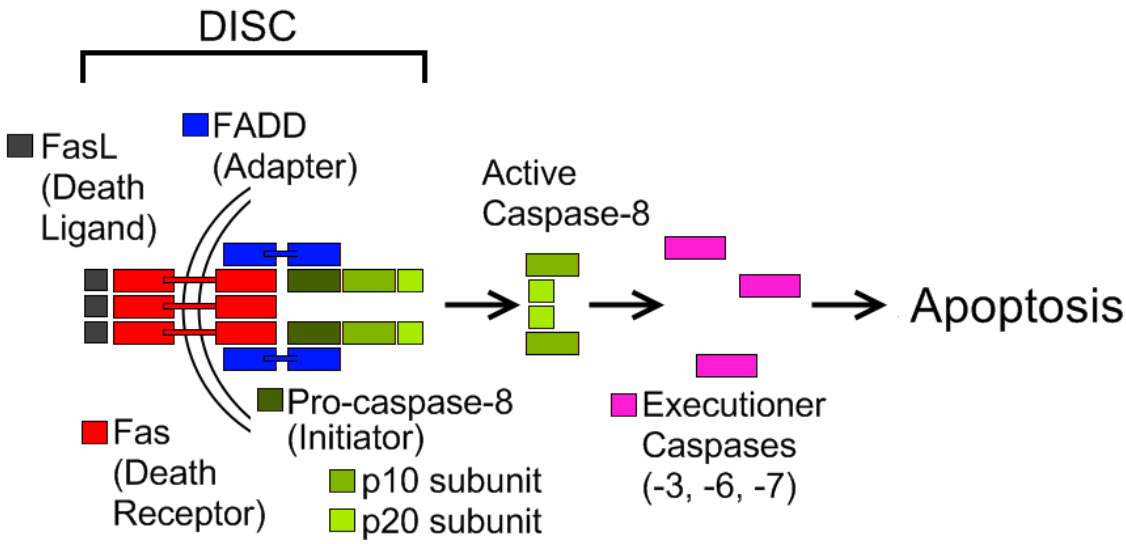

Figure 1.4: A brief overview of the extrinsic apoptosis pathway. Upon binding of a death inducing ligand the Death Inducing Signalling Complex is formed. Here caspase-8 is cleaved, dimerised and activated which leads to cleavage and activation of executioner caspases and apoptosis. Adapted from (Li and Yuan 2008), used with permission, 2015.

1.2.4.6 Initiator caspase-9

Several signalling pathways lead to apoptosis induction. The main pathways include the extrinsic and intrinsic pathways, as well as the immune-system related perforin/granzyme b pathway. The intrinsic pathway involves the permeabilisation of the mitochondria and release of caspase-9. This system is generally activated by an internal stimulus, such as DNA damage or mitochondrial damage due to reactive oxygen species (ROS). The extrinsic pathway involves receptor molecules on the surface of the cell which recognise certain ligands. As these receptors and their respective ligands lead to apoptotic death they have been termed death receptors and death ligands. Upon binding of these molecules caspase-8 is activated leading to apoptosis.

It should be noted that the pathways are not entirely distinct, as there is interactions between them. For example, Bid, a caspase-8 (extrinsic pathway) substrate induces mitochondrial permeabilisation (intrinsic) (Li, Zhu et al. 1998). It has also been suggested that caspase-8 cleaves caspase-9 (Srinivasula, Ahmad et al. 1996; Guo, Srinivasula et al. 2002; Gyrd-Hansen, Farkas et al. 2006; Poreba, Strozyk et al. 2013) and vice versa (Rooswinkel 2013).

Both of these pathways lead to the cleavage and activation of caspase-3. Caspase-3 cleaves many substrates ultimately leading to the morphological changes typical of apoptotic cells. As such it has been termed the executioner caspase.

Additionally, many proteins act on various components of these pathways to either inhibit them or promote them. An excellent example of this is the Bcl-2 family proteins which control the intrinsic apoptosis pathway and will be discussed later.

1.2.4.7 Intrinsic Pathway

The intrinsic apoptotic pathway is regulated by the Bcl-2 family proteins, and is generally initiated by an internal stimulus, such as DNA damage. This family includes both pro and anti-apoptotic proteins [reviewed by](Delbridge and Strasser 2015). The major pro apoptotic proteins include Bax, Bak, Bok and Bid. The major anti-apoptotic proteins include Bcl-2, Bcl-X_L, Bcl-w, Mcl-1, and Bfl-1/A1. These proteins regulate apoptosis by different mechanisms and interactions with each other (Delbridge and Strasser 2015). The main mechanism of the pro apoptotic action of Bcl-2 family members is to facilitate mitochondrial outer membrane permeabilisation [reviewed by](Baig, Seevasant et al. 2016). Once the membrane is permeabilised several proteins are released. Cytochrome c along with procaspase-9 and Apaf-1 form the apoptosome in a process which requires ATP, a complex comprised of seven copies of the adapter protein Apaf-1, cytochrome c and procaspase-9 [reviewed by](Bao and Shi 2007). Apaf-1 has a homologous protein in nematodes called CED-4. The apoptosome activates procaspase-9 by cleavage, and caspase-9 then goes on to cleave caspases-3 and -7 among others leading to apoptosis. Another protein that is released when the mitochondria are permeabilised is SMAC/diablo (Second Mitochondria-derived Activator of Caspases). SMAC/diablo acts by inhibiting the IAPs (Inhibitors of Apoptotic

Proteins) leading to apoptosis (Du, Fang et al. 2000; Kreuzaler and Watson 2012). Htr2a/Omi also acts by inhibiting the IAPs, however when it is expressed at high enough levels it leads to apoptosis by a serine protease dependent manner as opposed to a caspase dependent manner (Suzuki, Imai et al. 2001). Figure 1.5 shows a brief overview of the intrinsic apoptosis pathway.

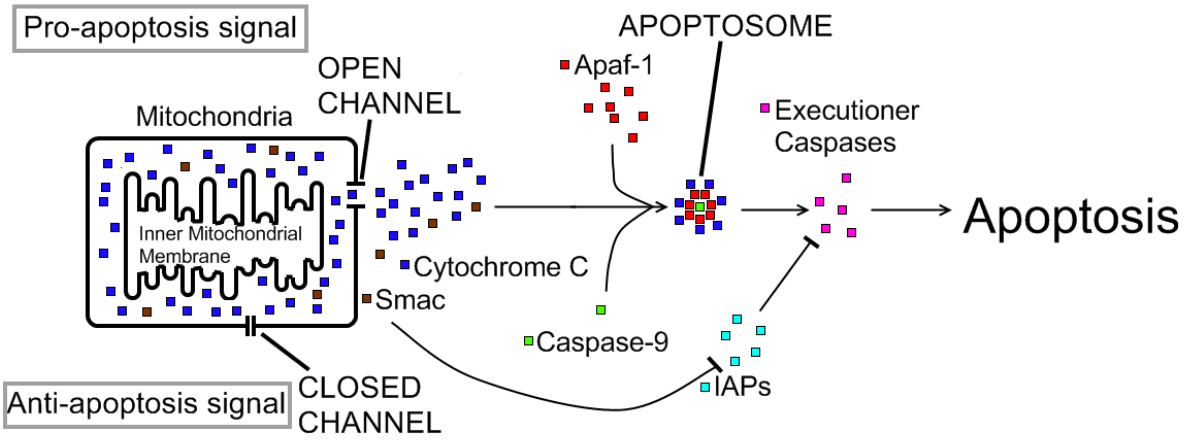

Figure 1.5: Overview of intrinsic apoptosis pathway. Apoptotic signalling events control the permeability of the outer mitochondrial membrane through the opening and closing of channels. Upon opening of these channels proteins are released and lead to the formation of the apoptosome. Here caspase-9 is activated and cleaves and activates the executioner caspases such as caspase-3 which leads to apoptosis. [Compiled/adapted from](Green and Evan 2002; Duprez, Wirawan et al. 2009; Monian and Jiang 2012; Arya and White 2015)

Another Bcl-2 family member with a vital role in apoptosis induction is Bid. Bid is a caspase-8 substrate, which once cleaved to truncated-Bid (tBid) acts on Bax and Bak to induce mitochondrial permeabilisation (Luo, Budihardjo et al. 1998; Slee, Keogh et al. 2000; Kuwana, Mackey et al. 2002). Bax and Bak are currently thought to create a protein channel in the mitochondria to permeabilise the membrane. The significance of Bid cleavage by caspase-8 is that the extrinsic pathway can activate the intrinsic pathway.

Pro-apoptotic Bcl-2 family proteins link the death receptors to the activation of apoptosis. These include Bim which is a microtubule associated protein as well as PUMA (p53 up-regulated modulator of apoptosis) and NOXA (Latin for damage), which are both activated by p53. (Debatin 2004). PUMA, once activated by p53 induces Bax translocation to the mitochondria (Zhang, Xing et al. 2009).

IAPs are Inhibitors of Apoptotic Proteins, a set of several proteins which act to prevent apoptosis under normal conditions. SMAC/DIABLO however is an inhibitor of these proteins and once it is released from the mitochondria the IAPs are inhibited and apoptosis is promoted. It should be noted that IAPs such as survivin and XIAP (X-linked inhibitor of apoptosis proteins) inhibit both the intrinsic and extrinsic pathways by interacting with executioner caspases (Tamm, Wang et al. 1998). Caspase-8, normally involved in the extrinsic pathway of apoptosis has been shown to respond to DNA damage by localising to the mitochondrial membrane indicating an example of crosstalk between the intrinsic and extrinsic pathways (Chandra, Choy et al. 2004).

1.2.5 The major players in apoptosis - Bcl-2 Family

1.2.5.1 Overview

Release of cytochrome c and control of mitochondrial permeabilisation is regulated by members of the Bcl-2 family. The Bcl-2 family of proteins is characterised by the presence of one or more conserved Bcl-2 homology motifs (BH1-BH4) [reviewed by] (Adams and Cory 1998; Delbridge and Strasser 2015). It contains both pro and anti-apoptotic members. The Bcl-2 family of proteins is divided into three subfamilies: Bcl-2, Bax and BH3. Members of the Bcl-2 subfamily are pro-survival, and members of the Bax and BH3 subfamilies are pro-apoptosis. The BH3 subfamily is unrelated to Bcl-2 excepting the BH3 domain (Hata, Engelman et al. 2015). The Bax subfamily resembles Bcl-2 except lack a functional BH4 domain. Expression of Bcl-2 was shown to prevent apoptosis in the nematode worm *C. Elegans* (Vaux, Weissman et al. 1992). Major pro-apoptotic members include Bax, Bak, Bok and Bid. Major anti-apoptotic members include Bcl-2, Bcl-X_L, Bcl-w and Mcl-1. Bcl-2 and Bcl-X_L are both homologous to the

nematode protein CED-9 (Hengartner and Horvitz 1994; Horvitz 2003). Bak was shown to have a conserved domain which mediates apoptosis and the protein interactions of Bak (Chittenden, Flemington et al. 1995). How the Bcl-2 family proteins determine whether the cell will undergo apoptosis is determined by the ratio of pro-apoptotic to anti-apoptotic expression [reviewed by](Adams and Cory 2007; Delbridge and Strasser 2015; Hata, Engelman et al. 2015; Pandey, Prasad et al. 2016). This was first demonstrated by preventing or inducing apoptosis by changing the expression ratio of Bcl-2 and Bax (Oltvai, Milliman et al. 1993). One of the mechanisms which are used to inhibit apoptosis induction is to prevent mitochondrial permeabilisation (Delbridge and Strasser 2015). Bcl-2 has been shown to prevent the release of cytochrome c from the mitochondria thereby preventing apoptosis (Kluck, Bossy-Wetzel et al. 1997). p53 interacts with several proteins in the Bcl-2 family of proteins including Bax, PUMA and NOXA [reviewed by](Delbridge and Strasser 2015; Hata, Engelman et al. 2015). Figure 1.6 shows the basic structural forms of Bcl-2 family proteins and a brief outline of their interactions.

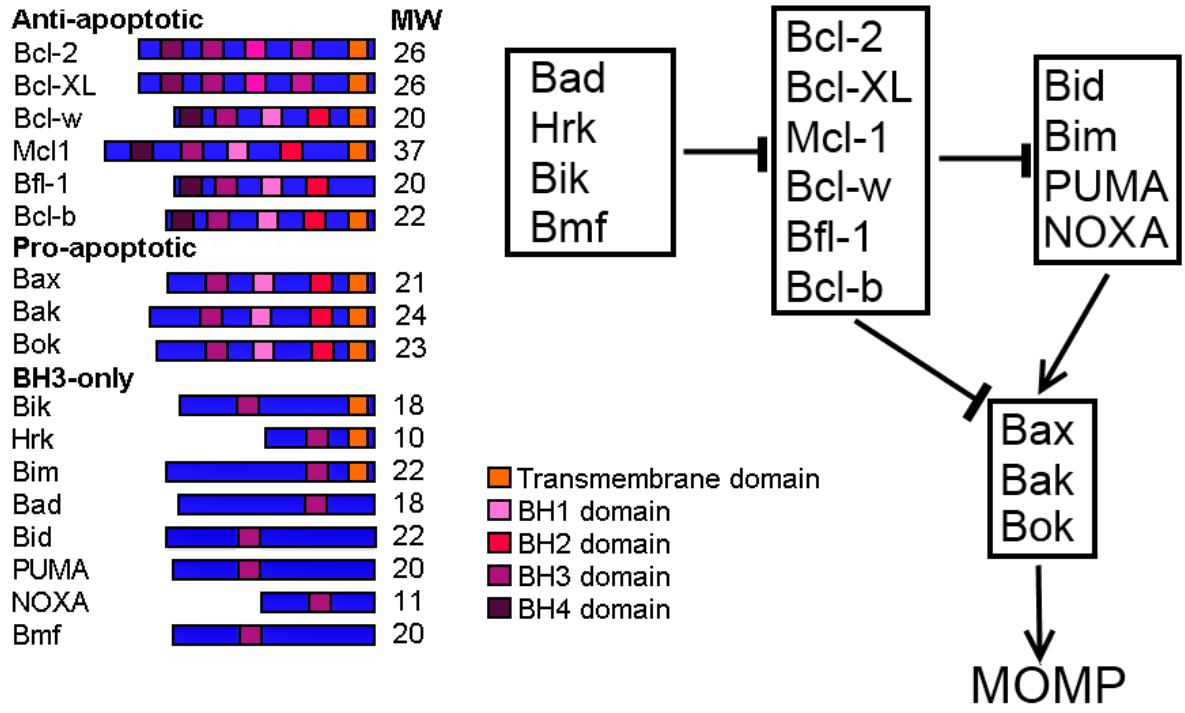

Figure 1.6: Brief overview of the structures and interactions of Bcl-2 family proteins. A complex equilibrium between the members of the Bcl-2 family controls the Mitochondrial Outer Membrane Permeability transition. Adapted from (Taylor, Cullen et al. 2008), used with permission, 2015.

Bcl-2 family proteins have many functions, but perhaps their main function is modulating the cellular response to cellular stresses and determining if the cell should undergo apoptosis [reviewed by] (Adams and Cory 1998; Pandey, Prasad et al. 2016). The Bcl-2 family of proteins can also regulate cell cycle progression (Brady, Gil-Gomez et al. 1996). BH3 only members of the Bcl-2 family function as damage sensors and direct antagonists of pro survival Bcl-2 family members. Bax like members of the Bcl-2 family function by acting to permeabilise the mitochondrial outer membrane [reviewed by](Adams and Cory 2007). Mice lacking both Bax and Bak expression only have a 10% survival rate into adulthood showing the importance of Bcl-2 family proteins in health and development (Lindsten, Ross et al. 2000). Bim and Bid are primarily responsible for the activation of Bax and Bak, however Bmf and NOXA can also activate Bax and Bak (Du, Wolf et al. 2011).

It is theorised that the BH1 and BH2 domains form a pore in the mitochondria or at least an insertion point in the mitochondrial membrane (Muchmore, Sattler et al. 1996). The BH4 domain is present only in the Bcl-2 subfamily pro-survival proteins. This pro-survival function may be in part due to the sequestering of pro-apoptotic Bcl-2 family members by the BH4 domain in pro-survival members (Huang, Adams et al. 1998)

However the mitochondria also play a role in extrinsic apoptosis in several cell lines. In these cases mitochondrial amplification of the death signal is required to initiate apoptosis, and this generally occurs through caspase-8 cleavage of Bid to tBid (Tang, Lahti et al. 2000). tBid induces mitochondrial permeabilisation by interacting with Bak and Bax inducing them to create pores in the mitochondrial outer membrane (Luo, Budihardjo et al. 1998). This discovery led to extrinsic cell death being classified into two distinct types: type I and type II (Scaffidi, Fulda et al. 1998). In type I, mitochondrial amplification of the death signal is not required and large amounts of active caspase-8 are produced at the DISC. Type II in contrast produces little active caspase-8 and requires mitochondrial activation to induce apoptosis (Scaffidi, Fulda et al. 1998; Barnhart, Alappat et al. 2003). The differences in type I and II cell death led to the finding that anti-apoptotic Bcl-2 members were only effective at inhibiting apoptosis in type II cells. Although it is known that Bak and Bax permeabilise the outer

mitochondrial membrane the mechanism of this is still not fully known. In 2000, Lindsten et al found that selective knockout of Bax or Bak alone did not produce a distinct phenotype in mice, but knockout of both genes together produced a lethal pairing. This suggested that both are involved in mitochondrial permeabilisation, perhaps as redundant pore forming proteins (Lindsten, Ross et al. 2000). It has since been revealed that Bax and Bak do indeed form pores in the mitochondrial membrane (Wei, Lindsten et al. 2000; Wei, Zong et al. 2001; Willis, Chen et al. 2005; Chipuk, Fisher et al. 2008; Westphal, Dewson et al. 2011; Westphal, Dewson et al. 2014; Kuwana, Olson et al. 2016).

1.2.5.2 DNA damage response

Under normal cellular conditions p53 is tightly regulated by Mdm2. Mdm2 binds to p53 and inhibits its activity. It also regulates the ubiquitinylation of p53 to target it for degradation (Coutts, Adams et al. 2009; Hrstka, Coates et al. 2009). Constant degradation of p53 keeps the levels low under normal conditions (Lavin and Gueven 2006; Mossalam, Matissek et al. 2012; Tichy, Stephan et al. 2013). However, once the cells receive a stress signal levels of p53 dramatically increase. This is because p53 undergoes a conformational change releasing it from Mdm2 and allowing it to become transcriptionally active, this release from Mdm2 also helps facilitate the accumulation of p53 as it is no longer targeted for ubiquitinylation [reviewed by](Coutts, Adams et al. 2009; Dai and Gu 2010). Mutated p53 is generally expressed at higher levels due to the fact that it cannot induce transcription of Mdm2 which normally acts to keep levels of p53 low (Vogelstein and Kinzler 1992). Yet another mechanism utilised by Mdm2 is to transport it from the nucleus to the cytoplasm, thus separating it from the DNA (Lakin and Jackson 1999). DNA damage causes activation of proteins such as ATM (ataxia telangiectasia mutated) and ATR (ataxia telangiectasia rad3 related protein) (Matsuoka, Ballif et al. 2007) [reviewed by](Elmore 2007; Kruse and Gu 2009). These proteins activate other proteins to either repair the cell's DNA or induce death of the cell. ATM phosphorylates p53 following DNA damage, especially in the form of DSBs (double stranded breaks) and ATR phosphorylates p53 when DNA repair enzymes are

non-functional [reviewed by](Lakin and Jackson 1999). Both of these proteins lead to the activation of p53. Following DNA damage, p53 acts on Bax, a mitochondrial pore forming protein (Chipuk, Kuwana et al. 2004). Bax, along with Bcl-X_L migrate to the mitochondria (Hsu, Wolter et al. 1997). This leads to mitochondrial outer membrane permeabilisation (MOMP). Permeabilisation of the mitochondrial membrane leads to release of several pro-apoptotic proteins including cytochrome c, SMAC/Diablo and Htr2a/Omi [reviewed by](Monian and Jiang 2012; Fuchs and Steller 2015). Additionally, Bax is a transcriptional target of p53 and is transcriptionally up-regulated by DNA damage in a p53 dependent manner (Han, Sabbatini et al. 1996). Post translational regulation of Bcl-2 family proteins has also been shown [reviewed by](Vazquez, Bond et al. 2008; Hrstka, Coates et al. 2009; Kruse and Gu 2009). For example, Bad is phosphorylated, promoting its sequestering by 14-3-3 proteins, thus preventing its inhibition of Bcl-X_L (Zha, Harada et al. 1996).

1.2.5.3 Regulation of the cell cycle by p53

p53 is a major regulator of the cell cycle. It also has a vital role in the induction of apoptosis as well as DNA repair (Kruse and Gu 2009). It is named as on Western blotting the protein appears to be approximately 53 kDa (DeLeo, Jay et al. 1979). p53 mutations are exceedingly common in cancers, with somewhere in the vicinity of 50% having mutated p53 and the other half believed to have alterations in p53 pathways (Ohnishi 2005). Because of this fact, p53 has been a target of research for some time. p53 knockout mice have been used to examine the importance of p53, and it has been found that these mice had extremely high susceptibility to cancer (Donehower 1996). p53 acts via two mechanisms: transcriptional regulation of proteins, and by direct interactions with proteins - particularly those related to mitochondrial permeabilisation.

1.2.5.4 Mitochondrial p53 interactions

In addition to p53's transcriptional activity, recent studies have indicated a mitochondrial role of p53 in apoptosis (Jamil, Lam et al. 2015). p53 was shown to interact with Bak, causing Bak oligomerisation and release of cytochrome c from mitochondria (Leu, Dumont et al. 2004; Tait and Green 2010). Additionally, p53 was shown to directly activate Bax leading to mitochondrial permeabilisation and apoptosis in mouse embryonic fibroblasts (Chipuk, Kuwana et al. 2004). When cells are subjected to hypoxic conditions the tumour suppressor protein Tid1 (also known as mitochondrial HSP40 (heat shock protein)) forms a complex with p53. This causes p53 translocation to the mitochondria and subsequent activation of the mitochondrial apoptosis pathway (Marchenko and Moll 2014). Down-regulation of Tid1 expression abrogated the apoptotic response, highlighting Tid1 as a regulator of apoptosis through p53 (Ahn, Trinh et al. 2010). p53 has been shown to localise to the mitochondria in proliferating cells (Ferecatu, Bergeaud et al. 2009). Additionally, p53 has been shown to trigger cell death in response to DNA damage prior to transcriptional activity (Erster, Mihara et al. 2004; Jamil, Lam et al. 2015). Furthermore, Bad – a Bcl-2 family protein which is transcriptionally regulated by p53 – physically interacts with cytoplasmic p53 and causes p53 to migrate to the mitochondria (Jiang, Du et al. 2006). Indeed several studies have shown that p53 leads to cell death via a mitochondrial interaction (Schuler, Bossy-Wetzel et al. 2000; Mihara, Erster et al. 2003; Vaseva, Marchenko et al. 2009; Mossalam, Matissek et al. 2012; Marchenko and Moll 2014; Matissek, Okal et al. 2014).

1.2.6 Other key regulators of apoptosis

1.2.6.1 Reactive Oxygen Species

Reactive Oxygen Species (ROS) have been shown to play a role in the induction of apoptosis in several cell lines following DNA damage [reviewed by](Ozben 2007). Malins et al, 2002 used the ROS depleting agent N-acetyl cysteine (NAC) to show that it was involved in apoptosis signalling, via inhibition of apoptosis. Furthermore, they found that NAC failed to inhibit apoptosis following FasL stimulation, indicating that ROS act upstream of DISC formation (Malins, Hellstrom et al. 2002). Additionally, the reactive oxygen species scavenger N-acetyl cysteine was effective in preventing apoptosis in Jurkat cells following gamma irradiation, however was unsuccessful in inhibiting apoptosis following Fas ligand death stimulation. From this the authors concluded that ROS act upstream of DISC formation to induce apoptosis (Huang, Fang et al. 2003). Conflicting with this Chiba et al (1996) indicated that N-acetyl cysteine effectively blocked Fas mediated apoptosis (Chiba, Takahashi et al. 1996). Although Fas is primarily involved in activation of the extrinsic apoptotic pathway, when caspases are inhibited it has been shown to induce caspase-independent cell death (CICD) (Chen, Chi et al. 2009). This cell death has been associated with the production of ROS by the mitochondria and cells gravitate toward necrosis rather than apoptosis.

1.2.6.2 Lipid Rafts

Lipid rafts are cholesterol and sphingomyelin enriched micro-domains of the plasma membrane that act as platforms for various signalling pathways. It was found that lipid raft clustering plays a role in formation of the DISC and caspase-8 activation (Bionda, Athias et al. 2008). Gajate et al (2009), provided evidence that lipid rafts are needed for apoptosis in some cell lines including Jurkat and multiple myeloma. Formation of lipid raft aggregates was inhibited by the depletion of cholesterol. The inhibition of lipid raft aggregates consequently prevented both caspase activation and loss of mitochondrial trans-membrane potential thus inhibiting apoptosis. Additionally, replenishment of cholesterol restored normal responses. They also provided evidence

that both extrinsic and intrinsic pathway elements were recruited to the raft domains and concluded that this may be a link between the two pathways (Gajate, Gonzalez-Camacho et al. 2009).

1.2.6.3 c-FLIP

A major regulator of the extrinsic apoptotic pathway is c-FLIP (FLICE-like Inhibitory Protein). C-FLIP is a regulator of both the DISC as well as TNFR1 complex IIa (Dickens, Powley et al. 2012). c-FLIP is a protein which is very similar to caspase-8, except it lacks catalytic activity (Wajant 2002). c-FLIP exists in three isoforms – c-FLIP$_L$, c-FLIP$_S$, and c-FLIP$_R$. Because of the similarity to caspase-8, it binds FADD, blocking caspase-8 binding and DISC formation. It has been shown that inhibition of c-FLIP expression induces spontaneous apoptosis in several cancer cell lines (Wilson, McLaughlin et al. 2007). Expression of cFLIP directly correlates with lack of caspase-8 activation (van Houdt, Muris et al. 2007).

1.2.6.4 TNF - Tumour Necrosis Factor

Tumour necrosis factor (TNF) is a typical member of the TNF superfamily of cytokines. The TNF superfamily activate signalling pathways for inflammation, cell proliferation, differentiation, cell survival and death (Micheau and Tschopp 2003). Many of these proteins lead to the activation of the transcription factor NFκB. TNF binds to TNF receptor 1 (TNFR1) and TNF receptor 2 (TNFR2) on the cell surface and leads to cell death through the formation of one of two complexes [reviewed by] (Dickens, Powley et al. 2012; Kreuzaler and Watson 2012). Complex-I is a ubiquitin dependent complex containing tumour necrosis factor receptor 1 associated death domain protein (TRADD), tumour necrosis factor receptor associated factor 2 (TRAF2), TRAF5, inhibitor of apoptotic proteins 1 (cIAP1), cIAP2, linear ubiquitin assembly complex (LUBAC) and receptor interacting protein 1 (RIP1) [reviewed by](Dickens, Powley et al. 2012; Kalliolias and Ivashkiv 2016). cIAP1 ubiquitination of components in this complex then lead to the activation of kinases needed for NFκB signalling (Jin and El-Deiry 2006).

This then leads to apoptosis through the activity of either caspase-8 or -10 [reviewed by](Pennarun, Meijer et al. 2009). In the absence of cIAPs, complex-I detaches from TNFR1 and recruits both FADD and caspase-8. This complex is called complex-IIb. Formation of this complex requires RIP1 (Dickens, Powley et al. 2012).

1.2.6.5 TRAIL – TNF-Related Apoptosis Inducing Ligand

TRAIL (TNF related apoptosis inducing ligand) is a promising new target for cancer therapy. This is because TRAIL has been shown to be cytotoxic to cancer cells, while showing no toxicity towards normal cells (Walczak, Miller et al. 1999). However, cancers may develop resistance to TRAIL. Binding of TRAIL to death receptors can also lead to cell proliferation and apoptosis evasion through the activity of MAPK (Monma, Harashima et al. 2013).

1.3 Necrosis

1.3.1 Overview

Necrosis was long considered to be the 'default' cell death pathway however this has since been shown to be false [reviewed by] (Moquin and Chan 2010; Fuchs and Steller 2015; Su, Yang et al. 2016). Necroptosis is the term used for regulated necrosis, however some groups define necroptosis as being programmed necrosis which is receptor interacting protein 1 (RIP1) dependent (Kroemer, Galluzzi et al. 2009). Necrosis occurs when the death stimulus is too severe for a more controlled cell death pathway to be activated. This can either be due to extensive damage to cellular components or the DNA itself [reviewed by](Borges, Linden et al. 2008; Kroemer, Galluzzi et al. 2009). Additionally certain compounds will selectively cause cells to undergo necrosis (Fuchs and Steller 2015; Su, Yang et al. 2016). Necrosis does not require energy in the form of ATP (Eguchi, Shimizu et al. 1997). It is also characterised by the random cleavage of DNA and proteins as well as the inhibition of protein and DNA synthesis (Malorni and Donelli 1992). However, necrosis rarely involves single cells as the death of the cell releases other compounds and components to the surroundings (Krysko, Vanden Berghe et al. 2008). Pro-inflammatory factors that are released include high motility group box 1 (HMGB1), HSP70, calreticuline and uric acid (Proskuryakov and Gabai 2010). Another cause of the large groups of affected cells in necrosis is the release of reactive oxygen species and reactive nitrogen species, damaging the surrounding cells [reviewed by](Rock and Kono 2008). These factors are the reasons for the death of large groups of cells in necrosis compared to the individual cells in apoptosis. When necrosis is activated in the absence of severe stimuli it is called programmed necrosis – or necroptosis (Degterev, Huang et al. 2005). This type of cell death is also called type III programmed cell death (Proskuryakov and Gabai 2010).

1.3.2 Triggers

Many stimuli which lead to apoptosis can also trigger necrosis depending on the severity of the stimulus. It has been demonstrated in several studies that the cell death type observed can be switched by the treatment with caspase inhibition, or depletion of ATP (Eguchi, Shimizu et al. 1997) [reviewed by] (Vanden Berghe, Kaiser et al. 2015). However, several stimuli preferentially cause cells to undergo necrosis. These stimuli include ischemia and hypoxia as well as binding of ligands such as TNF, Fas and TRAIL to death receptors under certain circumstances [reviewed by] (Krysko, Vanden Berghe et al. 2008; Kalliolias and Ivashkiv 2016).

1.3.3 Programmed Necrosis as a Cancer Treatment

Controversy has arisen about the use of programmed necrosis as a cancer treatment. This is because the necrotic cell death phenotype is damaging to surrounding cells and causes an inflammatory reaction [reviewed by] (Su, Yang et al. 2016). However, this may in some cases prove beneficial as the immune response may enhance the effectiveness of treatment (Guerriero, Ditsworth et al. 2008; Cuadrado-Castano, Sanchez-Aparicio et al. 2015). However caution must be used to find a beneficial balance in treatment (Edinger and Thompson 2004). Triggering necrosis could provide alternative treatments for cancers resistant to apoptosis signalling (Cho and Park 2014; Fulda 2014).

1.3.4 Major Players in Necrosis

RIP1 is a protein involved not only in necrosis signalling but also in apoptosis induction. Over-expression of RIP1 has been shown to induce apoptosis in a caspase dependent manner (Grimm, Stanger et al. 1996).

The necrosome is a complex which initiates necroptosis when caspases are inhibited (Holler, Zaru et al. 2000). In this complex RIP1 interacts with RIP3 via RHIM (RIP homotypic interaction motif) domains and forms complex II with a slight alteration – FADD and inactive caspase-8 are included. Formation of this complex leads to necrosis, however FADD is vital to the process (Dickens, Powley et al. 2012).

Heat shock proteins have been shown to suppress necrosis from ischemia, oxidative stress, RNS (reactive nitrogen species) and heat shock (Nylandsted, Gyrd-Hansen et al. 2004). A proposed possibility explaining this effect is that once chaperones are activated they suppress signal transduction pathways through sequestering proteins such as p38 mitogen activated protein kinase (p38 MAPK) and c-Jun N-terminal kinase (JNK) which leads to mitochondrial damage (Proskuryakov and Gabai 2010).

Bcl-2 family proteins can also modulate necrosis signalling. Bcl-2 has been shown to inhibit necrosis under certain conditions. These include anoxia (Shimizu, Eguchi et al. 1996), myocardial ischemia (Brocheriou, Hagege et al. 2000), hypoxia (Steinbach, Wolburg et al. 2003) and TNF stimulation (Thon, Mohlig et al. 2005). Additionally, Bax knockout was demonstrated to prevent necrosis (Moubarak, Yuste et al. 2007). Furthermore the association of Bcl-2 family protein BNIP3 (Bcl-2/adenovirus E1B 19 kDa protein-interacting protein 3) with mitochondria was disrupted by Necrostatin-1 treatment (Vande Velde, Cizeau et al. 2000).

1.3.5 Pathway of Necrosis

Although many stimuli can lead to the uncontrolled necrosis phenotype, programmed necrosis has distinct signalling events that trigger it. The first event is usually stimulation of a cell receptor such as TNF or Fas. Alternatively, massive DNA damage activates PARP1 on a large scale leading to depletion of NAD+ and ATP, steering the cell towards necrosis [reviewed by] (Kroemer, Galluzzi et al. 2009; Vanden Berghe, Kaiser et al. 2015). Energy depletion of cells is currently thought as the essential factor in determining the cell death pathway. Both of these events lead to the activation of RIP1 and JNK. Activation of these proteins promotes the recruitment of Nox1 (NADPH oxidase-1) to form a complex with TRADD. This complex generates ROS, specifically superoxide (Proskuryakov and Gabai 2010). Sustained activation of mitogen-activated protein kinase (MAPK) and JNK activation is required for necrosis (Kim, Morgan et al. 2007). The activation of these proteins leads to mitochondrial damage. Mitochondrial damage causes the release of pro-death factors such as cytochrome c, AIF (apoptosis inducing factor) as well as ROS. Indeed ROS production is almost universally associated with necrosis. Also, inhibition of ROS production is often sufficient to block necrosis (Proskuryakov and Gabai 2010). Additionally, mitochondria are the target of several pro-survival proteins such as Bcl-2 family proteins [reviewed by] (Delbridge and Strasser 2015; Karch and Molkentin 2015). In tandem with the mitochondrial damage several proteases are activated during necrosis – caspases (Faraco, Ledgerwood et al. 1999), calpains (Kohli, Madden et al. 1999), cathepsins and serine proteases. It should be noted that AIF and caspases are activated during necrosis, and are not solely apoptotic. These proteins have roles in both processes (Proskuryakov and Gabai 2010).

1.4 Cell death signalling platforms and other cell death types

1.4.1 Cell death signalling platforms

1.4.1.1 RIPoptosome

The RIPoptosome is a recently discovered cell death signalling platform which can induce cell death by either apoptosis or necrosis (Bertrand and Vandenabeele 2011). It is a large complex of approximately 2MDa which consists of RIP1, FADD and caspase-8. $FLIP_L$, $FLIP_s$ and RIP3 can also be included in the complex depending on the stimulus and cell type (Feoktistova, Geserick et al. 2011; Tenev, Bianchi et al. 2011). The activation and assembly of this complex occurs in the cytosol and is independent of cell surface death receptors such as TNF, Fas and TRAIL. RIPoptosome formation is induced by genotoxic depletion of IAP family proteins. The RIPoptosome has been demonstrated to form in response to etoposide induced DNA-damage in HT1080 fibrosarcoma cells (Tenev, Bianchi et al. 2011). $FLIP_L$ is an inhibitor of RIPoptosome mediated cell death. Additionally, ratios of FLIP isoforms appear to govern whether apoptosis or necroptosis is favoured (Feoktistova, Geserick et al. 2011; Imre, Larisch et al. 2011). Figure 1.7 demonstrates how the ratios of FLIP isoforms influence cell death outcomes. Supporting evidence for the RIPoptosome was provided when a different group found a complex containing RIP1, FADD and caspase-8 in response to depletion of IAPs by a drug called lexatumumab, which is a monoclonal antibody to TRAIL-R2 (Basit, Humphreys et al. 2012).

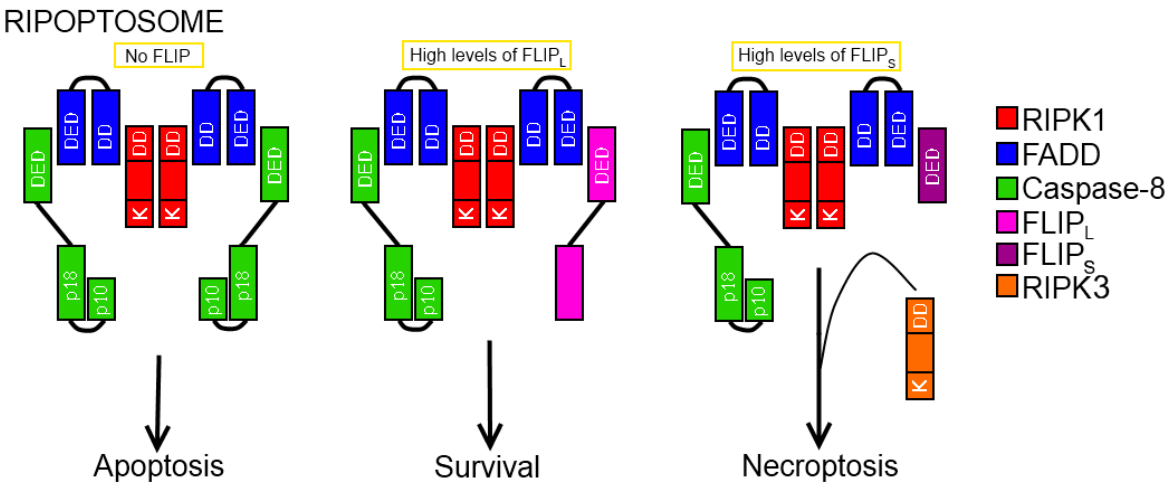

Figure 1.7: The RIPoptosome complex and ratios of FLIP isoforms affect cell death outcomes. RIP1 has also been shown to induce cell death in response to double stranded RNA. The response involves Toll-like receptor 3 activating caspase-8 in a RIP1 dependent manner. This activation is not dependent on FADD and is negatively regulated by expression of cIAP (Estornes, Toscano et al. 2012). Adapted from (Oberst and Green 2011), used with permission, 2015).

1.4.1.2 PIDDosome

The PIDDosome is an activation platform for caspase-2. The PIDDosome consists of PIDD (p53-induced protein with a death domain), RIP-associated ICH-1/CED-3 homologous protein with a death domain (RAIDD) and caspase-2. Caspase-2 is usually activated in response to heat shock, although has been shown to be activated in response to a variety of stimuli. The PIDDosome was found to be approximately 670 kDa. As this complex responds to induction by p53, this complex has been postulated to act in response to genotoxic stress (Tinel and Tschopp 2004). Figure 1.8 shows a diagram of the PIDDosome complex. Additionally, a study has indicated that caspase-2 knockdown in mouse embryonic fibroblasts (MEFs) only confers partial resistance to PIDD induced cell death, however is completely dependent on RAIDD (Berube, Boucher et al. 2005).

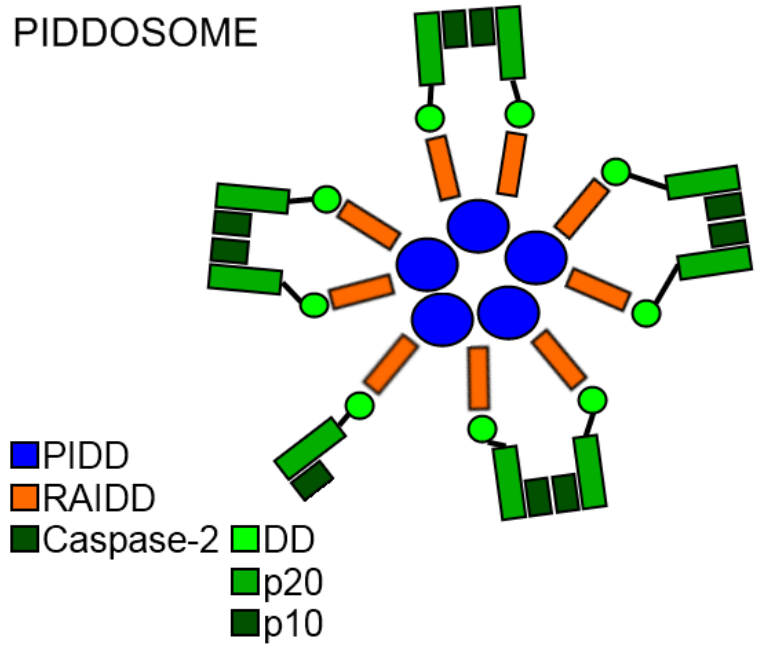

Figure 1.8: The PIDDosome complex is comprised of PIDD, the adapter protein RAIDD and caspase-2. Caspase-2 is divided into three domains – the death domain (DD) and the p10 and p20 subunits.

1.4.1.3 iDISC

The intracellular death-inducing signalling complex (iDISC) was identified as an activator of apoptosis with the requirement of caspase-8 as well as autophagy related genes. In a recent study it was found that this complex formed in response to sphingosine and proteasome inhibition in SV40 mouse embryonic fibroblasts. Caspase-8 was demonstrated to form a complex with ATG-5 (autophagy related gene protein 5) and co-localise with autophagy marker light chain 3 (LC3b) (and p62 at the autophagosomal membrane. This complex leads to the activation of caspase-8 and subsequently apoptosis. Furthermore, depletion of ATG-5 or ATG-3 markedly decreased caspase-8 activation and apoptosis (Young, Takahashi et al. 2012).

1.4.1.4 Inflammasome

Inflammasomes are multi-protein complexes which are formed in response to infection, cell damage or environmental stresses. They lead to the activation of caspase-1 and a rapid form of cell death called pyroptosis. However it has been shown that the inflammasome can also lead to apoptotic cell death through the association of Apoptosis -associated Speck-like protein containing a CARD (ASC) with caspase-8 (Sagulenko, Thygesen et al. 2013).

1.4.2 Other cell death types

There are several other types of cell death which should be briefly examined. Some more prominent cell death types include necrosis and autophagy, paraptosis, pyroptosis, CICD (caspase independent cell death) and pyronecrosis (Duprez, Wirawan et al. 2009; Kroemer, Galluzzi et al. 2009). Some more obscure cell death types which will not be discussed in detail including cornification - which is specific to epidermal cells, mitotic catastrophe - which occurs when mitosis is performed incorrectly, multi-nucleation - a DNA replication error during metaphase, anoikis, excitotoxicity, wallerian degeneration, and entosis – in which the cell is engulfed by a neighbouring cell and then dies in the phagosome. Paraptosis involves extensive cytoplasmic vacuolisation and mitochondrial swelling however presents no other apoptotic features. Pyronecrosis is necrosis which does not require caspase-1 for its activation (Willingham, Bergstralh et al. 2007).

Pyroptosis is distinct from necrosis and apoptosis. It requires the activation of caspase-1. Caspase-1 was the first caspase to be identified, and was originally termed interleukin 1ß converting enzyme (ICE). It is involved in inflammation and not activated in apoptotic cell death. It is activated like several other caspases by the formation of a signalling complex containing ASC, in this case called the pyroptosome (Fernandes-Alnemri, Wu et al. 2007). Activation of caspase-1 leads to formation of ion-permeable

pores in the plasma membrane, osmotic pressure on the cell then causes the cell to swell and burst. Additionally caspase-1 leads to activation of cytokines pro-IL-1ß and pro-IL-18 which are both released from the cell once activated. It should be noted that caspase-1 also cleaves several other proteins including other caspases (caspase-7), protein chaperones, and cytoskeletal proteins. Nuclear DNA condensing and fragmentation also occurs in pyroptosis but the laddering effect in apoptosis is not present (Duprez, Wirawan et al. 2009).

Caspase Independent Cell Death (CICD) is a form of programmed cell death morphologically similar to necrosis. It is a well regulated pathway and is activated by binding of a ligand to TNFR. The binding of the ligand to TNFR activates cell death through the activity of RIP1 (receptor-interacting protein 1). CICD has also been linked to autophagy by the formation of autophagosomes, however inhibitors of autophagy remain ineffective at preventing CICD (Chen, Chi et al. 2009).

1.5 Autophagy

1.5.1 Overview

Autophagy is a cellular process which enables a cell to tolerate the limited availability of nutrients. The name is derived from the Greek auto meaning “oneself” and phagy meaning “eat”. The term was coined by Nobel Prize winner Christian De Duve in 1963 at a symposium on lysosomes (Feng, He et al. 2014). This term was based on the early findings by Ashford and Porter showing sequestered organelles in rat hepatocytes following glucagon treatment (Ashford and Porter 1962). Under normal conditions autophagy functions to remove damaged organelles, clear cellular debris and in doing these things make metabolic precursors for the cell to use. Autophagy controls the turnover of mitochondria to maintain optimal levels in a process called mitophagy. Furthermore, autophagy clears protein aggregates which form when proteins are incorrectly folded in a process called aggrephagy. Autophagy also plays a role in infection by clearing intracellular pathogens. Deficiencies in autophagy have been linked to the progression of several diseases. Autophagy is widely known as the major cellular response to starvation conditions (Ryter, Cloonan et al. 2013).

It is also a mechanism of programmed cell death, under certain circumstances. This type of cell death is termed type II cell death (Torricelli, Salvadori et al. 2012). Autophagy is involved in many biological processes, including homeostasis, starvation, growth control, anti-aging and immunity. Along with apoptosis, autophagy maintains the balance of cells being produced with those being destroyed (Yang and Klionsky 2010; Ryter, Mizumura et al. 2014). It also has a prominent role in disease, such as cancer, metabolic diseases and neurodegenerative diseases (Ryter, Cloonan et al. 2013). The interaction of autophagy and cancer is quite complex. Autophagy normally functions to promote cell survival in the absence of nutrients however this is not the ideal situation in cancer. Autophagy has been associated with promoting survival of cancers, as the internal regions of tumours are often under nutrient deprivation

(Degenhardt, Mathew et al. 2006). The pro-survival role of autophagy has been demonstrated to be dependent on Bcl-2 family proteins under nutrient deprivation in neuroblastoma cells (Xu, Wu et al. 2013). Alternatively, autophagy can function to actively destroy the cancers, via autophagic cell death – which involves the extensive degradation of cellular components to the point which the cell cannot survive. These two roles have lead to extensive debate on whether triggering autophagy to combat cancer is a viable solution, or if it will just compound the problem. The general consensus at this stage is that only clinical trials will reveal if triggering autophagy is helpful in a particular instance (Kreuzaler and Watson 2012).

Understanding the complex interactions of autophagy in biological processes will help in our understanding of the diseases and processes it has a role in. Autophagy is activated in response to a number of stimuli hypoxia, overcrowding and high temperatures but is most commonly associated with the cellular response to starvation conditions (Levine and Klionsky 2004). Multicellular organisms are constantly subjected to periods of starvation due to dieting, night fasting and the scarcity of available food. Owing to this organisms have developed ways to tolerate starvation – one of the most important being autophagy (Caro-Maldonado and Muñoz-Pinedo 2011). Because autophagy functions as both a survival mechanism and cell death mechanism inhibiting autophagy or massively stimulating autophagy both lead to cell death (Torricelli, Salvadori et al. 2012).

Autophagy is divided into three types: microautophagy chaperone mediated autophagy and macroautophagy (Feng, He et al. 2014). Microautophagy involves the engulfment of cytoplasm directly at the lysosomal membrane. Macroautophagy is the proper name of what is simply called autophagy in the scientific community and is characterised by formation of double membrane vesicles (Levine and Klionsky 2004). Autophagy is primarily characterised by the formation of autophagosomes within the cell. An autophagosome is a membrane bound vesicle which contains enzymes from lysosomes for degradation of cellular components (Chikte, Panchal et al. 2013). An

autophagosome is formed by first making a small lipid bi-layer, which is expanded and enclosed into a vesicle around the cellular component to be destroyed. The initial source of the autophagosomal membrane can be from the golgi, endosomes, the endoplasmic reticulum, mitochondria or even the plasma membrane (Kang, Zeh et al. 2011). The autophagosomal membrane then fuses with lysosomes, releasing the enzymes required for degradation. Once the degradation is complete the contents of the autophagosome are released for the cell to recycle the components (Levine and Klionsky 2004; Yang and Klionsky 2010).

The proteins primarily responsible for autophagy are the autophagy-related genes (Atg). These proteins are homologues of the yeast autophagy-related genes (Levine and Klionsky 2004).

1.5.2 Molecular mechanisms in autophagy – ATG family

1.5.2.1 Autophagy in Yeast

The Atg family of proteins has been divided into functional subgroups in yeast. Atg proteins are named according to guidelines set out by Klionski et al in 2003, Atg meaning 'Autophagy-related' (Klionsky, Cregg et al. 2003). The first group forms the Atg1 complex containing Atg1, Atg11, Atg13, Atg17, Atg29 and Atg31 which functions as the initial complex that regulates the induction of autophagosome formation. The second group is based around Atg9 and its cycling system containing Atg2, Atg9 and Atg18 which facilitate membrane delivery and expanding of the phagophore. PtdIns 3-kinase complex which contains Vps34 (vacuolar protein sorting), Vps15, Vps30/Atg6, Atg14 controls vesicle nucleation. Finally two ubiquitin-like conjugation systems - Atg12 (Atg5, Atg7, Atg10, Atg12, Atg16) and Atg8 (Atg3, Atg4, Atg7, Atg8) perform vesicle expansion leading to the completion of autophagosomes (Yang and Klionsky 2010; Feng, He et al. 2014). Table 1.2 lists yeast ATG proteins and their mammalian homologues.

1.5.2.2 Mammalian Autophagy

Mammalian autophagy is under regulation by mammalian target of rapamycin (mTOR) which is a kinase and a major regulator of cell growth (Dunlop and Tee 2013). mTOR, in a complex called mammalian target of rapamycin complex 1 (mTORC1) negatively regulates the pro-autophagy complex containing ULK1 (UNC-51-like kinase 1), ATG13, ATG101 and FIP200 (Hosokawa, Hara et al. 2009). Thus inhibition of mTOR leads to autophagic cell death (Xie, White et al. 2013; Xie, Xie et al. 2013). Conversely, nutrient depletion inhibits mTORC1 leading to the activation of the ULK1 complex [reviewed by](Choi, Ryter et al. 2013; Feng, He et al. 2014). Another complex called the Beclin-1 interacting complex promotes autophagy, specifically the nucleation of the autophagosomal membrane. This complex contains Beclin-1, Bcl-2 family members, VPS34 (a PI3k protein) and ATG14L and is responsible for the generation of PI3P which directly promotes autophagosomal membrane nucleation. Finally, the autophagosomal membranes are elongated by one of two ubiquitin conjugation systems: ATG5-ATG12 or LC3b-ATG8 [reviewed by](Choi, Ryter et al. 2013; Feng, He et al. 2014).

Table 1.2: ATG proteins in yeast and mammals and their functions. [Table primarily adapted from](Mizushima, Yoshimori et al. 2011; Feng, He et al. 2014)

Complex and Role	**Yeast**	**Mammals**
Atg1/ULK complex (induction of autophagosome formation) [reviewed by] (Ryter, Cloonan et al. 2013)	Atg1	ULK1/2
	Atg11	
	Atg13	ATG13
	Atg17	RB1CC1/FIP200
	Atg29	
	Atg31	
Atg9 and cycling system (expansion of phagophore) [reviewed by] (Yang and Klionsky 2010; Choi, Ryter et al. 2013)	Atg2	ATG2
	Atg9	ATG9A/B
	Atg18	WIPI1/2
PtdIns3K complex (vesicle nucleation) [reviewed by] (Ryter, Cloonan et al. 2013)	Vps34	PIK3C3/VPS34
	Vps15	PIK3R4/VPS15
	Vps30/Atg6	Beclin-1
	Atg14	ATG14
Atg8 Ubl conjugation system (vesicle expansion) [reviewed by](Yang and Klionsky 2010)	Atg3	ATG3
	Atg4	ATG4A/B/C/D
	Atg7	ATG7
	Atg8	LC3A/B/C/D GABARAP GABARAPL1/2
Atg12 Ubl conjugation system (vesicle expansion) [reviewed by] (Yang and Klionsky 2010)	Atg5	ATG5
	Atg7	ATG7
	Atg10	ATG10
	Atg12	ATG12
	Atg16	ATG16L1

1.5.3 Pathway of autophagy

The phosphatidylinositol 3 kinase (PI3K)/mTOR (Mammalian target of rapamycin) pathway is a key regulator of cell survival and proliferation (Papadimitrakopoulou 2012). Upon inhibition of mTOR activity, mTOR dependent phosphorylation sites on the ULK1-ATG13-FIP200 induction complex become de-phosphorylated [reviewed by] (Ryter, Cloonan et al. 2013; Feng, He et al. 2014). This releases the activity of ULK1 which through auto-phosphorylation of different sites promotes assembly of the complex with ATG101 - a vertebrate specific Atg protein (Bodemann, Orvedahl et al. 2011). This complex then activates the PI3k complex Beclin1-ATG14L-VPS34-VPS15. This PI3k complex promotes coating of a cup shaped isolation membrane with phosphatidylinositol-3-phosphate (PI3P) – this initial formation of the membrane is termed autophagosomal nucleation (Ryter, Mizumura et al. 2014). This serves as a recruiting signal for the ATG16-ATG5/ATG12 isolation membrane elongation system. Two ubiquitin like molecules: ATG12 and LC3b conjugate to ATG5 and phosphatidylethanolamine respectively causing the formation of the autophagosome (Yang and Klionsky 2010; Ryter, Mizumura et al. 2014). In the first conjugation system ATG12 is activated by ATG7 and then transferred to ATG10, followed by a covalent linkage to ATG5 (Mizushima, Noda et al. 1998). In the second system microtubule-associated protein light chain 3 and ATG8 (LC3b-ATG8) are cleaved by the cysteine protease ATG4 exposing a C-terminal glycine (Amar, Lustig et al. 2006). ATG7 activates LC3b and transfers it to ATG3. LC3b is then conjugated to phosphatidylethanolamine with assistance from ATG5/ATG12. The lipidated LC3b coats both the inner and outer surfaces of the autophagosome providing a marker for autophagosomes (George, Baba et al. 2000; Bodemann, Orvedahl et al. 2011). These events happen in tandem with several dynamic membrane events which have currently not been fully defined. The autophagosomes then fuse with lysosomes leading to the degradation and recycling of cellular components (Hosokawa, Hara et al. 2009; Yang and Klionsky 2010; Dodson, Darley-Usmar et al. 2013; Blum and Kloog 2014). Figure 1.9 shows a simplified outline of the autophagy pathway.

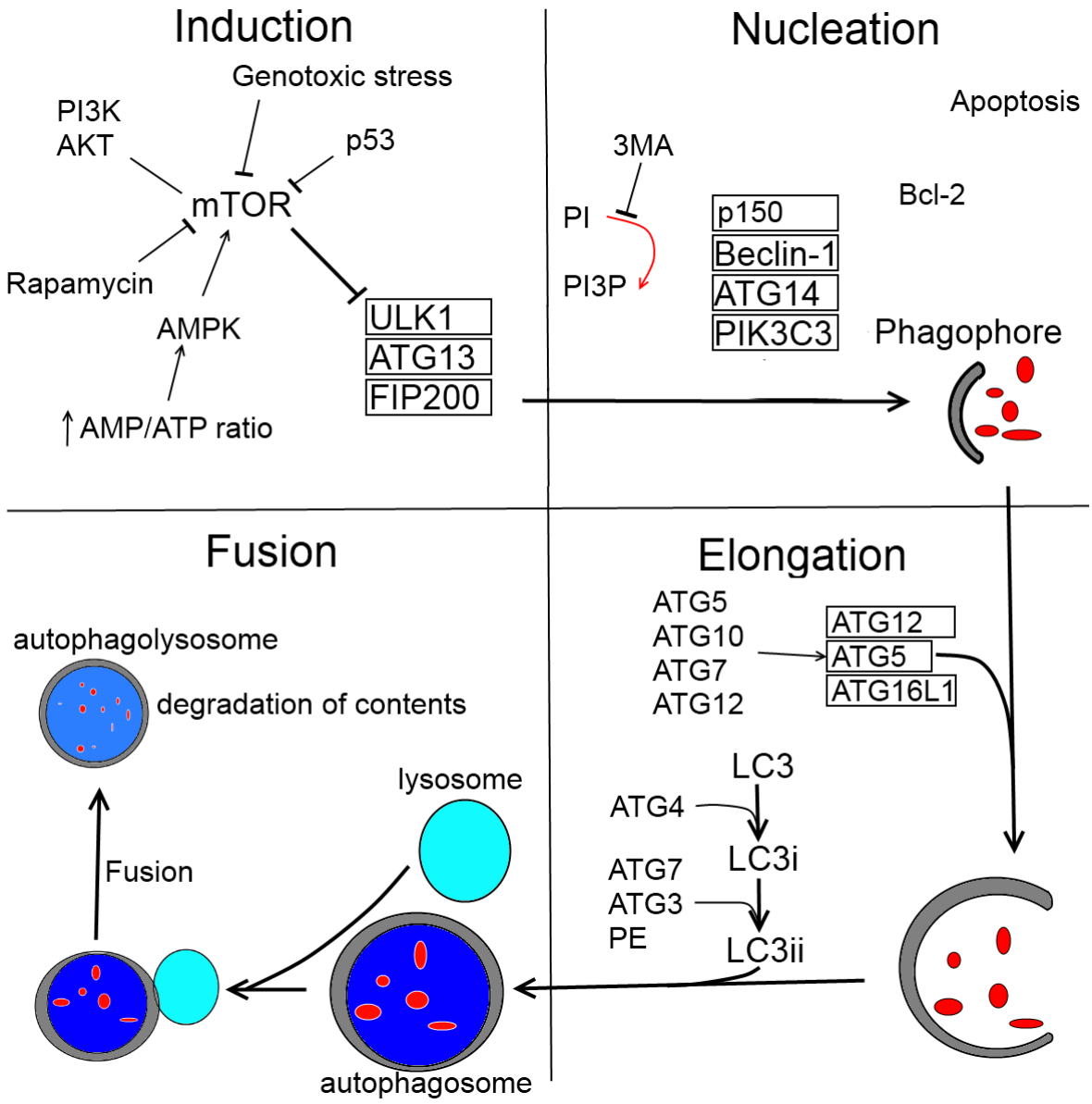

Figure 1.9: A brief overview of the autophagy pathway. Induction of autophagy is regulated primarily by mTOR and formation of a ULK1 containing complex is the initiating step. A Beclin-1 containing complex begins formation of a double membrane termed a phagophore around the targets. The membrane is elongated through two separate systems. When the membrane is complete it fuses with lysosomes and degradation of the proteins is achieved. (Choi, Ryter et al. 2013; Ryter, Cloonan et al. 2013; Feng, He et al. 2014)

In mammalian cells the ULK1/2 (yeast Atg1 homolog) complex is the equivalent of the yeast Atg1 complex and forms regardless of the presence of nutrients. This complex contains ATG13 (yeast Atg13 homolog), RB1CC1/FIP200 (yeast Atg17 homolog), C12orf44/ATG101 (no yeast homolog) and is approximately 3 MDa (3000 kDa) in size (Hosokawa, Hara et al. 2009). However, mTORC1 phosphorylates and inhibits ULK1/2

and ATG13. Under nutrient deprivation conditions mTOR is released causing the activation of ULK1/2 which then phosphorylates and activates Atg13 and RB1CC1 (retinoblastoma 1 inducible coiled-coil 1) (Hosokawa, Hara et al. 2009; Feng, He et al. 2014).

The class III phosphoinositide 3-kinase Vps34 homolog (PIK3C3), Vps15 (PIK3R4) and Vps30 (Beclin-1) are part of three important autophagy complexes. ATG14, Beclin-1, AMBRA1 (autophagy/Beclin-1 regulator 1) and Bcl-2 form the first complex. If AMBRA1 is in the complex autophagy is stimulated, but when Bcl-2 is in the complex autophagy is inhibited (Feng, He et al. 2014). The second complex contains UVRAG (ultraviolet radiation resistance-associated gene protein), Beclin-1 and the positive regulator SH3GLB1 (SH3 domain containing GRb2-like protein B 1), and this complex stimulates autophagy. The third complex contains UVRAG, Beclin-1 and KIAA0226/Rubicon and behaves as an inhibitor of autophagy through inhibition of UVRAG by Rubicon. In the mammalian conjugation system ATG4b (yeast Atg4 homolog) cleaves the pro-form of LC3b after the C-terminal glycine to form cytosolic LC3b-i. LC3b-i is subsequently conjugated to phosphatidylethanolamine to generate membrane associated LC3b-ii, leading to formation of the completed autophagosome (Feng, He et al. 2014). Beclin-1 inhibition leads to increased expression of LC3b-ii (Li, Yan et al. 2013).

Autophagy can be initiated by many stimuli, but perhaps the most common is nutrient deprivation. Upon withdrawal of nutrients from cells the mammalian target of rapamycin (mTOR) containing complex mTORC1 (mTOR complex 1) is inhibited. This leads to the activation of the ULK1 kinase complex which contains ULK1, ATG13 and ATG17. This leads to the formation of the Beclin-1 complex mentioned above (Hosokawa, Hara et al. 2009).

Another important component of the autophagy machinery is p62/SQSTM1 sequestosome-1. This adaptor protein helps in the trafficking of proteins to the autophagosome for degradation and is itself consumed in the process (Kreuzaler and Watson 2012). This protein is a polyubiquitin binding protein. p62 has links to ubiquitinylated protein aggregates in Parkinson's disease, Alzheimer's disease and Huntington's disease (Pankiv, Clausen et al. 2007). It has also been shown to bind LC3b proteins A and B (LC3a, LC3b). p62 forms small 'p62 bodies' which are transported to autophagosomes and degraded (Pankiv, Clausen et al. 2007).

A recent study has indicated that RalB – a Ras like small G protein and its effector protein exo84 (EXOC8) are required for autophagosome formation (Bodemann, Orvedahl et al. 2011). RalB is a close relative of the Ras GTPase family. The RalB/exo84 complex de-phosphorylates mTOR on the ULK1-ATG13-FIP200 complex causing assembly with ATG101. This then leads to recruitment of class III PI3K. The Beclin-1-ATG14L-VPS34-VPS15 complex is then formed in response which coats a cup like membrane with PI3P. RalB has also been shown to co-localise with Beclin-1. PI3P is a recruitment signal for ATG16-ATG5/ATG12, and ATG5 conjugates to ATG12 and LC3b. In the second system, running in parallel, ATG4 cleaves LC3b leading to autophagosome formation (Bodemann, Orvedahl et al. 2011).

1.6 Links Between Cell Death Pathways

Communication between apoptosis and autophagy is required to regulate cell death. Cleavage of the ATG5 autophagy protein creates a protein fragment which translocates to the mitochondria where it interacts with the Bcl-2 protein Bcl-X_L, leading to the activation of the mitochondrial apoptosis pathway (Yousefi, Perozzo et al. 2006; Young, Takahashi et al. 2012). Additionally, ATG5 has been shown to directly interact with FADD and induce caspase dependent cell death. Evidence has also been presented that the autophagosomal membrane acts as a platform for caspase activation (Young, Takahashi et al. 2012; Ryter, Mizumura et al. 2014). Additionally, following antigen receptor cross linking which causes apoptosis under normal conditions, when the activity of both FADD and caspase-8 was blocked in proliferating T-cells, autophagy was converted to a potent cell death mechanism instead of a cell stress survival mechanism (Bell, Leverrier et al. 2008). Figure 1.10 demonstrates a few links between different cell death types. Through intermediate proteins such as mTOR or direct interactions p53 can stimulate cells to undergo death via apoptosis autophagy or necrosis (Kruse and Gu 2009). Changes in levels of NAD+, depletion of ATP or production of ROS can all cause the cell to switch from an apoptotic cell death to a necrotic one (Krysko, Vanden Berghe et al. 2008; Proskuryakov and Gabai 2010). Caspases, whose primary function is the induction of apoptosis can also stimulate autophagy through caspase mediated cleavage of autophagy related proteins (ATG) or Beclin-1 cleavage (Li, Wang et al. 2011). Conversely, autophagic proteins can lead to the activation of FADD or Bcl-2 family members leading to apoptosis (Young, Takahashi et al. 2012; Ryter, Mizumura et al. 2014). Depletion of NAD+ or ATP lead to necrosis rather than apoptosis (Duprez, Wirawan et al. 2009). Elevation in ROS also tends to shift the equilibrium toward necrosis rather than apoptosis (Lee and Shacter 1999).

Caspases are important proteins in apoptosis signalling, however have also demonstrated the ability to lead to autophagic cell death [reviewed by] (Ryter, Mizumura et al. 2014). Caspase cleavage of the autophagic proteins has also been

recorded. Caspase-3 has been shown to cleave ATG4D (Kang, Zeh et al. 2011) and caspase-8 has been shown to cleave ATG3 (Oral, Oz-Arslan et al. 2012). Additionally, c-FLIP can act as a negative regulator of autophagy (Lee, Li et al. 2009). Autophagy has been shown to inhibit caspase-8, and caspase-3 inhibits autophagy. Inhibition of autophagy will often enhance apoptosis induced by chemotherapy (Ryter, Mizumura et al. 2014). ATG5 and Beclin-1 are both cleavage targets of calpains and caspases. For example, caspase-8 cleaves Beclin-1 (Li, Wang et al. 2011) and caspase-3 also cleaves Beclin-1 in a weak interaction (Djavaheri-Mergny, Maiuri et al. 2010). Furthermore, inhibition of autophagy can enhance the apoptotic response induced by chemotherapeutic drugs [reviewed by] (Sui, Chen et al. 2013). Beclin-1 knockdown decreases autophagy in several cell lines (Chen, McMillan-Ward et al. 2007). Blocking cleavage of Beclin-1 has no effect on apoptosis but results in chemoresistance (Wang, Wei et al. 2012).

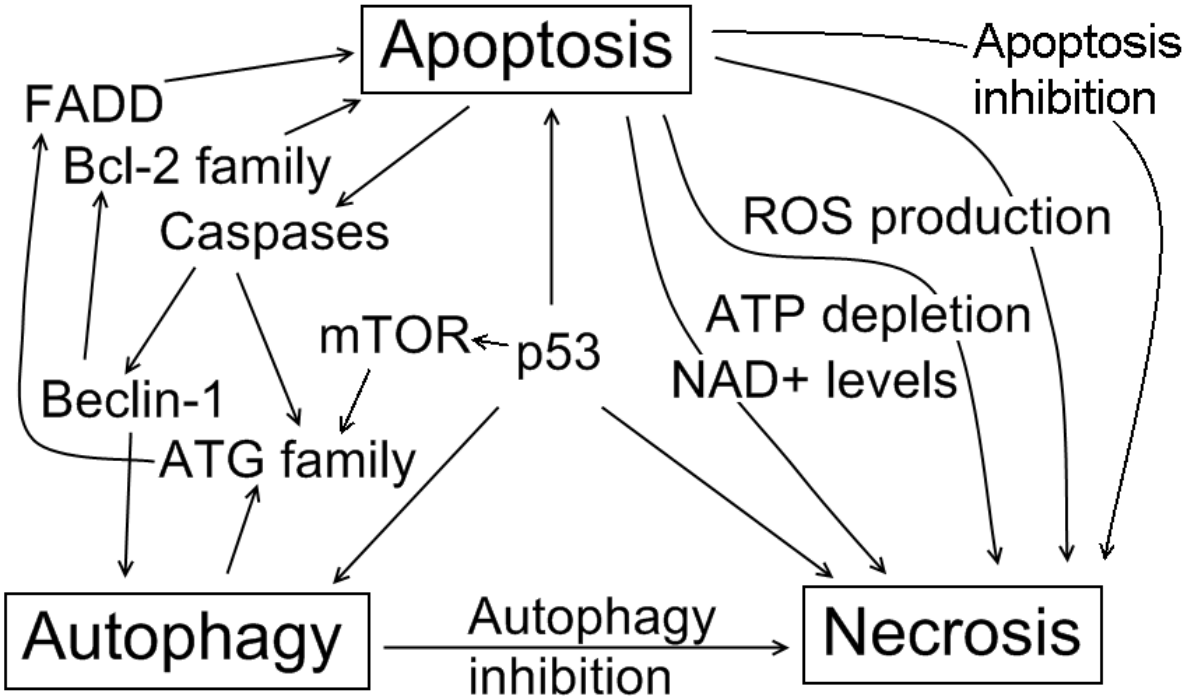

Figure 1.10: Examples of the crosstalk between different cell death pathways. A complex network of interactions can switch between apoptotic, autophagic or necrotic cell death types. (Yousefi, Perozzo et al. 2006; Krysko, Vanden Berghe et al. 2008; Kruse and Gu 2009; Kang, Zeh et al. 2011; Li, Wang et al. 2011; Ryter, Cloonan et al. 2013; Sui, Chen et al. 2013). Further information on these interactions can be found throughout the text of Section 1.6.

c-FLIP proteins are structurally similar to caspase-8, however possess no catalytic domain (Yeh, Itie et al. 2000; Kikuchi, Kuroki et al. 2012). c-$FLIP_L$ modulates the cellular response in determining whether the cell will undergo apoptosis or necrotic cell death (Feoktistova, Geserick et al. 2011; Tenev, Bianchi et al. 2011). T-cells deficient in c-$FLIP_L$ undergo a RIP1 dependent necroptosis cell death (He and He 2013). Furthermore caspase-8 activity was observed during this necroptosis cell death, a result previously unseen. Additionally, T-cells deficient in c-$FLIP_L$ exhibited enhanced autophagy. These findings clearly demonstrate the potential of c-$FLIP_L$ in linking cell death outcomes (He and He 2013).

RIP1 is another protein which under different circumstances can lead to either necrotic, apoptotic or autophagic cell death. Whether RIP1 leads to apoptosis or necrosis is largely dependent on the ratios of c-FLIP isoforms (Feoktistova, Geserick et al. 2011; Imre, Larisch et al. 2011). RIP1 has been shown in induce caspase-8 activation and apoptosis through the accumulation of ROS in T-lymphoma cells. Under these conditions the knockdown of caspase-8 expression changed the cell death phenotype observed to a simultaneous apoptosis and autophagy in the cell population (Kikuchi, Kuroki et al. 2012). Caspase-8 has also been demonstrated to be involved in necroptosis signalling by cleaving RIP1 shifting the equilibrium toward apoptosis rather than necrosis (Lin, Devin et al. 1999).

Expression of different Bcl-2 family proteins also control what type of cell death is initiated in response to stimuli. The Bcl-2 family of proteins are key in regulation of apoptosis however also can lead to autophagy induction [reviewed by] (Sui, Chen et al. 2013). For example, Bim is a BH3 only Bcl-2 family protein which is known to induce apoptosis by inactivating anti-apoptotic Bcl-2 family members and activating the pro-apoptotic Bcl-2 family members Bax and Bak (Luo and Rubinsztein 2013). However it has also been shown to interact with the autophagy protein Beclin-1 through dynein light chain 1, cytoplasmic (DYNLL1). Bim is phosphorylated by JNK under starvation conditions, which blocks the DYNLL1 interaction releasing Beclin-1 and allowing

autophagy to proceed. Bim has three splicing isoforms: BimEL (extra long), BimL (long) and BimS (short). BimEL and BimL interact strongly with Beclin-1 whereas BimS only has a weak interaction with Beclin-1 (Luo and Rubinsztein 2013).

Beclin-1 is an important protein in autophagy. This is highlighted by the observation that 75% of ovarian cancers, 50% of breast cancers and 40% of prostate cancers are haploinsufficient for Beclin-1 (Kreuzaler and Watson 2012). It is the mammalian ortholog of yeast Atg6 [reviewed by] (Kang, Zeh et al. 2011; Ryter, Mizumura et al. 2014). Beclin-1 is part of a class III phosphatidylinositol 3 kinase (PI3K) complex (Ryter, Mizumura et al. 2014). It is critical in formation of autophagosomal membranes and the localisation of other autophagy related proteins to these membranes. Over-expression of Beclin-1 has been shown to induce a large autophagic response and inhibit cancer growth (Kim, Yim et al. 2013). The PI3K pathway Beclin-1 is involved in regulates mTOR signalling and thus influences cell survival and death through both apoptosis and autophagy. (Kim, Yim et al. 2013)

Beclin-1 interacts with a wide variety of proteins including AMBRA-1, High mobility group box 1 (HMGB1), nPIST, VMP-1 (vacuolar membrane protein 1), SLAM (signalling lymphocyte activation molecule), IP3R (inositol tri-phosphate receptor), PINK (PTEN induced putative kinase 1) and Survivin (Kang, Zeh et al. 2011). Beclin-1 also possesses a BH3 only domain allowing it to interact with Bcl-2 family proteins; specifically Bcl-2 and Bcl-X_L (Kang, Zeh et al. 2011; Ryter, Mizumura et al. 2014). These two proteins are regulators of apoptosis (Xu, Wu et al. 2013). RalB – a protein which binds ULK-1 has recently been shown to drive assembly of Beclin-1 containing complexes (Bodemann, Orvedahl et al. 2011). Phosphorylation of Beclin-1 inhibits the interactions of the BH3 only domain (Kang, Zeh et al. 2011). Showing further interplay between autophagy and apoptosis Beclin-1 can be cleaved by caspases (Li, Wang et al. 2011; Li, Wang et al. 2011; Siddiqui, Mukherjee et al. 2015). The importance of Beclin-1 is highlighted by studies in mice where Beclin-1 null mice have embryonic lethality in 7.5 days (Kang, Zeh et al. 2011).

The BH3 domain of Beclin-1 is near the N-terminus at amino acids 114-123 (Kang, Zeh et al. 2011). Other notable structural features of Beclin-1 include a central coiled-coil domain at amino acids 144-269 as well as an evolutionary conserved domain at amino acids 244-337 (Kang, Zeh et al. 2011). The evolutionary conserved domain has been shown to be essential in the regulation of autophagy. This domain contains a short leucine rich domain which acts as a nuclear export signal. Beclin-1 proteins can self associate (Adi-Harel, Erlich et al. 2010). This may form platforms for rapid nucleation. Beclin-1 is transcriptionally regulated by NFκB, E2f and microRNAs. p65 up-regulates the expression of Beclin-1 (Kang, Zeh et al. 2011).

The tumour suppressor protein death associated protein kinase (DAPK) phosphorylates Beclin-1 at threonine 119 stimulating membrane blebbing by binding LC3b (Zalckvar, Berissi et al. 2009). As mentioned earlier phosphorylation of Beclin-1 releases Bcl-2 proteins. Alternatively, phosphorylation of Bcl-2 by c-Jun N-terminal kinase (JNK-1) reduces its interaction with Beclin-1 (Wei, Pattingre et al. 2008). HMGB1 promotes phosphorylation of Beclin-1 by extracellular signal regulated kinase (ERK) (Tang, Kang et al. 2010). The interactions of Beclin-1 are inhibited by tBid, Bad, BNIP3 however are not inhibited by Bax or Bak (Kang, Zeh et al. 2011).

p53 acts as a regulator of apoptosis, autophagy and necrosis (Kruse and Gu 2009). This occurs through modulation of Bcl-2 family proteins as well as other apoptotic proteins (Chipuk, Kuwana et al. 2004), and DRAM (damage regulated autophagic modulator) which itself can stimulate either apoptosis or autophagy (Crighton, Wilkinson et al. 2006). p53 can also act through the regulation of the mTOR pathway through AMPK (Ryter, Cloonan et al. 2013).

There are numerous links between the signalling of cell death pathways. Expression ratios of Bcl-2 family proteins or FLIP isoforms, p53 modulation of proteins or transcriptional regulation of protein as well as cleavage events between kinases involved in autophagy and apoptosis all contribute to the cell death outcome. The complex interplay between all these proteins are influenced by many factors including severity and type of the cell death stimulus, the availability of energy as well as the metabolic state of the cell.

1.7 Nutrient deprivation and metabolic dysregulation

1.7.1 Metabolic reprogramming

Metabolic reprogramming is another hallmark of cancer. These changes allow cancers to tolerate withdrawal of nutrients as well as enabling cancers to metabolise nutrients from other sources (Hanahan and Weinberg 2011). For example cancers often have up-regulated glycolysis instead of utilising aerobic respiration (Dang 2012).

1.7.1.1 Glycolysis

Long ago it was hypothesised that glycolysis is how cancers access the extra energy required for excessive cell proliferation, and how they may tolerate nutrient deprivation. This phenomenon was termed the Warburg effect after its discoverer Otto Warburg in the 1920's (Caro-Maldonado and Muñoz-Pinedo 2011; Puzio-Kuter 2011; Dang 2012). This phenomenon has since been shown to be caused by a constitutively active Ras (Rat sarcoma) pathway (Blum and Kloog 2014). Ras proteins are G proteins which act as molecular switches which are involved in several downstream signalling pathways (Munoz-Pinedo, El Mjiyad et al. 2012; Blum and Kloog 2014). Because of its involvement in these pathways Ras regulates cell survival, cell migration, cell cycle, metabolism and differentiation. Although glycolysis is far less efficient at energy production than oxidative phosphorylation several side effects of this energy production avenue could be beneficial to cancer survival (Ward and Thompson 2012). The first reason is decreased reliance on consistent oxygen supply as compared to oxidative phosphorylation at the mitochondria, despite it being aerobic glycolysis which is occurring (Munoz-Pinedo, El Mjiyad et al. 2012). Secondly, formation of glycolysis by-products such as lactic acid forms an acidity buffer which can help cancerous cells survive when there are changes in pH (Riganti, Gazzano et al. 2012). Third, the lactate build-up, a side effect of excessive glycolysis, interferes with the immune response as tumour infiltrating T lymphocytes rely on glycolysis also and

the high lactate content of the surroundings slows metabolism of the lymphocytes (Munoz-Pinedo, El Mjiyad et al. 2012; Blum and Kloog 2014). Finally, glycolytic intermediate products can be useful in anabolic processes as well as biosyntheses (Blum and Kloog 2014). Indeed, it has been observed that glycolysis is up-regulated in many cancer types, and that the normal energy generation method, oxidative phosphorylation is decreased (Bhardwaj, Rizvi et al. 2010; Dang 2012).

1.7.1.2 Glutamine

Glucose and glutamine are the primary sources of carbon for energy production (in the form of ATP) and biosynthesis in cancers where nutrients are lacking or the requirements for rapid proliferation are high (Wise and Thompson 2010; Dang 2012; Stine and Dang 2013; Blum and Kloog 2014). Glutamine is needed for the production of the non essential amino acids and also provides nitrogen for the synthesis of nucleotides (Wise and Thompson 2010; Munoz-Pinedo, El Mjiyad et al. 2012; Blum and Kloog 2014). Glutamine is one of the main metabolites in the tricarboxylic acid (TCA) cycle (Dang 2012; Munoz-Pinedo, El Mjiyad et al. 2012). The TCA cycle functions not only to make ATP, but also to synthesise fatty acids and non essential amino acids (Blum and Kloog 2014). In order to accommodate for the larger metabolic activity of cancer glutamine is used to synthesise nitrogen containing amino acids and nucleotides. In two enzymatic reactions for pyrimidine synthesis and three for purine synthesis, glutamine donates its amide group and is converted to glutamic acid. This means that while glutamine is a non-essential amino acid in normal cells it effectively becomes an essential amino acid in cancer (Blum and Kloog 2014). As a result of these factors glutamine consumption is increased in many cancers. This effect has been termed ‘glutamine addiction’ (Wise and Thompson 2010). In normal cells glutamine uptake is dependent on growth factors, however in cancer the cells switch to cell autonomous nutrient uptake, which leads to an increase in glutamine uptake (Wise and Thompson 2010; Dang 2012; Blum and Kloog 2014).

1.7.1.3 Pentose Phosphate Pathway

The Pentose Phosphate Pathway (PPP) is another important pathway in cancer. The main fuel source for this pathway is glucose-6-phosphate. The pentose phosphate pathway's primary function is the generation of NADPH – which is vital to the control of redox reactions (Dodson, Darley-Usmar et al. 2013). NADPH also fuels biogenesis reactions needed for growth. Furthermore, the pentose sugars generated in this pathway are used in the synthesis of nucleotides and amino acids. In pancreatic cancers mutated K-Ras promotes glucose uptake by the cell and stimulates the transfer of intermediates created into the PPP where they are used in the manufacture of nucleic acids. However, this activity shunted PPP activity away from the production of NADPH and more toward nucleic acid synthesis (Blum and Kloog 2005; Riganti, Gazzano et al. 2012; Blum and Kloog 2014).

1.7.1.4 Lipid Metabolism

Lipid metabolism is still not well understood. However it is known that there is a link to cancer. Lipogenesis is indeed increased in cancer cells for membranes, lipid rafts and signalling molecules (Munoz-Pinedo, El Mjiyad et al. 2012). High fat diets and obesity have been linked to several cancer types including pancreatic cancer (Dang 2012; Munoz-Pinedo, El Mjiyad et al. 2012). Addition of lipids has been shown to increase growth of pancreatic cancers however did not affect growth of other cancer types. This may be due to pancreatic cancers using the lipids as an energy source or through the regulation of hormones, growth factors and lipid messengers associated with lipids and finally through the bolstering of cellular membrane formation. (Blum and Kloog 2014)

1.7.1.5 AMPK

Another signalling protein responding to nutrient deprivation is AMPK. A lack of nutrients required to make ATP leads to activation of AMPK (Caro-Maldonado and Muñoz-Pinedo 2011). AMPK responds to changes in the ratio of ATP (adenosine tri-phosphate) to AMP (adenosine mono-phosphate). Low levels of glucose and glutamine lead to a lower ratio of ATP to AMP which in turn causes AMPK to increase energy production and limit energy usage (Dodson, Darley-Usmar et al. 2013). This is done through several ways including phosphorylation and inactivation of acetylCoA carboxylase which uses ATP for fatty acid synthesis, as well as activation of autophagy by phosphorylating ULK-1. AMPK also phosphorylates and activates TSC2 which inhibits mTOR, thus limiting cell growth [reviewed by](Dang 2012).

Once activated the mTORC1 kinase phosphorylates several proteins such as S6K1 and 4eBP1 leading to stimulation of translation, ribosome biogenesis and cell growth. Activated mTORC2 leads to stimulation of glycolysis through phosphorylation of hexokinase2, inhibition of apoptosis and an increase in mitochondrial biogenesis through phosphorylation of FOXO3a.

1.7.2 mTOR

Mammalian target of rapamycin is a serine/threonine protein kinase involved in regulating cell proliferation, cell migration, protein synthesis and transcription (Hosokawa, Hara et al. 2009; Choi, Ryter et al. 2013). It is a PI3K related family member (Zhou and Huang 2010; Mitra, Luna et al. 2015). It is the catalytic component of two protein complexes: mTORC1 and mTORC2 (Sancak, Thoreen et al. 2007; Peterson, Laplante et al. 2009). The mTORC1 complex consists of mTOR, regulatory-associated protein of mTOR (Raptor), mammalian lethal with SEC13 protein 8 (MLST8) and the non-core components PRAS40 (proline-rich Akt substrate of 40 kDa) and DEPTOR (DEP domain containing mTOR interacting protein) (Sancak, Thoreen et al. 2007; Peterson, Laplante et al. 2009; Zhou and Huang 2010; Dunlop and Tee 2013).

This complex monitors nutrient, oxygen and energy levels and controls protein synthesis (Dodson, Darley-Usmar et al. 2013; Dunlop and Tee 2013). The mTORC1 complex regulates protein synthesis through the phosphorylation of translational machinery such as S6 Kinase and eIF4e binding proteins (Zhou and Huang 2010; Caro-Maldonado and Muñoz-Pinedo 2011). Its activity is modulated by several factors including the concentrations of amino acids (Caro-Maldonado and Muñoz-Pinedo 2011). mTORC2 contains mTOR, rapamycin-insensitive companion of mTOR (RICTOR), MLST8, and mammalian stress-activated protein kinase interacting protein 1 (mSIN1) (Sancak, Thoreen et al. 2007; Peterson, Laplante et al. 2009; Zhou and Huang 2010). This complex regulates the cytoskeleton and phosphorylates Akt, controlling metabolism and survival (Zhou and Huang 2010). Inhibition of mTOR decreases Cdc2 activity which causes cell cycle arrest (Caro-Maldonado and Muñoz-Pinedo 2011). mTOR is a known regulator of autophagy (Dodson, Darley-Usmar et al. 2013). Inhibition of mTOR induces autophagic cell death in multiple cell lines (Xie, White et al. 2013).

Rapamycin (also known as Sirolimus) is a lipophilic macrolide antibiotic (Choi, Ryter et al. 2013; Dai, Gao et al. 2013). It is an inhibitor of the mTOR protein. It has also been reported that it has anti-proliferative effects in tumours (Dai, Gao et al. 2013). Rapamycin has been shown to induce both apoptosis and autophagy in PC-2 pancreatic cancer cells. Monitoring of expression levels of p53, Bax and Beclin-1 all showed up-regulation in a dose dependent manner in response to rapamycin (Dai, Gao et al. 2013). Rapamycin also increases the expression of the autophagy proteins p62 and LC3b (Xie, Xie et al. 2013).

1.7.2.1 mTOR Responds to Nutrient Levels

When there are sufficient nutrients mTORC1 is mainly localised to lysosomal membranes. The core mTORC1 proteins are mTOR, RAPTOR (regulatory associated protein of mTOR) and mLST8 (mammalian lethal with sec-13 protein 8). The complex shows sensitivity to rapamycin. RAPTOR is required for interactions of the complex with accessory proteins such as PRAS40 and Deptor (Sancak, Thoreen et al. 2007; Peterson, Laplante et al. 2009). Phosphorylation of RAPTOR at specific locations regulates mTORC1 activity. The various phosphorylation states of RAPTOR determine substrate specificity of the mTORC1 complex and the activity of mTOR in phosphorylating the substrate (Dunlop and Tee 2013).

Under nutrient deprivation conditions mTORC1 is largely inactive, and autophagy is activated. Inactivation of mTORC1 has been demonstrated to induce autophagy (Choi, Ryter et al. 2013; Ryter, Mizumura et al. 2014). Two separate protein complexes function to produce the phagophore membrane in the initiating step of autophagy. The complexes are ULK1-ATG13-FIP200 (200 kDa focal adhesion kinase family-interacting protein) and the Beclin1-VPS34 complex. Once the membrane is formed it is elongated through two ubiquitin like systems (Dunlop and Tee 2013).

ULK1 (Atg1) is widely regarded as the most upstream component of autophagy (Choi, Ryter et al. 2013; Feng, He et al. 2014; Ryter, Mizumura et al. 2014). It can be phosphorylated at several sites, and auto-phosphorylation is required for stabilisation and enhanced activity. ULK1 has also been demonstrated to inhibit mTORC1 activity through phosphorylation of RAPTOR at multiple sites (Dunlop and Tee 2013). AMPK positively regulates autophagy through phosphorylation of ULK1 (Dunlop and Tee 2013).

1.7.2.2 PI3K

The phosphoinositide 3-kinase (PI3K) family of enzymes are responsible for regulation of many cellular processes including growth, proliferation, migration, differentiation, survival and intracellular trafficking (Molejon, Ropolo et al. 2012; Arya and White 2015). They are a family of signal transducer enzymes. They are upstream of Protein Kinase B (PKB – also known as Akt) and the mTOR pathway (Sui, Chen et al. 2013). Activation of the PI3K/Akt pathway leads to enhanced glucose uptake and glycolysis. It also shifts glucose metabolism toward biosynthesis rather than energy production (Ward and Thompson 2012).

1.7.2.3 Reactive Oxygen Species

Reactive oxygen species (ROS) regulate autophagy (Alexander, Cai et al. 2010; Dodson, Darley-Usmar et al. 2013). This is through the effect of redox on glucose metabolic pathways and mitochondrial function. Superoxide – a reactive oxygen species, levels are regulated by superoxide dismutases and this function also modulates autophagy. Hydrogen peroxide also regulates autophagy through activation of class III PI3K proteins (Dodson, Darley-Usmar et al. 2013).

Reactive oxygen species are also generated at the peroxisomes as a by-product of fatty acid ß-oxidation. However the numbers of peroxisomes must be regulated as too many or too few lead to diseases. Autophagy is involved in regulation of peroxisomes in a process called pexophagy. Upon ROS production ATM is activated, which leads to the activation of ULK1. ULK1 then inhibits mTORC1 leading to the induction of autophagy. The peroxisome specific autophagy is achieved by ATM phosphorylation of PEX5 at serine 141, leading to ubiquitinylation of PEX5 (Zhang, Tripathi et al. 2015). This ubiquitinylation is recognised by the autophagy adapter protein p62 targeting autophagosomes to peroxisomes (Zhang, Tripathi et al. 2015). Additionally, ROS leads to the inhibition of mTORC1 through the tuberous sclerosis complex 2. AMPK is activated by ATM, and then AMPK phosphorylates TSC2 at several sites. Phosphorylated TSC2 then inhibits mTORC1 leading to the induction of autophagy (Alexander, Cai et al. 2010).

1.7.3 Bcl-2 Family

A lack of nutrients also influences Bcl-2 family proteins. Autophagy has been shown to be inhibited by Bcl-2 and Bcl-Xl (Wang, Wei et al. 2012). The Bcl-2 family of proteins was demonstrated to modulate autophagy in nutrient deprivation conditions. Bcl-2 itself was shown to be up-regulated in response to nutrient deprivation (Xu, Wu et al. 2013). Several studies have shown that lack of nutrients leads to cell death through the mitochondrial apoptosis pathway. Bax has been shown to translocate to the mitochondria leading to mitochondrial permeabilisation (Wolter, Hsu et al. 1997). Furthermore, glucose withdrawal induced death can be avoided by Bcl-2 or Bcl-X_L depending on the cell line. Bad is another Bcl-2 family member that has been linked to glucose metabolism and glucose withdrawal induced cell death. Bad helps mediate mitochondrial permeabilisation. Bim and Noxa induce death in response to ER stress and thus can also be linked to nutrient deprivation because nutrient deprivation causes ER stress. This ER stress is most likely triggered by glucose or amino acid withdrawal (Caro-Maldonado and Muñoz-Pinedo 2011).

1.8 Anti-Austerity

1.8.1 Overview

Anti-austerity refers to a class of compound with the ability to selectively kill cells in the absence of nutrients while leaving cells grown with nutrients unharmed. The term in this context was coined by Esumi and colleagues in 2002 (Esumi, Izuishi et al. 2002). This strategy of targeting cancer survival under nutrient deprivation led to the discovery of several compounds with anti-austerity properties through sample screening techniques (Lu, Kunimoto et al. 2004).

As a strategy to combat cancers with high tolerances to starvation conditions such as pancreatic cancer cells, Esumi and colleagues devised a screening process to identify compounds with preferential cytotoxicity to cells in nutrient deprivation conditions (Izuishi, Kato et al. 2000). In this screening process a cell line is grown in two culture conditions: nutrient deprived - which is culture medium free of glucose, serum or amino acids or complete culture medium - such as DMEM supplemented with FBS. The cultures are then incubated with various compounds and those with preferential toxicity to cells grown in nutrient deprived medium (NDM) are identified. This screening method has the advantage of not needing prior knowledge of protein targets (Magolan and Coster 2010). However, the nature of this test means that once an anti-austerity compound is identified no other information about its activity is known.

Several compounds with anti-austerity activity have been identified to date, the most potent ones from natural products. Particular focus has been given to compounds found in traditional herbal medicines (Magolan and Coster 2010). These compounds include angelmarin, arctigenin, kigamicin D, and samsoeum among others (Esumi, Lu et

al. 2004; Lu, Kunimoto et al. 2004; Awale, Nakashima et al. 2006; Gu, Qi et al. 2012; Kim, Yim et al. 2013). Despite the fact that all of these compounds show anti-austerity properties, differing signalling pathways are observed in response to different compounds.

The effectiveness of anti-austerity compounds is measured using observed preferential toxicity values – PC_{50} values, which are calculated by comparing cell viability against a concentration curve for the compound under nutrient deprivation conditions. The compounds must also demonstrate reduced toxicity under nutrient rich conditions (Magolan and Coster 2010).

1.8.2 Known Compounds with Anti-Austerity Properties

Compounds which induce a necrotic cell death phenotype include arctigenin, kigamicin D and pyrvinium pamoate. Arctigenin is found in several plants common in Chinese herbs including *Bardanae fructus*, *Saussurea medusa*, *Arctium lappa*, and *Forsythia intermedia*. Arctigenin is a compound which has been shown to selectively induce necrotic cell death in A549 human non-small cell lung cancer cells under glucose deprivation but leave cells under normal conditions intact (Gu, Qi et al. 2012). This was accomplished by limiting mitochondrial activity and increasing the build-up of ROS. Such compounds show promise as a possible selective treatment for solid cancers, which are often poorly vascularised. (Gu, Qi et al. 2012).

It was reported that Kigamicin D blocks the activation of Akt (Lu, Kunimoto et al. 2004). Kigamicin D was discovered from a screening experiment on *Actinomycetes* culture media searching for anti-austerity compounds. It has been demonstrated to have toxicity under nutrient deprivation conditions but not under normal conditions in pancreatic, skin and colon cancer cell lines. A necrotic phenotype was observed in

response to Kigamicin D under nutrient deprivation conditions. Glucose has been indicated as the key nutrient involved in the activity of Kigamicin D (Lu, Kunimoto et al. 2004).

Pyrvinium pamoate was also reported to show selective cytotoxicity to PANC-1 cells under glucose starvation conditions. Pyrvinium pamoate is clinically used as an anthelminthic (anti-parasite medicine). It is a synthesised cyanine dye (Beck, Saavedra et al. 1959; Downey, Chong et al. 2008; Demchenko and Callis 2010). Furthermore, Akt phosphorylation at Ser473 was indicated to be essential in the execution of cell death by pyrvinium pamoate. The authors concluded that the cell death type activated in response to pyrvinium pamoate was necrosis (Esumi, Lu et al. 2004).

Anti-austerity compounds which have been shown to induce an apoptotic phenotype include Heptaoxygenated xanthones, samsoeum and rottlerin (Dibwe, Awale et al. 2013; Kim, Yim et al. 2013). However rottlerin causes an autophagic cell death phenotype when apoptosis is inhibited (Torricelli, Salvadori et al. 2012).

Heptaoxygenated xanthones – isolated from the chloroform extract of *Securidae longepedunculata* have also been demonstrated to have anti-austerity activity in the PANC-1 pancreatic cancer cell line (Dibwe, Awale et al. 2013). These compounds induced an apoptosis like cell death as monitored by the annexin V/propidium iodide stain. Additionally, this cell death response was determined to be glucose dependent. The range of activity of heptaoxygenated xanthones showed PC_{50} values of 22.8-17.4 µM (Dibwe, Awale et al. 2013).

Samsoeum has traditionally been used as a herbal remedy for sickness including cough, fever and congestion for centuries in both China and Japan and is more commonly known as *Shensuyin* in China and *Jinsoin* in Japan (Kim, Yim et al. 2013). It

was found that Samsoeum selectively killed hepatocyte cancer cells while leaving normal cells unaffected. The cells were killed through both autophagic and apoptotic cell death types. Samsoeum was reported to affect the Akt and mTOR pathways – like many of the other anti-austerity compounds mentioned. Additionally, activation of the JNK signalling pathway was found, and inhibition of JNK blocked the activity of Samsoeum. An increase in phosphorylation of AMPK was also observed. (Kim, Yim et al. 2013).

Rottlerin is another possible candidate for an anti-austerity drug, which interacts with the Akt and ERK pathways and is a PKC-delta inhibitor. Rottlerin is a natural polyphenol purified from the kamala powder (Torricelli, Salvadori et al. 2012). Rottlerin has also been shown to sensitise MCF-7 breast cancer cells to apoptosis induction. Furthermore, Rottlerin promotes autophagy. It was found that Rottlerin induced cell death without nuclear fragmentation but with extensive vacuolisation. Testing for autophagy markers showed LC3b punctuate fluorescence, indicating autophagy as well as p62/SQSTM1 sequestosome-1 autophagic clearance (Torricelli, Salvadori et al. 2012). It was demonstrated that rottlerin induced apoptotic cell death in this cell line under nutrient deprivation conditions, however in the absence of caspase-3 an autophagic phenotype was observed.

Additionally, honokiol induced apoptotic cell death and inhibited the growth of tumours, specifically in the DBTRG-05MG glioblastoma multiforme cell line (Chang, Yan et al. 2013). Honokiol is a compound isolated from the Chinese herb *Magnolia officinalis*. Interestingly, upon treatment with Honokiol both apoptotic markers such as PARP-1 cleavage and Bcl-X_L cleavage and autophagy markers including increased Beclin-1 expression and LC3b puncta were detected. These findings highlight the difficulties in determining how any given cell line will respond to a particular anti-austerity agent (Chang, Yan et al. 2013).

Grandifloracin is yet another potential anti-austerity drug. This compound was isolated from the stem of the *Uvaria dac* plant (Awale, Ueda et al. 2012). It was shown to induce cell death in several pancreatic cancer cell lines including PANC-1 under nutrient deprivation conditions. It was found that the cell death type induced was not apoptotic, and was most likely autophagic as monitored by LC3b puncta fluorescence. The PC_{50} value observed for Grandifloracin was 14.5 µM. Grandifloracin was reported to act by inhibition of Akt and mTOR activity (Ueda, Athikomkulchai et al. 2013).

1.8.3 Angelmarin

In 2010, the Coster group synthesised an anti-austerity compound angelmarin (shown in Figure 1.11)(Magolan, Adams et al. 2011). Angelmarin is a natural product isolated from *Angelica pubescens* by Awale, Kadota and colleagues (Awale, Nakashima et al. 2006). The initial screening process for anti-austerity compounds was conducted on plant extracts from plants common in Japanese Kampo medicine (Awale, Nakashima et al. 2006). They found it to have selective toxicity to PANC-1 cells in nutrient deprived medium. The initial experiment to find anti-austerity compounds involved testing many compounds against pancreatic cancers under serum deprivation and normal conditions. Compounds which showed selective inhibition of cancer growth under nutrient deprivation but left cells under normal conditions unharmed were further examined (Magolan, Adams et al. 2011). This experiment isolated the natural product from which angelmarin is derived. Additionally, inhibition of glycolysis in recurring neuroblastoma using the glycolysis inhibitor 3-BrOP induced apoptotic cell death in the tumours. (Levy, Zage et al. 2012).

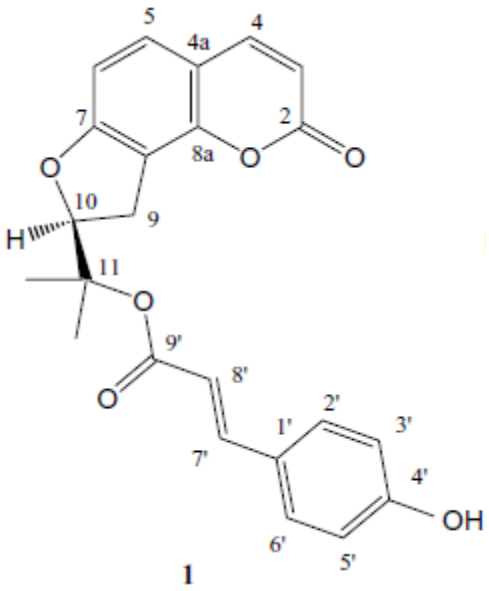

Figure 1.11: Structure of angelmarin as determined by IR spectrometry and NMR techniques by Awale and colleagues in 2006 (Awale, Nakashima et al. 2006). Image from (Magolan, Adams et al. 2011), used with permission, 2015).

1.8.4 Signalling pathways in response to angelmarin

Currently identified anti-austerity agents despite all targeting tolerance to nutrient deprivation, differ widely in the type of cell death observed. From the current information on these compounds it is exceedingly difficult to determine what pathways will be activated in response to any given compound. Therefore initial investigations of anti-austerity compounds should try to determine what type of cell death is activated. Following this, there are several signalling pathways which have been identified to respond to multiple anti-austerity compounds. Akt signalling pathways and mTOR both have been shown to respond to several compounds. Other cell stress response pathways should also be examined including PI3k and AMPK.

1.9 Previous Findings in the laboratory

Exploration of the effects of ionising radiation on BL30 cell lines have shown that following exposure to 20Gy of ionising radiation 100% of BL30A cells had undergone apoptosis, whereas BL30K cells had resistance to this level of irradiation (Waterhouse, Kumar et al. 1996). Furthermore an increase in ceramide in the irradiation sensitive cell line BL30A was found following treatment with ionising radiation but this increase was not present in the BL30K cell line (Michael, Lavin et al. 1997).

A separate study investigated the activities of synthesised caspase inhibitors. Preliminary tests indicated an unusual effectiveness of the caspase-8 inhibitor IETD-fmk at preventing apoptosis following gamma irradiation of the BL30A cell line. This finding was unusual because caspase-9 is the initiator caspase in the intrinsic apoptosis pathway which is normally activated in response to DNA damage. However activation of caspase-8 in response to DNA damage has been reported in several instances (Jones, Ganeshaguru et al. 2001; Afshar, Jelluma et al. 2006).

DNA damage induced by etoposide was also investigated in preliminary studies in our laboratory. It was found that 100% of BL30A cells had undergone apoptosis by 6 hours post treatment with etoposide, however delayed apoptosis was observed in BL30K cells. In the BL30K cells no apoptosis was visualised at 12 hours post treatment, while 50% apoptosis was observed at 24 hours (Lauren Finney and Dianne Watters, Unpublished). Additionally, the caspase-9 inhibitor LEHD-fmk was not effective at inhibiting DNA damage induced apoptosis.

In summary the preliminary findings have indicated a delay or resistance of the BL30K cell line to DNA damage induced apoptosis whereas the BL30A cell line remains sensitive. Also, caspase-8 has been implicated as the caspase responsible for apoptosis following DNA damage in BL30A cells. The mechanisms of resistance of the BL30K cell line to DNA damage induced apoptosis remain unknown.

1.10 Rationale, Project Aims and Overview

1.10.1 Rationale

Expanding the collective knowledge of cell death signalling pathways which are less well known provides avenues for drug discovery in targeted treatment of cancer. Additionally, use of drugs which target cancer cell tolerance to nutrient deprivation may provide an alternative treatment strategy for cancers which are highly resistant to current anti-cancer treatments, such as pancreatic cancer.

Cancers are continually evolving and develop multiple ways of surviving treatments or stresses (Greaves and Maley 2012). Therefore the need to develop new ways to trigger cell death remains high. Two approaches to examining cell death in cancer were chosen. Firstly, examining a pathway of cell death to find new targets may yield valuable insights for development of future cancer treatment strategies. Specifically, the unusual pathway of apoptosis in BL30A and BL30K cells was examined for the potential of finding new therapeutic targets. Of particular interest is how the BL30K cell line is resistant to triggering of this cell death pathway. Secondly, examining a new approach to cancer treatment using the novel anti-austerity approach on untested drugs may also prove to be a valuable tool. The anti-austerity compound angelmarin was tested for its potential to selectively kill PANC-1 pancreatic cancer cells under nutrient deprivation conditions. These two cancers were selected to demonstrate that each provides options for innovation in cancer treatments.

The cell lines were selected for their suitability in testing the different approaches. Preliminary data indicated that the Burkitt's lymphoma cell line BL30A may utilize an unusual pathway of apoptosis, and the related BL30K cell line was resistant to this pathway. The pancreatic cancer cell line PANC-1 has been shown in the literature to possess extraordinary tolerance to lack of nutrients and as such is ideal for use in testing anti-austerity compounds (Awale, Ueda et al. 2012; Ueda, Athikomkulchai et al. 2013). Both cancers provide opportunities to explore and develop novel cancer treatments.

1.10.2 Project aims and overview

This thesis examines evasion of different pathways of cell death in several cancer cell lines. It has examined the unusual pathway of apoptosis induction in the BL30A cell line, as well as the mechanisms of resistance to this pathway in the BL30K cell line. It also explored the potential of the anti-austerity compound angelmarin and its ability to selectively induce cell death in pancreatic cancer under nutrient deficient conditions. The aims that this thesis addresses are as follows:

(1) Investigate how the BL30A cell line undergoes apoptosis in response to DNA damage

The Burkitt's lymphoma cell line BL30A was examined for its unusual pathway of cell death in response to DNA damage. Previous results pointed to caspase-8 as an initiator of apoptosis in response to DNA damage. Chapter 3 explores the factors contributing to the cell death phenotype observed in BL30A. The activity of caspases and the proteins and complexes involved in the execution of apoptosis in response to DNA damage will be examined. The hypothesis to be tested is that an unusual pathway of apoptosis signalling which is dependent on caspase-8 is activated in response to DNA damage in BL30A cells.

(2) Investigate what factors contribute to the resistance of the BL30K cell line to apoptosis induced by DNA damage

The Burkitt's lymphoma cell line BL30K demonstrates resistance to the pathway of cell death shown in its sister cell line BL30A. Chapter 4 examines the proteins and pathways involved in providing this resistance to apoptosis induction by DNA damage. Expression of proteins with protective effects will be examined as well as expression differences between the apoptosis resistant BL30K cell line and the apoptosis sensitive BL30A cell line. The hypothesis to be tested is that the BL30K cell line has resistance to the pathway of apoptosis of the BL30A cells.

(3) Investigate the mechanisms of action of the anti-austerity compound Angelmarin in PANC-1 pancreatic cancer cells

The pancreatic cell line PANC-1 was selected to study the effects of the anti-austerity compound angelmarin. This cell line has been used in several studies to examine anti-austerity properties as it demonstrates extreme tolerance to nutrient withdrawal (Izuishi, Kato et al. 2000; Awale, Ueda et al. 2012). Chapter 5 explores the types of cell death involved, as well as the proteins which are important in the execution of cell death in response to angelmarin. The hypothesis of this chapter is that angelmarin selectively induces cell death in PANC-1 cells grown under nutrient deprivation while leaving cells grown under normal conditions unaffected. Additionally protective factors and influences on pancreatic cancer's sensitivity to angelmarin are examined.

Chapter 2

Materials and Methods

2.1 Reagents and Antibodies

2.1.1 Materials and Reagents

Table 2.1 lists the suppliers of chemicals and products used in this thesis. The majority of general laboratory supplies were from Chem Supply (Gillman, South Australia) and were of analytical grade or higher.

Table 2.1: Materials and Reagents

Company and Location	**Products**
BDH (Poole, United Kingdom)	Ammonium persulphate (APS)
Boehringer Roche (Mannheim, Germany)	Aprotinin, leupeptin, bovine serum albumin (BSA), DAPI, WST-1 cell proliferation assay
Bio-Rad Laboratories (Hercules, California, USA)	DC protein estimation, acrylamide/bis, N,N,N,N-Tetramethyl-Ethylenediamine (TEMED)
Gibco BRL-Invitrogen (Gaithersburg, Maryland, USA)	Dulbecco's modified Eagle medium (DMEM), penicillin/streptomycin, trypsin-EDTA, Glutamax, MEM non-essential amino acids, MEM amino acids, Foetal Bovine Serum, Roswell Park Memorial Institute (RPMI) 1640
PIERCE (Rockford, IL, USA)	Supersignal WestPico Chemiluminescent Detection Substrate
Sigma (St Louis, Missouri, USA)	2-mercaptoethanol, Ponceau-S, N-acetyl cysteine (NAC), sodium orthovanadate, phenylmethylsulfonyl fluoride, sodium pyrophosphate, Dithiothreitol (DTT), dimethyl sulphoxide (DMSO), trypan blue, bromophenol blue, ammonium persulphate, Etoposide, LEHD-fmk, PMSF, DEVD-fmk, IETD-fmk, Neocarzinostatin
Chem Supply (Gillman, South Australia, Australia)	EDTA, EGTA, Glycerol
MERCK (Darmstadt, Germany)	Glycine
Dynal (Invitrogen Dynal AS) (Ullernchausseen, Oslo, Norway)	M280 streptavidin beads
ICN Biomedicals (Aurora, Ohio, USA)	Nonidet P40 (NP-40)

Calbiochem (San Diego, California, USA)	Pansorbin cells, PD98059
GE Healthcare (Piscataway, New Jersey, USA)	Protein G-Sepharose fast flow beads
Millipore Corporation (Temecula, California, USA)	PVDF membranes
Tocris Bioscience (Ellisville, Missouri, USA)	SB203580
MP Biomedicals (Aurora, Ohio, USA)	bVAD-fmk
Research Organics (Cleveland, Ohio, USA)	CHAPS (3-[(3-Cholamidopropyl)dimethylammonio]-1-propanesulfonate)

2.1.2 Antibodies

Table 2.2 lists suppliers of antibodies used in production of this thesis. For each antibody used the dilution was optimised, however most were in the range of 1:500 to 1:2000.

Pathscan Western cocktail II is a signalling protein antibody mixture containing antibodies to phospho p90 RSK, phospho p53, phospho p38 MAPK, phospho S6 ribosomal protein and eIF4e as a loading control. eIF4e has been used by several groups as a loading control (Iwamaru, Iwado et al. 2007; Lorsch 2007; Mercado-Feliciano, Pharmacology et al. 2008; Mantwill, Naumann et al. 2013) and was used in the antibody cocktail as a loading control which does not conflict with the molecular weights of other components.

Table 2.2: Antibodies

Company and Location	Antibodies
Sigma-Aldrich (Missouri, USA)	ß-actin, ß-tubulin, secondary antibodies (FITC, TRITC, HRP conjugate)
Cell Signaling (Danvers, Massachusetts)	Bax, Caspase-2, Caspase-8, Cleaved Caspase-8, Caspase-9, Bad, Beclin-1, Pathscan Western cocktail 2, phospho-Bad, Bcl-2, LC3b, phospho-4eBP1
Roche (Penzberg, Upper Bavaria, Germany)	PARP, Bid
Santa Cruz (Dallas, Texas, USA)	Caspase-8, Caspase-9, Cytochrome c, FADD, Fas (Apo-1-1), Fas (c20), Golgi marker
BD Pharmingen (San Jose, California, USA)	Caspase-8, p53
Millipore (Billerica, Massachusetts, USA)	Fas CH-11 activating antibody

2.2 Cell Culture

For the growth and maintenance of cell lines in culture incubation was conducted using a humidified Hera Cell incubator (Heraeus, Hanau, Germany) at 37^{o}C and 5% partial pressure of CO_2. All subculture of cell lines was conducted in a Class II Biological Safety Cabinet. Adherent cells were washed with sterile phosphate-buffered saline (PBS) and then incubated at 37^{o}C and 5% CO_2 for 1-2 minutes with trypsin in PBS to detach cells from the flask surface. After the cells had detached, new medium was added and cells were seeded to the desired densities. All cell culture was conducted using standard plastic culture-ware such as 25cm^2 and 75cm^2 flasks or 24 well plates (TPP, Trasadingen, Switzerland).

2.2.1 Cell Lines

The BL30A and BL30K cell lines were previously referred to as BL30 and BL30(s) respectively (Khanna, Wie et al. 1996). The BL30A and BL30K Burkitt's lymphoma cell lines were maintained in RPMI 1640 medium (with L-glutamine) supplemented with 100 units/mL penicillin and 100 μg/mL streptomycin with 20% and 10% FBS (Foetal

Bovine Serum) respectively. The JHP lymphoblastoid cell line derived from Epstein-Barr virus transformation of human lymphocytes (Good, Lavin et al. 1978) was maintained in RPMI 1640 medium supplemented with 10% FBS. Cells were incubated at 37^{o}C and 5% partial pressure of CO_2.

The pancreatic adinocarcinoma cancer cell line PANC-1 was maintained in advanced DMEM medium (with L-glutamine) supplemented with 5% FBS and 100 units/mL penicillin and 100µg/mL streptomycin. Cells were incubated at 37^{o}C and 5% partial pressure of CO_2.

2.2.2 Preparations of frozen stocks for long term storage and preparation from frozen stocks

To maintain a stock of frozen cell lines for long term storage cells grown in culture were routinely harvested. Once a flask of cells had reached subconfluence they were harvested using trypsin (adherent cells only) and re-suspended in appropriate cell culture medium containing 10% FBS and 10% dimethyl sulfoxide (DMSO) as a cryopreservant at 4^{o}C. Cells were then placed in a Mr Frosty (Nalgene, Nalge Nunc, Denmark) container using isopropanol to provide a slow and even temperature decrease over time and placed in a -80^{o}C freezer overnight. Cell vials were then transferred to a liquid nitrogen dewar for long term storage.

To retrieve cells frozen in liquid nitrogen vials were quickly thawed using a 37^{o}C water bath. The cells were then suspended in appropriate culture medium for the cell line and centrifuged at 200g for 5 minutes to remove the DMSO cryopreservant. The supernatant was removed and the cell pellet was re-suspended in appropriate culture medium. Cells were then grown in the incubator as outlined above.

2.2.3 Apoptosis Induction

The apoptosis induction stimuli being investigated in this study was etoposide. Etoposide is a topoisomerase II inhibitor, which causes breaks in DNA (Slevin 1991; Corbett and Osheroff 1993). DNA topoisomerase II catalyses the relaxation of supercoiled DNA by covalently binding and temporarily cleaving both strands of the DNA followed by re-ligation. Topoisomerase II inhibitors stabilise the covalent intermediate which causes a decrease in re-ligation and consequently breaks in the DNA (Corbett and Osheroff 1993; Felix 2001). Etoposide is a well established agent used in the study of DNA damage in many cell lines including epithelial cell lines (Bortner, Oldenburg et al. 1995), small cell lung cancer, testicular cancer and Kaposi cells (Aisner and Lee 1991); Ramos Burkitt's lymphoma cells (Galluzzi, Brenner et al. 2008); HeLa cells (Kohler, Anguissola et al. 2008); Daudi and Raji cells (Simoes Magluta, Vasconcelos et al. 2009); colon carcinoma cells and Jurkat cells (Micheau, Solary et al. 1999). An etoposide stock solution of 68 mM was prepared in DMSO and aliquoted and stored at -20^{o}C. Etoposide was used at a final concentration 68 µM in medium containing approximately 10^{6} cells per mL. In samples without the addition of etoposide DMSO was added in equivalent volumes as a control. Previous studies in the laboratory have indicated that 68 µM of etoposide caused approximately 80% apoptosis by 8 hours in BL30A cells (Lauren Finney, unpublished) and others have reported similar numbers in Burkitt's lymphoma cell lines (Zhao, Song et al. 1998; Vrana, Bieszczad et al. 2002). This concentration of etoposide was selected to effectively induce apoptosis in a reasonable time frame for experiments to be performed.

2.2.4 Nutrient Deprivation

To examine the cellular responses to nutrient deprivation cells were grown under nutrient deprivation conditions. Following growth of cells to subconfluence PANC-1 cells were washed twice in PBS to remove nutrients from culture medium and then PBS containing calcium and magnesium and supplemented with MEM vitamin solution (Life Technologies) was added.

2.2.5 Treatment with Angelmarin

To investigate the effects of angelmarin, the drug was added to live cells grown in different media. Unless otherwise specified, angelmarin was added to a final concentration of 7.5 µM. Angelmarin was prepared as a stock solution of 10 mM in DMSO. In experiments, the control (or untreated) group was always incubated with an amount of DMSO equivalent to the sample with the highest amount of solvent.

2.3 Cellular Assays

2.3.1 Trypan Blue Exclusion Assay

Cell viability was assessed using the trypan blue exclusion assay. Live cells exclude the dye as their cell membrane is intact and actively restricts entry into the cells whereas dead cells – or those which have lost their membrane integrity permit the dye in and are thus stained blue. In this assay cells are incubated in 0.8 mM trypan blue solution in PBS for 10 minutes at 37^{o}C and then visualised using an Eclipse TS100 light microscope (Nikon, Japan). The number of unstained cells excluding trypan blue indicated the viable cell population. Experiments were repeated three times and conducted in duplicate.

2.3.2 WST-1 Cell Proliferation Assay

The WST-1 cell proliferation assay was used to monitor cell growth. The assay is based on the reduction of the tetrazolium salt to soluble formazan by electron transport across the plasma membrane of dividing cells. The shift in colour was then assayed using a plate reader at 450 nm wavelength.

2.3.3 Resazurin Cell Survival Assay

Cell viability was also assessed using the Resazurin (alamar blue) cell viability assay. This assay measures the metabolic capacity of cells as an indicator of cell viability. Viable cells reduce resazurin to resorufin, which is highly fluorescent (Bueno, Villegas et al. 2002). In this assay cells were incubated for 2 hours (1-6 hours recommended) in culture conditions with the addition of 10µL of 0.01% w/v resazurin per well (100µL total/well) in a 96 well microtiter plate. The plate was then read in a plate reader using the fluorescence wavelengths of 530-570 nm excitation and 590-620 nm emission. Higher values indicate more viable cells.

2.3.4 Caspase Activity Assay

A caspase activity assay was used to determine when caspases are activated in response to stimuli. Peptide AFC (7-amino-4-trifluoromethyl coumarin) conjugates are fluorigenic substrates cleaved after a specific peptide sequence (e.g. DEVD-afc). Once the AFC is cleaved from the peptide, free AFC fluoresces and can be detected by excitation at 400 nm and emission at 505 nm. In this assay 10 µg of cell lysate per sample from etoposide time courses or treatment with angelmarin was diluted in caspase assay buffer (100 mM HEPES pH 7.5, 20% glycerol v/v, 0.5 mM EDTA, 3.3 mM DTT). Appropriate AFC conjugated peptide caspase substrate was added to a final concentration of 40µM. The peptide sequences were DEVD-afc, IETD-afc and LEHD-afc for caspases-3, -8 and -9, respectively. Samples were incubated at 37^{o}C for 30 minutes then fluorescence was measured using a plate reader. Further readings were made at 1 hour, 4 hours and 24 hours. The protocol was adapted from the protocol outlined by Zapata and colleagues (Zapata, Takahashi et al. 1998).

2.4 Protein Extraction

2.4.1 Whole Cell Lysate

Protein lysates were extracted from cells for use in experiments. Adherent cells undergoing exponential growth were scraped with a cell scraper (TPP, Switzerland) from the flask surface and transferred to a 10 mL centrifuge tube. Suspension cells were simply transferred to a 10 mL centrifuge tube. The cells were then centrifuged at 200g and 4^{o}C for 5 minutes. The cell pellets were re-suspended in PBS and centrifuged at 200g and 4^{o}C for 5 minutes. The cell pellet was then re-suspended in whole cell lysis buffer (50 mM Tris-HCl, pH 7.4, 120 mM sodium chloride, 10 mM sodium fluoride, 200 µM sodium orthovanadate, 1 mM phenylmethylsulfonyl fluoride, 0.4% Nonidet 40 (v/v) (ICN Biomedicals Inc., Aurora, Ohio, USA), and protease inhibitors. Alternatively the RIPA cell lysis buffer (20 mM Tris-HCl, pH 7.4, 150 mM sodium chloride, 1 mM EDTA, 1 mM EGTA, 2.5 mM sodium pyrophosphate, 1% triton x100 (v/v), 1 mM phenylmethylsulfonyl fluoride, 1 mM ß-glycerophosphate, 1 mM sodium orthovanadate and protease inhibitors) was used . Cells were incubated at 4^{o}C for 20 minutes. Samples were then centrifuged at 16000g at 4^{o}C for 15 minutes to pellet debris. The supernatant was removed and protein estimation was conducted as outlined in section 2.4.3. Aliquots were then stored at -80^{o}C until required.

2.4.2 Immunoprecipitation

Adherent cells undergoing exponential growth were scraped with a cell scraper (TPP, Switzerland) from the flask surface and transferred to a 10 mL centrifuge tube. Suspension cells were simply transferred to a 10 mL centrifuge tube. The cells were then centrifuged at 200g and 4^{o}C for 5 minutes. The cell pellets were re-suspended in PBS and centrifuged at 200g and 4^{o}C for 5 minutes. The cell pellet was then re-suspended in universal immunoprecipitation buffer (UIB) (50 mM Tris-HCl, pH 7.4, 150 mM sodium chloride, 0.2% Triton-X100, 0.3% Nonidet 40 (v/v), 2 mM EDTA, 2 mM EGTA, 25 mM sodium fluoride, 25 mM ß–glycerophosphate, 200 µM sodium orthovanadate, 1 mM phenylmethylsulfonyl fluoride, 1 mM dithiothreitol, and

protease inhibitors. Cells were incubated at 4°C for 20 minutes. Samples were then centrifuged at 16000g at 4°C for 15 minutes to pellet debris. The supernatant was removed and protein estimation was conducted. 0.5-2 mg of protein was incubated for 30 minutes using a rotator in 30 µL of Protein-A coated pansorbin cells (Calbiochem, Merck, Darmstadt, Germany) that had been washed with UIB three times. Samples were then centrifuged at 16000g at 4°C for 1 minute to remove the pansorbin cells which were used to remove the immunoglobulin heavy chains by binding the F_c region. The supernatant was transferred to a clean tube and the immunoprecipitating antibody was added at a concentration of 1 µg/mL. 30 µL of protein G-Sepharose beads were used to sequester the antibody protein complex by rotating overnight at 4°C. Samples were then washed in freshly prepared UIB by centrifugation at 16000g at 4°C for 1 minute to pellet protein the G-Sepharose and protein-antibody complex and re-suspended in UIB several times. The supernatant was removed and the beads were re-suspended in loading buffer for polyacrylamide gel electrophoresis.

2.4.2.1 Alternate Immunoprecipitation protocol

This protocol was employed as an additional confirmation of the presence or absence of target proteins found previously in section 2.4.2. Samples of cells were obtained at specific time points and lysis was performed using RIPA lysis buffer. 50µL of Protein G Sepharose fast flow beads per sample were pre-prepared by washing three times in NT-80 buffer (20 mM Tris-HCl pH 7.4, 80 mM NaCl) by centrifugation at 200g for 3 minutes at 4°C followed by aspiration of supernatant. To avoid damaging the beads pipetting was done using a p200 pipette with 5 mm of the pipette tip cut off. To pre-clear the protein samples 1 mg of lysate per sample was incubated with Protein G Sepharose beads for 15 minutes at room temperature. The pre-cleared lysates (supernatant) were then transferred to a clean tube and incubated with primary antibody overnight at the manufacturers recommended dilution. Alternatively, control samples were incubated with animal appropriate pre-immune serum. The protein conjugated to primary antibody was then transferred onto more pre-prepared Protein G Sepharose fast flow beads and incubated for 2 hours at 4°C. The beads were then washed twice in solution c (50 mM Tris-HCl pH 7.4, 150 mM NaCl, 0.2% Triton X-100)

by centrifugation at 200g and aspiration of supernatant. The beads were then washed three times in NT-80 buffer, followed by a final wash in PBS before storage (at -80^{o}C) or analysis.

2.4.2.2 Immunoprecipitate – mass spectrometry

To identify protein interactions with proteins of interest an immunoprecipitate was paired with mass spectrometry analysis. The immunoprecipitate was prepared as outlined in section 2.4.2.1 and then sent for analysis. This work was undertaken at APAF (Australian Proteome Analysis Facility) in Sydney, Australia, the infrastructure provided by the Australian Government through the National Collaborative Research Infrastructure Strategy (NCRIS).

2.4.3 Protein Estimation

To assess the concentrations of protein in samples the BioRad DC protein assay was used. A serial dilution of bovine serum albumin in the lysis buffer used was prepared as a standard. The assay was applied to the samples as per the manufacturer's instructions. Samples were then compared to the standard curve once read using a Thermo Max micro plate reader (Molecular Devices) using SOFTmax Pro v5 software. Samples were diluted and test re-run if outside the concentration range. Values for protein concentrations in samples were then calculated in mg/mL.

2.4.4 Subcellular Fractionation

Following etoposide treatment cells were washed in isotonic sucrose buffer (ISB) (250 mM sucrose, 10 mM HEPES pH 7.5, 10 mM KCl, 1.5 mM $MgCl_2$, 1 mM EDTA, 1 mM EGTA) and incubated for 1 minute in ISB plus 0.05% digitonin. Samples were then centrifuged at 900g to extract a crude cytoplasmic fraction. The pellet was re-suspended in ISB plus 0.5% Triton X-100 for 10 minutes and then centrifuged at 1000g to extract a mitochondrial fraction. This protocol was adapted from those described by

Foucher and colleagues and Hide and colleagues (Foucher, Papadopoulou et al. 2006; Hide, Ritleng et al. 2008).

2.5 Western Blotting

2.5.1 SDS-PAGE

SDS-PAGE was used to examine the expression of proteins in samples under different conditions. SDS-PAGE was performed according to the method of Laemmli (Laemmli 1970). Following determination of protein concentration using the BioRad DC assay, 50-100µg of protein sample was denatured by adding loading buffer (62.5 mM Tris-HCl pH 6.8, 2% sodium dodecyl sulphate (v/v), 10% glycerol (v/v), 5% ß-mercaptoethanol (v/v) and 0.0025% bromophenol blue (v/v)) and heating at 95^{o}C for 5 minutes. A separating SDS polyacrylamide gel of appropriate percentage between 5-15% (e.g. 10%) was prepared and cast in the gel apparatus (BioRad Mini Protean 3). The separating gels contained 375 mM Tris-HCl pH 8.8, 0.1% SDS (v/v), 0.05% ammonium persulphate (w/v), 0.1% TEMED (v/v) and ranged from 5%-15% acrylamide/bis. Saturated n-butyl alcohol was added on top to ensure a level interface surface. Once the gel had set the n-butyl alcohol was washed off using electrode buffer (25 mM Tris-HCl pH 8.3, 192 mM glycine, 0.1% SDS (v/v)). The 4% stacking gel was then prepared and added on top of the separating gel with a well comb inserted. The stacking gel consisted of 125 mM Tris-HCl pH 6.8, 0.1% SDS, 4% acrylamide/bis (v/v), 0.05% ammonium persulphate (w/v) and 0.05% TEMED (v/v). Between 20-100µg of each protein sample was denatured by adding loading buffer (62.5 mM Tris-HCl pH 6.8, 2% sodium dodecyl sulphate (v/v), 10% glycerol (v/v), 5% ß-mercaptoethanol (v/v) and 0.0025% bromophenol blue (v/v)) and heating at 95^{o}C for 5 minutes. The denatured samples were then loaded into the wells in 1x sample buffer. Any empty wells were filled with sample buffer. The gel apparatus was then filled with electrode buffer and the gel was run at 30mA per gel using a BioRad power pack. Electrophoresis was stopped once the dye front ran off the edge of the gel. The molecular weight marker pre-stained protein ladder plus SM1811 (Fermentas, Waltham, Massachusetts, USA) was used for immunoblot analysis.

2.5.2 Western Transfer to Membrane

Following SDS-PAGE proteins were transferred to a 0.45µm Immobilon-P polyvinylidene fluoride (PVDF) (Millipore Corporation, Billerica, MA, USA) microporous membrane. PVDF membranes were prepared by soaking in methanol for 20 seconds, followed by rinsing in MilliQ water for 5 minutes. The membranes were then equilibrated by soaking in transfer buffer (50 mM Tris-HCl, 40 mM glycine, 0.1% SDS, 20% methanol (v/v)) for 5 minutes. The membrane and gel were loaded into a cassette between blotting paper. Proteins were transferred using Western blotting apparatus (BioRad) containing transfer buffer and run at 100 Volts at 4^{o}C for 1-2 hours. The membrane was then removed and proteins were visualised by staining with 0.2% Ponceau-S diluted in 3% acetic acid. The stain was removed by washing several times in MilliQ filtered water. The membranes were then blocked in 1% bovine serum albumin overnight at 4^{o}C. The membranes were then washed three times for a total of 30 minutes in PBS containing Tween-20 and incubated overnight with primary antibodies in PBS containing 1% BSA. Primary antibodies (as listed in Table 2.2) were used at concentrations ranging from 1:500-1:5000, however unless otherwise stated were used at 1:1000 dilution. Membranes were then washed three times for a total of 30 minutes with PBS containing Tween-20 and incubated with secondary antibody conjugated to horse radish peroxidase for 2 hours at room temperature or overnight at 4^{o}C. Secondary antibodies (listed in Table 2.2) were used at concentrations ranging from 1:2000-1:20000, however unless otherwise stated were used at 1:10000 dilution. Again, membranes were washed three times for a total of 30 minutes and antibody-protein complexes were visualised.

2.5.3 Chemiluminescence

In order to detect the proteins separated by Western blotting the chemiluminescence of horse radish peroxidase (HRP) was detected using WestPico Supersignal enhanced chemiluminescence reagent (Pierce Supersignal) according to manufacturer's instructions. The primary antibody concentrations used generally ranged from 1/500 to 1/5000. The secondary antibody concentrations generally ranged from 1/2000 to

1/20000. Following Western blotting, proteins marked with antibodies were visualised on membranes using the chemiluminescence imaging system LAS-3000 (Fuji Photo Film Company, Ltd, Tokyo, Japan) instrument equipped with a cooled CCD camera for light detection. The images were captured using Science Lab 2001 Image Reader and analysed with Image Gauge v4.0 software (Fuji Photo Film Company, Ltd, Tokyo, Japan).

2.5.4 Immunoblotting – Fluorescence

Specialised Western blotting membranes suitable for fluorescence were used to obtain images for antibodies which were ineffective in chemiluminescence. The membranes used were Immun-Blot Low Fluorescence PVDF Membrane (Bio-Rad Laboratories, Hercules, California, USA). As with chemiluminescence membranes, the fluorescence membranes were probed with primary antibodies, however the secondary antibodies used were fluorescent antibodies such as FITC or TRITC conjugates. Fluorescence on the membranes was visualised using a FLA-5000 fluorescence imager (Fuji Photo Film Company, Ltd, Tokyo, Japan).

2.5.5 Native PAGE

Native PAGE was used as an initial assessment of the presence of a high molecular weight complex as a possibility for caspase-8 activation. Native PAGE is a method similar to SDS-PAGE however is conducted in the absence of reducing agents or SDS. Because of the mild conditions used proteins in complexes can often be visualised as opposed to SDS-PAGE where all protein complexes are denatured (Wittig and Schagger 2005). Western blotting gels and buffers were prepared in the absence of SDS and following suspension in sample buffer 50 µg of samples were added to each lane of the gel (5%). The gel was run at 30mA until the dye front had reached the end of the gel and the proteins were transferred to a PVDF membrane. The membrane was stained with coomassie blue 250 for 2 hours at room temperature under agitation and then de-stained for visualisation using acetic acid and methanol initially at (30% v/v acetic

acid, 70% v/v methanol) and then (7% v/v acetic acid, 40% v/v methanol). Bands were then photographed using the Geliance 600 UV transilluminator (Perkin Elmer, Waltham, Massachusetts, U.S.) with an EtBr/UV filter at an exposure time of 80ms.

2.5.6 Apical Caspase Trapping

In order to determine the first activated caspase in response to etoposide treatment in BL30 A cells, a biotinylated form of the pan-caspase inhibitor zVAD-fmk was used. In this assay the biotinylated caspase inhibitor was added to cells growing in culture medium prior to treatment which would lead to caspase activation. The inhibitor acts as a substitute substrate which irreversibly binds the caspase, thus stopping further activity. Once the apical caspase is bound it can be isolated using the biotin signal and examined through Western blotting techniques (Tu, McStay et al. 2006).

2.5.7 Quantification of Western Blots

Following each Western blot, band intensities of proteins of interest along with their paired loading control intensities were measured using GelQuant.net software. The intensities of the loading control bands were divided by the highest intensity band from the loading controls to obtain a ratio for each column. The intensities of the bands from proteins of interest were then divided by the loading control ratio to obtain normalised values for proteins of interest. Normalised values were then scaled so that control (0 hour) samples were represented as unity. These values were then graphed with the values from the other replicate experiments and statistical analyses were performed using Graphpad Prizm software.

2.6 Inhibitor Assays

2.6.1 Caspase Inhibitors

Caspase inhibitors were employed to assess the effects of their inhibition on cellular processes. The caspase inhibitors used were peptide sequences linked to a fluoromethylketone group. The peptide sequence is the substrate cleavage site for the

specific caspase however once the caspase attempts to cleave the peptide it becomes irreversibly bound to the FMK group and thus cannot cleave other substrates. The irreversible caspase inhibitors were used at 50 μM and levels of apoptosis were monitored using DAPI (4',6-diamidino-2-phenylindole) staining. The selective caspase-8, -9 and -3 inhibitors IETD-fmk, LEHD-fmk and DEVD-fmk were added to cells at the same time as addition of etoposide to determine their effect on apoptosis induction by etoposide. The caspase inhibitors were prepared as 50 mM stock solutions in DMSO. In experiments, the control (or untreated) group was always incubated with an amount of DMSO equivalent to the sample with the highest amount of solvent.

2.6.2 Other Inhibitors

Several inhibitors of cellular functions were used to assess the activity of etoposide on Burkitt's lymphoma cells or to assess the activity of angelmarin on PANC-1 cells. These inhibitors include necrostatin-1 – an inhibitor of RIP1 activity, pifithrin-α and pifithrin-μ – both of which are p53 inhibitors, PD98059 an inhibitor of MEK in the ERK/MAPK signalling pathway, SB203580 an inhibitor of p38 MAPK, chloroquine – a small molecule which disrupts lysosomal function, hydroxypropyl ß-cyclodextrin (HPBCD) – which disrupts lipid rafts, and N-acetyl cysteine (NAC) – a reactive oxygen species scavenger. The inhibitors were prepared as stock solutions in DMSO. In experiments, the control (or untreated) group was always incubated with an amount of DMSO equivalent to the sample with the highest amount of solvent.

2.7 Microscopy and fluorescence immunohistochemistry

2.7.1 Cell Fixation

Fixation of cells for later staining or antibody labelling was done using paraformaldehyde. Cells were fixed to coverslips in 24 well plates using 4% paraformaldehyde in PBS. For cells growing in suspension, 500μL of medium containing approximately 10^6 cells per mL was transferred to the well and centrifuged at 200g for 5 minutes at room temperature. Adherent cells were grown on the 24

plate containing coverslips. The supernatant was then carefully removed from the side of the wells and 200µL of PBS containing 4% paraformaldehyde was added. The plate was then centrifuged at 200g for 5 minutes at room temperature and then left at room temperature for 20 minutes for fixation. The supernatant was then removed and approximately 1 mL of PBS was carefully added. Samples were stored at 4^{o}C shortly until staining and visualisation.

2.7.2 DAPI Staining

The nuclear stain 4',6-diamidino-2-phenylindole (DAPI) was used to visualise the nuclei of cells and thus assess the percentages of apoptosis as determined by nuclear fragmentation. Following fixation, DAPI was added to a concentration of 0.5µg/mL in PBS and incubated for 30 minutes at room temperature in a container protected from light. Coverslips were then thoroughly washed with PBS and mounted on slides using a small drop of anti-fade fluorescent mounting medium (1 mg/mL p-phenylenediamine, 90% glycerol in PBS pH 8.0). Cells were then viewed using a fluorescent microscope. Six random fields of cells were viewed and counted and photographed at 200x or 400x magnification. The ratio of normal to apoptotic cells was then calculated.

2.7.3 Visualisation – Brightfield

Brightfield microscopy was used for quick visualisation of cell appearance and growth. It was also used for cell counting using the hemocytometer. A TS100 light microscope (Nikon, Japan) was used at 100x to 400x magnification.

2.7.4 Visualisation – Immuno-fluorescence

Following fixation and staining or labelling with primary and secondary antibodies coverslips were transferred to slides and mounted using a small drop of anti-fade fluorescent mounting medium (1 mg/mL p-phenylenediamine, 90% glycerol in PBS pH 8.0). Slides of cells stained with DAPI or fluorescently stained antibodies were viewed

using a Nikon Eclipse E800 fluorescence microscope. Images were obtained using the V++ precision digital imaging system 4.0 software by Digital Optics. This software was also used to create merged images for comparisons.

2.8 Flow cytometry

Flow cytometry was conducted to determine the levels of surface Fas receptors. For each sample 2.5 mL of cells (at approximately $1x10^6$ cells/mL) were used. For each sample 2 mL of cells were transferred to a 10 mL tube and centrifuged at 200g for 5 minutes at room temperature. The supernatant was removed and the pellet was resuspended in 0.5 mL of 4% paraformaldehyde in PBS. The samples were then incubated at 37^{o}C for 10 minutes, followed by chilling at 4^{o}C for 1 minute. Samples were then centrifuged at 200g at 4^{o}C and washed in 2 mL of 0.5% BSA in PBS. The pellet was resuspended in 100µL of 0.5% BSA in PBS and incubated at room temperature for 10 minutes. Rabbit anti-Fas (C-20) antibody was added at a 1/100 dilution and incubated for 1 hour at room temperature. The samples were then washed as above in 0.5% BSA in PBS. Secondary antibody (FITC anti rabbit IgG) was then added and incubated for 30 minutes at room temperature. The samples were then washed in 0.5% BSA in PBS and two times and resuspended in 0.5 mL PBS. The cells were then analysed by flow cytometry in a Becton Dickinson FACS Calibur instrument using a 488 nm laser for detection of fluorescence emission. 20000 events were accumulated per sample. FACS analysis was performed with the assistance of Dr. Bernadette Bellette.

2.9 Software for Data Analysis

Statistical analysis was performed using Graphpad Prism v3 by Graphpad Software Incorporated (San Diego, California, USA). Graphpad Prism v3 was also used to create graphs of data sets. Software used for quantification of Western blots was GelQuant.NET software provided by biochemlabsolutions.com. Flow cytometric data was analysed with the help of Dr. Bernadette Bellette using Summit v4.3 software by Becton Dickinson.

Chapter 3

Apoptosis Pathways of BL30A Cells

3.1 Introduction

3.1.1 Burkitt's Lymphoma Cell Lines

BL30A and BL30K cell lines were selected as both are derived from a singular parent cell line, and BL30A remains sensitive to apoptosis, whereas BL30K has developed resistance (Waterhouse, Kumar et al. 1996). After 8 hours of treatment with 20Gy of ionising radiation 80-90% of the BL30A cells had undergone apoptosis however less than 5% of the BL30K cells had undergone apoptosis. Burkitt's lymphoma is a common cancer type, especially in Africa. This is because of the link between Epstein Barr Virus (EBV) and the lymphoma. This virus greatly increases the risk of developing Burkitt's lymphoma, assumedly through the damage of DNA in the host cells. As such these lymphomas are classed as either EBV+ or EBV- (Ferry 2006). However the BL30 cell lines are derived from an EBV negative BL biopsy. BL cell lines are classed in groups based on their appearance of growth in cell suspension. The BL30A cell line is classed as group I whereas the BL30K cell line is classed as group II/III. Group I BL cells are sensitive to apoptosis and tend to grow in single cell suspension, whereas group II/III cells are resistant to apoptosis and tend to grow in clumps (Khanna, Wie et al. 1996). Furthermore, BL cell lines with wildtype p53 are usually more susceptible to apoptosis induction whereas mutant p53 expression is usually associated with apoptosis resistance (Khanna, Wie et al. 1996). Khanna et al (1996) also reported that BL30A cells have a mutant p53 allele and a deletion of the other p53 allele (Farrell, Allan et al. 1991; Khanna, Wie et al. 1996). BL30K cells have been reported to have 2 mutant p53 alleles (Khanna, Wie et al. 1996). Owing to their origins (one parent cell line) they make an excellent model for the study of apoptosis resistance. For comparison with the experiments in this chapter Figure 3.1 shows a time course of etoposide treatment in BL30A cells at a concentration of 68 μM. Approximately 75-80% of cells are shown to be apoptotic by 6 hours post treatment.

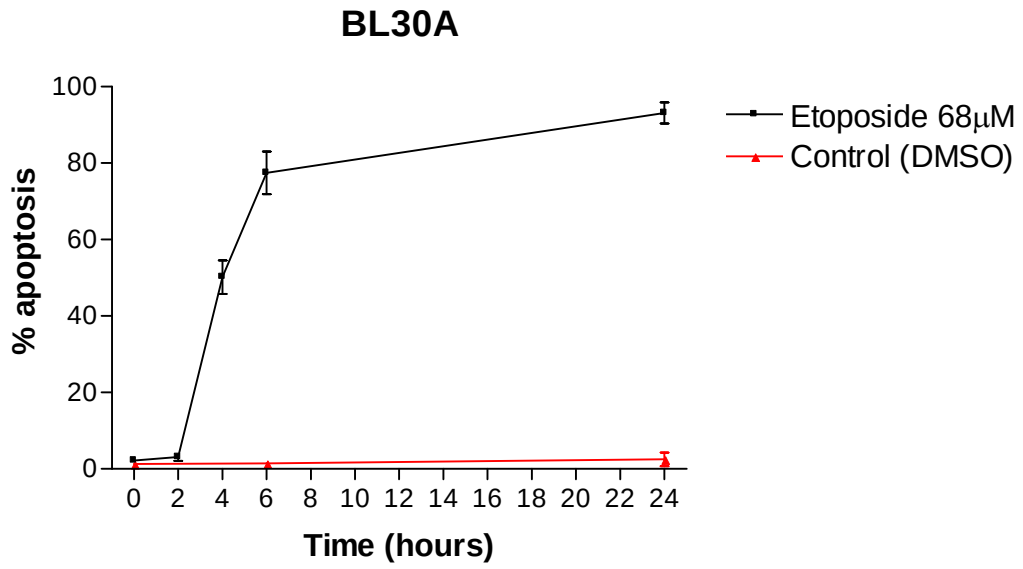

Figure 3.1: Apoptosis induction by etoposide in BL30A cells. Time course of apoptosis by etoposide induction (68μM) in BL30A cells was monitored by DAPI staining. Results expressed are the mean ± SEM of three replicate experiments. Percentages of apoptosis were obtained by counting six fields of cells under 200X magnification and dividing the number of apoptotic cells by the total number of cells.

3.2 Investigations of caspases

3.2.1 Inhibition of caspase-8 by IETD-fmk was effective at preventing apoptosis

Caspase-8 is the initiator caspase associated with the extrinsic apoptotic pathway. However, previous work in our laboratory has indicated that caspase-8 is required for apoptosis to proceed following DNA damage in this cell line (Lauren Finney, Unpublished). To confirm that inhibition of caspase-8 and not other caspases prevents apoptosis following DNA damage, the irreversible caspase inhibitors IETD-fmk (fluoro-methyl ketone), LEHD-fmk and DEVD-fmk, specific for caspases -8, -9 and -3 respectively were used. The inhibitors were added individually with etoposide to induce apoptosis. Inhibition of caspase-8 by IETD-fmk was the most effective at preventing apoptosis, whereas inhibiting caspases-9 or -3 with LEHD-fmk and DEVD-fmk respectively was less effective. BL30A cells incubated with etoposide and IETD-fmk showed levels of apoptosis similar to the untreated control, whereas cells incubated with etoposide and LEHD-fmk showed levels of apoptosis similar to samples treated with etoposide only (Figure 3.2).

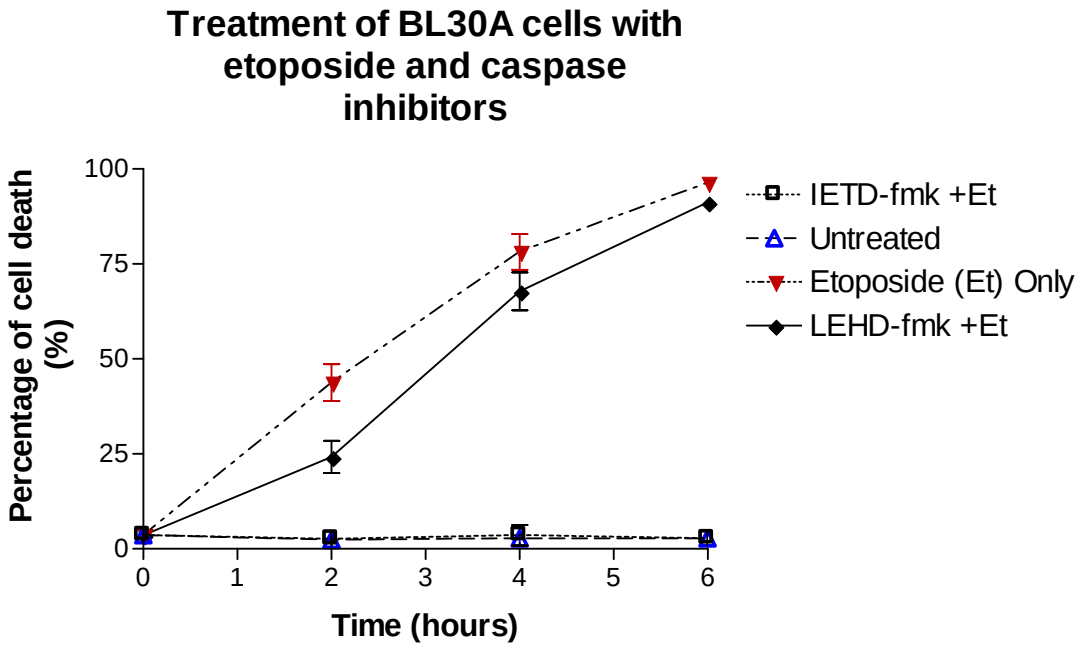

Figure 3.2: Treatment of BL30A cells with etoposide and caspase inhibitors. BL30A cells were treated with etoposide alone (68 µM) or etoposide with either IETD-fmk (20 µM) or LEHD-fmk (20 µM) and levels of cell death were monitored using DAPI nuclear staining at the indicated time points. Percentages of apoptosis were obtained by counting six fields of cells under 200X magnification and dividing the number of apoptotic cells over total number of cells. Results expressed are the mean ± SEM of three replicate experiments.

3.2.2 Caspase-8 and caspase-9 are activated nearly simultaneously following DNA damage

Experiments were then performed to test the time course of activation of caspases-8 and -9 using a fluorimetric assay. In this assay caspase substrates containing 7-amino-4-trifluoromethyl coumarin (AFC) were used to assess the activity of caspases in whole cell lysates at time points following treatment with etoposide to induce DNA damage. These AFC substrates fluoresce once cleaved by their respective caspases giving an indication of caspase activity. Caspase-8 activity was detected at approximately 2 hours 15 minutes post treatment and caspase-9 activity was also detected at 2 hours 15 minutes post treatment (Figure 3.3). Activation of the executioner caspase-3 was also detected at 2 hours 30 minutes post treatment, however at far higher levels than the initiator caspases (Figure 3.3).

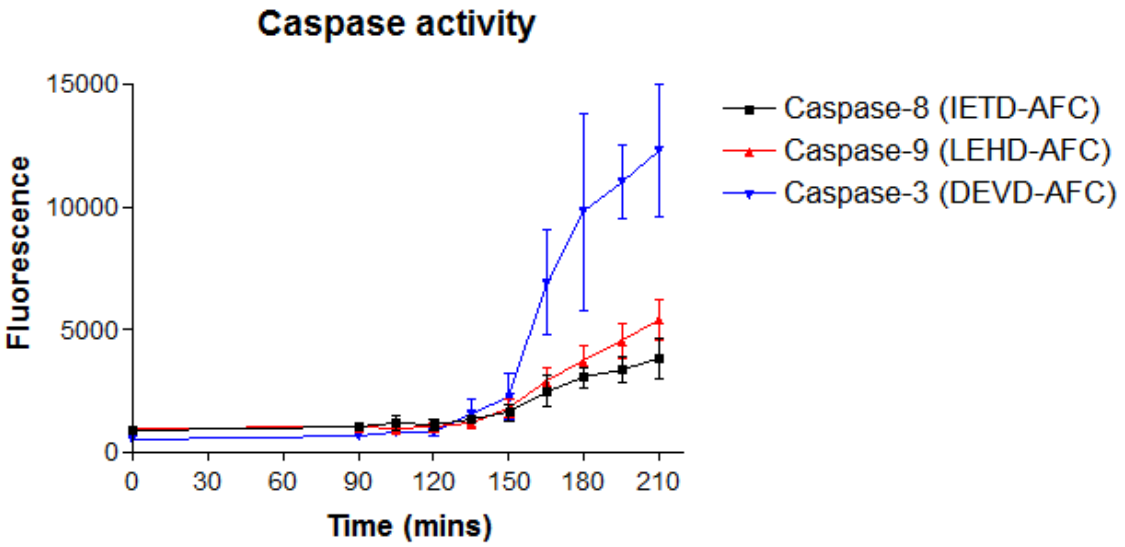

Figure 3.3: Caspase activity assay in BL30A cells. The caspase-8 substrate IETD-AFC (IETD-7-amino-4-trifluoromethyl coumarin) (4 µM), caspase-9 substrate (LEHD-AFC) (4 µM) and the caspase-3 substrate (DEVD-AFC) (4 µM) were used on whole cell lysates from the time points indicated following etoposide (68 µM) treatment. The released AFC concentration – indicating caspase activity - was estimated from a standard curve. Results expressed are the mean ± SEM of three replicate experiments.

Caspases are activated by cleavage, therefore Western blotting of lysates from etoposide time courses can be used to monitor caspase activation. Western blotting of caspase-8 provides further evidence of caspase activation by detection of the fully cleaved caspase fragments. However this was only detectible at 3 hours post treatment (Figure 3.4). This was likely because cleavage detection by Western blotting is a less sensitive method to detect small amounts of caspase activation than the caspase activity assay. The full length form of caspase-8 is seen at approximately 60 kDa at levels decreasing with time, however the fully cleaved form was first seen at approximately 15 kDa at 3 hours post etoposide treatment (Figure 3.4).

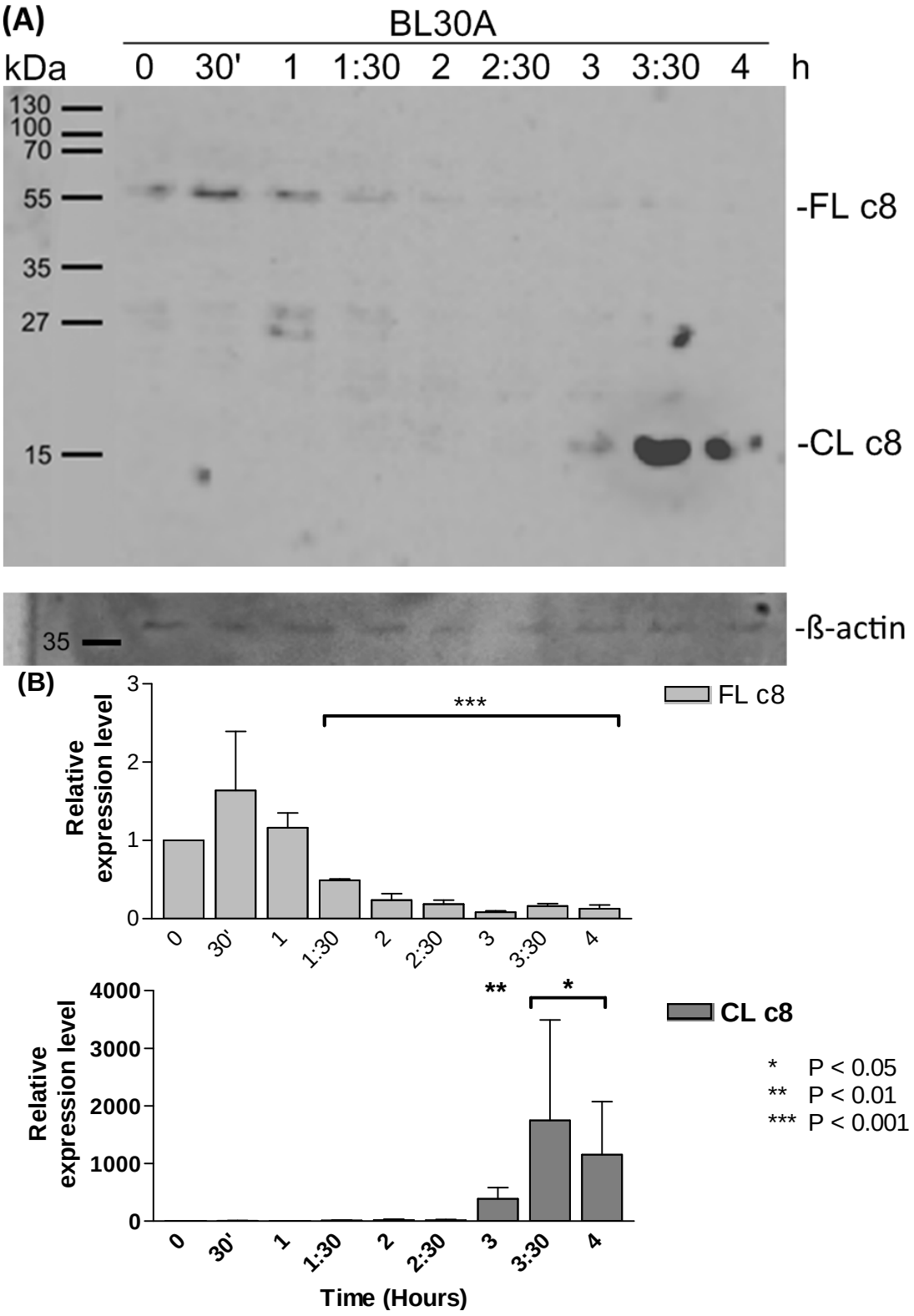

Figure 3.4: Western blotting of caspase-8 in BL30A cells. **(A)** Western blot of BL30A cells at different times after etoposide (68 µM) treatment probed with anti-caspase-8 antibody (Cell Signaling). The blot was re-probed with ß-actin (Sigma) as a loading control. FL c8 – full length caspase-8, CL c8 – cleaved caspase-8. The blot is representative of three biological replicates. **(B)** Quantified histogram of the expressed proteins normalised to ß-actin. Results expressed are the mean ± SEM. Asterisks indicate significant differences from unity.

Caspase-2 was also monitored using Western blotting. Caspase-2, as mentioned in the introduction is involved in apoptosis induction primarily in response to heat shock, however has also been demonstrated to be activated in response to DNA damage. Western blotting of caspase-2 revealed levels of full length caspase-2 decreasing at 4 hours (Figure 3.5). Also at 4 hours cleaved caspase-2 was first detectable, indicating a later activation time than caspase-8.

Additionally, caspase-9 was monitored using Western blotting. Caspase-9 is the caspase primarily responsible for the execution of the intrinsic pathway of apoptosis. Western blotting of caspase-9 showed levels of full length caspase-9 increased at 4 hours (Figure 3.6). Also at 4 hours cleaved caspase-9 levels increased dramatically, indicating activation of caspase-9.

Eukaryotic translation initiation factor 4E (eIF4E) is a protein which functions in translation to bind the mRNA cap and deliver it to the ribosome (Anthony, Carter et al. 1996). eIF4E is activated by mTORC1. This is done by mTORC1 phosphorylating 4EBP-1 causing it to release eIF4e activating it (Zhou and Huang 2010). mTORC1 is a protein complex which functions as a nutrient, energy and redox sensor in addition to controlling protein synthesis (Zhou and Huang 2010). eIF4e has been used as a housekeeping protein to show equal loading by several groups (Iwamaru, Iwado et al. 2007; Lorsch 2007; Mercado-Feliciano, Pharmacology et al. 2008; Mantwill, Naumann et al. 2013).

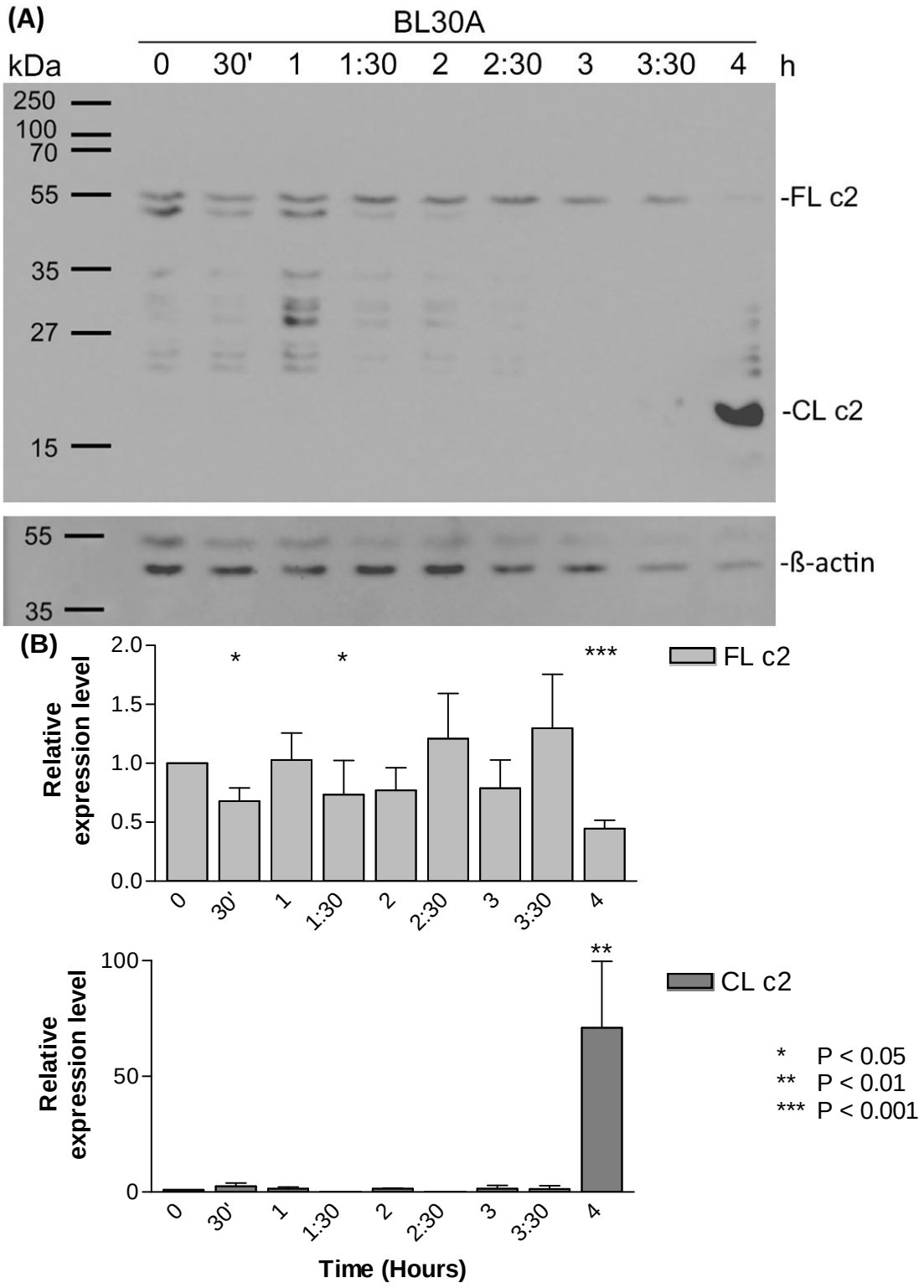

Figure 3.5: Western blotting of caspase-2 in BL30A cells. **(A)** Western blot of BL30A cells at different times after etoposide (68 µM) treatment probed with anti-caspase-2 antibody (Cell Signaling). The blot was re-probed with ß-actin (Sigma) as a loading control. FL c2 – full length caspase-2, CL – cleaved caspase-2. The blot is representative of three biological replicates. **(B)** Quantified histogram of the expressed proteins normalised to ß-actin. Results expressed are the mean ± SEM. Asterisks indicate significant differences from unity.

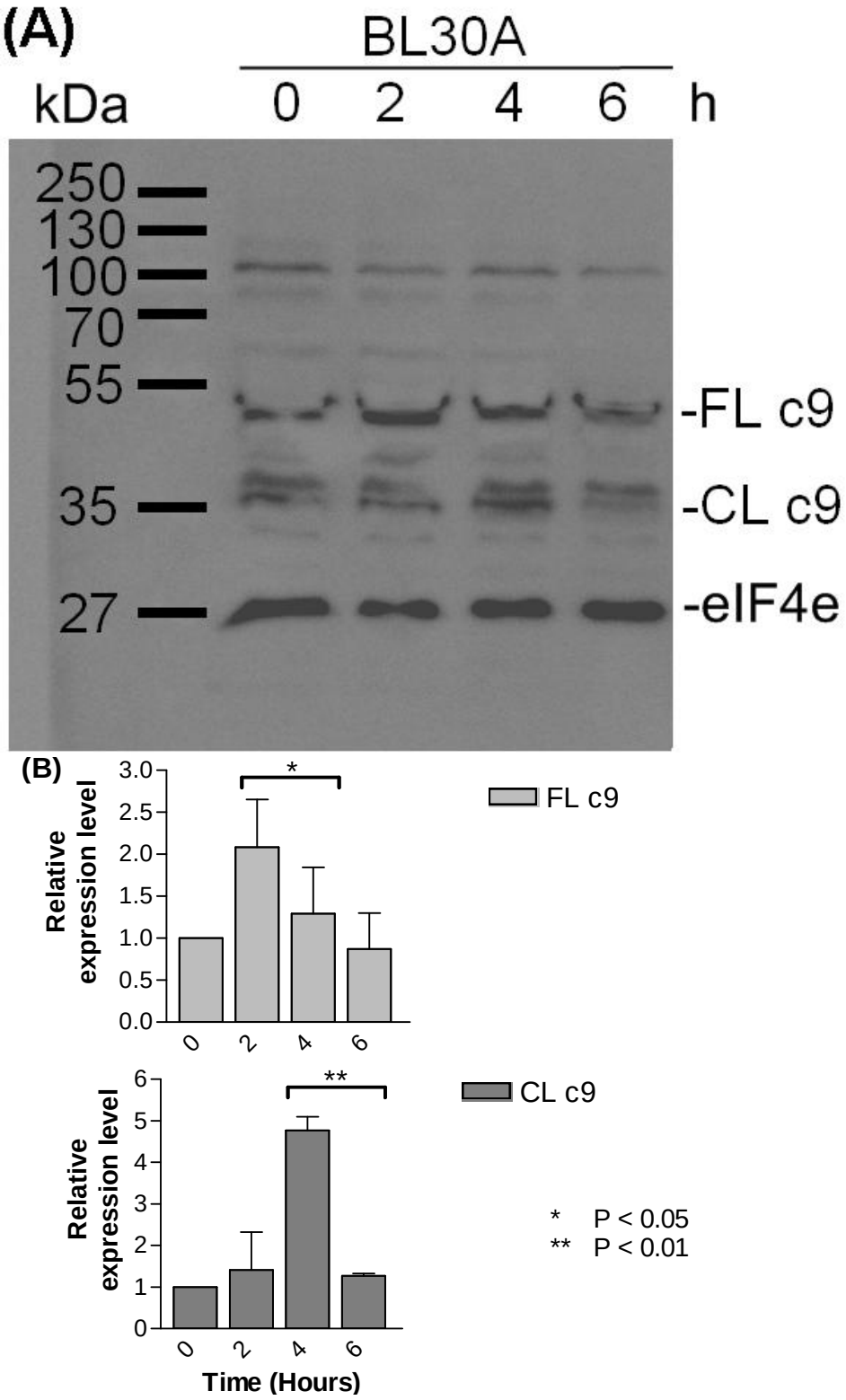

Figure 3.6: Western blotting of caspase-9 in BL30A cells. **(A)** Western blot of BL30A cells at different times after etoposide (68 µM) treatment probed with anti-caspase-9 antibody (Cell Signaling). FL c9 – full length caspase-9, CL c9 – cleaved caspase-9. eIF4e is shown as a loading control. The blot is representative of three biological replicates. **(B)** Quantified histogram of the expressed proteins normalised to eif4e. Results expressed are the mean ± SEM. Asterisks indicate significant differences from unity.

3.2.3 Trapping of the apical caspase using biotinylated pan-caspase inhibitor

To provide further evidence for which caspase is the first activated caspase following DNA damage in BL30A cells the biotinylated pan-caspase inhibitor bVAD-fmk was used. In this experiment cells are pre-treated with bVAD-fmk and then treated with apoptosis inducing stimuli. The first caspase to be activated then attempts to cleave the inhibitor and becomes irreversibly bound to it. The biotin tag is then used to isolate the caspase for identification by Western blotting. Upon probing the blot with anti-caspase-8 the partially cleaved form was visible, indicating that caspase-8 was the apical caspase. It should be noted that this experiment is very difficult to perform and many researchers had not been able to replicate the experimental findings from D. Green's laboratory (Pop, Salvesen et al. 2008). Bands of approximately 45 kDa were detected using this protocol which is the approximate molecular weight of partially cleaved caspase-8 (Figure 3.7). This provides evidence that caspase-8 was the first activated caspase in response to DNA damage. Furthermore, the biotinylated pan-caspase inhibition experiment failed to trap caspase-9 (Figure 3.8) providing evidence that caspase-9 is not the initiator caspase.

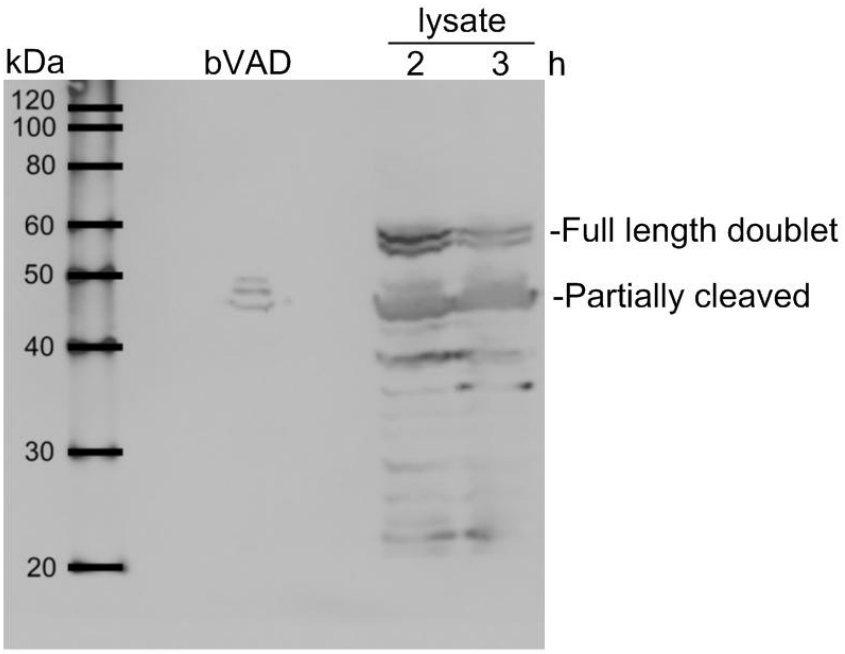

Figure 3.7: Apical caspase trapping experiment in BL30A cells – caspase-8. The biotinylated apical caspase inhibitor bVAD-fmk was used at a concentration of 50 µM to isolate the apical caspase following etoposide treatment (68 µM). The blot was probed with mouse anti caspase-8 (BD Pharmingen). bVAD is biotinylated VAD-fmk, lysate samples from etoposide treatment are shown for comparison. The blot is representative of two biological replicates.

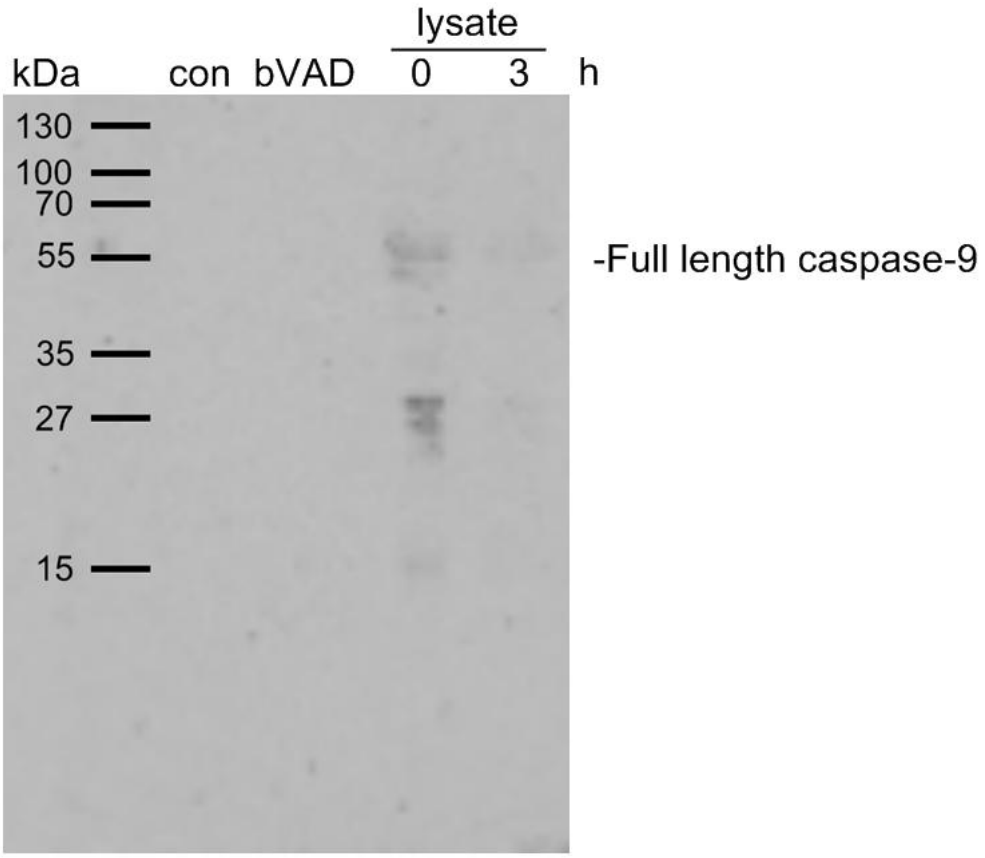

Figure 3.8: Apical caspase trapping experiment in BL30A cells – caspase-9. The biotinylated apical caspase inhibitor bVAD-fmk was used at a concentration of 50 µM to isolate the apical caspase following etoposide treatment (68 µM). The blot was probed with mouse anti caspase-9 (Santa Cruz). bVAD is biotinylated VAD-fmk, lysate samples from etoposide treatment are shown for comparison. The blot is representative of two biological replicates.

3.3 Investigation of p53 and mitochondrial involvement

3.3.1 Mitochondrial membrane permeabilisation was not evident until 3 hours post treatment

Caspase-9 is activated upon permeabilisation of the outer mitochondrial membrane, releasing cytochrome c which forms the apoptosome – the caspase-9 activating platform (Aslan and Thomas 2009). Additional evidence that indirectly supports caspase-8 as the primary caspase over caspase-9 was that mitochondrial outer membrane permeabilisation is not detectible by Western blotting of lysates separated

by subcellular fractionation until later times. Digitonin was used to selectively permeabilise the plasma membrane in a protocol originally devised by Fiskum and colleagues (Fiskum, Craig et al. 1980). The protocol used was derived from those described by Foucher and colleages and Hide and colleagues (Foucher, Papadopoulou et al. 2006; Hide, Ritleng et al. 2008). Cytochrome c release was not detected until 3 hours post etoposide treatment (Figure 3.9). A band for cytochrome c was seen at approximately 15 kDa. Decreasing levels are shown in the mitochondrial fraction at 3 hours, at the same time cytochrome c was first observed in the cytoplasm. Probing of the blot with ß-actin showed bands only in the cytoplasmic fractions at equal levels, as would be expected.

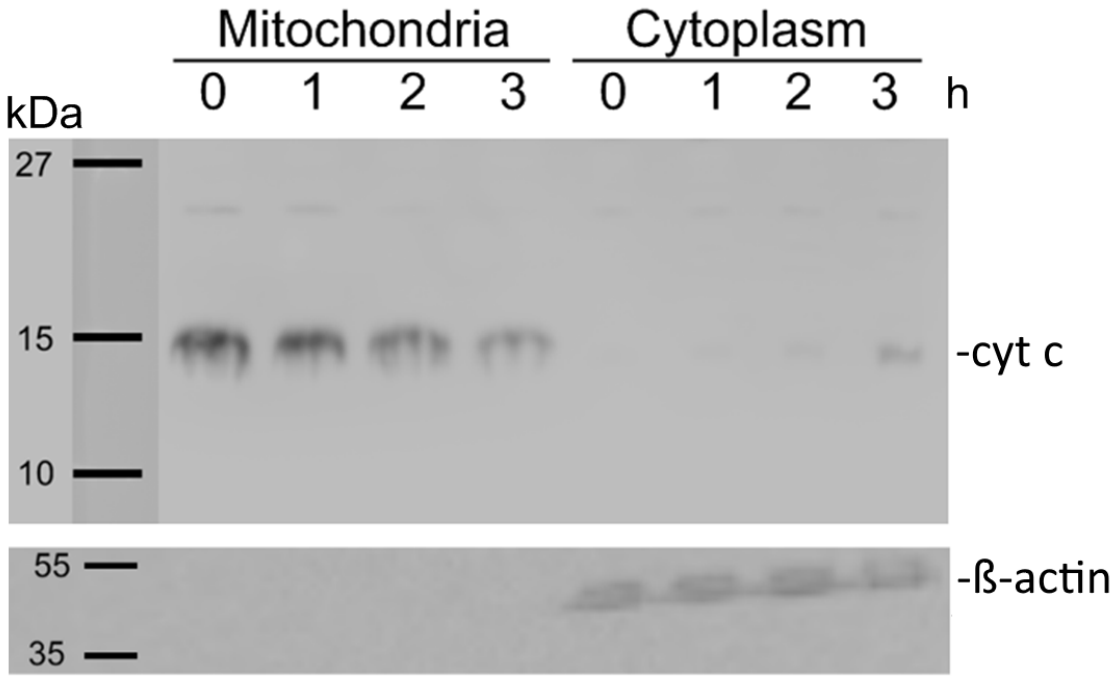

Figure 3.9: Cytochrome c release in BL30A cells. Western blot of lysates from etoposide (68 µM) time course in BL30A separated into crude cytoplasmic and mitochondrial fragments by subcellular fractionation and probed with anti-Cytochrome c antibody (Santa Cruz). The blot was re-probed with ß-actin (Sigma) as a loading control. The blot is representative of three biological replicates.

The mitochondria are major generators of reactive oxygen species. Reactive oxygen species have been shown to influence cell survival in response to DNA damage (Huang, Fang et al. 2003; Kobashigawa, Kashino et al. 2015). N-acetyl cysteine (NAC) is a reactive oxygen species scavenger which is used to deplete ROS. However treatment with etoposide and NAC showed no difference with etoposide only (Figure 3.10). This suggested that ROS are not necessary for induction of apoptosis in BL30A cells.

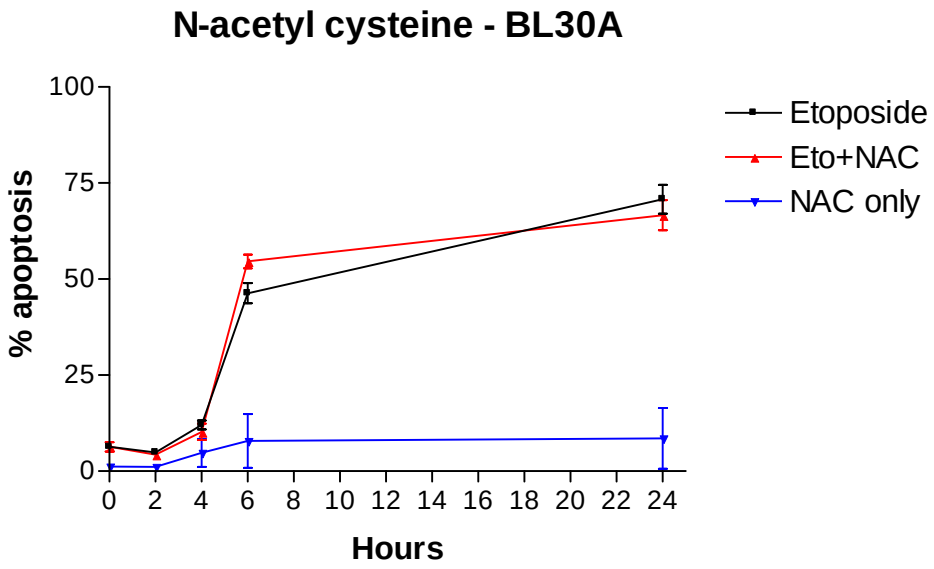

Figure 3.10: Depletion of ROS in BL30A cells using N-acetyl cysteine. Percentages of apoptotic cell death as assessed by DAPI nuclear staining at the indicated times after treatment with etoposide (68 µM) alone, etoposide plus N-acetyl cysteine (5 mM), or NAC alone. Percentages of apoptosis were obtained by counting six fields of cells under 200X magnification and dividing the number of apoptotic cells over total number of cells. Results expressed are the mean ± SEM of three replicate experiments.

3.3.2 p53 transcription appears inactive

Further examination of mitochondrial outer membrane permeabilisation led to the investigation of Bax levels. Bax is a Bcl-2 family protein which facilitates mitochondrial permeabilisation. Additionally Bax is a p53 transcriptionally regulated protein (Chipuk, Kuwana et al. 2004) which is up-regulated upon stress signals (Hickman, Moroni et al. 2002). p53 is largely responsible for regulating the cellular response to DNA damage. Using Western blotting it was found that Bax protein levels were unchanged up to 6 hours post treatment (Figure 3.11). This provided indirect evidence that p53 was not transcriptionally active following DNA damage.

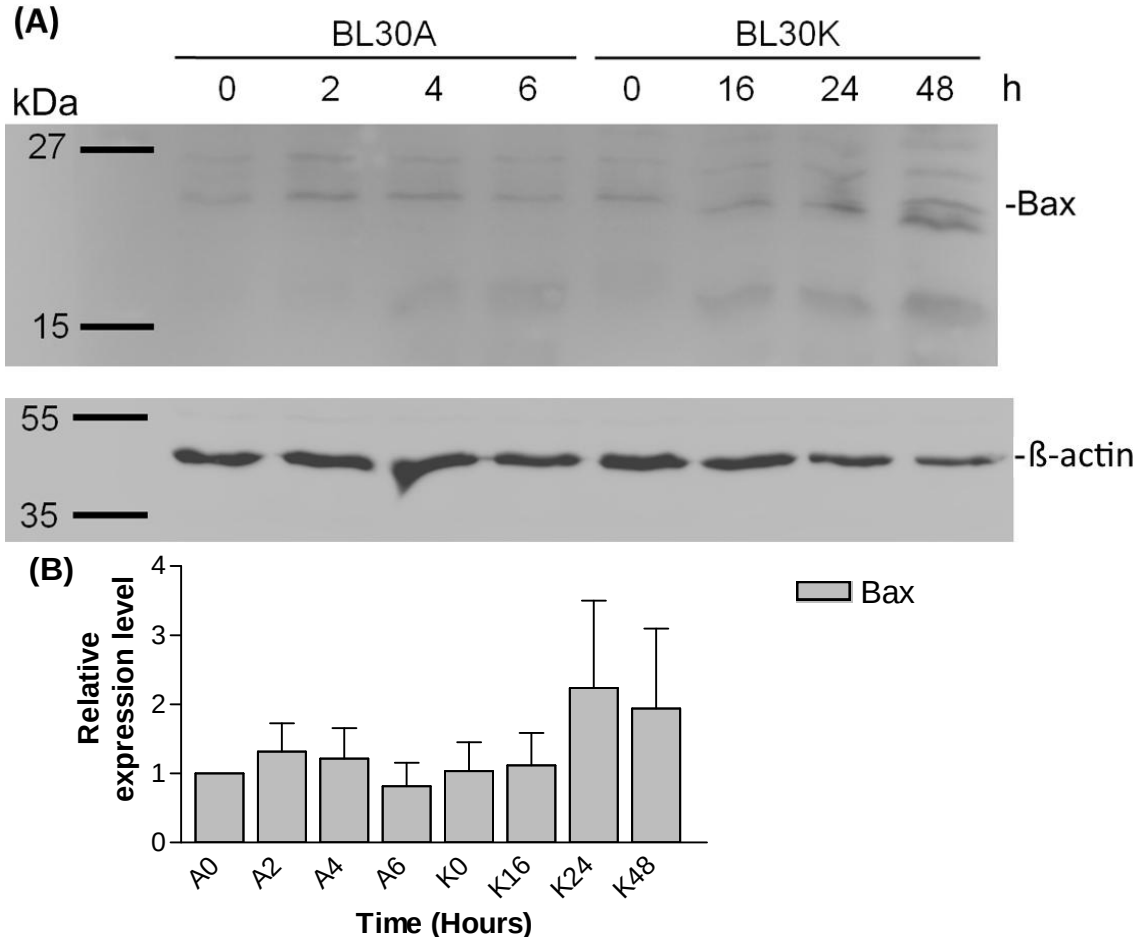

Figure 3.11: Bax protein levels in BL30A and BL30K cells. **(A)** Western blot of BL30A and BL30K cells at different times after etoposide (68 µM) treatment probed with anti-Bax antibody (Cell Signaling). The blot was re-probed with anti-ß-actin (Sigma) as a loading control. The blot is representative of three biological replicates. **(B)** Quantified histogram of the expressed proteins normalised to ß-actin. Results expressed are the mean ± SEM. No statistical significance was observed between samples.

3.3.3 p53 inhibitors indicate a mitochondrial role for p53

p53 has been shown to interact with various Bcl-2 family members, which govern mitochondrial permeabilisation (Green and Kroemer 2009). To investigate the role of p53 in apoptosis induction in the BL30A cell line, selective inhibitors of the cytoplasmic and transcriptional activity of p53 were used to determine if it was required for this apoptotic response. There are two types of pifithrin (**p fi**fty-**thr**ee **in**hibitor): Pifithrin-α inhibits the transcriptional activity of p53, and pifithrin-μ inhibits the mitochondrial interactions of p53 (Strom, Sathe et al. 2006). Pifithrin-α has also been demonstrated to protect mice from side effects of cancer therapy (Komarov, Komarova et al. 1999). Pifithrin-μ has been shown to block interaction between p53 and Bcl-XL (Hagn, Klein et al. 2009). Pifithrin-α was ineffective at preventing apoptosis, however pifithrin-μ was effective at preventing etoposide induced apoptosis in this cell line. Pifithrin-μ treatment together with etoposide treatment resulted in only baseline levels of apoptosis, whereas treatment with pifithrin-α and etoposide showed a large increase in apoptosis levels (Figure 3.12). These results suggest that the mitochondrial activity of p53 was important in this pathway of apoptosis, however transcriptional activity of p53 was not required.

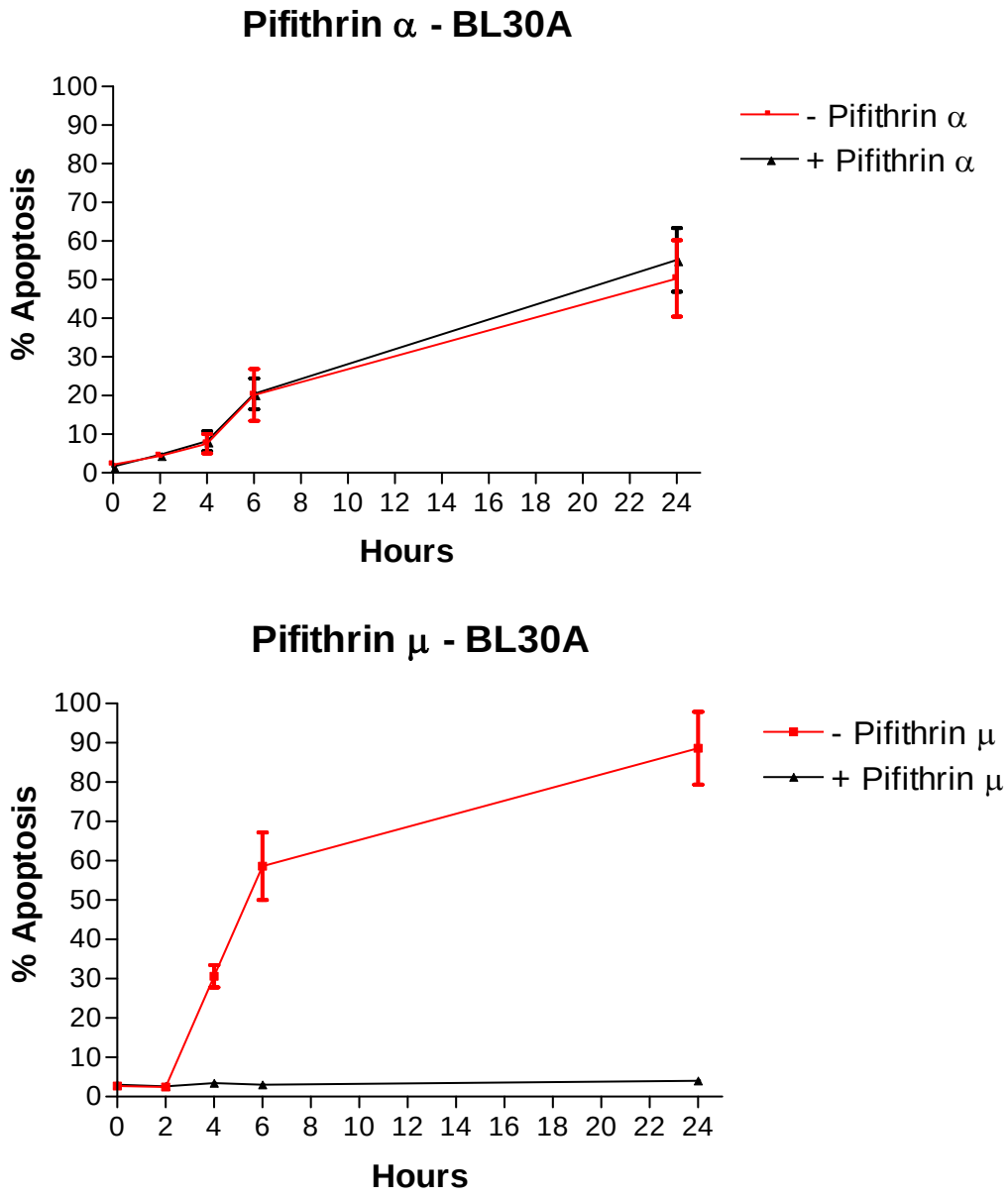

Figure 3.12: p53 inhibition experiments in BL30A cells. Percentages of apoptotic cell death as assessed by DAPI nuclear staining at the indicated times after treatment with etoposide (68 μM) and either Pifithrin-α (30 μM) or Pifithrin-μ (30 μM). Percentages of apoptosis were obtained by counting six fields of cells under 200X magnification and dividing the number of apoptotic cells over total number of cells. Results expressed are the mean ± SEM of three replicate experiments.

3.4 The extrinsic apoptotic pathway appears not to be involved

3.4.1 Fas activating antibody fails to induce apoptosis in BL30A cells

p53 is a regulator of many death pathways, however the mechanism of caspase-8 activation still remained elusive. It was hypothesised that caspase-8 and the extrinsic apoptotic pathway was activated in this cell line in response to DNA damage by an unknown mechanism. Fas – the receptor for FasL, is a component of the extrinsic signalling pathway of apoptosis (Itoh, Yonehara et al. 1991; Park 2012). It is involved in the initial step of the pathway in formation of the DISC, which is the normal activation platform for caspase-8 (Park 2012). To test if the death receptor pathway was functional addition of a death ligand was used to induce apoptosis. Fas activating antibody CH-11, which mimics FasL was used to induce apoptosis (Yonehara, Ishii et al. 1989; Landowski, Gleason-Guzman et al. 1997; Park, Choi et al. 2003). Addition of Fas activating antibody CH-11 at a concentration of 100 ng/mL was ineffective at inducing apoptosis in BL30A cells, however successfully induced apoptosis in the positive control cell line, JHP (Figure 3.13). The lymphoblastoid cell line JHP was created by EBV transformation of normal B cells.

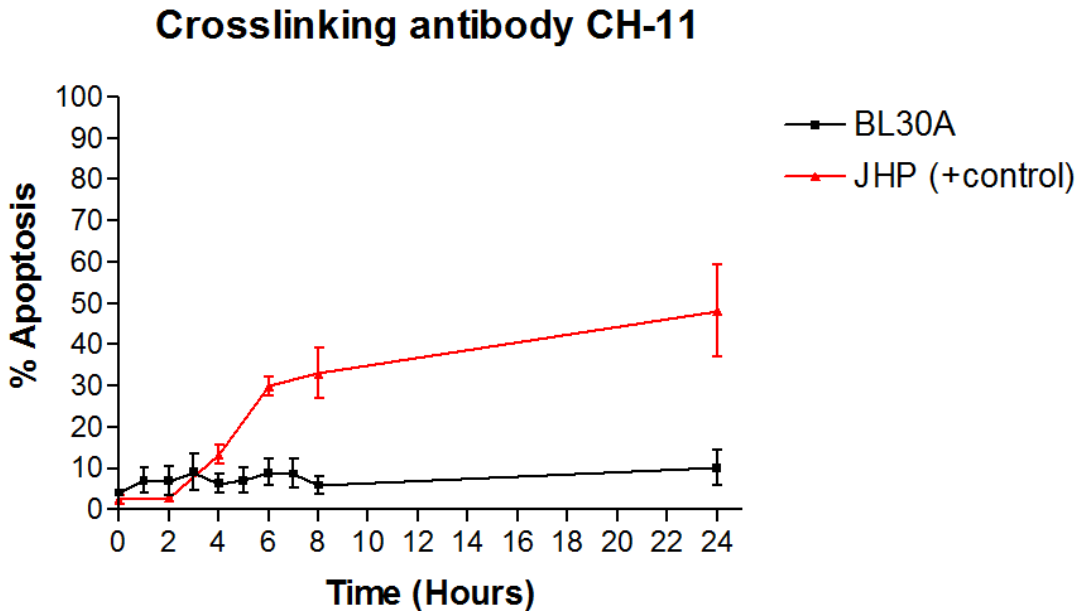

Figure 3.13: Apoptosis induction by Fas activating antibody CH-11 in BL30A cells. Addition of the Fas activating antibody (CH-11)(Millipore) at a concentration of 100 ng/mL was used to induce apoptosis. Apoptosis was measured at the indicated time points post treatment using DAPI nuclear staining. Percentages of apoptosis were obtained by counting six fields of cells under 200X magnification and dividing the number of apoptotic cells over total number of cells. Results expressed are the mean ± SEM of three replicate experiments.

Additionally, immunoprecipitation of Fas in BL30A cells was performed (Figure 3.14). It should be noted that the molecular weight of native Fas is approximately 36 kDa however it often appears larger on SDS-PAGE due to glycosylation (Itoh, Yonehara et al. 1991). The manufacturers datasheet for the antibody indicates that Fas runs at approximately 40 kDa using this antibody. The immunoprecipitation experiment revealed Fas in both the untreated and 2 hour samples, however levels of Fas appeared low as the exposure time used was very long and on the highest sensitivity setting on the machine. However, the immunoprecipitation failed to bind FADD as it was undetectable in both samples. This result provides evidence that Fas does not form the DISC in BL30A cells.

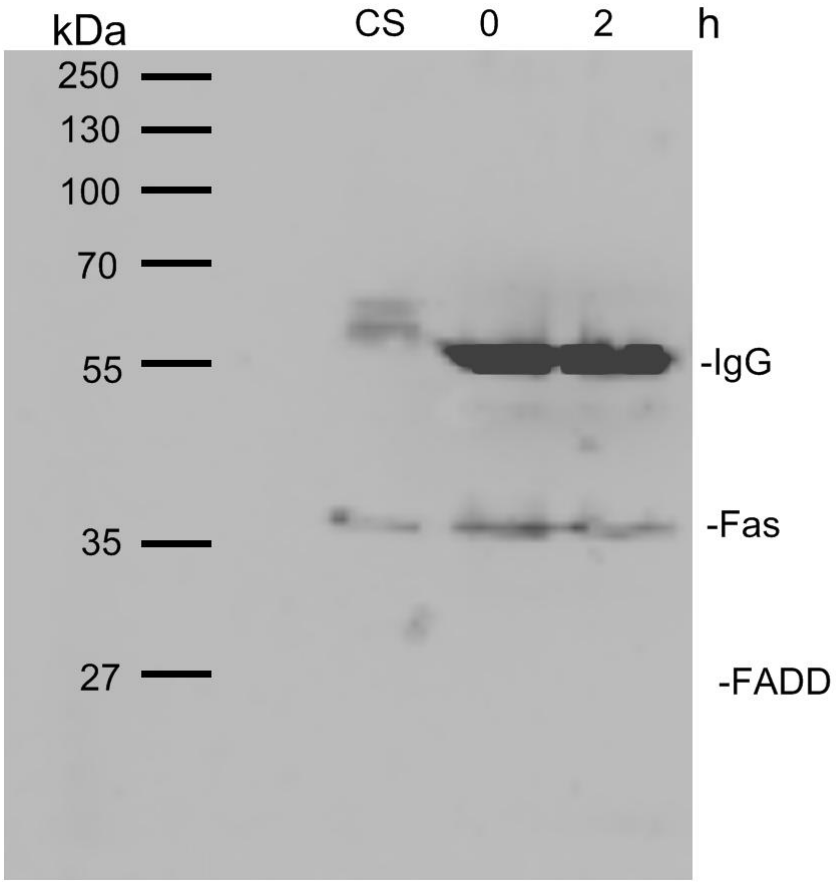

Figure 3.14: Immunoprecipitation of Fas in BL30A cells probing for Fas and FADD. Immunoprecipitation of Fas (apo-1-1) (Santa Cruz) probing for Fas (apo-1-1) (Santa Cruz) at 1/1000 dilution and FADD (Santa Cruz) at 1/500 dilution. Exposure time was 10 minutes on ultra exposure. CS- control pre-immune serum, 0 – 0 hours post etoposide treatment, 2 – 2 hours post etoposide treatment. The blot is representative of three biological replicates.

3.4.2 The extrinsic apoptosis pathway may be blocked by down-regulation of surface Fas

This finding led to the investigation of why the extrinsic pathway appeared inactive. Levels of the death receptor Fas on the surface of the cells were assessed using flow cytometry. Haynes et al (2002) reported that in group I Burkitt's lymphoma cells high levels of Fas receptor were found in the Golgi, with none present on the cell surface. In contrast, group III cells had levels of Fas receptor expressed both on the surface of the cell and internally. The authors concluded that membrane trafficking may play a role in the expression of Fas. The authors also suggested that the internalisation of Fas had developed as a mechanism of evasion of apoptosis (Haynes, Daniels et al. 2002). The JHP cell lymphoblastoid cell line was used as a control sample as a point of reference for normal levels of Fas expression. Figure 3.15 shows the expression of Fas as determined by flow cytometric analysis. The differences in fluorescence between the control samples and the non-permeabilised samples represent the expression of Fas on the cell surface. The difference in fluorescence between the non-permeabilised samples and the permeabilised samples show the expression of Fas internally. In the BL30A cells there was very little difference between the control sample and the non-permeabilised sample indicating that expression of Fas on the surface of the cell was very low. However there was an increase in fluorescence in BL30A when comparing the non-permeabilised sample to the permeabilised sample which indicates that there was expression of Fas internally. In contrast, expression of Fas on the cell surface of JHP cells was seen (compare control to non-permeabilised) as well as expression internally (compare non-permeabilised to permeabilised). Furthermore, fluorescence of Fas was higher in the JHP cell line when compared to the BL30A cell line indicating that BL30A has low expression of Fas compared to the control cell line.

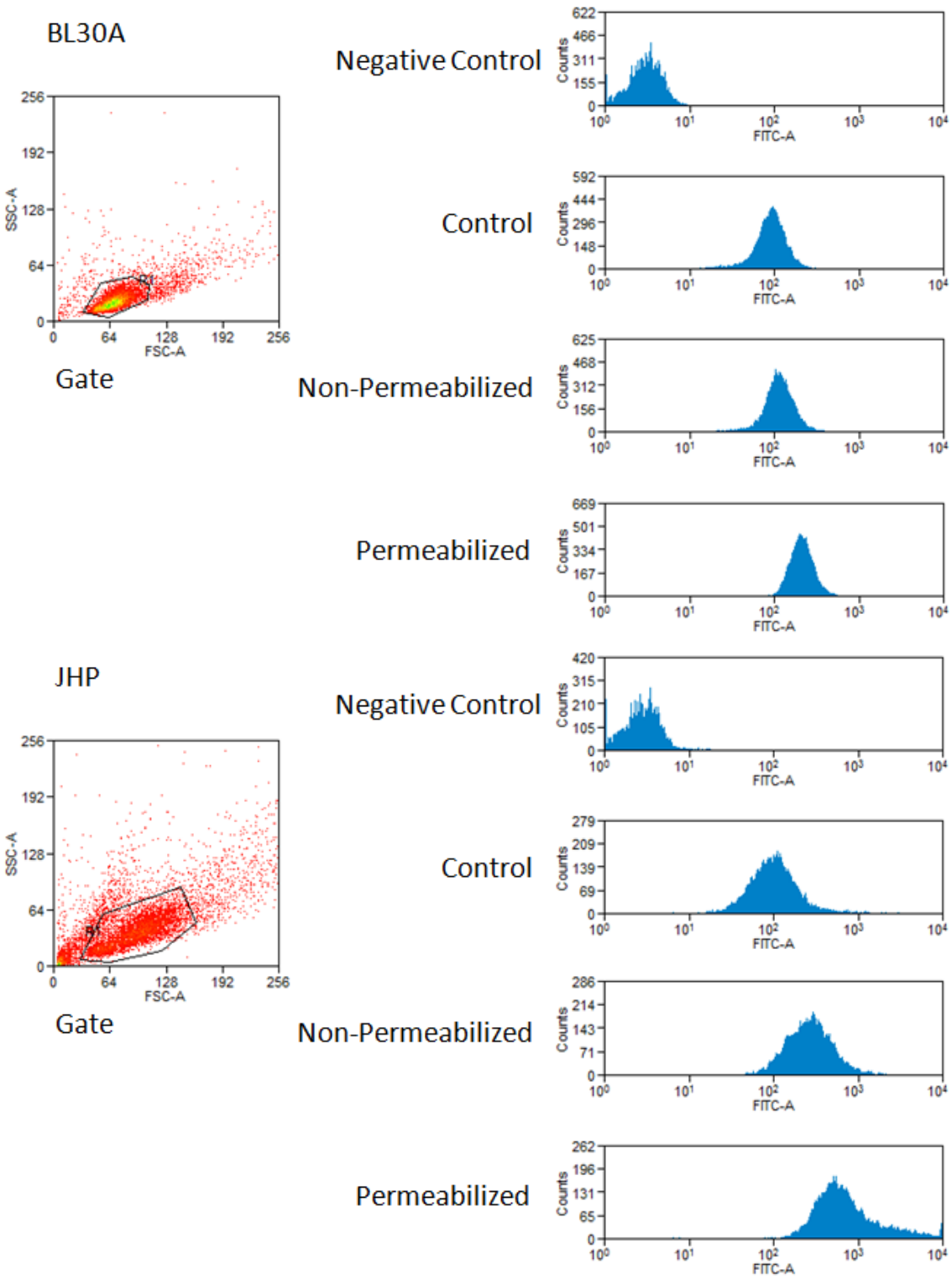

Figure 3.15: Fas expression in BL30A cells. Fas expression in BL30A and JHP cells was analysed using a flow cytometry instrument. Fluorescence intensities of Fas labelled cells are shown. Cells were fixed using 4% paraformaldehyde and then treated with anti-Fas antibody (Santa Cruz) followed by FITC conjugated secondary antibody. Negative control samples (to test for auto-fluorescence) have no antibodies added, and control samples have only secondary antibody. Cells were permeabilised by 0.1% Triton X-100 in PBS where applicable. Results expressed are representative of two replicate experiments.

3.4.3 Surface cholesterol depletion

To further exclude a role for the DISC, and indeed other membrane bound signalling complexes in DNA damage induced apoptosis an experiment was conducted in which lipid raft formation is disrupted. Lipid rafts are the platforms on which signalling complexes like the DISC are formed, and cholesterol is a vital component of these rafts (Pike 2004). The cholesterol depletion agent hydroxy-propyl ß-cyclodextrin (HPBCD) (Zidovetzki and Levitan 2007) was used to deplete the surface cholesterol of the cells – disrupting lipid raft formation. It was found that depletion of surface cholesterol did not affect the levels of apoptosis following etoposide treatment in the BL30A cell line. Levels of apoptosis observed were indistinguishable between cells treated with etoposide or etoposide and HPBCD (Figure 3.16). This result suggested that caspase-8 was activated in a manner that does not require the use of a membrane bound signalling platform such as the DISC.

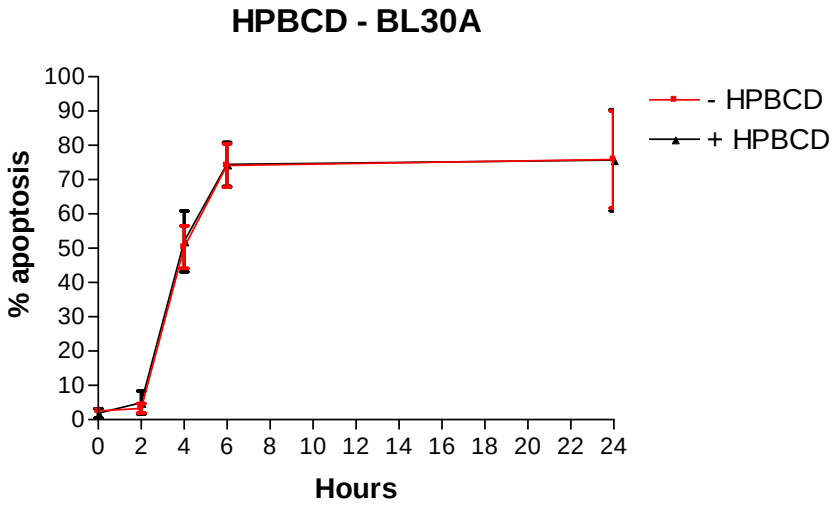

Figure 3.16: Cholesterol depletion in BL30A cells. Time course of apoptosis induction by etoposide (68µM) in BL30A cells as monitored by DAPI staining. Samples were pre-treated for 30 minutes in either the presence or absence of 2% (w/v) hydroxy propyl ß-cyclodextrin (HPBCD). Samples were then resuspended in complete culture medium and etoposide added. Percentages of apoptosis were obtained by counting six fields of cells under 200X magnification and dividing the number of apoptotic cells over total number of cells. Results expressed are the mean ± SEM of three replicate experiments.

3.5 A high molecular weight complex as an activation platform for caspase-8

3.5.1 Caspase-8 forms a complex of high molecular weight in response to DNA damage

Owing to the findings that the DISC was not involved in activation of caspase-8 other activation mechanisms were explored. Initiator caspase activation occurs by a process called autocatalytic cleavage, meaning that once two caspase molecules are in close proximity they cleave each other (Muzio, Stockwell et al. 1998; Chen, Orozco et al. 2002). To enable this cleavage a high molecular weight signalling complex is often recruited. Such platforms include the DISC, the apoptosome, TNF complex 1, and the more recently discovered RIPoptosome. Using blue native PAGE, a form of PAGE where proteins are left in their native configuration by use of mild conditions, proteins are separated based on their size and charge, and protein-protein interactions are also maintained. Because of this, large complexes of proteins can be identified.

Native page experiments revealed a high molecular weight complex containing FADD in BL30A cells in the 2 hours 30 minutes sample and the 4 hour sample indicated by the arrow (Figure 3.17). However this complex was not detectable in the 0 hour sample. A high molecular weight complex was also detected containing FADD in both the 0 and 4 hour post etoposide treatment samples in BL30K cells indicated by the arrow (Figure 3.17). Furthermore, native page experiments also revealed a high molecular weight complex containing caspase-8 in the 2 hour 30 minutes post etoposide treatment BL30A sample (Figure 3.18). This technique is limited however as it does not provide any information about the complexes or even if it is the same complex being detected in different samples. Additionally, use of antibodies to smaller proteins such as caspase-8 and FADD is unable to resolve these proteins in high molecular weight complexes and their native sizes simultaneously as the molecular weight difference is too large. Furthermore, this technique can only resolve proteins with low pI values as proteins are not universally charged as in SDS-PAGE (Wittig and Schagger 2005).

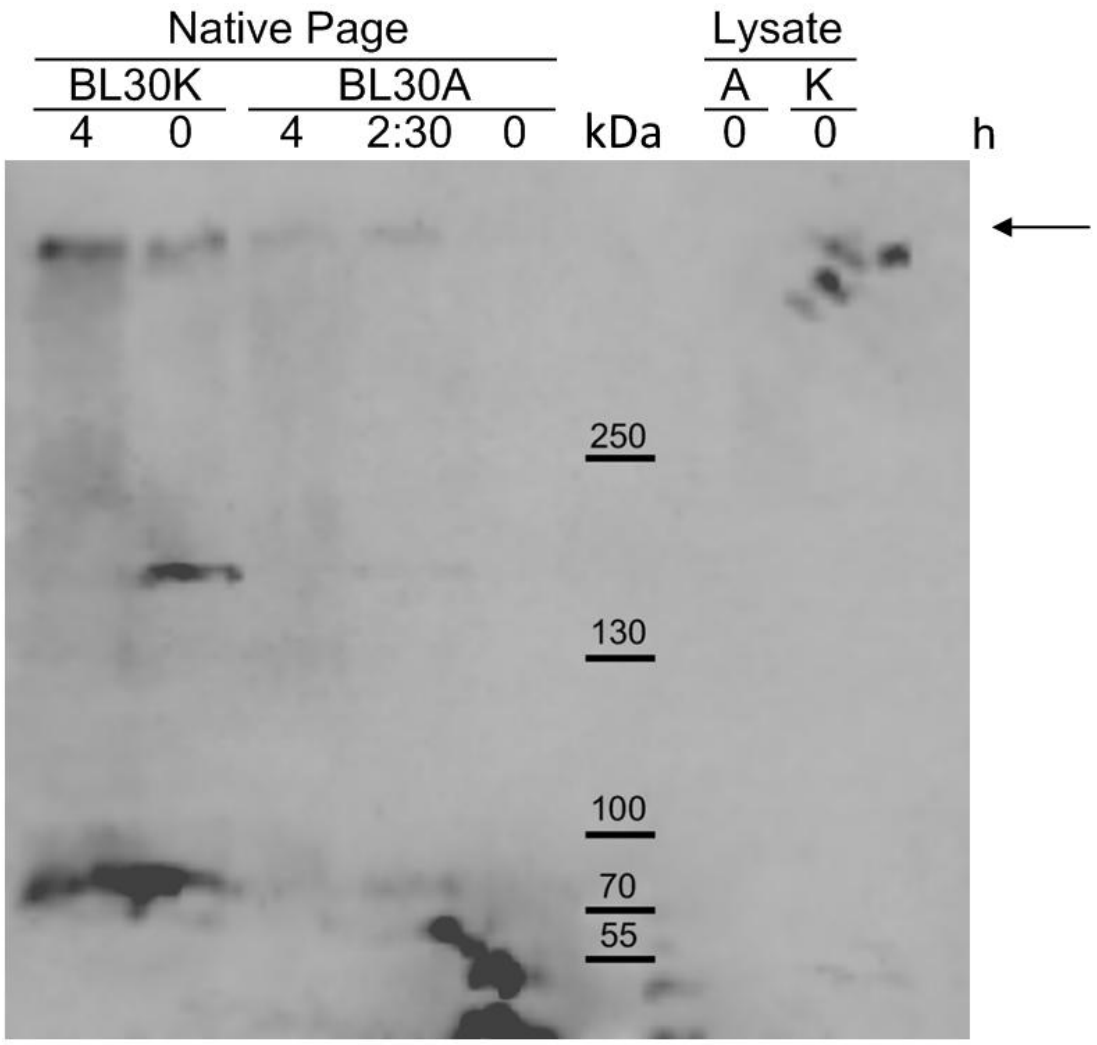

Figure 3.17: Native page of BL30A and BL30K cells probing for FADD. Native page performed on BL30A cells following etoposide treatment. The blot was probed with FADD (BD Pharmingen) and secondary antibody conjugated to HRP. Exposure time was 5 minutes on super exposure. The blot is representative of two replicate experiments.

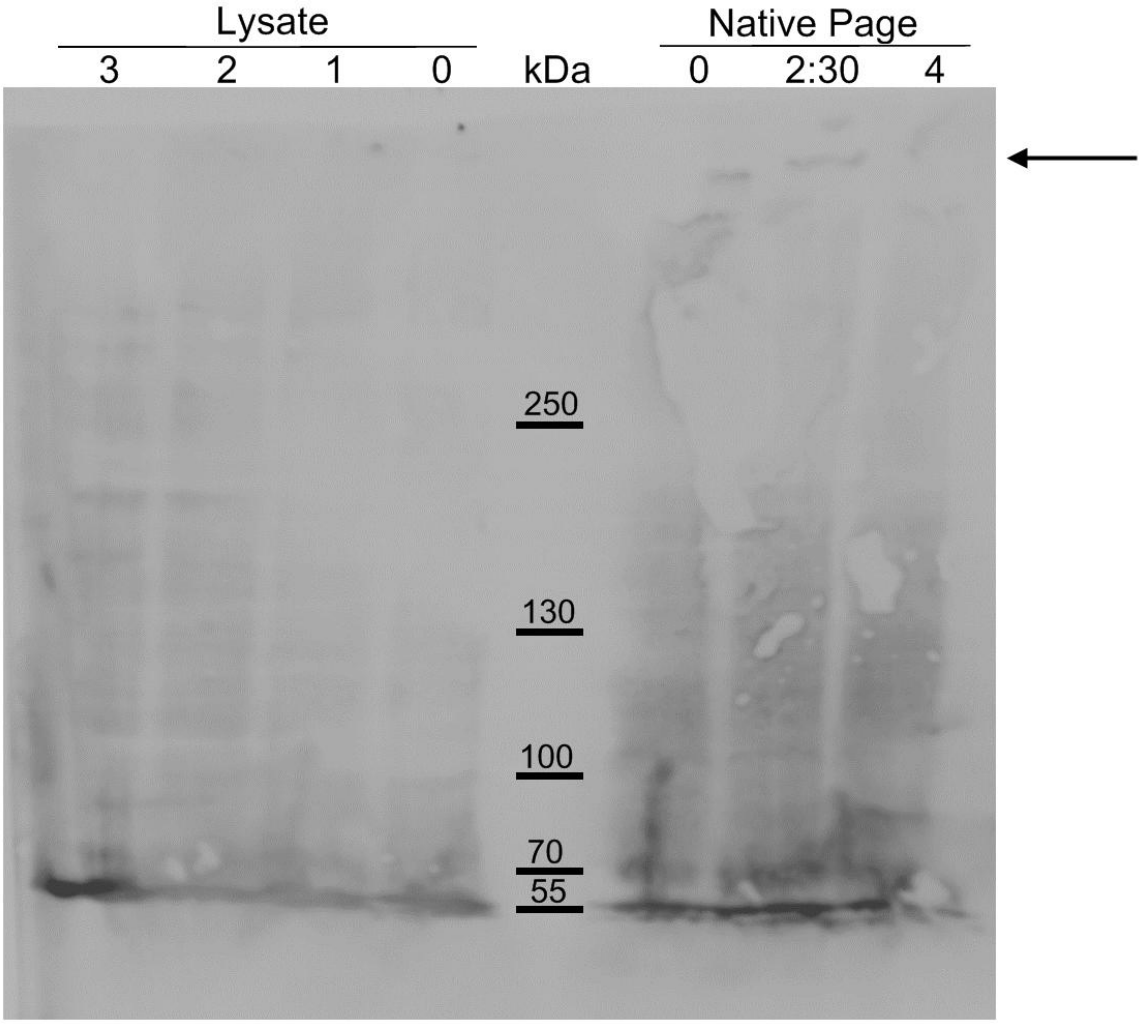

Figure 3.18: Native page of BL30A cells probing for caspase-8. Native page performed on BL30A cells following etoposide treatment. The blot was probed with mouse anti-caspase-8 (Cell Signaling) and secondary antibody conjugated to HRP. Exposure time was 5 minutes on super exposure. Arrow indicates high molecular weight complex. The blot is representative of two replicate experiments.

3.5.2 Immunoprecipitation experiments show complex containing FADD, caspase-8 and possibly RIP1

Immunoprecipitation experiments were conducted in order to determine which proteins interact with caspase-8 and FADD and lead to caspase-8 activation. Immunoprecipitation of FADD revealed that caspase-8 does indeed interact with FADD (Figures 3.19a and 3.19b). It should be noted that caspase-8 is approximately the same molecular weight as IgG (approximately 55 kDa). Initial probing of the

membrane with anti-FADD antibody revealed bands at 55 kDa indicating IgG (Figure 3.19a), but failed to show a band at the correct molecular weight of FADD (27 kDa). Re-probing of the blot with caspase-8 antibody revealed bands in the cell lysate lanes and the immunoprecipitation lanes at 55 kDa at far greater levels than the initial probing with FADD (Figure 3.19b). Additionally, a band of approximately 25 kDa was detected in both lysate lanes but not in the immunoprecipitation lanes. These findings will be discussed later.

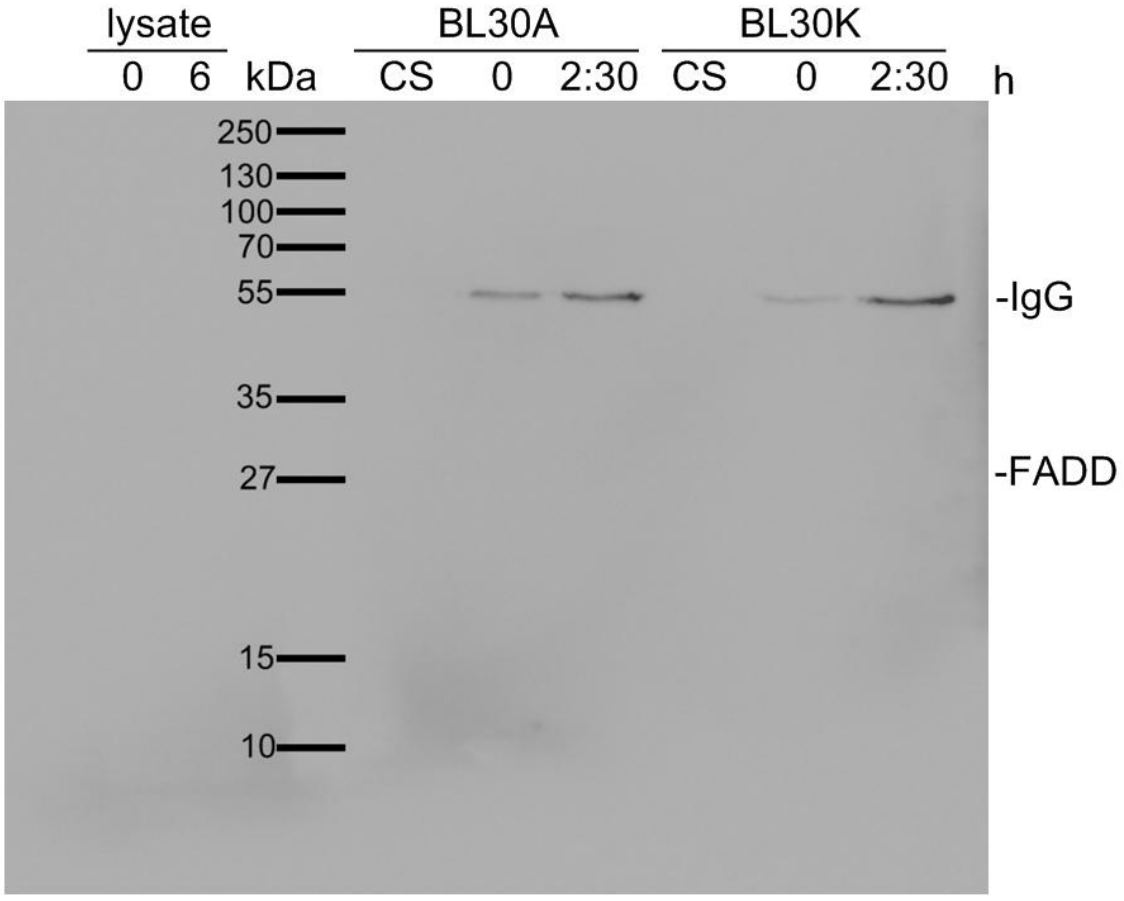

Figure 3.19a: Immunoprecipitation of FADD probing for FADD in BL30A and BL30K cells. The blot was probed with anti-FADD (BD Pharmingen) at 1/500 dilution and secondary antibody conjugated to HRP. Lysate indicates samples from BL30A cells treated with etoposide and is shown for comparison. CS indicates control serum (samples treated with pre-immune serum instead of primary antibody). The blot is representative of two replicate experiments.

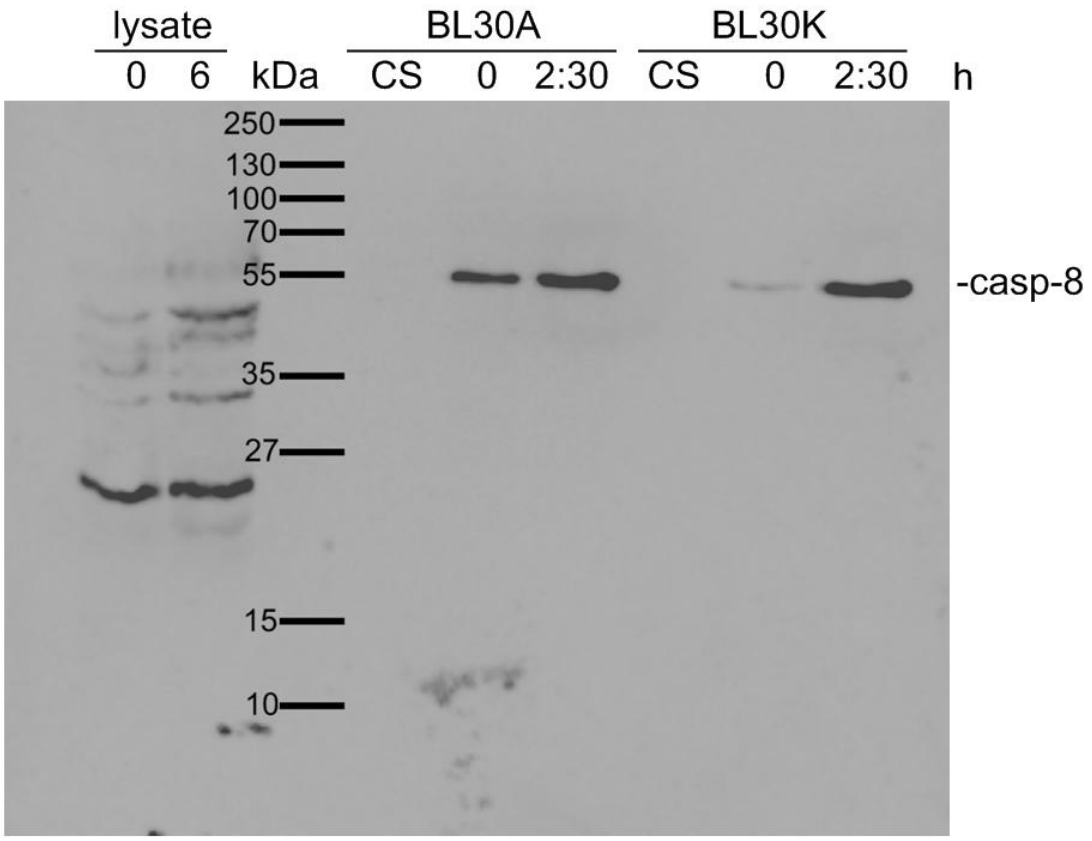

Figure 3.19b: Immunoprecipitation of FADD probing for caspase-8 in BL30A and BL30K cells. The blot was probed with antibody to caspase-8 (Cell Signaling) and secondary antibody conjugated to HRP. The blot had previously been probed with FADD. Lysate indicates samples from BL30A cells treated with etoposide and is shown for comparison. CS indicates control serum (samples treated with pre-immune serum instead of primary antibody). The blot is representative of two separate experiments.

Immunoprecipitation of caspase-8 was also conducted (Figure 3.20). Probing of the blot with anti-RIP1 antibody revealed RIP1 in the lysate samples indicated by bands at 74 kDa (Figure 3.20a). These bands of 74 kDa were not detected in the immunoprecipitation lanes. However, several bands at molecular weights of approximately 250 kDa, 130 kDa, 50 kDa 40 kDa, 35 kDa and 20 kDa were detected upon probing with RIP 1 which were present only in the immunoprecipitate lanes, and not in the control pre-immune serum lanes (Figure 3.20a). These findings will be discussed later.

The immunoprecipitation of caspase-8 was re-probed with anti-caspase-8 (Figure 3.20b). Caspase-8 was detected in both of the lysate samples, and also in the 0 and 4 hour immunoprecipitate samples but not in the pre-immune serum control samples (Figure 3.20b). The band of approximately 60 kDa shows the classical doublet, sometimes observed with caspase-8 probing on Western blotting (Scaffidi, Medema et al. 1997). This result indicates that the immunoprecipitation of caspase-8 was successful at pulling down caspase-8.

Probing for FADD in the immunoprecipitation of caspase-8 showed FADD in both the lysate samples, as well as the 4 hour post etoposide immunoprecipitation sample (Figure 3.20c). However FADD was not detectable in either of the pre-immune serum control samples or the 0 hour post etoposide immunoprecipitation. This finding indicated that caspase-8 forms a complex with FADD in response to DNA damage.

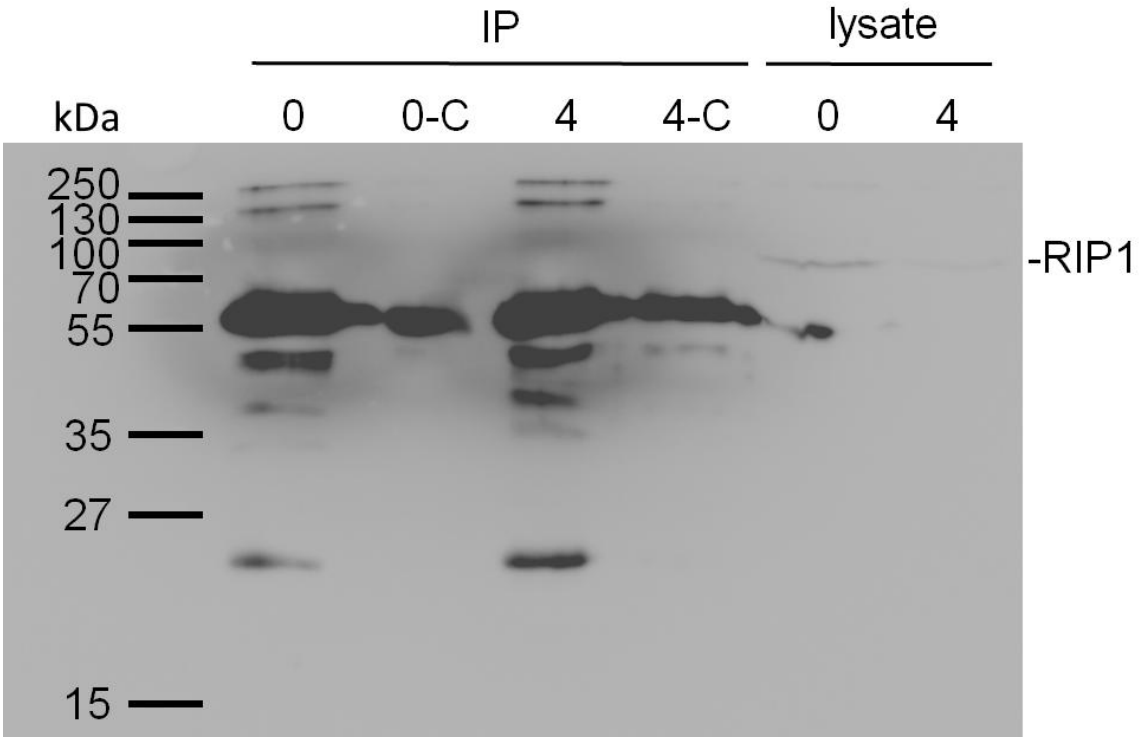

Figure 3.20a: Immunoprecipitation of caspase-8 1c12 antibody (Cell Signaling) probing for RIP1 in BL30A cells. The blot was probed with antibody to RIP1 (Cell Signaling) and secondary antibody conjugated to HRP. C indicates control serum (samples treated with pre-immune serum instead of primary antibody). The blot is representative of two replicate experiments.

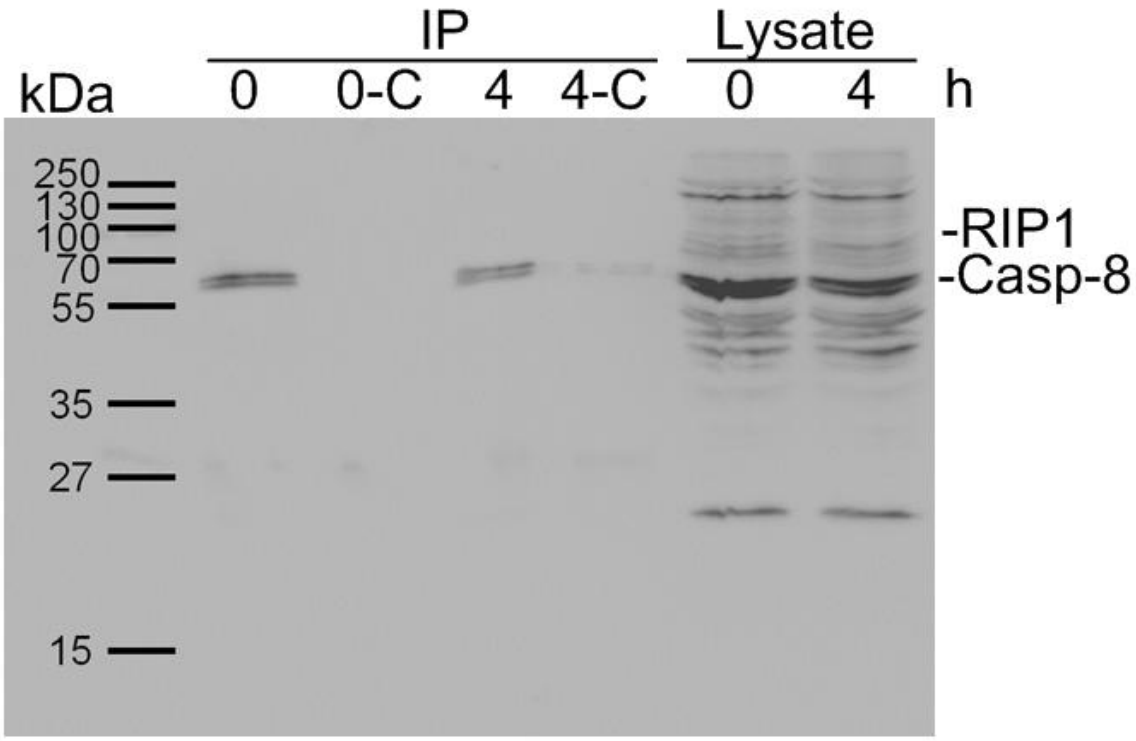

Figure 3.20b: Immunoprecipitation of caspase-8 probing for caspase-8 in BL30A cells. The blot was probed with antibody to caspase-8 1c12 (Cell Signaling) and secondary antibody conjugated to HRP. The blot had previously been probed with RIP1. The blot is representative of two replicate experiments.

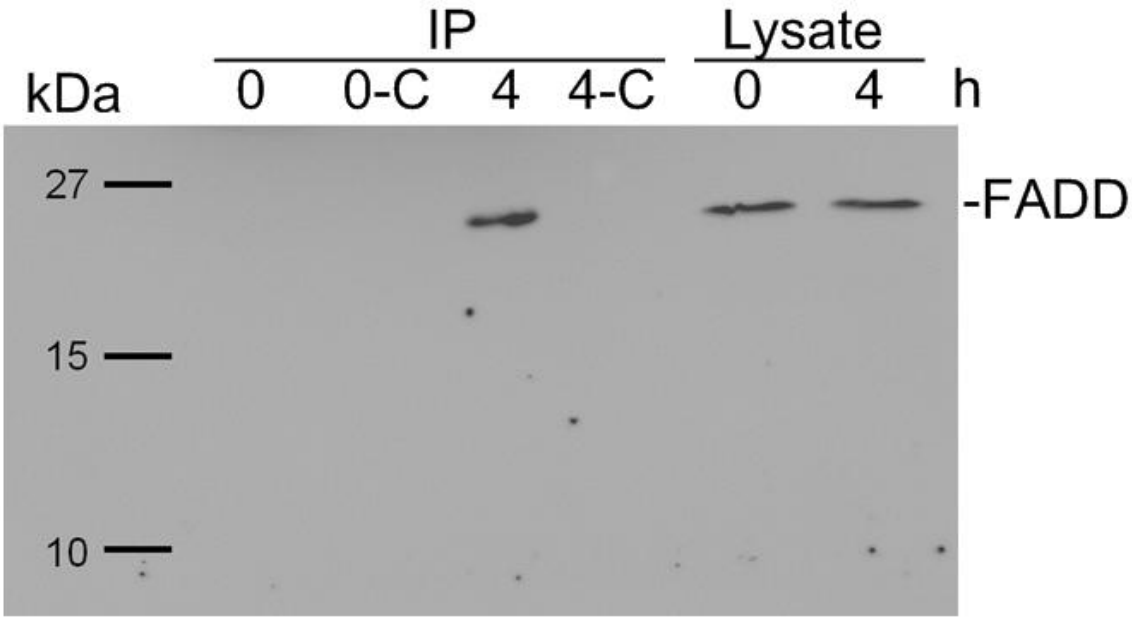

Figure 3.20c: Immunoprecipitation of caspase-8 probing for FADD (Zymed) in BL30A cells. The blot was probed with antibody to FADD (Zymed) and secondary antibody conjugated to HRP. The blot had previously been probed with RIP1 and caspase-8. The blot is representative of two separate experiments.

3.5.3 Necrostatin-1 reduces apoptosis levels in response to etoposide in BL30A cells

Results regarding RIP1 from the immunoprecipitation experiments were inconclusive. Therefore the involvement of RIP1 was investigated by use of a RIP1 inhibitor. Inhibitor studies revealed that RIP1 inhibition by necrostatin-1 reduced the level of apoptosis observed in response to DNA damage by etoposide (Figure 3.21). Additionally, inhibition of MEK in the MAPK/ERK signalling pathway by PD98059 also reduced the apoptosis levels observed. The MAPK/ERK signalling pathway is primarily involved in cell growth, but has been shown to modulate cell death and survival. Inhibition of MEK has been demonstrated to promote apoptosis when used in combination with Bcl-2 inhibition (Milella, Estrov et al. 2002; Corcoran, Cheng et al. 2013). p38 MAPK has been demonstrated to promote survival of cells through phosphorylation and inactivation of caspase-8 and caspase-3 (Alvarado-Kristensson, Melander et al. 2004). However, inhibition of p38 MAPK by SB203580 showed no detectable reduction in apoptosis levels.

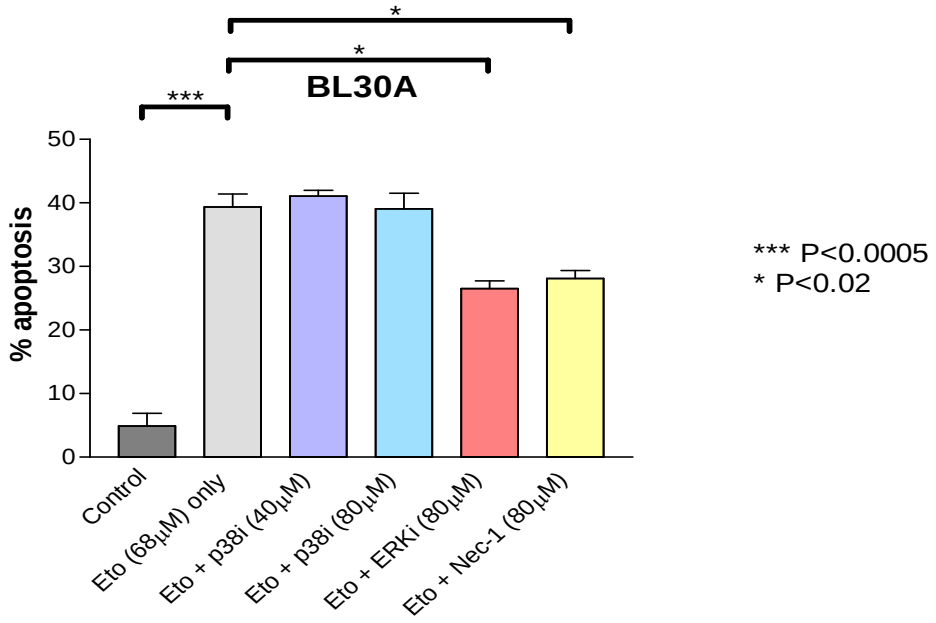

Figure 3.21: Effects of various inhibitors on apoptosis in BL30A cells. Several inhibitors were added to BL30A cells to determine if they affect the levels of cell death observed in response to DNA damage. The inhibitors used were SB203580 (40 μM and 80 μM) for p38 inhibition, PD98059 (80 μM) for ERK inhibition and necrostatin-1 (80 μM) for RIP1 and RIP3 inhibition. The cells were grown in the presence of etoposide (68 μM) and the indicated concentrations of inhibitors for 6 hours and then the percentages of apoptosis were assessed using DAPI staining. Percentages of apoptosis were obtained by counting six fields of cells under 200X magnification and dividing the number of apoptotic cells over total number of cells. Results expressed are the mean ± SEM of three replicate experiments.

3.5.4 Western blotting for RIP expression levels

Following the finding that necrostatin-1 decreased apoptosis levels in response to DNA damage RIP1 expression levels were monitored. RIP1 expression remained constant until 4 hours post treatment when the levels began to decrease (Figure 3.22a) when compared to the ß-actin loading control. Interestingly, RIP1 expression was lower in the apoptosis resistant BL30K cell line, which will be discussed in the next chapter. Full length caspase-8 levels appeared to decrease over time in the BL30A cells however levels in the BL30K cell line began lower – approximately equal to levels of 6 hour post treatment in the BL30A cell line and remained consistent between time points (Figure 3.22b).

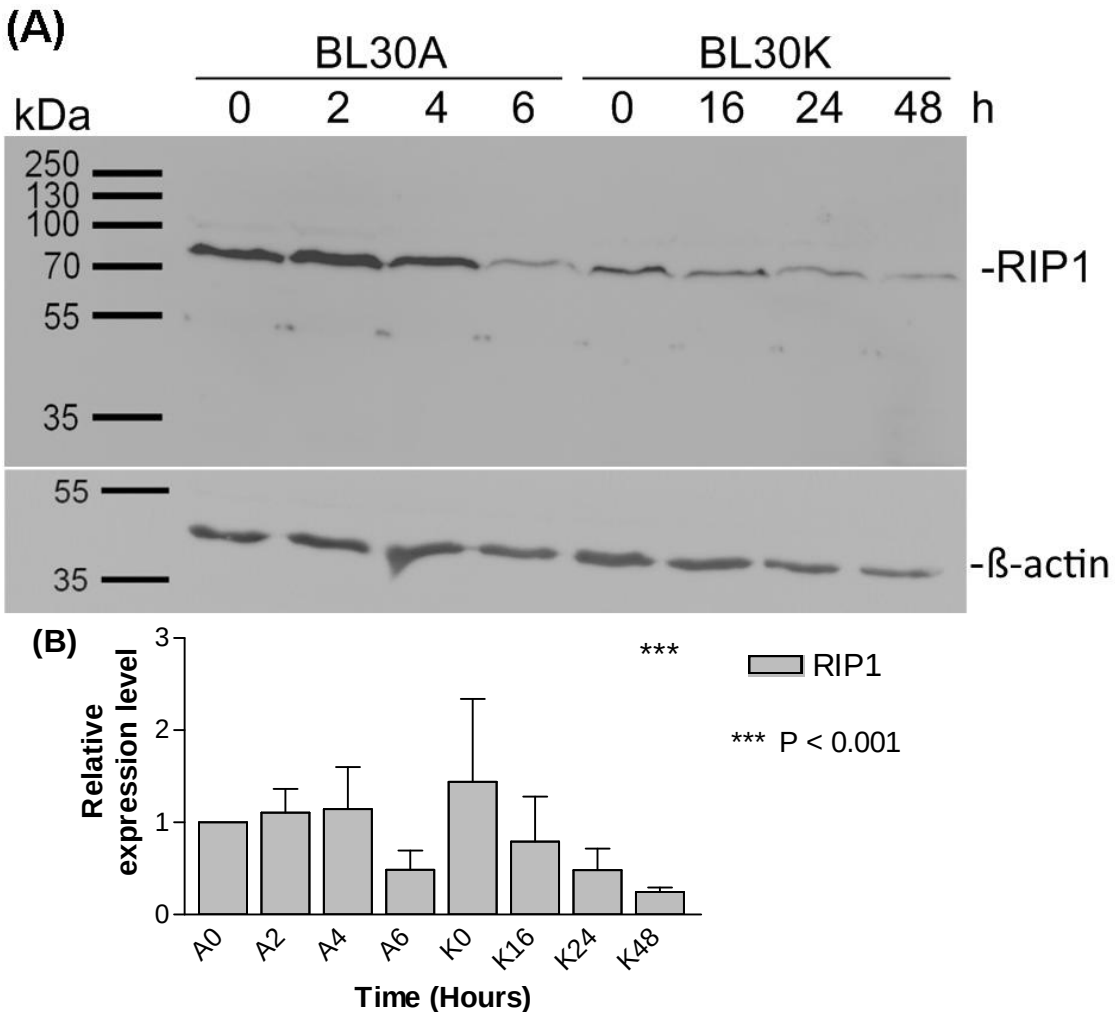

Figure 3.22a: Western blot of RIP1 in BL30A and BL30K cells. **(A)** Western blotting of etoposide time course probing for RIP1 (Cell Signaling) and secondary antibody conjugated to HRP. Re-probing of the blot with ß-actin (Sigma) is shown as a loading control. This is the same Western blot as Figure 3.11 reprobed with different antibodies. The blot is representative of three biological replicates. **(B)** Quantified histogram of the expressed proteins normalised to

ß-actin. Results expressed are the mean ± SEM. Asterisks indicate significant differences from unity.

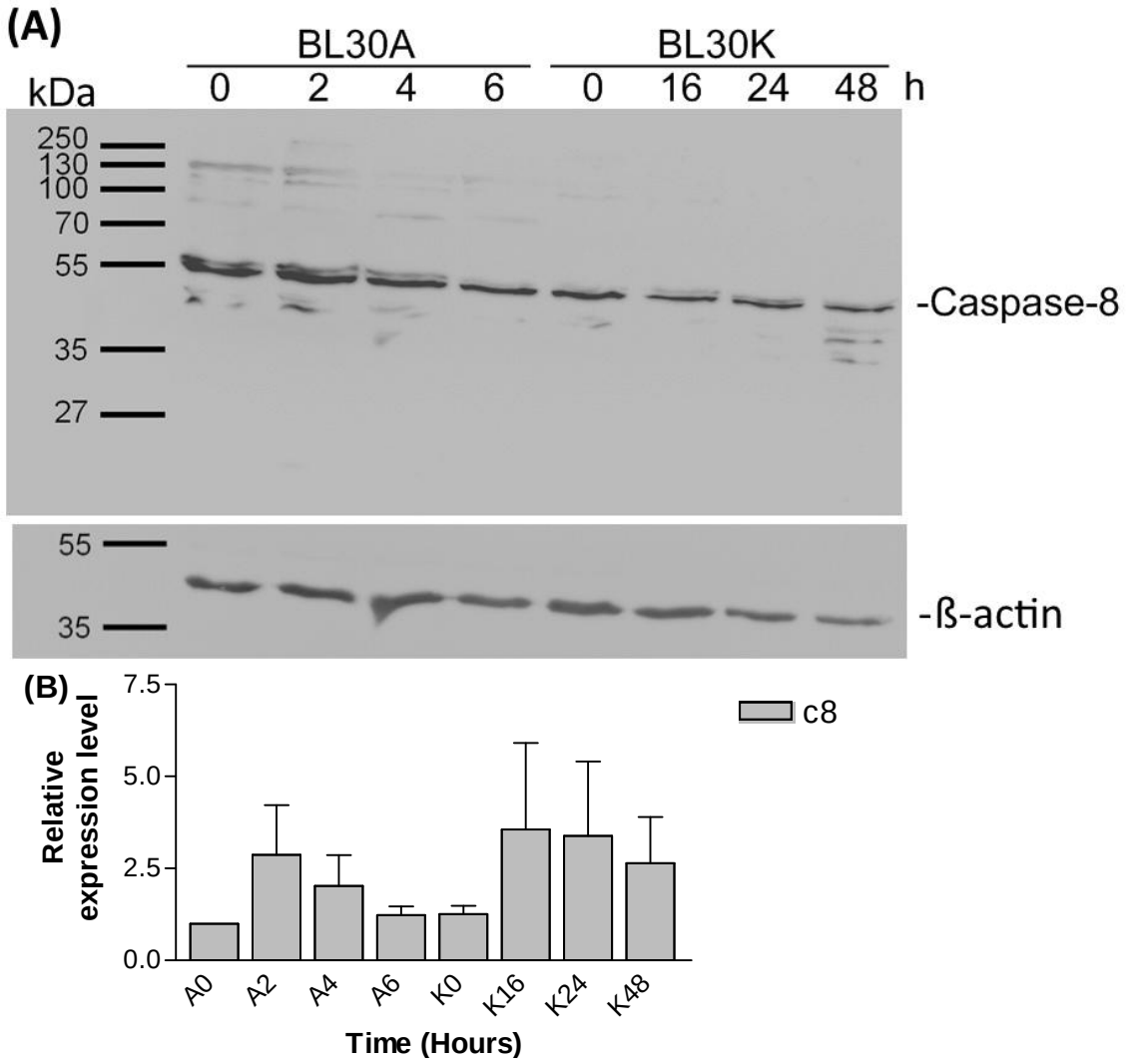

Figure 3.22b: Western blot of caspase-8 in BL30A and BL30K cells. **(A)** Western blotting of etoposide time course probing for caspase-8 (Cell Signaling) and secondary antibody conjugated to HRP. The blot had previously been probed with antibody to RIP1 (Cell Signaling). Re-probing of the blot with ß-actin (Sigma) is shown as a loading control. This is the same Western blot as Figure 3.11 reprobed with different antibodies.The blot is representative of three biological replicates. **(B)** Quantified histogram of the expressed proteins normalised to ß-actin. Results expressed are the mean ± SEM. No statistical significance was observed between samples.

3.5.5 Western blotting for FADD expression levels

As FADD was shown to interact with caspase-8 in BL30A cells and because FADD is known to form a complex with RIP1 in several cell lines (Tenev, Bianchi et al. 2011) its

expression levels were monitored. It was found that FADD levels increased over time, peaking at 4 hours post etoposide treatment in BL30A cells (Figure 3.23). The blot was cropped close to the top as the band for ß-actin was close at the exposure time used. It should also be noted that FADD expression in BL30K was higher in the untreated samples with decreasing levels and was undetectable by 24 hours.

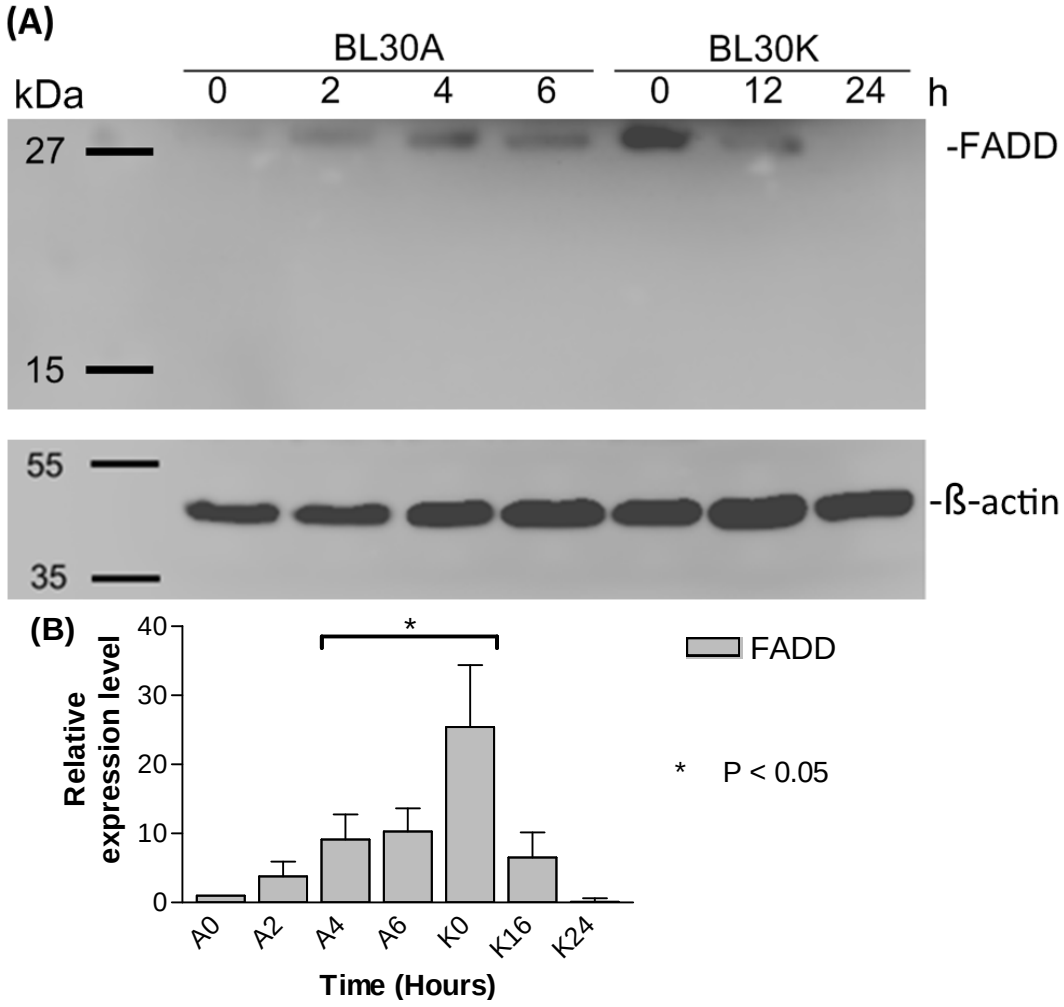

Figure 3.23: Western blot of FADD in BL30A and BL30K cells. **(A)** Western blot of lysates from BL30A and BL30K cells following etoposide (68 µM) treatment. The blot was previously probed with caspase-8. The blot was probed with 1/500 FADD (Santa Cruz), and secondary antibody conjugated to HRP. Exposure time was 5 minutes on ultra exposure. Re-probing with ß-actin (Sigma) is shown as a loading control. The blot is representative of three biological replicates. **(B)** Quantified histogram of the expressed proteins normalised to ß-actin. Results expressed are the mean ± SEM. Asterisks indicate significant differences from unity.

To summarise, evidence has been provided evidence that upon treatment with etoposide to damage DNA, apoptosis induction begins between 2 and 3 hours, and was dependent on caspase-8 activation. Mitochondrial permeabilisation – investigated as an early event in the intrinsic pathway of apoptosis occurs as a later event in the apoptotic response. p53 translational activity appears uninvolved in regulation of apoptosis however inhibition of cytoplasmic p53 activity prevents apoptosis in response to etoposide. Inhibition of MEK in the ERK/MAPK signalling pathway reduced the levels of apoptosis observed, however inhibition of p38 MAPK was ineffective at preventing apoptosis. The mechanism for activation of caspase-8 does not require Fas in the DISC, and must be activated by an alternate mechanism. A complex of high molecular weight forms in response to DNA damage in the BL30A cell line. This complex contains FADD and caspase-8. Inhibition of RIP1 reduced the levels of apoptosis observed and expression of RIP1 was higher in the apoptosis sensitive cell line BL30A than the apoptosis resistant BL30K cell line. FADD expression also increased throughout the time course of etoposide treatment in BL30A cells.

3.6 Discussion

The pathway of cell death in the BL30A cell line was explored in this chapter. Figure 3.1 shows that etoposide induces apoptosis in BL30A cells with 75-80% apoptosis by 6 hours post treatment. Previous findings involving caspase inhibitor studies led us to investigate the involvement of caspase-8 in cell death in response to etoposide induced DNA damage. Inhibition of the initiator caspases -8, -9 as well as the executioner caspase-3 show that caspase-8 inhibition was effective at preventing apoptosis following DNA damage (Figure 3.2). The caspase-9 and -3 inhibitors were ineffective at preventing apoptosis. It should be noted however that inhibition of the executioner caspase-3 is not always effective at preventing apoptosis as there are other executioner caspases, such as caspase-7 which have overlapping substrates (Lamkanfi and Kanneganti 2010). Caspase-9 inhibition would be expected to be effective if the intrinsic apoptosis pathway is the primary pathway and if caspase-9 was indeed the initiator caspase. It has been reported that the fmk caspase inhibitors are not be entirely specific to their targeted caspase (Benkova, Lozanov et al. 2009). Inhibition of the caspases is achieved however partial inhibition of other caspases is often observed (Benkova, Lozanov et al. 2009; Tenev, Bianchi et al. 2011).

Examination of the activation times of caspases-8 and -9 showed no detectable difference in activation time with time points as little as 15 minutes apart (Figure 3.3). Both initiator caspases were activated at 2 hours and 15 minutes post etoposide treatment as measured using the fluorigenic AFC caspase substrates. Caspase-3 activity was also detected beginning at 2 hours and 15 minutes, again highlighting that caspases, once activated, have a very quick chain reaction of activation. Caspase-3 activity had much higher levels which increased over time when compared to the initiator caspases. This finding is consistent with the activation cascade and amplification observed in caspase activation.

Caspase activation is also commonly monitored by Western blotting and detection of cleavage fragments as caspases are cleaved to become active. Caspase-8 cleavage was monitored using Western blotting. However, the antibodies tested had very limited effectiveness at detection of the cleaved forms of caspase-8. Figure 3.4 shows caspase-8 cleavage fragments detectable beginning at 3 hours post DNA damage. When compared to the 2 hours and 15 minutes activation time observed in the caspase activity assay (Figure 3.3) the differences in activation time observed can be explained by the sensitivity of the different assays, the fluorigenic assay being more sensitive. This being said, both results point to the activation of caspase-8 between 2 and 3 hours.

Caspase-2 is another initiator caspase which is normally activated in response to heat shock (Bouchier-Hayes, Oberst et al. 2009). However, caspase-2 has been shown to be activated in response to DNA damage in several cell lines (Robertson, Enoksson et al. 2002; Lin, Chen et al. 2004; Zhivotovsky and Orrenius 2005; Olsson, Vakifahmetoglu et al. 2009). Caspase-2 activation was monitored using Western blotting (Figure 3.5). Levels of the full length form of caspase-2 decreased at 4 hours post etoposide treatment, and at the same time the cleaved form of caspase-2 was detected. This indicated a far later activation time for caspase-2 than caspase-8, providing evidence that caspase-2 was not the initiator caspase.

Caspase-9 – the initiator caspase for the intrinsic apoptotic pathway was also monitored using Western blotting. A large increase in cleaved caspase-9 was detectable at 4 hours post treatment with etoposide in BL30A (Figure 3.6), consistent with the activation observed in the caspase activity assay. Following these findings an experiment was used to trap the apical (or first activated) caspase using a biotinylated irreversible pan-caspase inhibitor (Tu, McStay et al. 2006). The sample was then run on a Western blot and probed with anti-caspase antibodies. Probing of the Western blot of this experiment with caspase-8 antibody appeared to indicate that caspase-8 was the apical caspase in response to DNA damage in BL30A cells. A partially cleaved form of caspase-8 was detected providing more evidence of caspase-8 as the initiator caspase (Figure 3.7). This protocol has been shown to trap the partially cleaved form

of caspase-8 rather than the uncleaved pro-form (Mohr and Zwacka 2007). Additionally, upon probing of the trapped caspase sample with caspase-9 antibody nothing was detected (Figure 3.8). This result was obtained twice however we were unable to obtain a third replicate using the biotinylated pan-caspase inhibitor reagent available to us. These findings were however consistent with caspase trapping experiments performed by Lauren Finney previously in our laboratory (Lauren Finney - Honours thesis, 2007). As mentioned earlier, this experiment is extremely difficult to perform and many other research groups have struggled to replicate the experimental results of the initial authors (N. Waterhouse personal communication, (Pop, Salvesen et al. 2008)).

Having provided evidence that caspase-8 was the first activated caspase the mechanism of activation still remained to be determined. The release of components from the mitochondria is a step in the intrinsic apoptotic pathway, or an amplification step in the extrinsic pathway. Cytochrome c is a protein expressed in the mitochondria and important to the intrinsic apoptotic pathway for activation of caspase-9 in the apoptosome. To monitor this mitochondrial outer membrane permeabilisation, cytochrome c levels in fractions separated into mitochondrial and cytoplasmic fractions were visualised by Western blotting. Cytochrome c was detected only in the mitochondrial fractions until 3 hours post treatment when it became detectable in the cytoplasm (Figure 3.9). The activation of caspase-9 prior to detectable cytochrome c release may be because the assay did not detect low levels of cytochrome c release from mitochondria. Alternatively, caspase-9 can be activated independently of cytochrome c by caspase-8 cleavage of pro-caspase-9 (McDonnell, Wang et al. 2003). Probing with anti-ß-actin antibody only showed ß-actin in the cytoplasmic fractions at equal levels, but not in the mitochondrial fractions. However because inhibition of caspase-9 was not able to prevent apoptosis (Figure 3.2) it has lead to the conclusion that mitochondrial outer membrane permeabilisation and the mitochondrial pathway of apoptosis is activated only as an amplification step and not the primary contributor to the cell death phenotype observed.

The mitochondria are the energy generators of the cell, and as a by-product produce reactive oxygen species. ROS have been demonstrated to modulate apoptosis (Huang, Fang et al. 2003; Ozben 2007). Therefore, the effect of ROS on apoptosis induction in BL30A cells was monitored. N-acetyl cysteine is a reactive oxygen species scavenger which was used to deplete ROS. However treatment with N-acetyl cysteine failed to reveal any difference between cells treated with etoposide and N-acetyl cysteine and cells treated with etoposide only (Figure 3.10). This finding provides evidence that ROS are not modulating apoptosis in response to DNA damage in BL30A cells.

The regulation of cell death is heavily influenced by the activity of p53 (Kruse and Gu 2009). To begin exploring the involvement of p53 in cell death in BL30A cells, Bax - a p53 transcriptional target was examined. However Bax expression did not change throughout the time course of etoposide treatment (Figure 3.11). This indicated that the transcriptional activity of p53 was not up-regulated over the time course examined in response to DNA damage. p53 inhibitors were also used to explore the involvement of p53. Pifithrin-α - an inhibitor of p53 transcriptional activity failed to rescue the cell from DNA damage induced apoptosis (Figure 3.12). Furthermore, pifithrin- α has been shown to inhibit PIDD dependent caspase-2 activation in response to cisplatin (another DNA damaging agent) in renal tubular epithelial cells (Seth, Yang et al. 2005). No difference was observed between BL30A cells treated with etoposide plus pifithrin-α and cells treated with etoposide only. It also provides weak evidence against caspase-2 as an initiator of apoptosis in response to DNA damage in BL30A. The ineffectiveness of pifithrin-α to prevent apoptosis is consistent with the lack of change in Bax expression observed in showing that p53 was not transcriptionally regulating apoptosis in BL30A cells. Additionally, when paired with the later activation time of caspase-2 observed it provides evidence that the PIDDosome was not the apoptosis activating platform. Pifithrin-μ is an inhibitor of p53 interactions at the mitochondria, and was effective at preventing apoptosis in response to etoposide treatment (Figure 3.12). BL30A cells treated with etoposide only showed high levels of apoptosis, however cells treated with etoposide and pifithrin-μ only showed baseline levels of apoptosis. This result points to a role of p53 in the cytoplasm in the regulation of apoptosis. However, pifithrin-μ inhibition of apoptosis should be examined more thoroughly as pifithrin-μ

has since been shown to have interactions with HSP70 from the heat shock family of proteins (Kaiser, Kuhnl et al. 2011; Leu, Pimkina et al. 2011). It has been reported that both BL30A and BL30K have mutant p53 (Khanna, Wie et al. 1996), however the finding that pifithrin-μ blocks apoptosis may indicate that p53 is functional, at least in its cytoplasmic role. p53 may indeed be mutant in BL30A and BL30K cells as translational regulation does not appear to be activated in response to DNA damage, however p53 regulation of apoptosis in a non-translational role appears likely.

Due to the involvement of caspase-8 in apoptosis induction in response to DNA damage the expression of Fas, the death receptor which is primarily responsible for caspase-8 activation must be investigated. Firstly, the Fas activating antibody (CH-11), which mimics the death ligand of Fas was used (Yonehara, Ishii et al. 1989; Landowski, Gleason-Guzman et al. 1997; Park, Choi et al. 2003). Addition of the ligand failed to induce apoptosis in BL30A cells, however it effectively induced apoptosis in the positive control cell line JHP (Figure 3.13). Additionally, immunoprecipitation of Fas failed to pull down FADD – a vital component of the DISC and extrinsic apoptosis signalling (Figure 3.14). Furthermore, expression of Fas was monitored using flow cytometric analysis. Flow cytometric analysis revealed that BL30A cells expressed very low levels of Fas when compared to the lymphoblastoid control cell line JHP (Figure 3.15). Expression of Fas on the cell surface was extremely low in BL30A cells, and only low levels were detected internally. This was determined by comparing the control sample to the non-permeabilised sample for surface expression and comparing the non-permeabilised and permeabilised sample for internal expression. Comparatively, the JHP control cell line expressed Fas both on the cell surface and internally at much higher levels than BL30A. These results are not quite in agreement with findings by Haynes and colleagues (Haynes, Daniels et al. 2002). Haynes found that Group I BL cells - of which BL30A is a member did not express Fas on the cell surface, however BL30A was not specifically investigated in the study. Lack of cell surface expression of Fas is consistent with these findings, however Haynes reported high levels of Fas internally, whereas this data indicates low levels in BL30A. In addition, depletion of surface cholesterol was used to disrupt any potential cell surface signalling platforms. Surface cholesterol is important in the formation of lipid rafts and cell surface

signalling platforms such as the DISC - primary activator of the extrinsic apoptotic pathway. However depletion of surface cholesterol using hydroxy-propyl ß-cyclodextrin had no effect on the apoptosis levels observed posing more evidence that the formation of a cell surface signalling complex was not involved (Figure 3.16). These results taken together provide strong evidence that the DISC is not involved in the activation of apoptosis in BL30A cells in response to DNA damage. In agreement with these findings it has been reported that etoposide induced activation of caspase-8 and apoptosis occurs independently of death receptors in MDA-MB-231 human breast adinocarcinoma cells and HT1080 fibrosarcoma cells (Tenev, Bianchi et al. 2011). Caspase-8 activation in response to etoposide in Jurkat T cells has also been demonstrated in the absence of Fas (Boesen-de Cock, de Vries et al. 1998; Bantel, Engels et al. 1999).

The question of how caspase-8 is activated in response to DNA damage still remained. A possible explanation is that a high molecular weight complex which is activated by p53 brings caspase-8 proteins into proximity for activation. Platforms such as the apoptosome, PIDDosome or RIPoptosome could facilitate caspase-8 activation (Tinel and Tschopp 2004; Feoktistova, Geserick et al. 2011; Tenev, Bianchi et al. 2011). Native page techniques were used to investigate if caspase-8 formed a high molecular weight complex in response to DNA damage. Western blotting for FADD under non-denaturing conditions revealed a high molecular weight complex in BL30A cells treated with etoposide detectable at 2 hours 30 minutes and 4 hours post treatment (Figure 3.17), however FADD was not detected in the 0 hour sample. Additionally Western blotting for caspase-8 under non-denaturing conditions showed a complex containing caspase-8 in the 2 hours and 30 minutes sample. These findings provide evidence that caspase-8 and FADD were involved in high molecular weight complexes in response to DNA damage. Platforms documented to involve both FADD and caspase-8 include the DISC and TNFR complex 2, the necrosome, RIPoptosome and the iDISC (Imre, Larisch et al. 2011; Tenev, Bianchi et al. 2011; Dickens, Powley et al. 2012; Kreuzaler and Watson 2012; Young, Takahashi et al. 2012).

Immunoprecipitation experiments were then used to examine interactions between FADD and caspase-8 and the complexes they are involved in. Figure 3.19a shows an immunoprecipitate of FADD probing for FADD however a band of the correct molecular weight of FADD was not seen. Re-probing with caspase-8 (Figure 3.19b) showed much darker bands in the IP samples at 55 kDa. Immunoprecipitations of caspase-8 probing for FADD were also conducted as an alternate approach. Immunoprecipitation of caspase-8 revealed the presence of FADD in 4 hour post etoposide treated samples (Figure 3.20c). Successful immunoprecipitation was confirmed by probing with caspase-8 and it was detected in the 0 and 4 hour samples, but not the pre-immune serum control samples (Figure 3.20b). Interestingly, upon probing of the caspase-8 IP with RIP1 several bands were revealed which were present only in the IP lanes and not in the pre-immune serum control lanes (Figure 3.20a). The differences in expression between the 0 and 4 hour sample differed in that the 40 kDa and 20 kDa fragments were more highly expressed in the 4 hour samples, and the 35 kDa sample was only present in the 4 hour sample. The finding of an approximately 35 kDa fragment only in the 4 hour post etoposide treatment sample is similar to a finding that a 42 kDa RIP1 cleavage fragment was observed solely in apoptotic cells in HeLa, HEK293 and Jurkat cells (Lin, Devin et al. 1999). This finding should be investigated further with antibodies to RIP1 from a different manufacturer and proteins with interactions with RIP1 should also be explored.

The use of several inhibitors was then employed to provide further insight into what pathways and proteins are involved in cell death in response to DNA damage. Inhibition of p38 MAPK in the ERK/MAPK signalling pathway by SB203580 failed to decrease the levels of apoptosis, pointing away from the necessity of p38 MAPK in the cell death response (Figure 3.21). This finding is consistent with findings suggesting p38 MAPK is not required for apoptosis signalling in response to IR in BL30A cells (Michael-Robinson, Spring et al. 2001). However, inhibition of MEK in the ERK/MAPK signalling pathway by PD98059 decreased the observed apoptosis levels demonstrating a possible role of proteins in the ERK family in modulating cell death in response to DNA damage (Figure 3.21). Additionally, necrostatin-1 which is an inhibitor of RIP1 decreased the cell death response to DNA damage, suggesting the

involvement of RIP1 in apoptosis induction in DNA damage induced apoptosis. It should be noted however that necrostatin-1 inhibits IDO in immune signalling and inflammation (Vandenabeele, Grootjans et al. 2013). Indeed it was reported that inhibition of RIP1 kinase activity by necrostatin-1 triggered interactions between RIP1, caspase-8 and FADD leading to apoptosis in acute lymphoblastic leukaemia cells (Loder, Fakler et al. 2012). Necrostatin-1 inhibition of apoptosis combined with the detection of RIP1 at unusual molecular weight bands highlight the need for further investigation of RIP1.

Western blotting of RIP1 revealed higher relative expression of RIP1 in BL30A cells than the apoptosis resistant BL30K cells (Figure 3.22a). Levels of RIP1 in BL30A remained at high levels until 4 hours post etoposide treatment when levels sharply decreased as compared to ß-actin (Figure 3.22c). Levels of full length caspase-8 also decreased over time beginning between 2 and 4 hours (Figure 3.22b). Expression of FADD in BL30A appeared quite low at 0 hour post etoposide treatment, levels increased at 2 hours and appeared to peak at 4 hours before beginning to decline again at 6 hours (Figure 3.23) as compared to ß-actin. The expression levels of FADD in response to etoposide coincide with the times of apoptosis induction in response to etoposide in BL30A. This would seem to suggest that FADD is involved in apoptosis induction in response to DNA damage.

The findings in this chapter have indicated that caspase-8 is the apical caspase in response to DNA damage in BL30A cells. This was determined through caspase inhibition studies, caspase activation assays and Western blotting of caspases. Additionally, caspase-8 is activated independently of the DISC or cell surface signalling complexes as determined through immunoprecipitation experiments, flow cytometric analysis of Fas expression, resistance to Fas activating antibody induced apoptosis and the ineffectiveness of cholesterol depletion in preventing apoptosis. p53 transcription appears uninvolved in apoptosis induction as determined through monitoring of p53 regulation of Bax as well as the p53 transcriptional inhibitor pifithrin-α. However activity of p53 in the cytoplasm appears vital to apoptosis induction as determined through pifithrin-μ inhibition. The mitochondria were permeabilised during the

apoptosis process and caspase-9 was activated however activation of caspase-9 was not essential for apoptosis to proceed and may only serve as an amplification mechanism. The mechanism of caspase-8 activation still remains to be determined however FADD was involved in its activation as determined by native page, immunoprecipitation experiments and Western blotting. A high molecular weight complex is likely to be involved in the activation of caspase-8, and there is a strong possibility that RIP1 is involved in regulation of apoptosis in response to DNA damage in BL30A cells.

Future studies should thoroughly examine the involvement of RIP1 in the execution of apoptosis in response to DNA damage. Additionally, the ERK/MAPK signalling pathway should be explored as a regulatory mechanism in this pathway. Furthermore, the cytoplasmic role of p53 should be defined in determining how it is activated and what proteins are activated by p53, including direct interactions with proteins such as Bcl-2 family proteins which lead to apoptosis.

Chapter 4

Apoptosis Resistance of BL30K cells

4.1 Introduction

The BL30K cell line is derived from the same parent cell line as BL30A, however has developed resistance to apoptosis induction. This chapter explores the mechanism of resistance to DNA damage induced apoptosis in an effort to better understand how cancers resist current anti-cancer treatments.

4.2 Apoptosis Resistance or Delay

In order to assess the level of resistance of the BL30K cell line to DNA damage induced apoptosis, a cell death response curve to etoposide was created. Treatment with an equivalent concentration of etoposide (68μM) as the BL30A cell line yields approximately 75% apoptosis by 24 hours for BL30K cells (Figure 4.1), as opposed to 80% at 6 hours for BL30 cells. Additionally, apoptosis only appeared at approximately 12 hours post treatment with 25% apoptosis visualised.

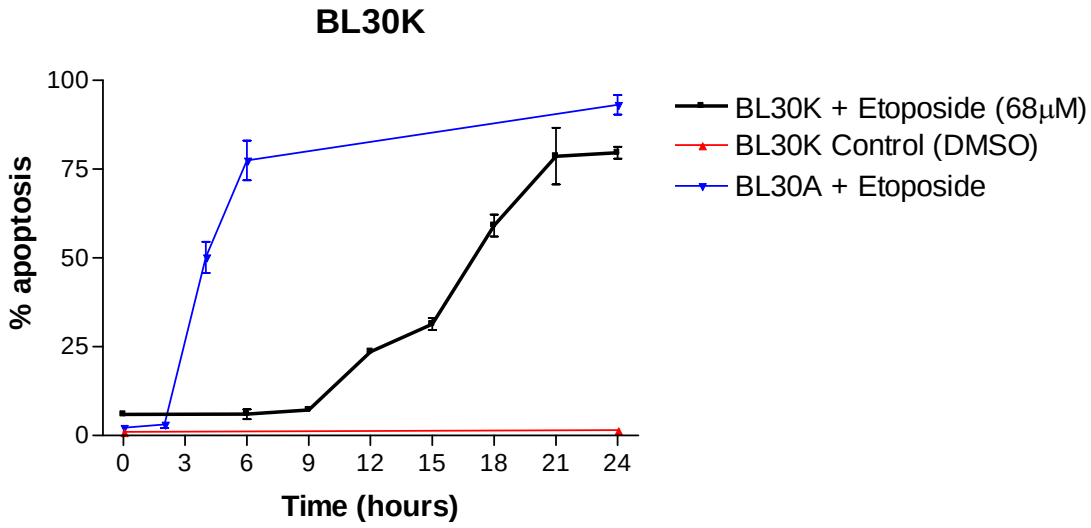

Figure 4.1: Etoposide time course in BL30K cells. Time course of apoptosis by etoposide induction (68μM) in BL30K cells as monitored by DAPI staining. Etoposide treatment of BL30A (from Figure 3.1) is shown for comparison. Percentages of apoptosis were obtained by counting six fields of cells under 200X magnification and dividing the number of apoptotic cells over the total number of cells. Results expressed are the mean ± SEM of three replicate experiments.

4.2.1 Caspase activation in response to DNA damage

This delayed apoptosis response in the BL30K cell line led us to investigate the times at which caspases are activated. Studying caspases, being the primary effectors of apoptosis should provide insight into how the apoptosis process is delayed in this cell line. Previous findings in the laboratory have indicated caspase-8 inhibition was effective in reducing apoptosis levels in response to DNA damage in BL30K cells (Lauren Finney, Honours thesis, 2007). Therefore caspase inhibition was examined. It was found that inhibition of caspase-9 had no effect on cell death in BL30K whereas inhibition of caspase-8 inhibited apoptosis (Figure 4.2). Addition of IETD-fmk – the inhibitor of caspase-8 – with etoposide showed only baseline levels of apoptosis in response to etoposide treatment. BL30K cells treated with LEHD-fmk – the caspase-9 inhibitor showed levels of apoptosis similar to cells treated with etoposide only.

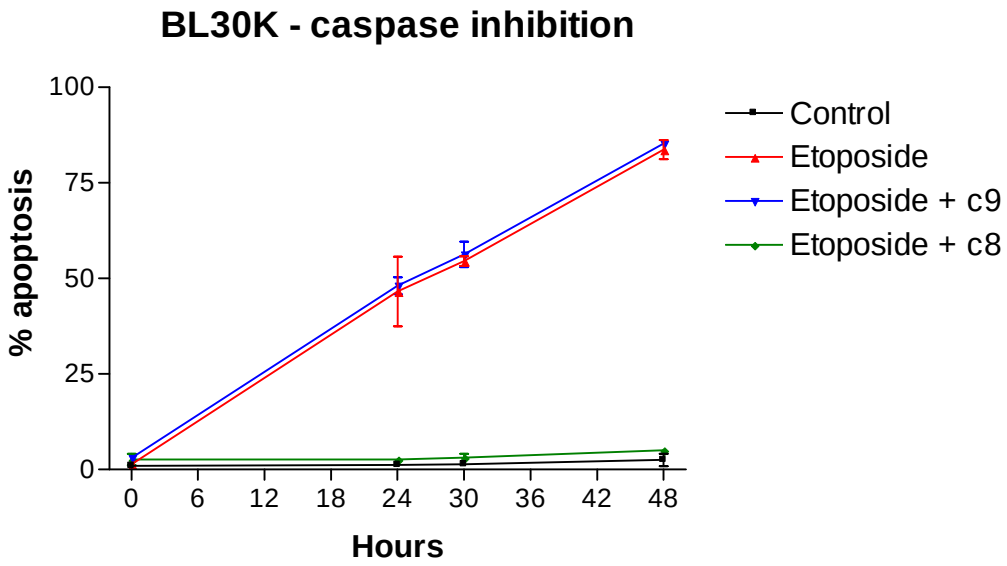

Figure 4.2: Treatment of BL30K cells with etoposide and caspase inhibitors. BL30K cells were treated with etoposide (68 µM) or etoposide with either IETD-fmk (4 µM) or LEHD-fmk (4 µM) and levels of cell death were monitored using DAPI nuclear staining at the indicated time points. Percentages of apoptosis were obtained by counting six fields of cells under 200X magnification and dividing the number of apoptotic cells over total number of cells. Results expressed are the mean ± SEM of three replicate experiments.

Western blotting of caspases was also conducted to assess caspase activation. Full length caspase-8 in the BL30A cells increases in levels following stimulation with etoposide peaking at 2 hours post treatment and declining to baseline levels by 6 hours (Figures 4.3 and 4.4). Comparatively, in the BL30K cell line caspase-8 levels appear to increase post etoposide treatment also, but the peak was at 16 hours post treatment and levels do not decline to baseline levels until 48 hours post treatment. Caspase-8 cleavage fragments were detected in BL30K cells beginning at 16 hours post treatment in contrast to 3 hours in the BL30A cells. Quantification revealed it was approximately a 3 fold increase in BL30K at 16 hours compared to 0 hours. It should also be noted that a band of approximately 70-100 kDa appears at the time which corresponds to apoptosis occurring – 4 hours in BL30A and 16 hours in BL30K. Figure 4.3 and 4.4 both show the caspase-8 doublet which will be explored in the discussion. Figure 4.4 was a repeat experiment of Figure 4.3 shown to highlight the high molecular weight band observed and to visualise fully cleaved caspase-8.

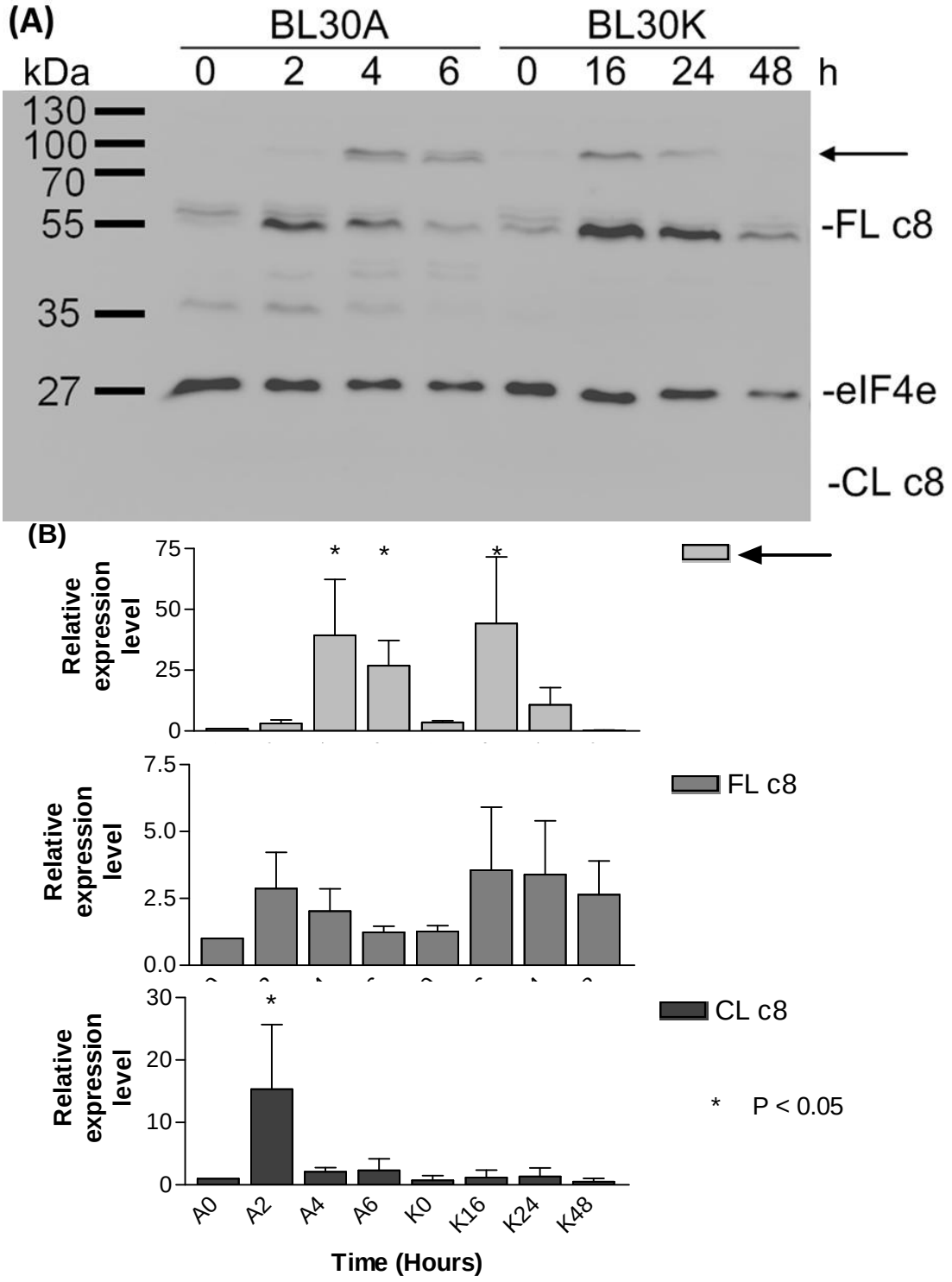

Figure 4.3: (A) Western blot of etoposide (68 µM) time course in BL30A and BL30K cells probing for caspase-8. The blot was treated with caspase-8 (Cell Signaling) antibody and then anti mouse secondary antibody conjugated to HRP at 1/20000 dilution. Exposure time was 10 minutes on standard. The blot had previously been probed with Western cocktail II. FL c8 – full length caspase-8, CL c8 – cleaved caspase-8, arrow indicates high molecular weight band to be discussed (likely multimers of cleaved caspase-8). eIF4e is shown as a loading control. The blot is representative of three biological replicates. **(B)** Quantified histogram of the expressed proteins normalised to eIF4e or ß-actin. Results expressed are the mean ± SEM. Asterisks indicate significant differences from unity.

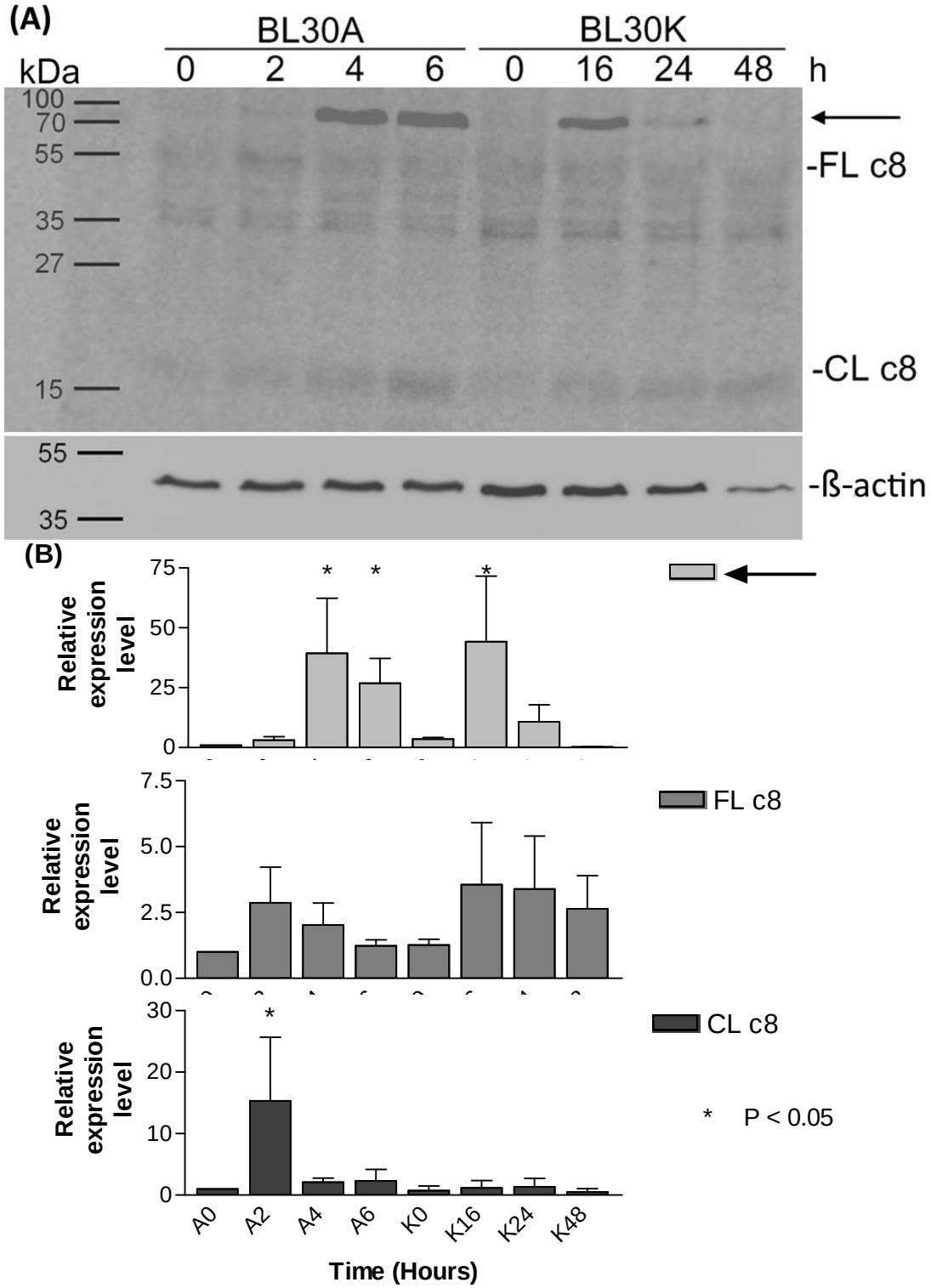

Figure 4.4: (A) Alternative Western blot of etoposide (68 µM) time course in BL30A and BL30K cells probing for caspase-8. Blot was treated with caspase-8 (Cell Signaling) antibody and then anti mouse secondary antibody conjugated to HRP at 1/20000 dilution. Exposure time was 5 minutes on super exposure. FL c8 – full length caspase-8, CL c8 – cleaved caspase-8, arrow indicates high molecular weight band to be discussed (likely multimers of cleaved caspase-8). The blot was re-probed with ß-actin (Sigma) as a loading control. The blot is representative of three biological replicates. **(B)** Quantified histogram of the expressed proteins normalised to eIF4e or ß-actin. Results expressed are the mean ± SEM. Asterisks indicate significant differences from unity.

Western blotting of caspase-9 was conducted to complement the inhibitor data. Caspase-9 cleavage in BL30K cells was not evident until 24 hours post treatment with etoposide, however the levels were very low (Figure 4.5).

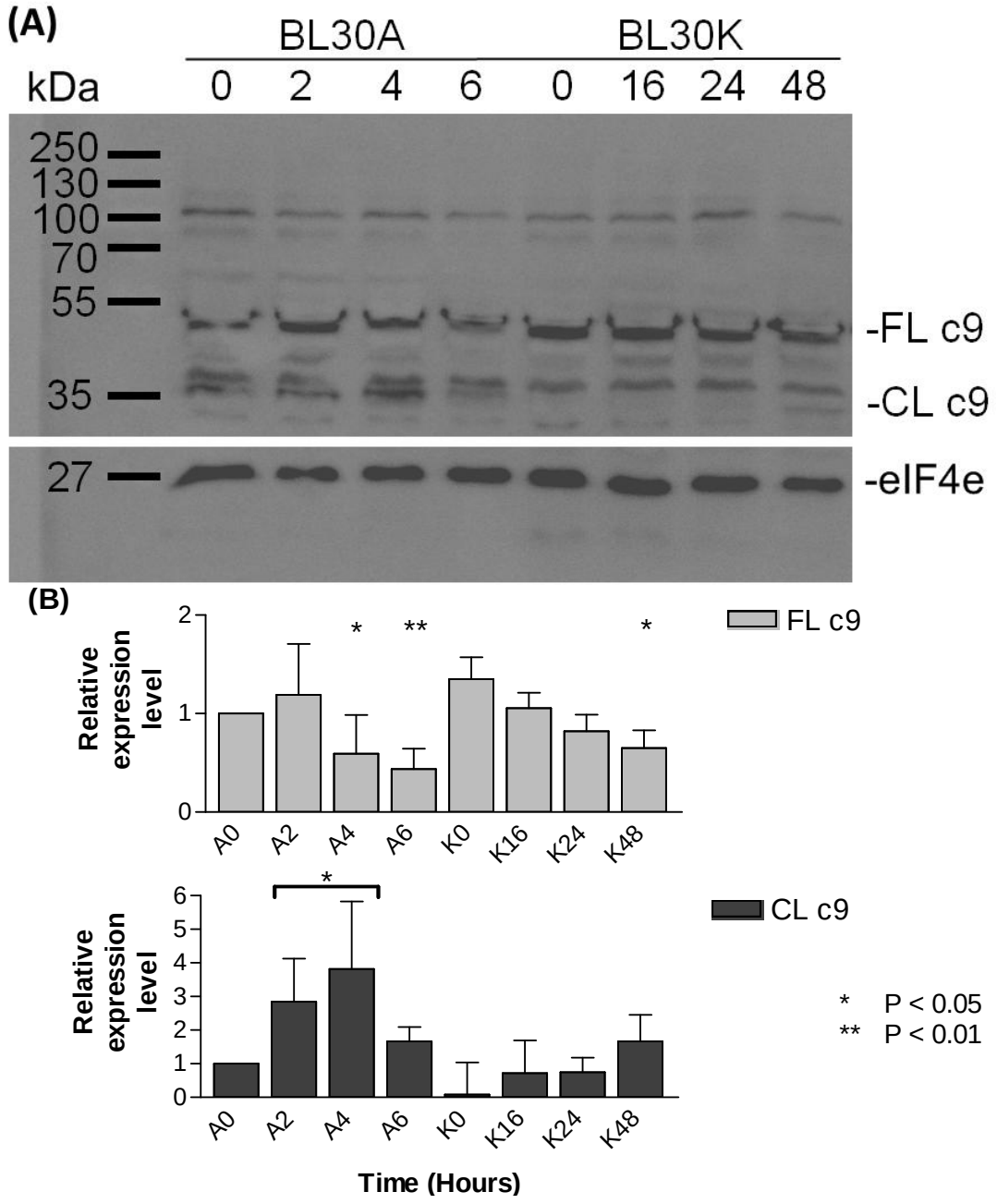

Figure 4.5: (A) Western blot of etoposide (68 µM) time course in BL30A and BL30K cells probing for caspase-9. The blot was treated with caspase-9 antibody (Cell Signaling) and then anti mouse secondary antibody. Exposure time was 10 minutes on standard exposure. FL c9 – full length caspase-9, CL c9 – cleaved caspase-9. eIF4e is shown as a loading control. This is the same Western blot as Figure 4.3 reprobed with different antibodies. The blot is representative of three biological replicates. **(B)** Quantified histogram of the expressed proteins normalised to eIF4e. Results expressed are the mean ± SEM. Asterisks indicate significant differences from unity.

4.3 Cell survival signalling in BL30K cells

Further investigation of upstream signalling events following DNA damage was also conducted. This was primarily looking at signalling pathways often modulated in response to DNA damage. p53 is one such protein, possibly the most well known protein activated in response to cellular stress. It has previously been reported that p53 is mutated in the BL30 cell line investigated (Khanna, Wie et al. 1996). Western blotting revealed that phosphorylated p53 was detected in BL30K cells even at the 0 hour time point (Figure 4.6). Furthermore, there was a marked increase in phospho p53 at 16 hours post etoposide indicating levels are increased in response to DNA damage. The BL30A cell line shows no detectable phospho p53 at 0 hours post treatment, and an increase at 2 hours to roughly the equivalent to the BL30K baseline level. These changes in phospho p53 levels were all compared using eIF4e as a loading control. BL30K cells were also probed with Bax to monitor the transcriptional activity of p53 (Figure 3.10). However there was little change in the expression of Bax indicating that p53 transcriptional regulation was not activated in response to etoposide treatment in BL30K.

The phosphorylated form of p38 MAPK – a key protein in the ERK/MAPK signalling pathway was also detected using Western blotting. Phospho p38 MAPK as mentioned earlier has been shown to inhibit activation of caspases (Alvarado-Kristensson, Melander et al. 2004). Phospho p38 MAPK was detected in BL30K cells at 16 hours post etoposide treatment (Figure 4.6). The BL30A cell line also shows an increase in phospho p38 MAPK at 2 hours post treatment.

Additionally, the phosphorylated form of S6 ribosomal protein was detected. S6 ribosomal protein is phosphorylated by p70 S6 kinase 1 and p70 S6 kinase 2 both of which also phosphorylate Bad (Harada, Andersen et al. 2001). Phosphorylation of Bad inactivates it preventing its interaction with Bcl-2 family proteins which promote mitochondrial permeabilisation (Adams and Cory 2007). Therefore, phosphorylation of S6RP could provide some indication of Bad phosphorylation also. Phospho S6 RP was detected at 0 and 16 hours in BL30K cells but declining at 24 hours and completely absent after 48 hours (Figure 4.6). The levels detected however were much lower in BL30K compared to BL30A. Phospho S6 ribosomal protein was detected to a higher degree in the BL30A cells when compared to the BL30K cells with highest expression at 0-4 hours and declining at 6 hours post treatment. It should be noted that phospho Bad was examined with Western blotting, unfortunately the antibody used failed to detect phospho Bad, and therefore that data was not included. Nonetheless, the finding that phosphorylation of S6RP was higher in BL30A than BL30K when it would be expected to induce apoptosis provides weak evidence against Bad being involved in apoptosis induction, but phosphorylation of Bad should be examined in future studies.

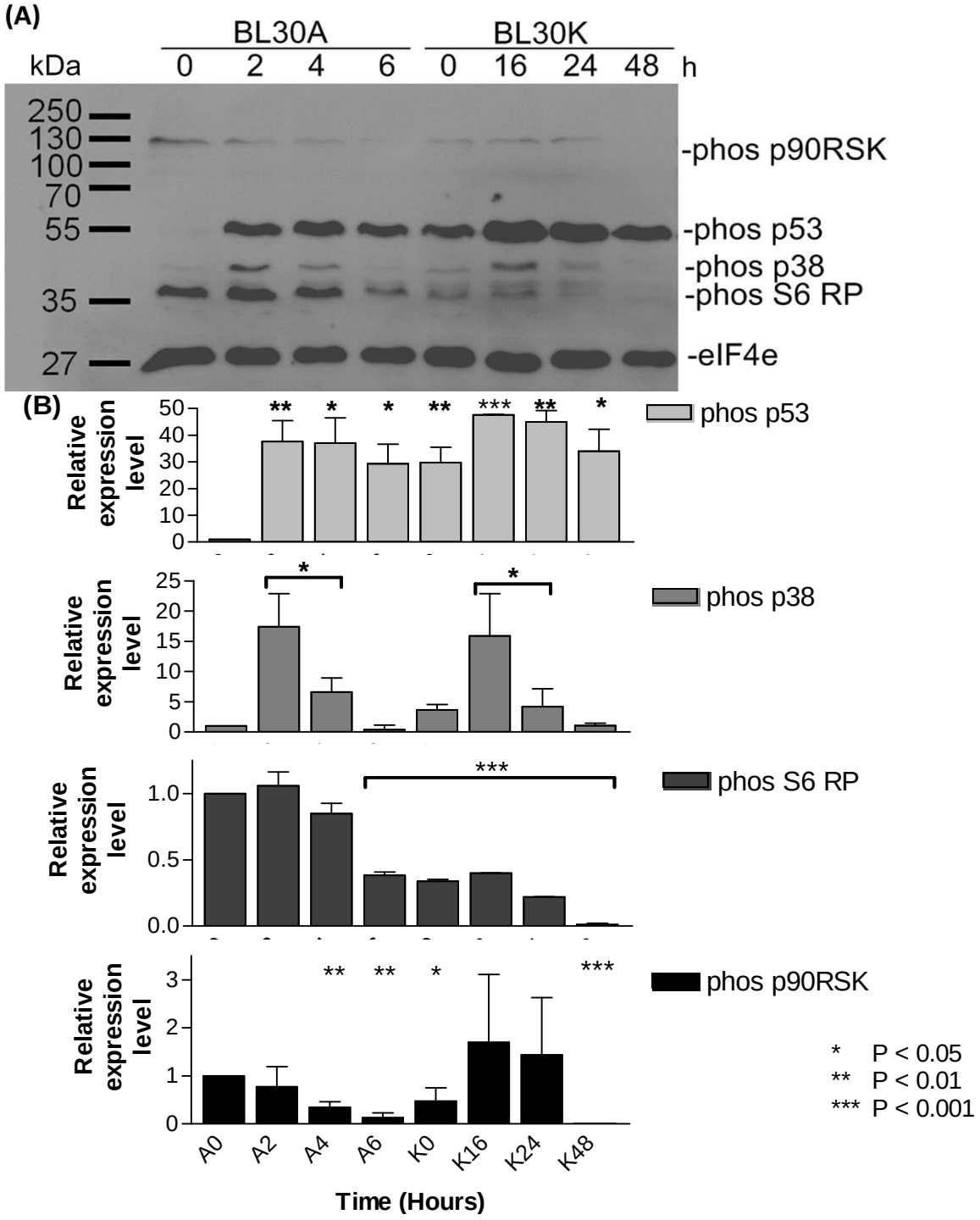

Figure 4.6: (A) Western blot of etoposide (68 µM) time course in BL30A and BL30K cells probing for Western cocktail II. Blot was treated with Western cocktail II (Cell Signaling) dilution and then anti mouse secondary antibody conjugated to HRP at 1/20000 dilution. Exposure time was 5 minutes on standard. Phos p90RSK – phospho p90RSK, phos p53 – phospho p53, phos p38 – phospho p38 MAPK, phos S6 RP – phospho S6 ribosomal protein. eIF4e acts as the loading control. This is the same Western blot as Figure 4.3 reprobed with different antibodies. The blot is representative of three biological replicates. **(B)** Quantified histogram of the expressed proteins normalised to eIF4e. Results expressed are the mean ± SEM. Asterisks indicate significant differences from unity.

Phosphorylation of Akt at Ser473 – involved in cell growth signalling pathways, was also monitored. Akt can activate mTOR by phosphorylating and inhibiting the TSC1 and TSC2 complexes (Dodson, Darley-Usmar et al. 2013). mTOR then acts to inhibit autophagy (Annovazzi, Mellai et al. 2009). There was a slight increase in phospho Akt beginning at 4 hours in BL30A, and a substantial increase at 48 hours in BL30K (Figure 4.7). Previous probing of the blot shows eIF4E as a loading control for comparison.

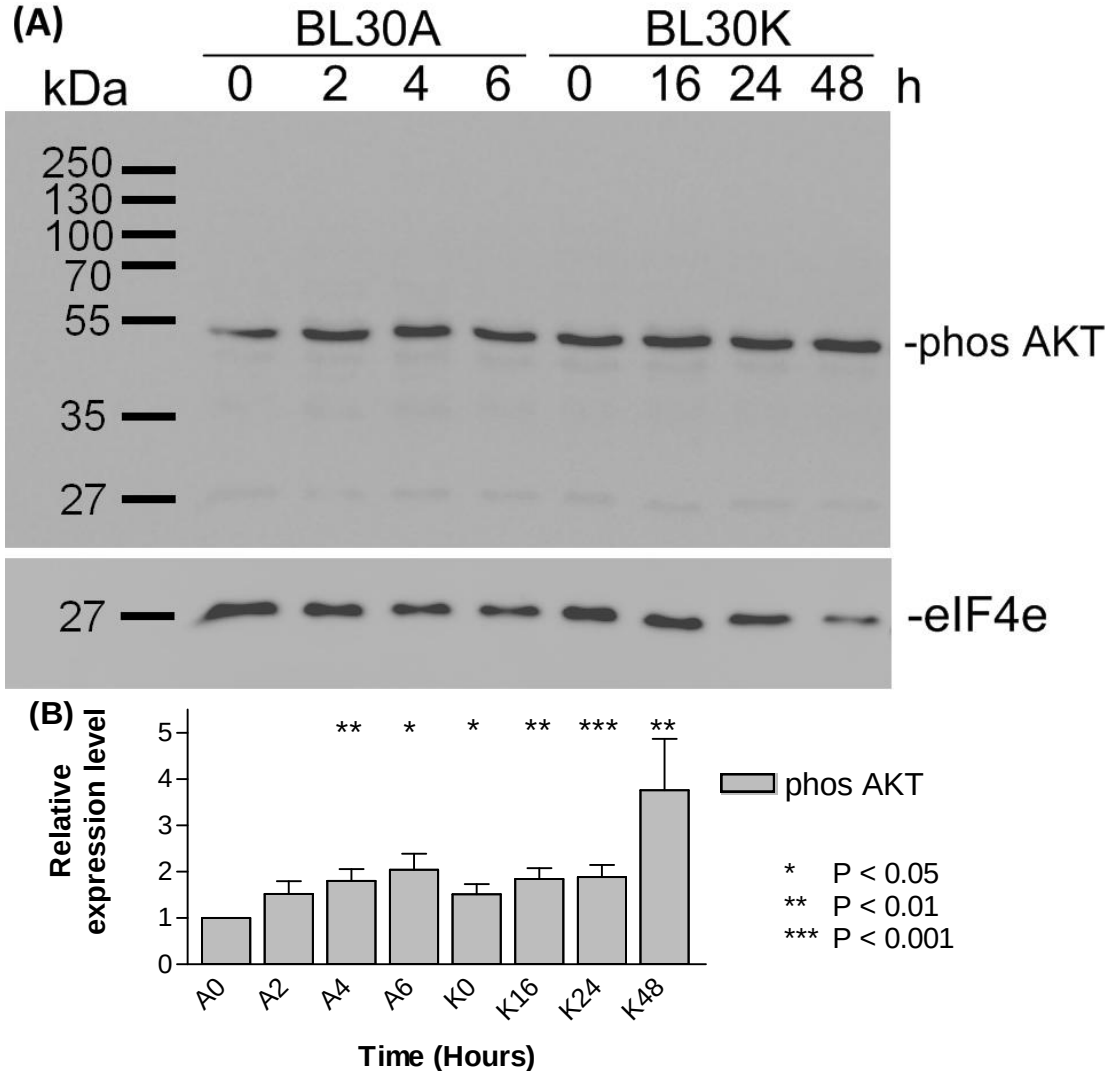

Figure 4.7: (A) Western blot of etoposide (68 µM) time course in BL30A and BL30K cells probing for phospho Akt. The blot was probed with phospho Akt (Ser473) (Cell Signaling) at dilution and then anti mouse secondary antibody conjugated to HRP at 1/20000 dilution. Exposure time was 2 seconds on high. Phos Akt – phospho Akt (Ser473). The blot had previously been probed with eIF4e as a loading control. This is the same Western blot as Figure 4.3 reprobed with different antibodies. The blot is representative of three biological replicates. **(B)** Quantified histogram of the expressed proteins normalised to eIF4e. Results expressed are the mean ± SEM. Asterisks indicate significant differences from unity.

4. 4 Surface Fas in BL30K cells

Because of the possible involvement of caspase-8, expression of the extrinsic death receptor protein Fas may be a factor in resistance of BL30K cells. Flow cytometric analysis of Fas showed expression of Fas at low levels in BL30K in both permeabilised and non permeabilised cells. Comparing the non-permeabilised secondary antibody only sample and the non-permeabilised primary and secondary antibody sample Fas is expressed on the surface of BL30K cells at low levels. This indicated that Fas is expressed on the surface of the cell (Figure 4.8a). Additionally, comparing the primary and secondary antibody in non-permeabilised cells sample and the primary and secondary antibodies in permeabilised samples there does not appear to be Fas expressed internally in BL30K cells. BL30A cells showed lower levels of Fas expression compared to BL30K cells (Figure 4.8b).

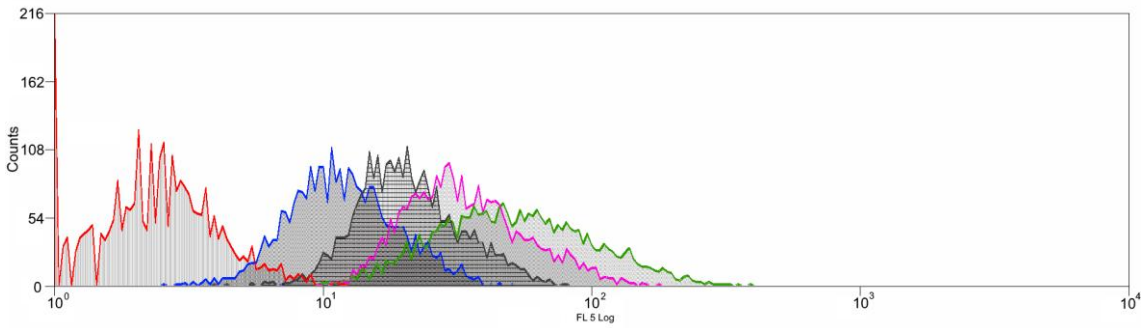

Figure 4.8a: Flow cytometric analysis of Fas in BL30K cells. Fluorescence intensities of Fas labelled cells are shown. Cells were fixed and then treated with anti-Fas antibody (Santa Cruz) followed by FITC secondary antibody (Sigma). Cells were permeabilised by 0.1% Triton X-100 in PBS where applicable. Samples are as follows: no antibodies control in permeabilised cells (red), secondary antibody only in permeabilised cells (gray), anti-Fas primary and secondary antibody in permeabilised cells (pink), secondary antibody only in non-permeabilised cells (blue), anti-Fas primary and secondary antibody in non-permeabilised cells (green). Results expressed are representative of two biological replicates.

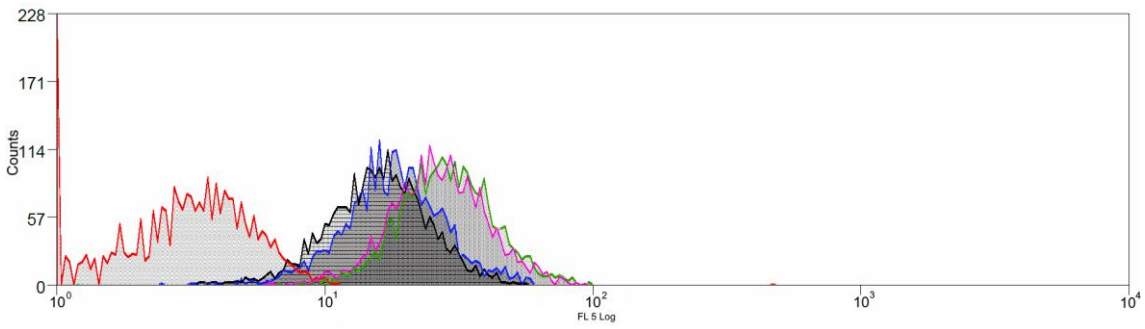

Figure 4.8b: Flow cytometric analysis of Fas in BL30A cells. Fluorescence intensities of Fas labelled cells are shown. Cells were fixed and then treated with anti-Fas antibody (Santa Cruz) followed by FITC secondary antibody (Sigma). Cells were permeabilised by 0.1% Triton X-100 in PBS where applicable. Samples are as follows: no antibodies control in permeabilised cells (red), secondary antibody only in permeabilised cells (gray), anti-Fas primary and secondary antibody in permeabilised cells (pink), secondary antibody only in non-permeabilised cells (blue), anti-Fas primary and secondary antibody in non-permeabilised cells (green). Results expressed are representative of two biological replicates.

As there was a small amount of expression of Fas at the cell surface induction of apoptosis using the Fas activating antibody CH-11 was assessed. However, Fas activating antibody CH-11 at a concentration of 100 ng/mL was ineffective at inducing apoptosis in BL30K cells, but successfully induced apoptosis in the positive control cell line, JHP (Figure 4.9).

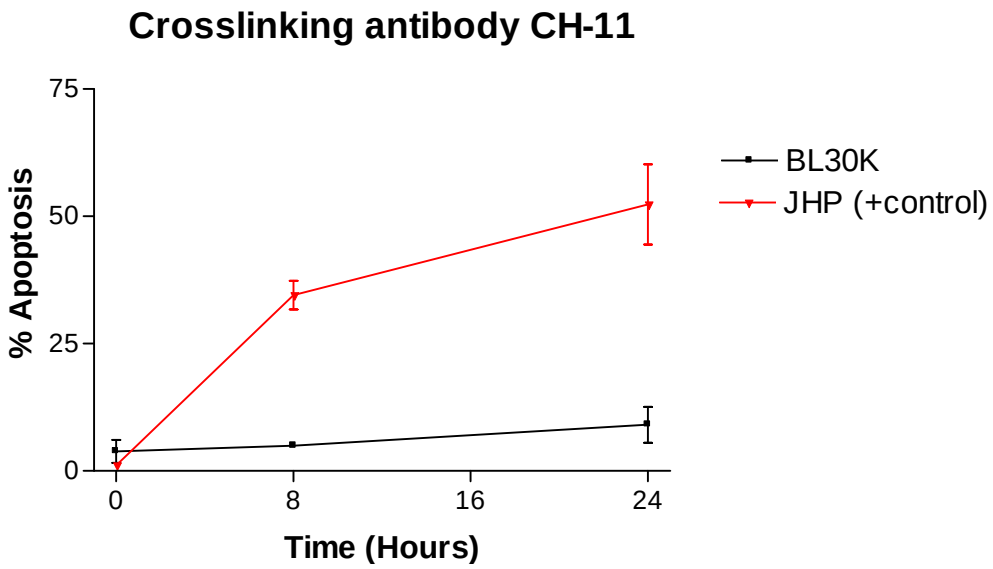

Figure 4.9: Apoptosis induction by Fas activating antibody CH-11 in BL30K cells. Addition of the Fas activating antibody (CH-11)(Millipore) at a concentration of 100 ng/mL was used to induce apoptosis. Apoptosis was measured at the indicated time points post treatment using DAPI nuclear staining. Percentages of apoptosis were obtained by counting six fields of cells under 200X magnification and dividing the number of apoptotic cells over total number of cells. Results expressed are the mean ± SEM of two replicate experiments.

4.5 RIP1 as a regulator of apoptosis

As Fas expression in BL30K cells was low, as in BL30A, an alternative activation mechanism of caspase-8 must be explored. RIP1 (otherwise known as RIP1) is an important protein in a complex called the RIPoptosome. This complex can not only initiate cell death via apoptosis or necroptosis but can also promote cell survival. Western blotting of RIP1 levels showed that RIP1 expression in BL30K cells is at lower levels than in BL30A cells (Figure 4.10). Re-probing of the blot with anti ß-actin is shown for comparison. RIP1 levels remain unchanged at 16 hours post etoposide treatment however levels begin to decrease at 24 hours post treatment. In the BL30A cell line RIP1 levels again remain relatively consistent until 4 hours post etoposide treatment where they begin to decline.

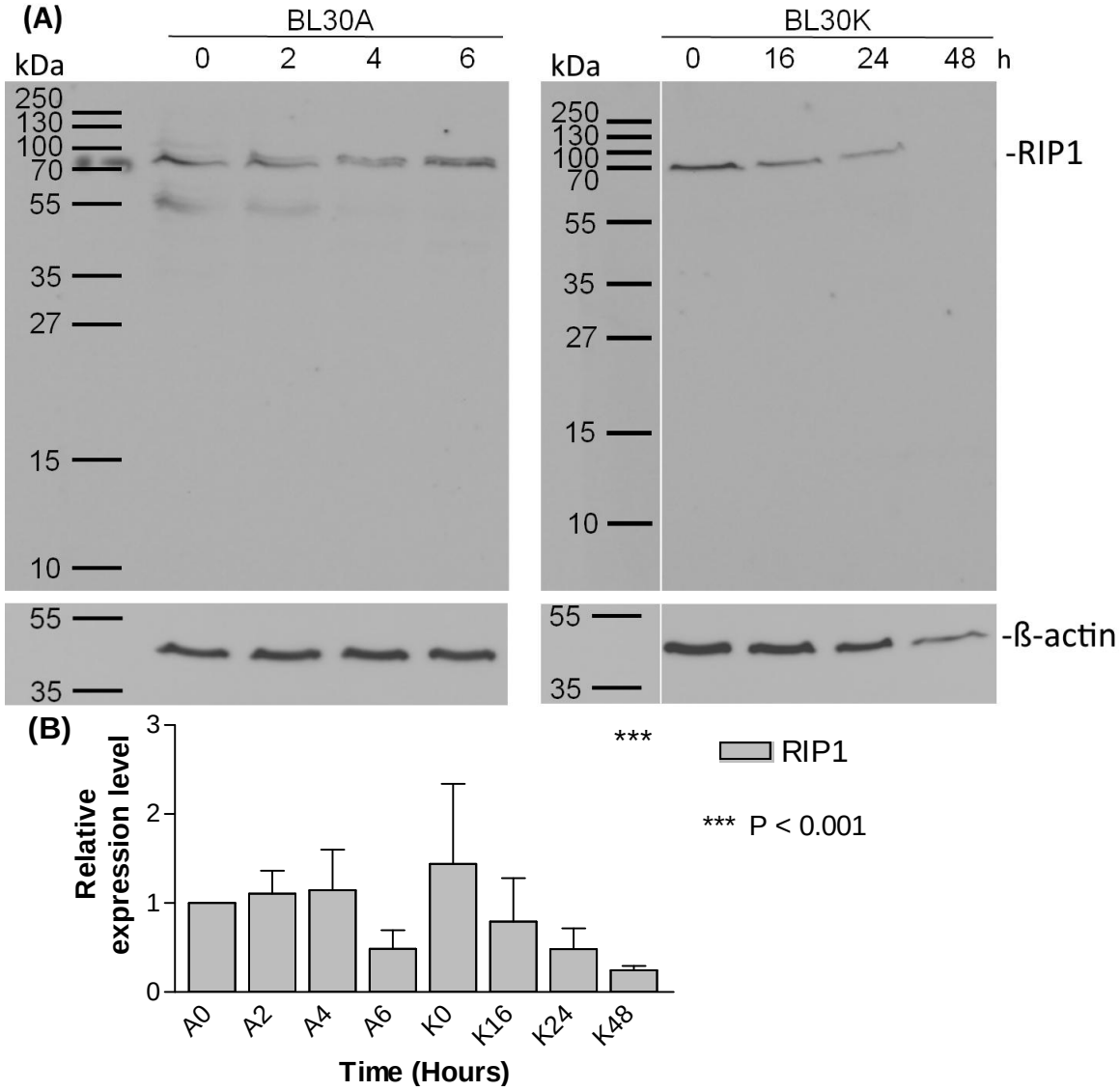

Figure 4.10: (A) Western blots of etoposide time course in BL30A and BL30K cell lines probing for RIP1. The blots were treated with mouse anti-RIP1 (BD Pharmingen) and then anti mouse secondary antibody conjugated to HRP. Exposure time for each was 20 minutes on high exposure. The blots were re-probed with ß-actin (Sigma) as a loading control. The blots are representative of three biological replicates. **(B)** Quantified histogram of the expressed proteins normalised to eIF4e. Results expressed are the mean ± SEM. Asterisks indicate significant differences from unity.

4.6 Involvement of FADD in BL30K apoptosis

FADD is a protein involved in cell death signalling in not only the extrinsic apoptosis pathway but also in the RIPoptosome. Expression of FADD in BL30K cells showed that levels were highest in untreated samples and decreased in response to etoposide (Figure 4.11). Re-probing of the blot with anti ß-actin as a loading control is shown for comparison. FADD was still detectable at 12 hours, but appeared absent at 24 hours post treatment. In the BL30A cell line began low but rose to a peak at 4 hours and then levels began to decrease. It should be noted that even at its peak in BL30A levels were higher in the untreated BL30K samples.

Native page analysis of FADD from chapter 3 revealed FADD in a high molecular weight complex in BL30K cells in both 0 and 4 hours post etoposide treatment (Figure 3.16). Additionally, immunoprecipitation of FADD revealed an interaction with caspase-8 in BL30K cells. These findings could suggest a complex involved in dysregulation of caspase-8 in BL30K cells.

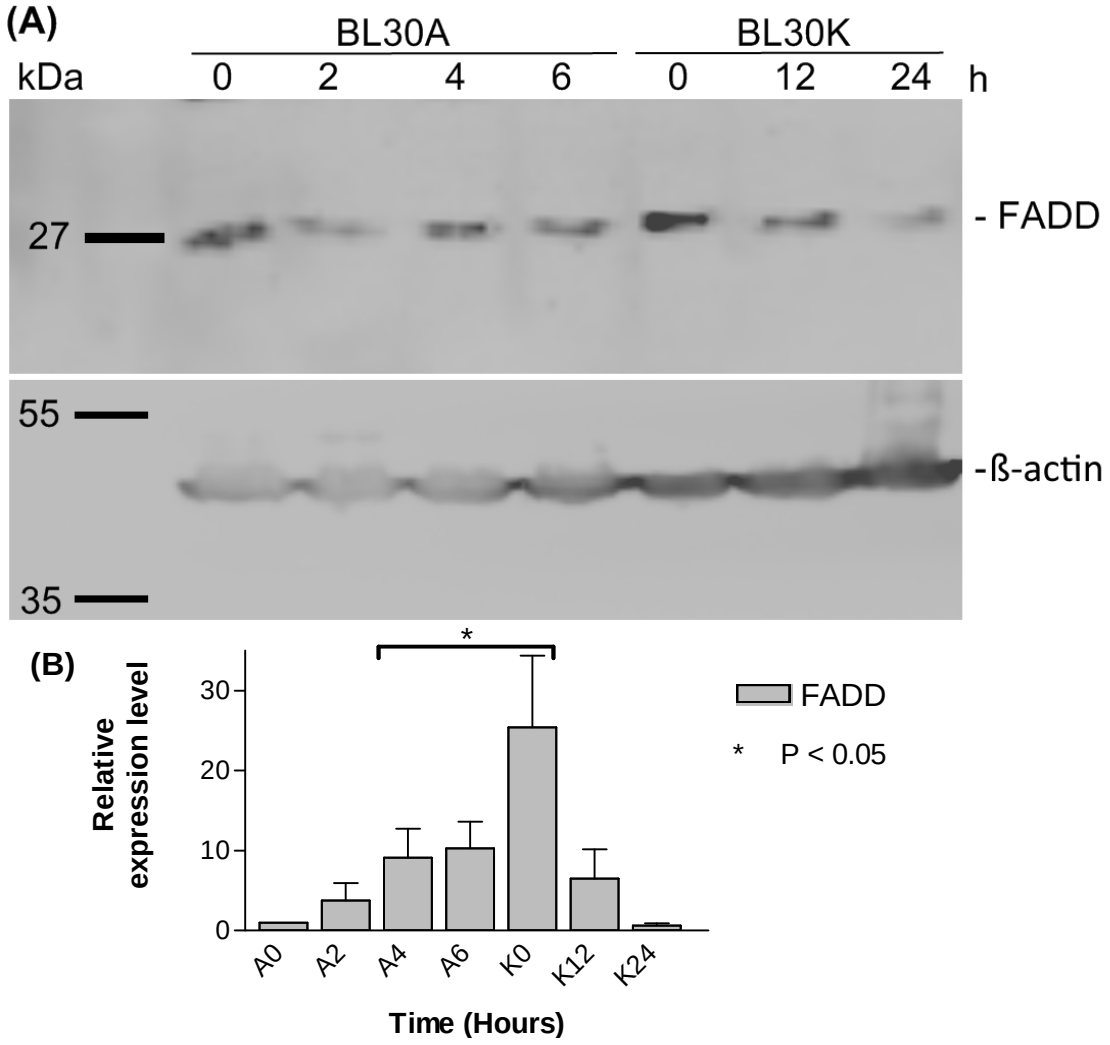

Figure 4.11: (A) Western blot of etoposide (68 µM) time course in BL30A and BL30K cells probing for FADD. The blot was previously probed with FADD (BD Pharmingen) (MW 28 kDa) and caspase-8 (Cell Signaling). The blot was probed with 1/500 FADD, and secondary antibody conjugated to HRP. Exposure time was 5 minutes on ultra exposure. ß-actin (Sigma) is shown in the middle panel as a loading control. The blot is representative of three biological replicates. **(B)** Quantified histogram of the expressed proteins normalised to eIF4e. Results expressed are the mean ± SEM. Asterisks indicate significant differences from unity.

4.7 Co-Immunoprecipitation and Mass Spectrometry of Caspase-8 comparing BL30A and BL30K cells

In order to determine the differences in protein interactions with caspase-8 in BL30A and BL30K cells a co-immunoprecipitation technique paired with mass spectrometry was used. In this technique a 'bait protein' is used to 'pull down' any other proteins interacting with the protein. The proteins 'pulled down' are then subjected to mass spectrometry for identification and the two cell lines can be compared. This work was undertaken at APAF (Australian Proteome Analysis Facility) the infrastructure provided by the Australian Government through the National Collaborative Research Infrastructure Strategy (NCRIS).

An immunoprecipitation of caspase-8 BL30A and BL30K cells 4 hours post treatment with etoposide was conducted as outlined in the methods section 2.4.21. However instead of the Protein G Sepharose beads being re-suspended in gel loading buffer they were stored in PBS at -80^{o}C and sent to the analysis facility via Express Post keeping the samples frozen using dry ice.

The samples were then subjected to on bead digestion in which 300µL of 100 mM triethylammonium bicarbonate (TEAB) and 1% sodium deoxycholate (SDC) was added to the beads and incubated at 95^{o}C for 5 minutes to release proteins from the beads. The samples were then reduced and alkylated with dithiothreitol (DTT) and iodoacetamide followed by digestion with trypsin at 37^{o}C overnight. The digestion was quenched by adding 2 µL formic acid and the precipitated SDC was removed by centrifugation (14,100g). The samples were dried and reconstituted in the loading buffer (2% acetonitrile, 0.1% formic acid) prior to nanoLC analysis.

The sample (10 µL) was injected onto a peptide trap (Michrome peptide Captrap) for pre-concentration and desalted with 0.1% formic acid, 2% ACN at 10 µL/min for 5 minutes. The peptide trap was then switched into line with the analytical column. Peptides were eluted from the column using a linear solvent gradient, with steps, from H_2O:CH_3CN (95:5; + 0.1% formic acid) to H_2O:CH_3CN (5:95; + 0.1% formic acid) with constant flow (550 nL/min) over an 80 minute period. The LC eluent was subject to positive ion nanoflow electrospray MS analysis in an information dependant acquisition mode (IDA). In the IDA mode a TOFMS survey scan was acquired (m/z 350-1500, 0.25 seconds), with ten largest multiply charged ions (counts >150) in the survey scan sequentially subjected to MS/MS analysis. MS/MS spectra were accumulated for 200 milli-seconds (m/z 100-1500) with rolling collision energy.

The raw data files (.wiff) were converted to mascot generic files (.mgf) using AB SCIEX CommandDriver software. They were submitted to Mascot (Matrix Science, UK) and searched against Homo sapiens in the SwissProt database.

The analysis revealed numerous interactions with caspase-8, many of which are interactions with high abundance proteins and non-relevant, such as keratins or immunoglobulins. Table 4.1 shows the results of the analysis. Unshaded cells indicate proteins expressed in both BL30A and BL30K, cells shaded green indicate proteins specific to their cell line. Proteins of interest include glucose regulated protein 78 (GRP78) – a glucose regulated protein with demonstrated effects on cell death signalling (Rao, Peel et al. 2002; Kong, Zhang et al. 2013), and heat shock cognate 71 kDa protein (HSP7C) – which is a stress response chaperone protein (Suk, Lin et al. 2015). GRP78 was immunoprecipitated by antibodies to caspase-8 in both BL30A and BL30K cells whereas HSP7C was only immunoprecipitated by antibodies to caspase-8 in BL30K cells (Table 4.1).

Table 4.1: Results of co-immunoprecipitation mass spectrometry in BL30A and BL30K cells 4 hours post etoposide treatment. White cells show commonalities between the two samples, green show the differences.

BL30A	
K2C1_HUMAN	Keratin, type II cytoskeletal 1 OS=Homo sapiens GN=KRT1 PE=1 SV=6
K22E_HUMAN	Keratin, type II cytoskeletal 2 epidermal OS=Homo sapiens GN=KRT2 PE=1 SV=2
K1C10_HUMAN	Keratin, type I cytoskeletal 10 OS=Homo sapiens GN=KRT10 PE=1 SV=6
GRP75_HUMAN	Stress-70 protein, mitochondrial OS=Homo sapiens GN=HSPA9 PE=1 SV=2
K1C9_HUMAN	Keratin, type I cytoskeletal 9 OS=Homo sapiens GN=KRT9 PE=1 SV=3
K2C6B_HUMAN	Keratin, type II cytoskeletal 6B OS=Homo sapiens GN=KRT6B PE=1 SV=5
K2C5_HUMAN	Keratin, type II cytoskeletal 5 OS=Homo sapiens GN=KRT5 PE=1 SV=3
K1C14_HUMAN	Keratin, type I cytoskeletal 14 OS=Homo sapiens GN=KRT14 PE=1 SV=4
K1C16_HUMAN	Keratin, type I cytoskeletal 16 OS=Homo sapiens GN=KRT16 PE=1 SV=4
ACTB_HUMAN	Actin, cytoplasmic 1 OS=Homo sapiens GN=ACTB PE=1 SV=1
TBA1A_HUMAN	Tubulin alpha-1A chain OS=Homo sapiens GN=TUBA1A PE=1 SV=1
H4_HUMAN	Histone H4 OS=Homo sapiens GN=HIST1H4A PE=1 SV=2
FUS_HUMAN	RNA-binding protein FUS OS=Homo sapiens GN=FUS PE=1 SV=1
TBB5_HUMAN	Tubulin beta chain OS=Homo sapiens GN=TUBB PE=1 SV=2
EF1A1_HUMAN	Elongation factor 1-alpha 1 OS=Homo sapiens GN=EEF1A1 PE=1 SV=1
GRP78_HUMAN	78 kDa glucose-regulated protein OS=Homo sapiens GN=HSPA5 PE=1 SV=2
HNRH1_HUMAN	Heterogeneous nuclear ribonucleoprotein H OS=Homo sapiens GN=HNRNPH1 PE=1 SV=4
FILA2_HUMAN	Filaggrin-2 OS=Homo sapiens GN=FLG2 PE=1 SV=1
IGKC_HUMAN	Ig kappa chain C region OS=Homo sapiens GN=IGKC PE=1 SV=1
RLA2_HUMAN	60S acidic ribosomal protein P2 OS=Homo sapiens GN=RPLP2 PE=1 SV=1
H2B1A_HUMAN	Histone H2B type 1-A OS=Homo sapiens GN=HIST1H2BA PE=1 SV=3
H3C_HUMAN	Histone H3.3C OS=Homo sapiens GN=H3F3C PE=1 SV=3
H2A1B_HUMAN	Histone H2A type 1-B/E OS=Homo sapiens GN=HIST1H2AB PE=1 SV=2
RLA0L_HUMAN	60S acidic ribosomal protein P0-like OS=Homo sapiens GN=RPLP0P6 PE=5 SV=1
TIAR_HUMAN	Nucleolysin TIAR OS=Homo sapiens GN=TIAL1 PE=1 SV=1
IGHM_HUMAN	Ig mu chain C region OS=Homo sapiens GN=IGHM PE=1 SV=3
ROA2_HUMAN	Heterogeneous nuclear ribonucleoproteins A2/B1 OS=Homo sapiens GN=HNRNPA2B1 PE=1 SV=2

Table 4.1 (continued)

BL30K	
K2C1_HUMAN	Keratin, type II cytoskeletal 1 OS=Homo sapiens GN=KRT1 PE=1 SV=6
K1C10_HUMAN	Keratin, type I cytoskeletal 10 OS=Homo sapiens GN=KRT10 PE=1 SV=6
GRP75_HUMAN	Stress-70 protein, mitochondrial OS=Homo sapiens GN=HSPA9 PE=1 SV=2
K22E_HUMAN	Keratin, type II cytoskeletal 2 epidermal OS=Homo sapiens GN=KRT2 PE=1 SV=2
K1C9_HUMAN	Keratin, type I cytoskeletal 9 OS=Homo sapiens GN=KRT9 PE=1 SV=3
TBA1B_HUMAN	Tubulin alpha-1B chain OS=Homo sapiens GN=TUBA1B PE=1 SV=1
K2C5_HUMAN	Keratin, type II cytoskeletal 5 OS=Homo sapiens GN=KRT5 PE=1 SV=3
K1C14_HUMAN	Keratin, type I cytoskeletal 14 OS=Homo sapiens GN=KRT14 PE=1 SV=4
HSP7C_HUMAN	Heat shock cognate 71 kDa protein OS=Homo sapiens GN=HSPA8 PE=1 SV=1
IGHM_HUMAN	Ig mu chain C region OS=Homo sapiens GN=IGHM PE=1 SV=3
ACTB_HUMAN	Actin, cytoplasmic 1 OS=Homo sapiens GN=ACTB PE=1 SV=1
G3P_HUMAN	Glyceraldehyde-3-phosphate dehydrogenase OS=Homo sapiens GN=GAPDH PE=1 SV=3
PROF1_HUMAN	Profilin-1 OS=Homo sapiens GN=PFN1 PE=1 SV=2
GRP78_HUMAN	78 kDa glucose-regulated protein OS=Homo sapiens GN=HSPA5 PE=1 SV=2
EF1A1_HUMAN	Elongation factor 1-alpha 1 OS=Homo sapiens GN=EEF1A1 PE=1 SV=1
RS16_HUMAN	40S ribosomal protein S16 OS=Homo sapiens GN=RPS16 PE=1 SV=2
FUS_HUMAN	RNA-binding protein FUS OS=Homo sapiens GN=FUS PE=1 SV=1
H4_HUMAN	Histone H4 OS=Homo sapiens GN=HIST1H4A PE=1 SV=2
TBB5_HUMAN	Tubulin beta chain OS=Homo sapiens GN=TUBB PE=1 SV=2
RLA2_HUMAN	60S acidic ribosomal protein P2 OS=Homo sapiens GN=RPLP2 PE=1 SV=1
IGKC_HUMAN	Ig kappa chain C region OS=Homo sapiens GN=IGKC PE=1 SV=1
DCD_HUMAN	Dermcidin OS=Homo sapiens GN=DCD PE=1 SV=2
S10A9_HUMAN	Protein S100-A9 OS=Homo sapiens GN=S100A9 PE=1 SV=1
UBP2L_HUMAN	Ubiquitin-associated protein 2-like OS=Homo sapiens GN=UBAP2L PE=1 SV=2
BRD3_HUMAN	Bromodomain-containing protein 3 OS=Homo sapiens GN=BRD3 PE=1 SV=1

4.8 Discussion

The BL30K cell line has been shown to be resistant to DNA damage induced apoptosis. It was shown that there was a delay in apoptosis induction and the cause for this resistance when compared to the BL30A cell line was explored. BL30K cells begin to undergo apoptosis at 12 hours post treatment with etoposide (Figure 4.1) compared with 2-3 hours post treatment in the BL30A cells (Figure 3.1). The delay in apoptosis would seem to indicate a protective mechanism in the BL30K cells which is not present in the BL30A cells which delays the onset of apoptosis. Other factors influencing cell survival may be involved. Despite the differences in the time frame of apoptosis induction in BL30A compared to BL30K, inhibition of caspase-8 was effective at preventing the apoptotic response in BL30K (Figure 4.2). Cell death levels when comparing BL30K cells treated with etoposide and caspase-9 inhibitor were indistinguishable between levels of cells treated with etoposide only. Inhibition of caspase-8 activity however abrogated the apoptosis response with levels of apoptosis comparable to control untreated cells.

Western blotting of caspase-8 showed decreasing levels of the full length form, as would be expected with its activation. The lower molecular weight cleavage fragments were detected in BL30K as early as 16 hours post treatment, consistent with the observed levels of apoptosis in BL30K. However, detection of a band of approximately 70 kDa upon probing with caspase-8 antibody was consistently found in the BL30K 16 and 24 hour post treatment time points as well as the BL30A 4 and 6 hour time points. Quantification revealed approximately an 8-fold increase in this band at 4 hours post treatment in BL30A and 16 hours in BL30K. These times coincide with observed apoptosis induction. Non-specific binding of the antibody could theoretically be responsible for this band, however the very specific expression times merit a different explanation. This finding may indicate that the partially cleaved caspase-8 fragment or a subset of cleaved caspase-8 fragments are forming a complex at this higher molecular weight. Although it is widely regarded that complexes cannot form under

SDS-PAGE conditions it has been documented that under certain circumstances complexes are sometimes visualised on SDS-PAGE (Sweadner 1991; Linderoth, Model et al. 1996; Soulie, Moller et al. 1996; Rath, Glibowicka et al. 2009; Tulumello and Deber 2009). Papers reporting this phenomenon are scarce, as many research groups would dismiss the results owing to the observation of incorrect molecular weight bands. Furthermore, upon seeing this phenomenon it would often go unreported and measures would be taken to ensure these complexes cannot form. One such method is the addition of a large concentration of urea to the sample buffer (Soulie, Moller et al. 1996). Membrane proteins are also prone to formation of complexes in SDS-PAGE conditions as well as proteins with very strong interactions (Tulumello and Deber 2009). Nevertheless, this 70 kDa band was detected at times corresponding with apoptosis upon probing with caspase-8. Additionally, detection of this band was seemingly inversely proportional to full length caspase-8 levels. This provides some evidence of the cleavage and activation of caspase-8, and for the formation of a multimeric cleaved caspase complex. This finding is consistent with the current knowledge base of activated caspase-8 forming dimers. Future studies should attempt to identify the protein in this band through mass spectrometry techniques.

The finding that apoptosis does not begin until 12 hours post treatment and that inhibition of caspase-8 but not caspase-9 inhibits apoptosis provide evidence for a caspase-8 regulated pathway of apoptosis occurring in response to DNA damage in the BL30K cell line. The cause for the delay in the apoptotic response however remains unresolved. Upstream signalling events must be contributing factors to provide the delay in apoptosis induction. Signalling pathways which influence cellular responses to stress must therefore be explored. Phosphorylation of p53 was clearly elevated in the BL30K cell line when compared to the BL30A cell line (Figure 4.6). This difference highlights an important disparity between the two cell lines. Under normal conditions p53 levels should remain low owing to regulation by Mdm2 (Coutts, Adams et al. 2009). However BL30K expressed high levels of phosphorylated p53, even when untreated. Furthermore, upon DNA damage phospho-p53 levels in BL30K increased sharply by 16 hours post treatment indicating its activation in response to the insult.

Quantification revealed an approximate 2-fold increase in phospho p53 by 16 hours post etoposide treatment. Levels of p53 then began to slowly decline back to baseline levels by 48 hours post treatment. Increases in phospho-p53 levels coinciding with apoptosis may point to p53 promoting the apoptosis response, however the complexities of p53 involvement in survival and death responses makes drawing this conclusion unjustified without further evidence and investigation. Transcriptional activity of p53 was monitored by Bax expression (Figure 3.10), however no notable differences in expression were observed over the time course of treatment indicating that transcriptional activity of p53 is not involved in BL30K apoptosis signalling.

Phosphorylation of p38 MAPK was also observed at times consistent with the induction of apoptosis. p38 MAPK has the potential to modulate the death survival continuum and could be a contributing factor in the delayed apoptosis induction in BL30K. p38 MAPK has been shown to interact with caspases-8 and -3 and promote cell survival by phosphorylation of the caspases in neutrophil cells (Alvarado-Kristensson, Melander et al. 2004). Phospho p38 MAPK was detected in BL30K cells at 16 hours post etoposide treatment (Figure 4.6). The BL30A cell line also shows an increase in phospho p38 MAPK at 2 hours post treatment. However, as caspases are being activated in response to etoposide, p38 inhibition is ineffective at preventing apoptosis (Figure 3.21) and p38 MAPK has been reported to not be needed in apoptosis induced by IR in BL30A (Michael-Robinson, Spring et al. 2001), p38 MAPK involvement does not appear to be necessary in the apoptotic response.

Phosphorylation of Akt at Ser473 was also monitored. Akt can activate mTOR by phosphorylating and inhibiting the TSC1 and TSC2 complexes (Dodson, Darley-Usmar et al. 2013). mTOR then acts to inhibit autophagy (Annovazzi, Mellai et al. 2009). Akt is known to exert anti-apoptotic effects (Tang, Okada et al. 2001). There was only a marginal increase in phosphorylation of Akt in BL30A cells, and only at 4 hours – after apoptosis had begun (Figure 4.7). Little change in phosphorylation of Akt was seen in BL30K until 48 hours where there was a large increase, however this was after

apoptosis was already occurring (Figure 4.7). This provided evidence against Akt as a regulator of apoptosis in response to DNA damage in BL30A and BL30K cells.

Another possibility for the resistance of BL30K cells to apoptosis was the down-regulation of Fas – a protein involved in activation of caspase-8. Expression of Fas on the surface of the cell appeared slightly higher in BL30K cells compared to BL30A cells (Figure 4.8). This finding is in agreement with findings that Group III BL cells – of which BL30K is a member, express Fas on the cell surface (Haynes, Daniels et al. 2002). However, induction of apoptosis by Fas activating antibody CH-11 was ineffective in BL30K cells providing evidence against Fas involvement (Figure 4.9). It remains unlikely that apoptosis is activated through Fas as expression levels were very low and Fas activating antibody did not induce apoptosis in BL30K cells.

Components of the RIPoptosome were also examined as a possibility of resistance. The RIPoptosome is a complex capable of regulating cell death by not only apoptosis but by necroptosis also (Imre, Larisch et al. 2011). RIP1 levels were indeed higher in BL30A cells than BL30K (Figure 4.10). As the RIPoptosome can cause apoptosis induction, the higher levels of RIP1 in BL30A could explain the earlier apoptotic response in BL30A. FADD – another RIPoptosome component was expressed at increasing levels over time in BL30A but expressed at higher background levels in BL30K which decreased over time (Figure 4.11). Additionally, native PAGE analysis of FADD from chapter 3 revealed a high molecular weight complex at 0 and 4 hour post etoposide treatment samples in BL30K cells (Figure 3.17). Immunoprecipitation experiments of FADD were inconclusive and IP of caspase-8 in BL30K cells should be conducted to reveal an interaction between caspase-8 and FADD in BL30K cells (Figure 3.19a and 3.19b). Caspase-8 is the third component of the RIPoptosome and can be activated by the complex, however several factors influence this activation such as the ratios of FLIP isoforms (Feoktistova, Geserick et al. 2011). These findings would be consistent with the presence of a high molecular weight complex which regulates cell

death. Unfortunately we were unable to investigate FLIP isoforms in this study but this would be a worthwhile exploration avenue in the future.

Additionally, a preliminary co-immunoprecipitation mass spectrometry assay was performed (Table 4.1). This assay highlighted some differences between protein interactions of caspase-8 in BL30A and BL30K. Many of the proteins detected using this assay were high abundance proteins and not relevant to apoptosis, however there were a few proteins of interest, which the literature has indicated to modulate apoptosis signalling. Of note was a protein called heat shock cognate 71 (HSP7C also called HSPA8 and HSC70) – which was only seen in the BL30K samples. HSP7C is a stress response chaperone protein (Suk, Lin et al. 2015). It has been shown to interact with Dredd (the Drosophila caspase-8 homolog) and modulate the immune response to bacteria (Fukuyama, Ndiaye et al. 2012). HSP7C has also been shown to be modulated in response to the anti-cancer drug bortezomib in mantle cell lymphoma (Weinkauf, Zimmermann et al. 2009). HSP7C up-regulation was observed upon treatment with bortezomib in Burkitt's lymphoma cells (Suk, Lin et al. 2015). Staurosporine treatment induced apoptosis and also increased expression of HSP7C in neuroblastoma cells (Short, Heron et al. 2007). Furthermore, inhibition of HSP7C in tandem with inhibition of HSP72 led to extensive apoptosis in HCT116 human colon cancer cells (Powers, Clarke et al. 2008). These results may indicate a protective role for HSP7C in BL30K apoptosis taking into account literature regarding HSP7C protein interactions. However, owing to time constraints, HSP7C was not investigated further. To confirm the interaction of HSP7C and caspase-8 immunoprecipitations should be conducted using antibodies to HSP7C and Western blotting. Another protein of interest was glucose regulated protein 78 (GRP78). This protein was detected in both BL30A and BL30K cells. GRP78 is a regulator of translocation across the ER membrane and also acts as an apoptotic regulator in response to ER stress (Rao, Peel et al. 2002). GRP78 interacts with caspases-7 and 12 to form a complex which down-regulates apoptosis (Rao, Peel et al. 2002; Kong, Zhang et al. 2013). Although GRP78 was seen in both cell lines, the affinity of the interaction is unknown and because it has been shown to modulate the cell death response GRP78 warrants further investigation.

Again, immunoprecipitations of GRP78 and caspase-8 should be conducted to confirm the interaction between the proteins.

To summarise, delayed apoptosis in response to etoposide treatment was observed in BL30K cells compared to BL30A. The apoptosis of BL30K cells appears dependent on caspase-8 and not caspase-9 activation. Other factors must therefore be promoting cell survival to counteract the induction of the apoptosis. These may include p53, which was phosphorylated to a higher degree in response to DNA damage in BL30K cells or possibly p38 MAPK which was also phosphorylated in response to the DNA damage. Phosphorylation of p53 was detectable even in the untreated sample which contrasts with BL30A where phospho p53 only became detectable post treatment. Phosphorylation of Akt (Ser473) did not occur until after apoptosis induction in BL30A and BL30K cells, likely precluding its involvement. Additionally, the expression of Fas appeared to be unaffected by DNA damage indicating it is likely uninvolved in apoptosis induction in response to DNA damage in BL30A and BL30K cells. However RIP1 expression appears lower in the resistant BL30K cell line than its apoptosis sensitive sister cell line BL30A highlighting a difference which may contribute to the resistance to apoptosis observed in BL30K cells.

Chapter 5

The Anti-Austerity Compound Angelmarin

5.1 Introduction

5.1.1 Pancreatic Cancer

Pancreatic cancer is the 10th and 9th most prevalent cancer in men and women respectively in the United States (Blum and Kloog 2014). Pancreatic cancer is considered to be one of the more lethal cancers, with a mean 5 year survival of only 4-5% (Bhardwaj, Rizvi et al. 2010; Ueda, Athikomkulchai et al. 2013). Current cancer treatment is largely ineffective against pancreatic cancer (Dai, Gao et al. 2013; Blum and Kloog 2014). Several factors contribute to the ineffective treatment of pancreatic cancer. Firstly, due to the location of the pancreas in relation to other organs diagnosis is very difficult. Early symptoms are not specific to pancreatic cancer and diagnosis is often not made until late stages – approximately 85% after the tumour has metastasised and is no longer only locally confined to the pancreas (Shore, Vimalachandran et al. 2004; Magolan and Coster 2010). Pancreatic cancer most often metastasises to regional lymph nodes, the liver and the peritoneal cavity. Additionally, owing to its location surgical intervention is often impossible (Bhardwaj, Rizvi et al. 2010). Secondly, a major challange in the treatment of Pancreatic cancer is that there is a very high level of heterogeneity between pancreatic cancers (Biankin, Waddell et al. 2012). Investigations of pancreatic cancer genomes showed that a significant proportion of pancreatic cancers have amplifications of oncogenes, however the majority of amplifications presented at low individual prevalence, demonstrating that progression of pancreatic cancer is influenced by a diverse range of mechanisms (Waddell, Pajic et al. 2015). An extensive study of genomes of more than 450 PDACs has recently demonstrated the great extent of heterogeneity in pancreatic cancer showing more than 20,000 coding mutations as well as more than 20,000 genomic rearrangements. The research group has divided PDACs into four sub-types based on gene expression profiles: squamous, pancreatic progenitor, immunogenic, and aberrantly differentiated endocrine exocrine (ADEX) (Bailey, Chang et al. 2016). Understanding the vast genetic differences between pancreatic cancers is needed for the development of effective treatment strategies, especially in the hopes of developing targeted treatments for the molecular phenotype of individual patients

(Biankin, Waddell et al. 2012; Waddell, Pajic et al. 2015; Bailey, Chang et al. 2016). Finally, chemotherapeutic drugs are largely ineffective against pancreatic cancer (Shore, Vimalachandran et al. 2004). Therefore alternative treatments must be considered.

Adding to the difficulty of treatment, several pancreatic cancers show high tolerance to starvation in comparison to other cancer types and high expression of Akt was associated with this tolerance (Izuishi, Kato et al. 2000; Awale, Ueda et al. 2012). Pancreatic cancers are capable of surviving up to 72 hours without nutrients where other cell lines die within 24 hours (Awale, Ueda et al. 2012; Ueda, Athikomkulchai et al. 2013). PANC-1 pancreatic cancer cells were shown to have greater than 50% survival after 48 hours in complete nutrient deficiency conditions (Izuishi, Kato et al. 2000). Akt is thought to be at least partially responsible for this tolerance, and under nutrient deprivation conditions in PANC-1 cells is phosphorylated within 2 hours (Izuishi, Kato et al. 2000).

5.1.2 Anti-Austerity

An area of study which is being examined here is the possibility of using anti-austerity drugs to destroy pancreatic cancer. Austerity, in this context is the ability of cells to survive withdrawal of nutrients, oxygen, or other metabolites. Such compounds have been theorised to be useful in combating cancer as tumours are often poorly vascularised thus leading to cancer cells being undernourished (Vaupel, Kallinowski et al. 1989; Momose, Ohba et al. 2010; Dang 2012). The advantages of using anti-austerity drugs to destroy cancer cells is that normal cells, likely to have sufficient nutrients, will be unaffected by the addition of the drug, and selectively kill the cancer cells. Akt and AMPK are closely related to the tolerance of pancreatic cancers to nutrient deprivation (Suzuki, Kusakai et al. 2003).

5.2 Nutrient Deprivation

In order to assess PANC-1 response to nutrient deprivation conditions, cells were grown under several different conditions. Following washing with PBS to remove the nutrients, growth conditions included complete culture medium (DMEM supplemented with glucose, and 10% FBS), nutrient deprivation medium (PBS supplemented with MEM vitamin solution), and deprivation medium supplemented with either glucose, 10% FBS or amino acids. Cell growth and viability was then assessed after 24 or 48 hours on incubation at 37^{o}C and 5% CO_2. Cell staining with trypan blue was used to monitor cell death by loss of cell membrane integrity. Cell growth was monitored using the WST-1 cell proliferation assay to monitor mitochondrial activity.

Pancreatic cancer demonstrates a remarkable tolerance to nutrient deprivation. The pancreatic cancer cell lines PANC-1, AsPC-1, BxPC-1, and KP-3 all demonstrate high tolerance to nutrient deprivation (Izuishi, Kato et al. 2000). The PANC-1 cells used in this study when grown in the complete absence of nutrients, that is PBS supplemented with vitamins, showed less than 10% cell death after 24 hours, and less than 25% cell death after 96 hours (Figure 5.1). This tolerance to nutrient starvation is quite remarkable, even among cancer cells.

Supplementation of 25 mM glucose to nutrient deprived conditions further increased cell survival of PANC-1 cells. Slightly higher levels of cell death were observed at 24 and 48 hours in PANC-1 cells supplemented with glucose compared to cells grown without glucose. At 96 hours less than 20% cell death was observed using the trypan blue stain (Figure 5.1).

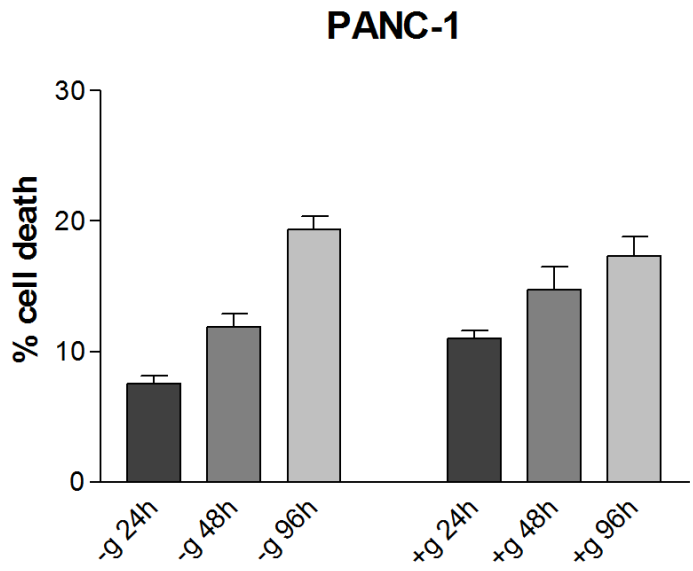

Figure 5.1: Tolerance of PANC-1 cells to nutrient deprivation. PANC-1 cells were grown in PBS containing vitamins, magnesium and calcium without glucose (-g) or supplemented with 25 mM glucose (+g). Cells were grown up to 96 hours in the absence of nutrients. Results expressed are the mean ± SEM of three replicate experiments.

5.3 Angelmarin

5.3.1 Toxicity of angelmarin in nutrient deprivation

To test angelmarin as an anti-austerity compound in pancreatic cancer, PANC-1 cells were treated with 7.5 µM angelmarin under a variety of growth conditions. Previous experiments have indicated that 7.5 µM angelmarin caused approximately 50% cell death in complete nutrient deprivation conditions after 24 hours (see Figure 5.3), therefore testing of this concentration of angelmarin under different growth conditions should reveal if the addition of nutrients provide protection. Under complete nutrient deprivation conditions (PBS supplemented with vitamins), angelmarin had a profound effect- its addition significantly increased cell death from 40% without angelmarin to 100% with angelmarin (Figure 5.2). Contrasting with this finding, the addition of glucose, glutamine or 10% FBS largely mitigated the effect, and cells grown in complete culture medium showed no effect of angelmarin.

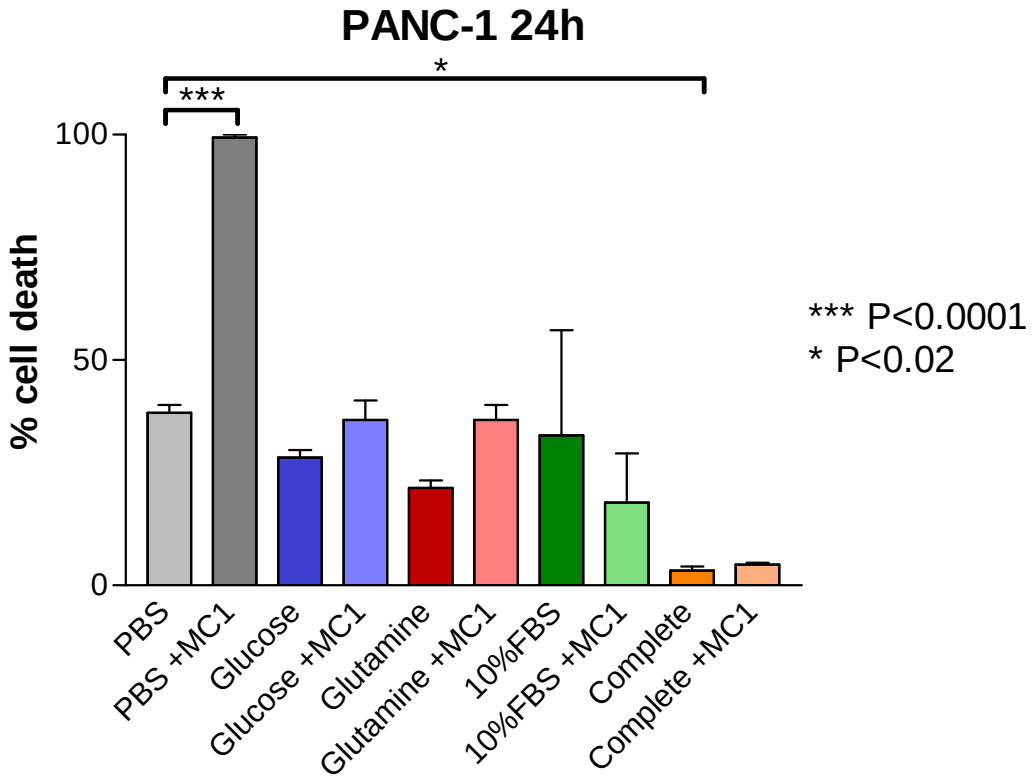

Figure 5.2: Response of PANC-1 cells to addition of 7.5 µM angelmarin under various growth conditions. PANC-1 cells were grown for 24 hours under various growth conditions in the presence and absence of angelmarin. Cell viability was assessed using trypan blue staining. PBS – PBS supplemented with vitamins, glucose – supplemented with 25 mM glucose, glutamine – supplemented with 2 mM glutamine, 10% FBS – supplemented with 10% FBS, complete – DMEM supplemented with 10% FBS, MC1 – 7.5 µM angelmarin. Results expressed are the mean ± SEM of three replicate experiments.

5.3.2 Complete medium and glucose protect cells from angelmarin

Addition of angelmarin to PANC-1 cells grown in complete culture medium showed no effect (Figures 5.2 and 5.4). This demonstrates that there is something protective in culture medium which protects from angelmarin. Nutrient deprivation medium supplemented with glucose showed approximately 40% cell death after 24 hours of angelmarin at 10 µM. Cells grown in nutrient deprivation medium without glucose showed approximately 50% cell death after 24 hours of treatment with 7.5 µM and 100% if treated with 10 µM angelmarin (Figure 5.3).

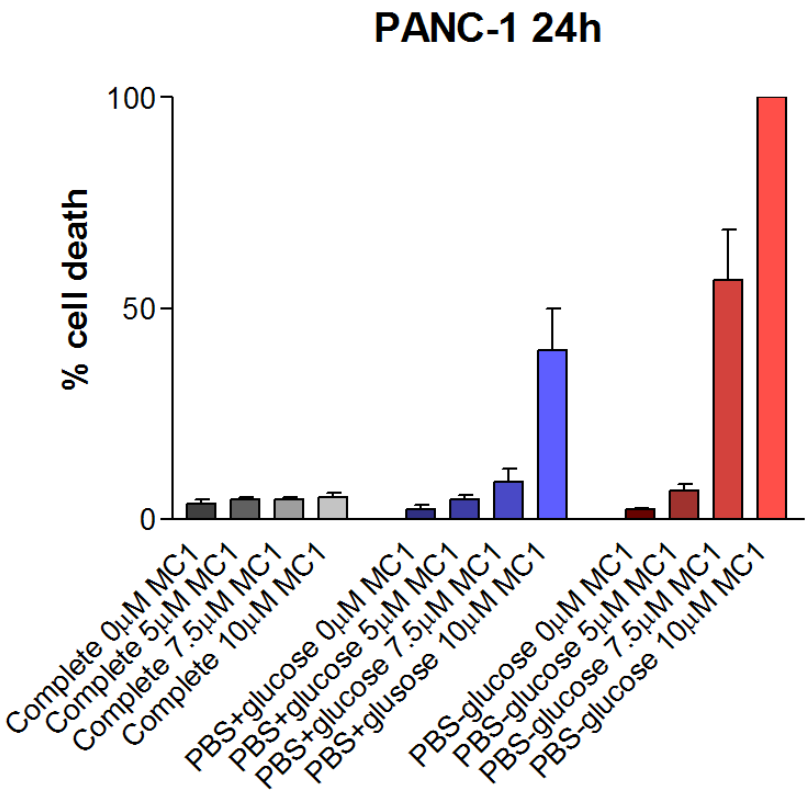

Figure 5.3: Response of PANC-1 cells to addition of angelmarin in the presence or absence of glucose. PANC-1 cells were grown for 24 hours in complete culture medium (Complete), PBS supplemented with vitamins (PBS-glucose) or PBS supplemented with vitamins and 25 mM glucose (PBS+glucose). Cells were grown in the presence of the indicated concentrations of angelmarin (MC1). Cell viability was assessed using trypan blue staining. Results expressed are the mean ± SEM of three replicate experiments.

5.3.3 Cells grown in complete medium are unaffected by high dose of angelmarin

PANC-1 cells grown in complete culture medium were also treated with angelmarin in order to determine the toxicity of the drug under normal conditions. However, addition of angelmarin at an extremely high dose of ten times the PC_{50} calculated for PBS with vitamins (75 μM) had no effect on the levels of cell death observed, as seen in Figure 5.4.

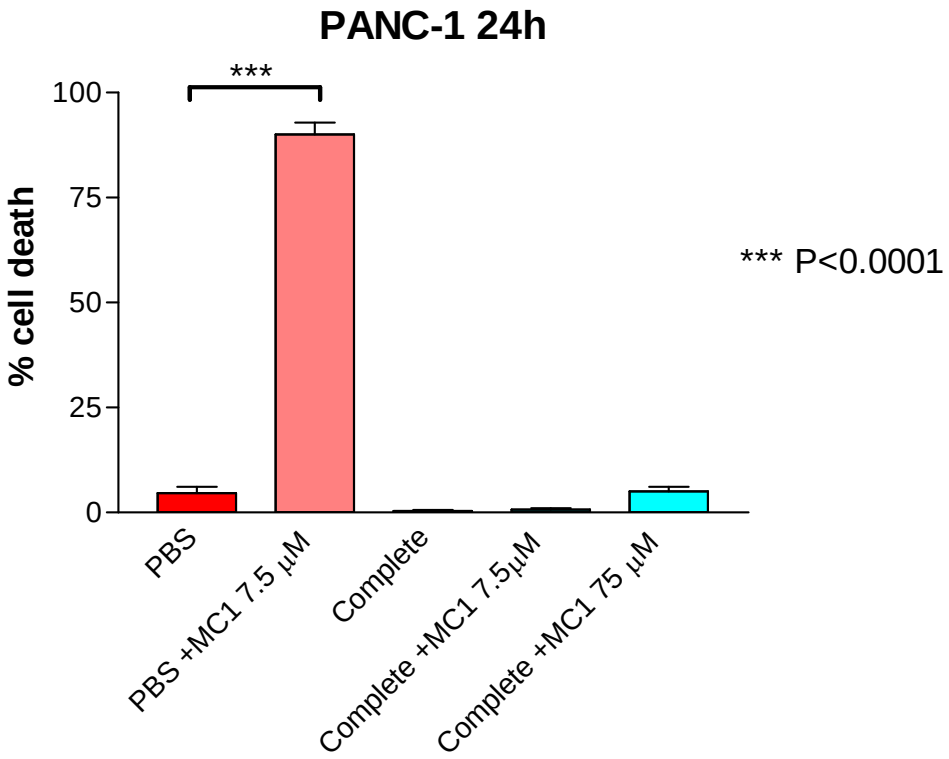

Figure 5.4: Angelmarin toxicity in complete culture medium in PANC-1 cells. PANC-1 cells were grown in PBS supplemented with vitamins (PBS) or DMEM supplemented with 10% FBS (complete) for 24 hours in the presence and absence of angelmarin (MC1) at the indicated concentrations. Cell viability was assessed using staining with trypan blue. Results expressed are the mean ± SEM of three replicate experiments.

5. 4 Angelmarin Butyl Ester

In an effort to increase the activity of angelmarin chemical synthesis of several derivatives of angelmarin was conducted by the Coster group at the Eskitis Institute for Drug Discovery, Griffith University, Don Young Rd, Nathan, Queensland 4111, Australia (Magolan, Adams et al. 2011). Angelmarin Butyl ester is one such compound. This compound shows higher activity in PANC-1 cells grown in the absence of nutrients. Angelmarin butyl ester showed a PC_{50} of 0.2 µM under nutrient deprivation conditions (PBS containing vitamins) (Figure 5.5), compared to angelmarin's PC_{50} of 7.5 µM under the same conditions.

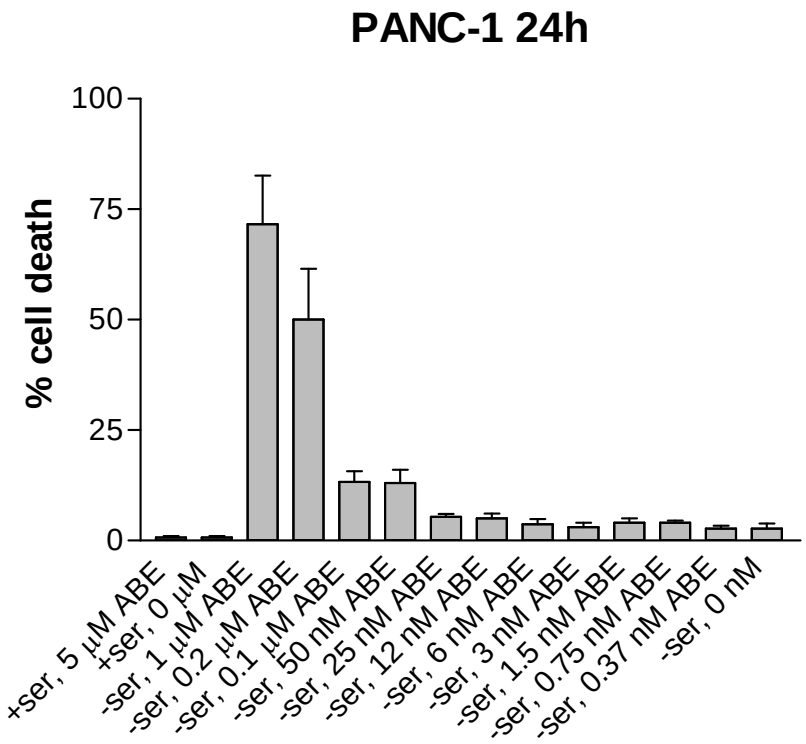

Figure 5.5: Angelmarin butyl ester cell death curve in PANC-1 cells. PANC-1 cells were grown for 24 hours at different concentration of angelmarin butyl-ester (ABE)(an angelmarin derivative) in PBS supplemented with 10% FBS (+ser) or without 10% FBS (-ser). Cell viability was assessed using staining with trypan blue. Results expressed are the mean ± SEM of three replicate experiments.

5.5 Cell death type involved in response to angelmarin

5.5.1 LC3b immunofluorescence shows marginally increased autophagy

LC3b is a commonly used marker of autophagy (Young, Takahashi et al. 2012). LC3b is involved in the formation of autophagosomes (Young, Takahashi et al. 2012). It is expressed diffusely in cells under normal conditions but forms in to puncta which are associated with autophagosome formation in cells undergoing autophagy (Ravikumar, Sarkar et al. 2010; Choi, Ryter et al. 2013). LC3b immunofluorescence shows an increase in LC3b fluorescent puncta in angelmarin treated cells in the absence of nutrients, but consistent levels in all the other samples (Figure 5.6a). This indicates that autophagy was being up-regulated by angelmarin under nutrient deprivation conditions. Figure 5.6b shows counted and graphed data of the percentages of cells with autophagosomes.

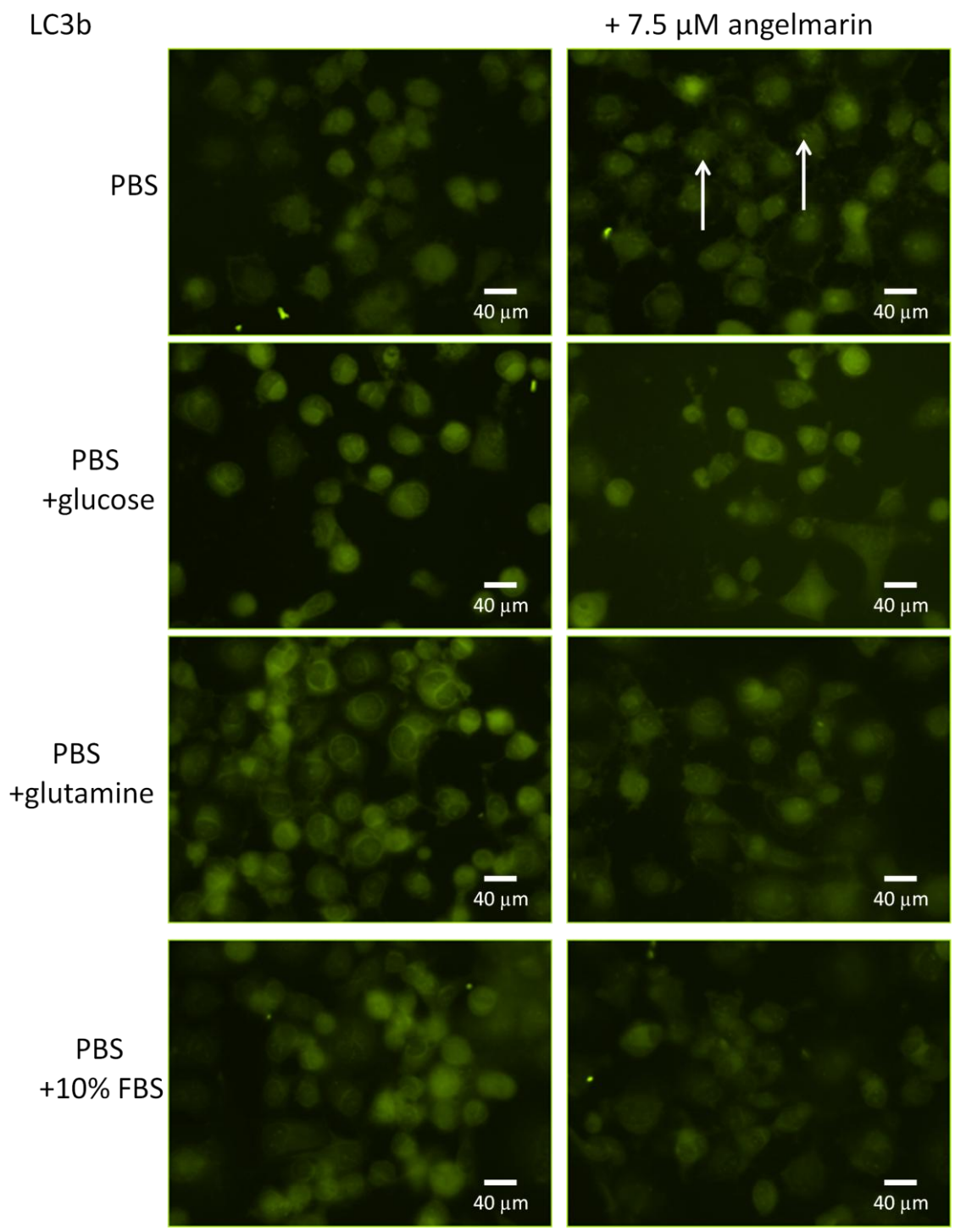

Figure 5.6a: Immunofluorescence of LC3b (Cell Signaling) in PANC-1 cells grown for 24 hours under various conditions in the presence and absence of angelmarin (7.5 µM). Arrows indicate LC3b punctate fluorescence. PBS – phosphate-buffered saline with vitamins, + glucose – supplemented with 25 mM glucose, glutamine – supplemented with 2 mM glutamine, +10% FBS – supplemented with 10% FBS. The cells were viewed at 200x magnification on a Nikon Eclipse E800 fluorescence microscope. Results expressed are representative of two replicate experiments.

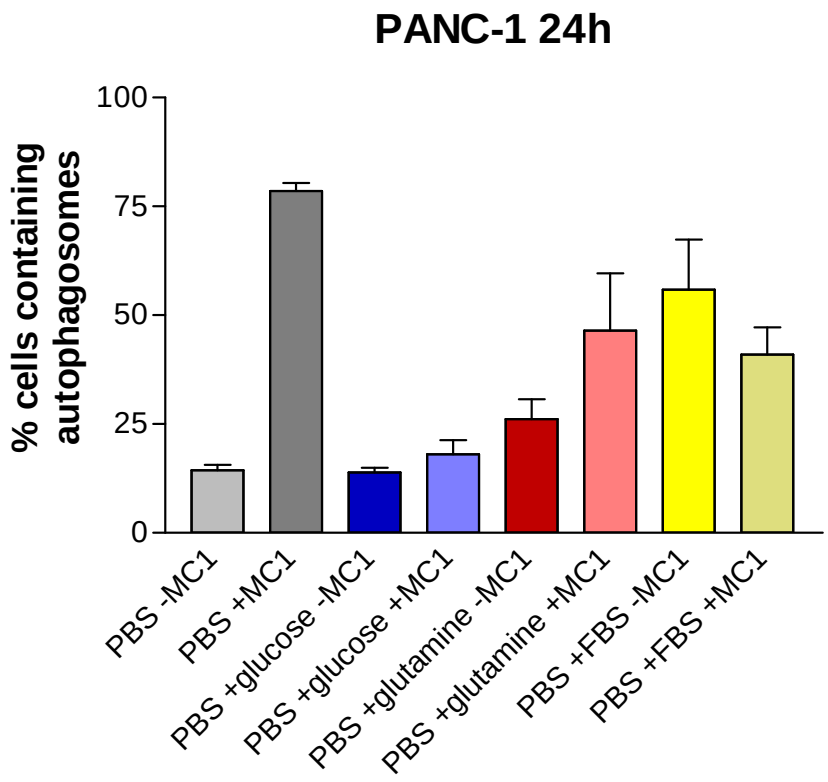

Figure 5.6b: Graphed data of cell counts comparing cells containing autophagosomes compared to those without detectable autophagosomes. Three random fields were counted for a total of approximately 300 cells per sample. PBS – PBS containing vitamins, m – 7.5 μM angelmarin (MC1), glucose – 25 mM glucose, glutamine – 2 mM glutamine, FBS – supplemented with 10% FBS. Results expressed are the mean ± SEM of two replicate experiments.

5.5.2 DAPI staining reveals no nuclear fragmentation

To investigate whether apoptosis is occurring nuclear staining was used to detect nuclear fragmentation – a morphological sign of apoptosis. Nuclear staining with DAPI shows that the nuclei remain intact in PANC-1 cells regardless of the addition of angelmarin in PBS supplemented with vitamins, or PBS supplemented with vitamins and either glucose, glutamine or 10% FBS (Figure 5.7). This provides evidence that apoptosis is not the mechanism of cell death in response to angelmarin as the nuclei would break apart and fragment if apoptosis were occurring.

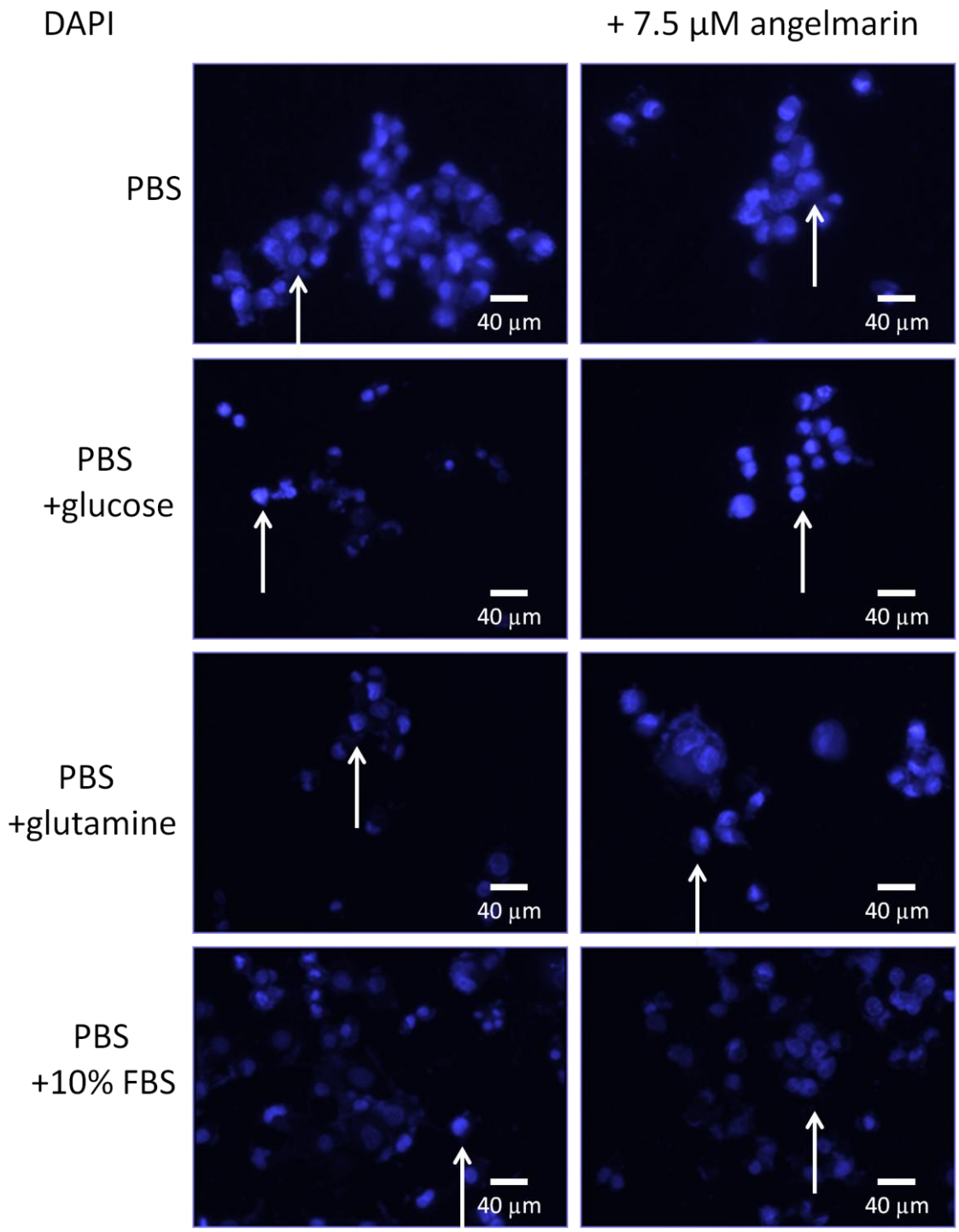

Figure 5.7: DAPI staining in PANC-1 cells grown for 24 hours under various conditions in the presence and absence of angelmarin (7.5 µM). Arrows show examples of intact nuclei. PBS – phosphate-buffered saline with vitamins, + glucose – supplemented with 25 mM glucose, glutamine – supplemented with 2 mM glutamine, +10% FBS – supplemented with 10% FBS. The cells were viewed at 200x magnification on a Nikon Eclipse E800 fluorescence microscope. Results expressed are representative of three replicate experiments.

5.6 Cell survival signalling proteins

5.6.1 Beclin-1 expression is down-regulated

Examination of autophagy related proteins by Western blotting was conducted to provide insight into the mechanism behind autophagy in PANC-1 cells. Expression of Beclin-1 after 24 hours of treatment was consistent between cells grown without nutrients or angelmarin, cells grown in the presence of glucose regardless of angelmarin and cells grown in the presence of glutamine regardless of angelmarin. A large decrease in expression of Beclin-1 was observed in PBS without nutrients in the presence of angelmarin (Figure 5.8). These results suggest that Beclin-1 is modulated in response to angelmarin however may not be essential for its execution. Indeed, Torricelli et al (2012) demonstrated that autophagy can be activated in a Beclin-1 independent manner in response to rottlerin – a cytotoxic compound with efficacy in both apoptosis competent and incompetent cells. Wu et al has also demonstrated autophagy occurring in a Beclin-1 independent manner using si-Beclin-1 knockdown (Wu, Huang et al. 2014).

5.6.2 Regulation of the mTOR pathway

Proteins involved in the mTOR cell survival signalling pathway were examined as this signalling pathway is activated in response to cellular stresses. Phosphorylation of p53 was detected at 0 hours however levels decreased to an undetectable amount in the 24 hour nutrient deprived medium (Figure 5.9). Phospho p38 MAPK levels also appeared reduced at 24 hours when compared to the 0 hour time point in nutrient deprived medium (Figure 5.9). Levels of phospho p53 and phospho p38 MAPK both appeared unchanged between the 0 and 24 hour incubation times in media supplemented separately with glucose, glutamine or serum (Figure 5.9).

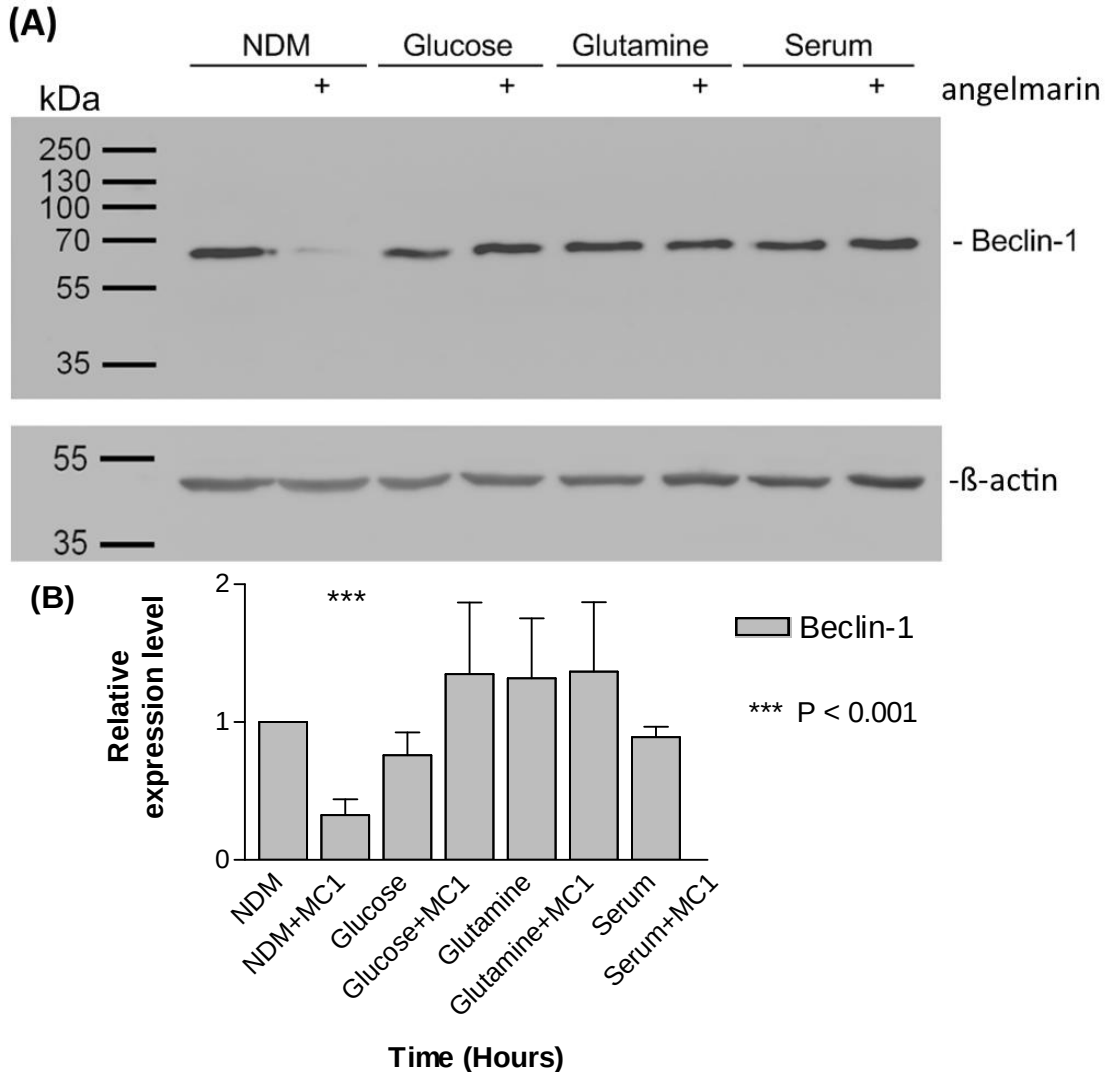

Figure 5.8: (A) Beclin-1 expression in PANC-1 cells. PANC-1 cells were grown for 24 hours in PBS containing vitamins (NDM) supplemented with glucose, glutamine, or 10% FBS (Serum) in the presence or absence of 7.5 µM angelmarin. The Western blot membrane was probed using Beclin-1 (60 kDa) (Cell Signaling) antibody and incubated overnight at 4°C. Secondary antibody conjugated to HRP was used at 1/5000 dilution. ß-actin (Sigma) is shown as loading control. The blot is representative of three biological replicates. **(B)** Quantified histogram of the expressed proteins normalised to ß-actin. Results expressed are the mean ± SEM. Asterisks indicate significant differences from unity.

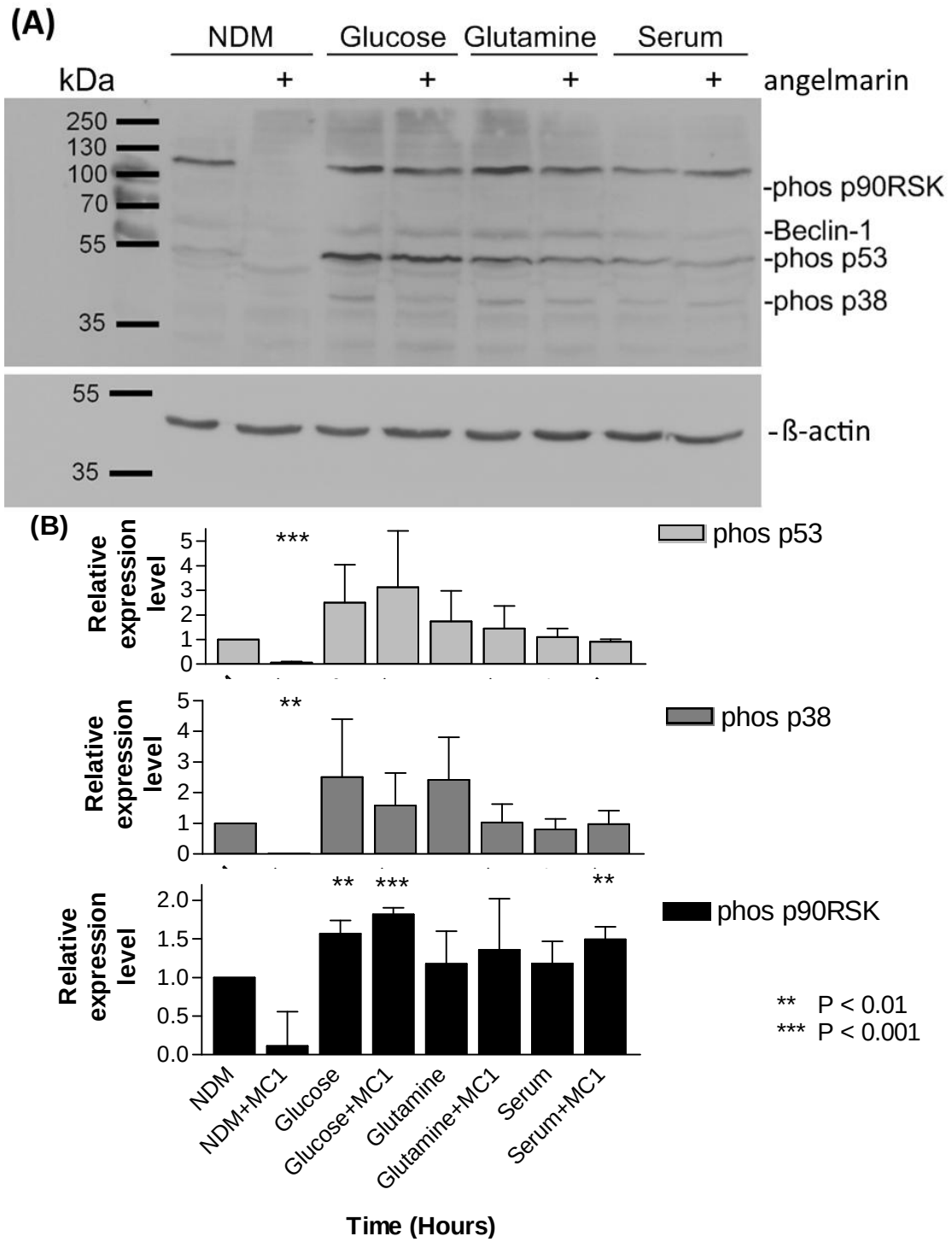

Figure 5.9: (A) Western blotting of cell signalling proteins in PANC-1 cells under different growth conditions. PANC-1 cells were grown for 24 hours in PBS containing vitamins (NDM) supplemented with glucose, glutamine or 10% FBS (Serum) in the presence or absence of 7.5 µM angelmarin. The membrane was probed using Western Cocktail II (Cell Signaling) antibody at a 1/500 dilution and incubated overnight at 4°C. Secondary antibody conjugated to HRP was used at 1/5000 dilution. The membrane was exposed for 8 minutes on high sensitivity. Phos p90RSK – phospho p90 ribosomal S6 kinase, phos p53 – phospho p53, phos p38 – phospho p38 MAPK. ß-actin (Sigma) is shown as loading control. The blot is representative of three biological replicates. **(B)** Quantified histogram of the expressed proteins normalised to ß-actin. Results expressed are the mean ± SEM. Asterisks indicate significant differences from unity.

p90RSK is important in MAPK signalling and survival of cells (Yoo, Cho et al. 2015). Phosphorylation of Raptor by p90RSK leads to mTORC1 activation (Zhou and Huang 2010). PANC-1 cells were grown with 7.5 μM angelmarin in the absence of nutrients and levels of phosphorylated proteins were monitored. Phosphorylated p90RSK was detected at the 0 hour time point in PANC-1 cells, however was not detectable as early as 2 hours post angelmarin treatment (Figure 5.10). The phosphorylated form of p38 MAPK was also detectable at 0 hours post angelmarin treatment (Figure 5.10) but was undetectable at 2 hours post treatment and beyond.

p53 as mentioned previously is vital in cell death and survival signalling. The phosphorylated form of p53 was detected at high levels at 0 hours post angelmarin treatment (Figure 5.10). However levels had dropped a large amount by as early as 2 hours post treatment, and were undetectable at 24 hours. Expression of the p53 regulated protein Bax showed decreased levels at 2 hours post angelmarin treatment in PANC-1 cells (Figure 5.11).

Phosphorylation of Akt, a protein involved in cell survival signalling and modulation of apoptosis was monitored using Western blotting. A 2-3 fold increase in phosphorylation of Akt at Ser473 was observed at 24 hours post treatment with angelmarin (Figure 5.12).

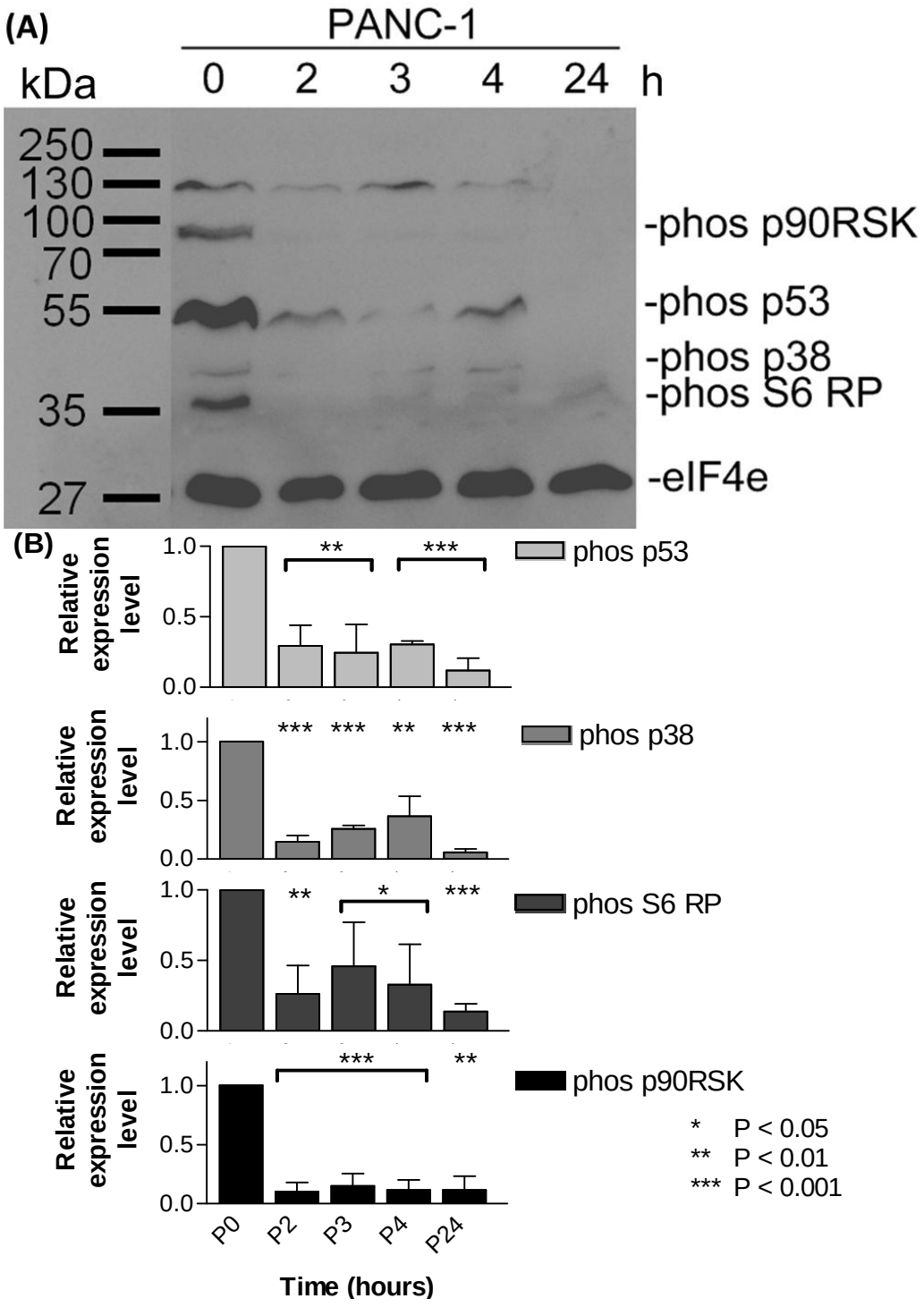

Figure 5.10: **(A)** Western blot of angelmarin time course in PANC-1 cells probing for Western cocktail II. PANC-1 cells were grown in DMEM without glucose or FBS in the presence of 7.5 µM angelmarin for the indicated times. Lysates from the samples were then used for Western blotting. The blot was treated with Western cocktail II (Cell Signaling) and then anti mouse secondary antibody conjugated to HRP at 1/20000 dilution. Exposure time was 5 minutes on standard exposure. Phos p90RSK – phospho p90 ribosomal S6 kinase, phos p53 – phospho p53, phos p38 – phospho p38 MAPK, phos S6 RP – phospho S6 ribosomal protein. eIF4e is shown as a loading control. The blot is representative of three biological replicates. **(B)** Quantified histogram of the expressed proteins normalised to eIF4e. Results expressed are the mean ± SEM. Asterisks indicate significant differences from unity.

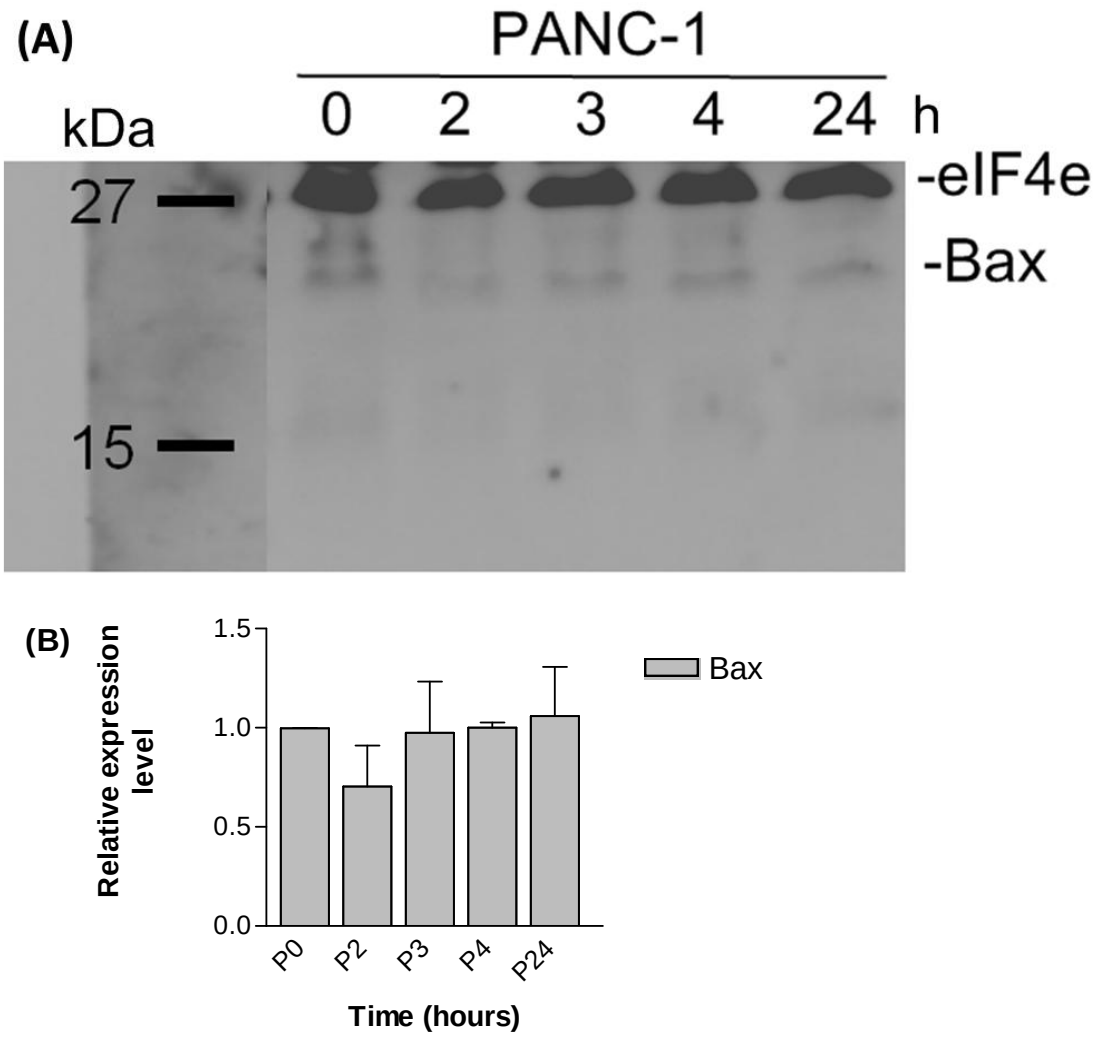

Figure 5.11: (A) Western blot of angelmarin time course in PANC-1 cells probing for Bax. PANC-1 cells were grown in DMEM without glucose or FBS in the presence of 7.5 µM angelmarin for the indicated times. Lysates from the samples were then used for Western blotting. The blot was treated with anti Bax antibody (Cell Signaling) and then anti mouse secondary antibody conjugated to HRP. Exposure time was 5 minutes on super exposure. eIF4e is shown as a loading control. This is the same Western blot as Figure 5.10 reprobed with different antibodies. The blot is representative of three biological replicates. **(B)** Quantified histogram of the expressed proteins normalised to eIF4e. Results expressed are the mean ± SEM. No statistical significance was observed between samples.

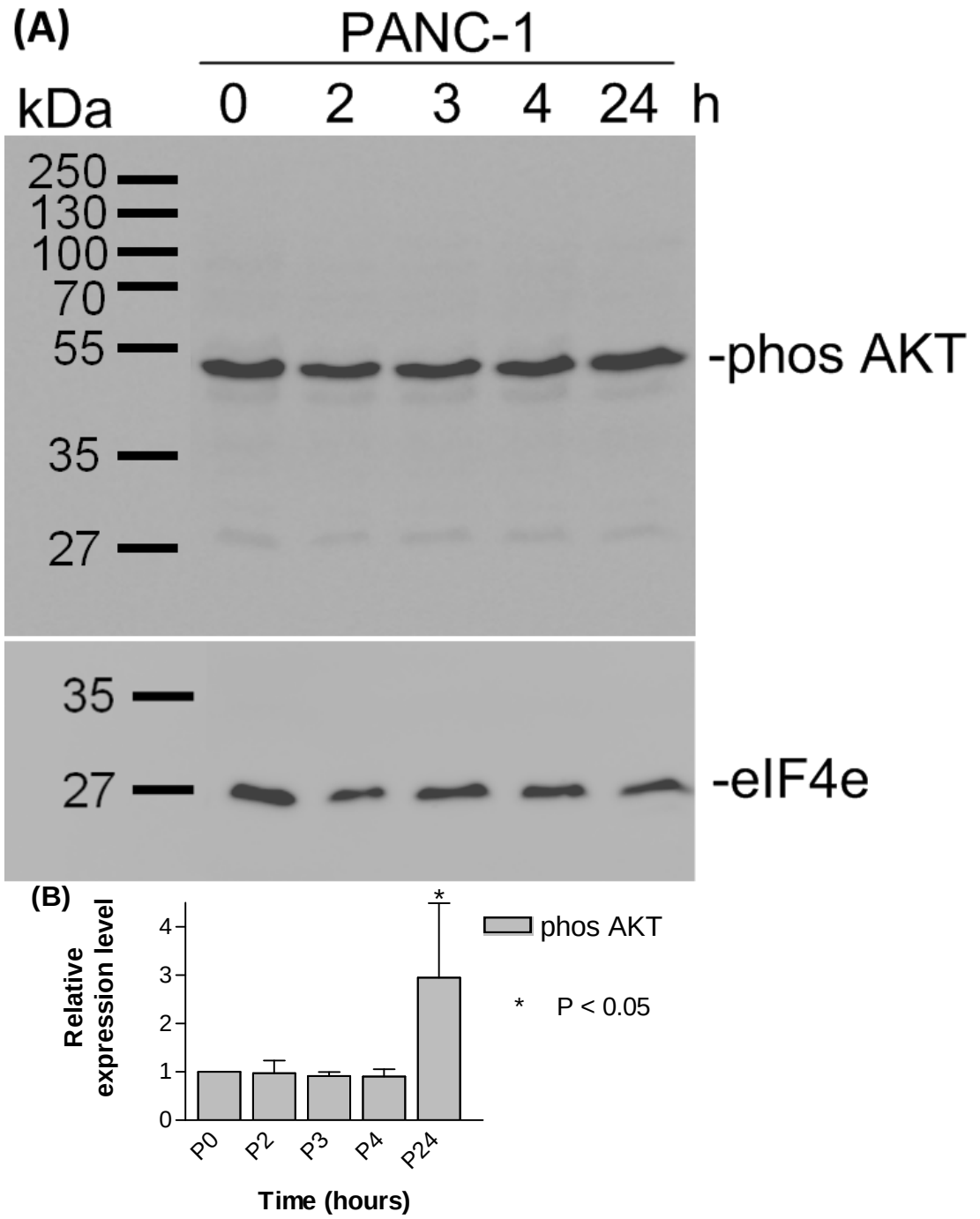

Figure 5.12: (A) Western blot of angelmarin time course in PANC-1 cells probing for phospho Akt. PANC-1 cells were grown in DMEM without glucose or FBS in the presence of 7.5µM angelmarin for the indicated times. Lysates from the samples were then used for Western blotting. The blot was treated with phospho Akt (Ser473) (Cell Signaling) antibody and then anti mouse secondary antibody conjugated to HRP. Exposure time was 4 minutes on super. eIF4e is shown as a loading control. This is the same Western blot as Figure 5.10 reprobed with different antibodies. The blot is representative of three biological replicates. **(B)** Quantified histogram of the expressed proteins normalised to eIF4e. Results expressed are the mean ± SEM. Asterisks indicate significant differences from unity.

5.7 Caspases

5.7.1 Caspase expression in PANC-1 cells

The two major initiator caspases responsible for the starting apoptosis were monitored by Western blotting. Expression of full length caspase-8 was higher in the untreated samples, decreased in the 2-4 hour samples, and completely absent in the 24 hour sample (Figure 5.13). Expression of caspase-8 cleavage fragments was completely undetectable, indicating that caspase-8 is not activated.

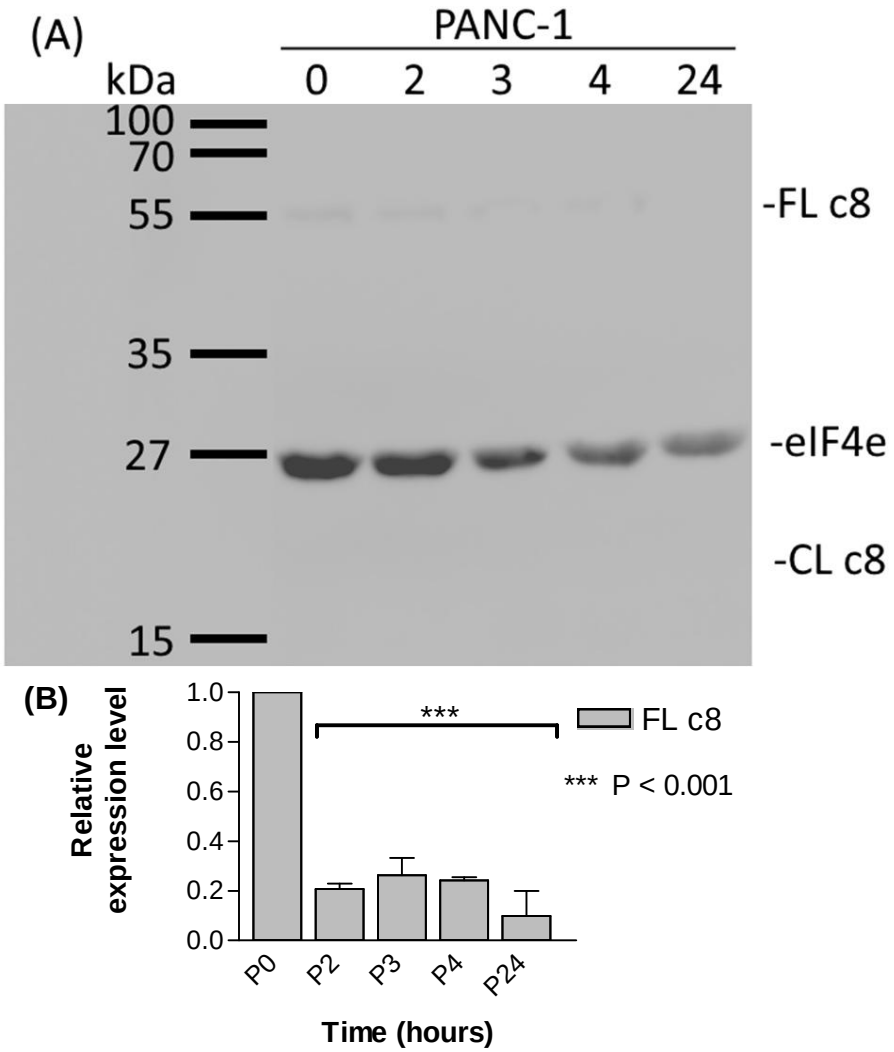

Figure 5.13: (A) Western blot of angelmarin time course in PANC-1 cells. The blot was treated with caspase-8 antibody (Cell Signaling) and then anti mouse secondary antibody conjugated to HRP at 1/20000 dilution. Exposure time was 10 minutes on standard. The blot had previously been probed with Western Cocktail II (Cell Signalling. FL c8 – full length caspase-8, CL c8 – cleaved caspase-8. eIF4e is shown as a loading control. The blot is representative of three biological replicates. **(B)** Quantified histogram of the expressed proteins normalised to eIF4e. Results expressed are the mean ± SEM. Asterisks indicate significant differences from unity.

Over the 24 hour time course, by which time a large amount of cells were dead, the expression of full length caspase-9 had not changed (Figure 5.14). Levels of caspase-9 cleavage fragments did not change, and were nearly undetectable at all time points, indicating that caspase-9 is not activated.

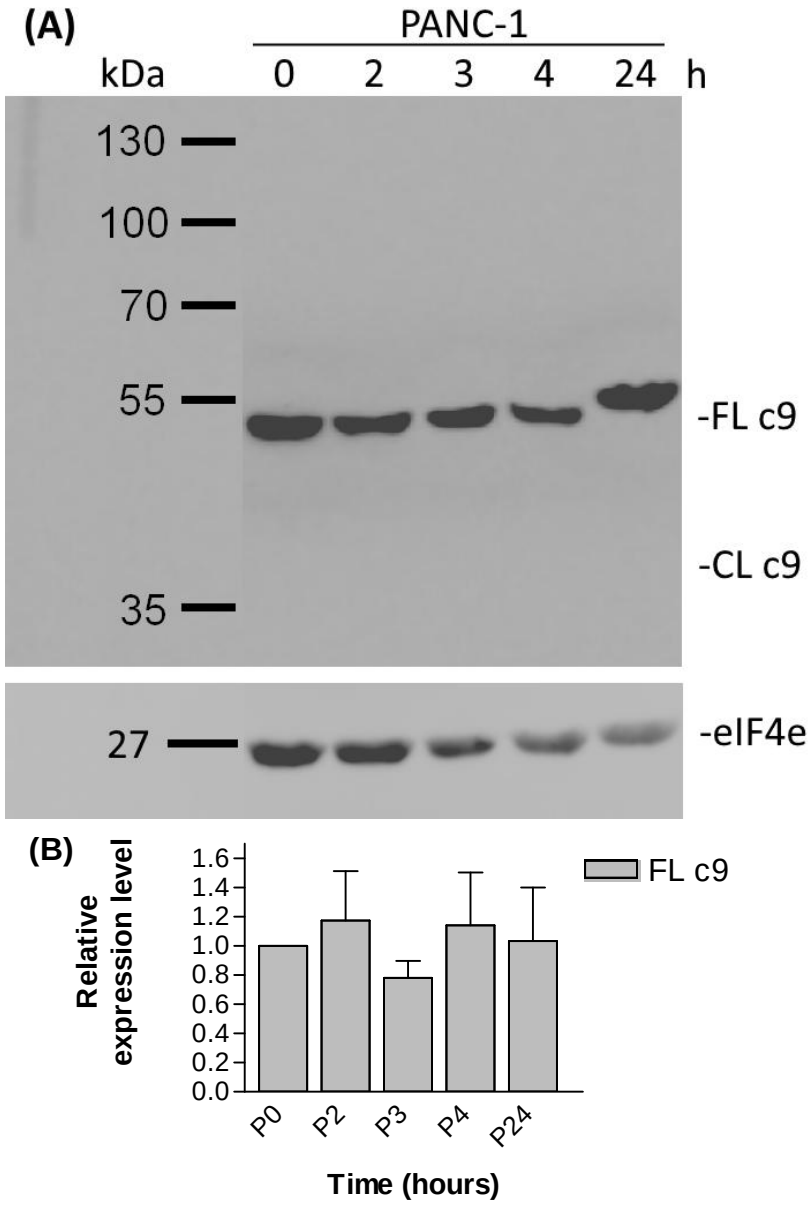

Figure 5.14: Western blot of angelmarin time course in PANC-1 cells probing for caspase-9. PANC-1 cells were grown for 0, 8, 16 and 24 hours in PBS containing vitamins in the presence or absence of 7.5 µM angelmarin. The membrane was probed using caspase-9 (Cell Signaling) antibody at a 1/500 dilution and incubated overnight at 4°C. Secondary antibody conjugated to HRP was used at 1/5000 dilution and incubated for 4 hours at room temperature. The membrane was exposed for 5 seconds on standard sensitivity. eIF4e is shown as a loading control. This is the same Western blot as Figure 5.13 reprobed with different antibodies. The blot is representative of three biological replicates. **(B)** Quantified histogram of the expressed proteins normalised to eIF4e. Results expressed are the mean ± SEM. No statistical significance was observed between samples.

5.7.2 Caspase activation

Because of the differences in caspase-8 expression observed, caspase activity was measured. However the levels of caspase-8, caspase-9 and caspase-3 activation remained low and consistent over the 24 hour time course when compared to etoposide treated BL30A cell line, which was used as a positive control for apoptosis induction (Figure 5.15).

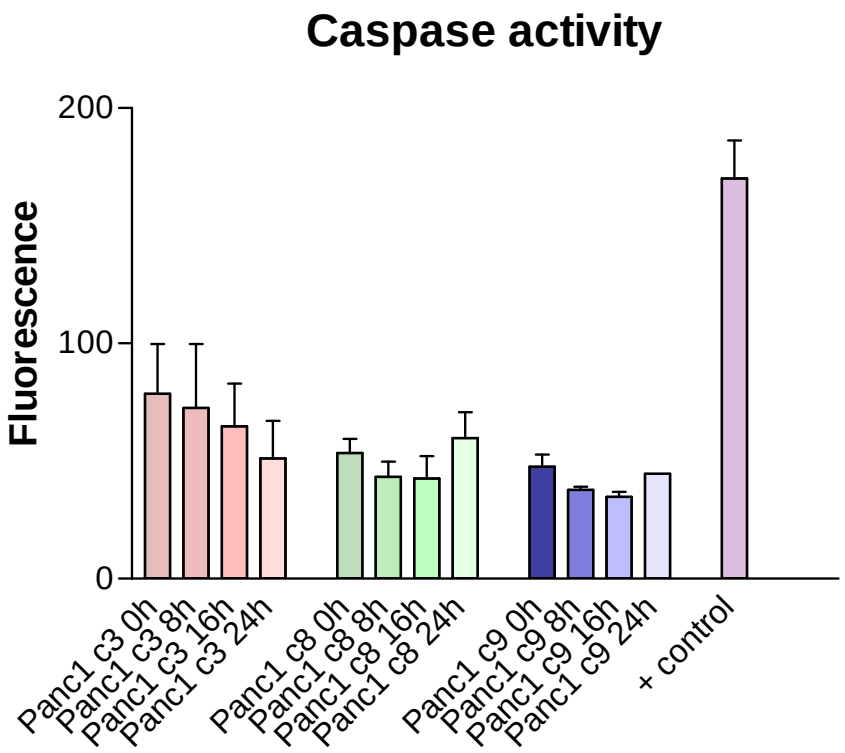

Figure 5.15: Caspase activity assay in PANC-1 cells. PANC-1 cells were grown in PBS supplemented with vitamins with 7.5 µM of angelmarin for the indicated times. The BL30A cell line was used for a positive control sample treated with caspase-3 substrate. Caspase-3 (c3), caspase-8 (c8) and caspase-9 (c9) activation is reflected by arbitrary values of fluorescence. Results expressed are the mean ± SEM of three replicate experiments. One way Anova revealed no difference between samples, excluding the positive control.

5.7.3 Caspase inhibition

Additionally, inhibition of caspase activation using irreversible fmk inhibitors failed to protect cells from cell death induced by angelmarin treatment (Figure 5.16). DEVD-fmk, IETD-fmk and LEHD-fmk - inhibitors for caspase-3, caspase-8 and caspase-9 respectively all had no effect on cell death in response to angelmarin.

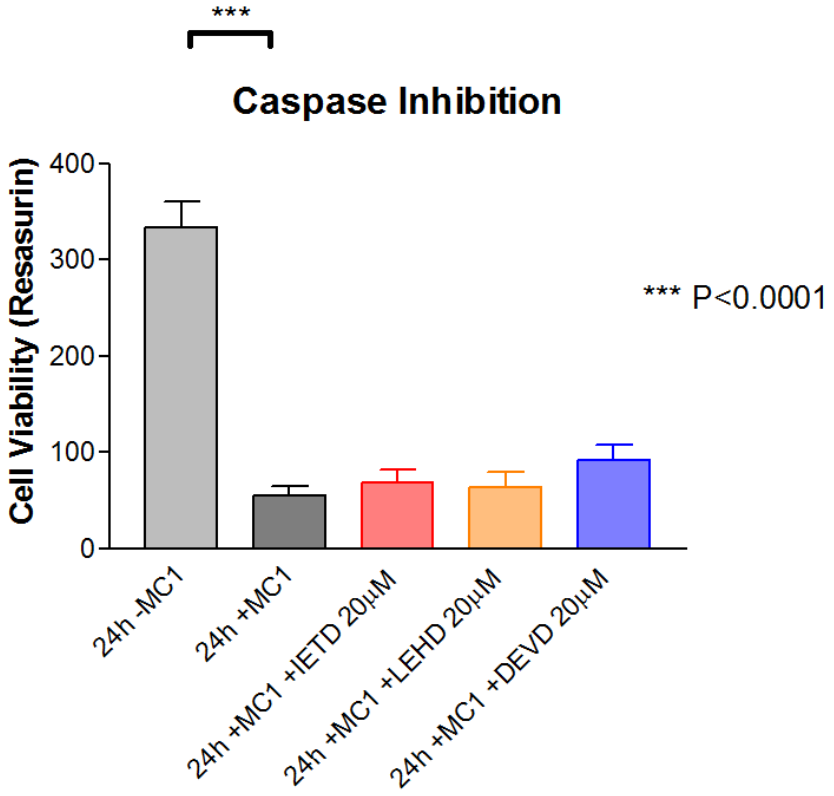

Figure 5.16: Caspase inhibitors effect on angelmarin treatment of PANC-1 cells. PANC-1 cells were grown in PBS supplemented with vitamins for 24 hours in the presence and absence of 7.5 µM angelmarin (MC1) and inhibitors for caspase-3 (DEVD), caspase-8 (IETD) and caspase-9 (LEHD) at 20 µM each. Cell viability was assessed using the resazurin stain. Results expressed are the mean ± SEM of three replicate experiments.

5.8 RIP-1 involvement in angelmarin response

Another protein that was examined was RIP1, which can modulate cell entry into apoptosis, necrosis or even encourage cell survival. A large amount of expression of RIP1 was detected between 0 hours and 4 hours with comparable levels, however by 24 hours RIP1 was undetectable (Figure 5.17). Re-probing of the blot with ß-actin and ß-tubulin is shown for comparison.

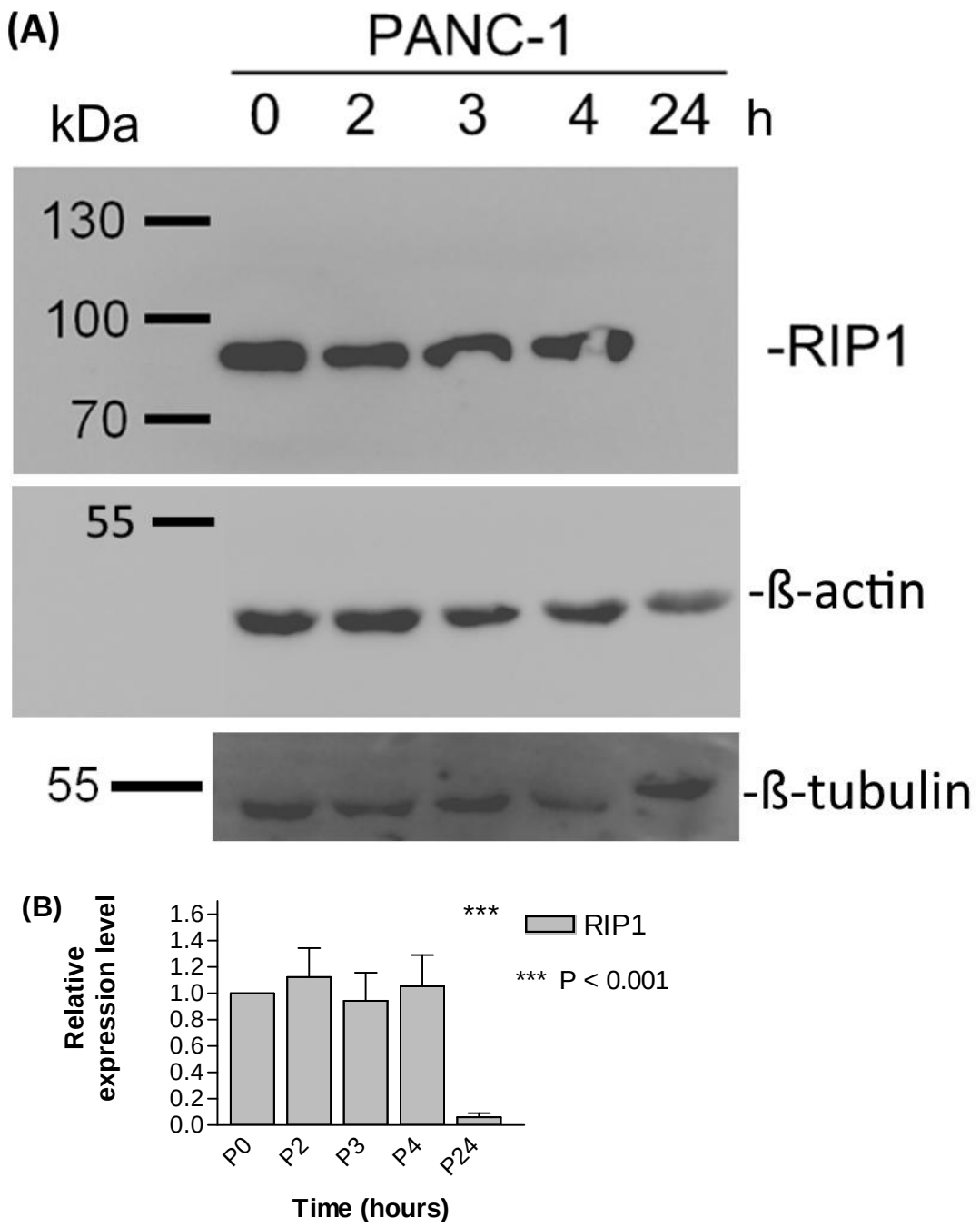

Figure 5.17: (A) Western blotting of angelmarin time course in PANC-1 cells probing for RIP1. The blot was probed with anti RIP1 antibody (BD Pharmingen) and then anti mouse secondary antibody conjugated to HRP. The blot was re-probed with ß-actin (Sigma) antibody and ß-tubulin III antibody for loading controls. The blot is representative of three biological replicates. **(B)** Quantified histogram of the expressed proteins normalised to ß-actin. Results expressed are the mean ± SEM. Asterisks indicate significant differences from unity.

5.9 Inhibitor studies

Several inhibitors of cell signalling pathways or proteins of interest were used to determine if their inhibition affects the survival of PANC-1 cells in response to angelmarin treatment. Necrostatin-1 is an inhibitor of RIP1 (Degterev, Huang et al. 2005; Degterev, Hitomi et al. 2008) that was used to further investigate the involvement of RIP1. Inhibition of RIP1 by necrostatin-1 decreased the observed amounts of cell death (Figures 5.18 and 5.19).

Other inhibitors were also investigated for their modulation of cell death in response to angelmarin. Inhibition of p38 MAPK in the ERK/MAPK signalling pathway by the inhibitor SB203580 at a concentration of 20μM did not significantly reduce cell death caused by angelmarin in PBS supplemented with vitamins (Figure 5.18). Inhibition of MEK in the ERK/MAPK signalling pathway by the inhibitor PD98059 at a concentration of 20μM also did not significantly reduce cell death caused by angelmarin in PBS supplemented with vitamins (Figure 5.18).

Chloroquine was used as an inhibitor of lysosome associated functions. Addition of a high concentration of chloroquine (50-100μM) abrogated the cell death response caused by angelmarin under nutrient deprivation conditions (Figures 5.18 and 5.19). Inhibition of the mitochondrial activity of p53 by using the inhibitor pifithrin-μ marginally decreased the amount of cell death observed (Figure 5.18).

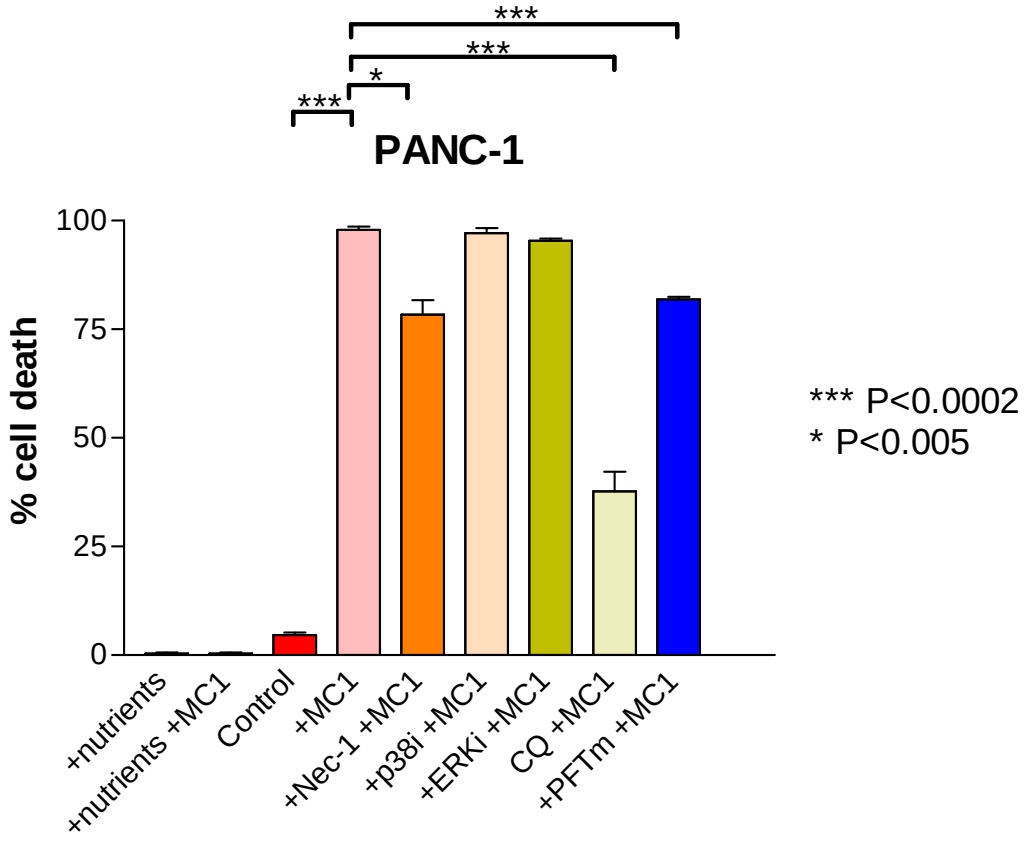

Figure 5.18: Effect of several inhibitors on angelmarin treatment in PANC-1 cells. Cell death of PANC-1 cells was monitored using the trypan blue stain. Trypan blue selectively stains cells which have lost their membrane integrity while leaving healthy cells unstained. Following washing in PBS cells were incubated for 24 hours in nutrient deprivation medium in the presence and absence of angelmarin and several inhibitors. MC-1 – Angelmarin (7.5 µM), Nec-1 – Necrostatin-1 (20 µM), p38i – SB203580 (20 µM), ERKi – PD98059 (20 µM), CQ – Chloroquine (50 µM), PFTm - Pifithrin-µ (9 µM). Results expressed are the mean ± SEM of three replicate experiments.

Rottlerin is a natural product known to induce potassium channel opening in mitochondria, and enhance phosphorylation and activation of Akt (Miura, Tanno et al. 2010; Clements, Cordeiro et al. 2011). Rottlerin reduced the observed levels of cell death in response to angelmarin (Figure 5.19).

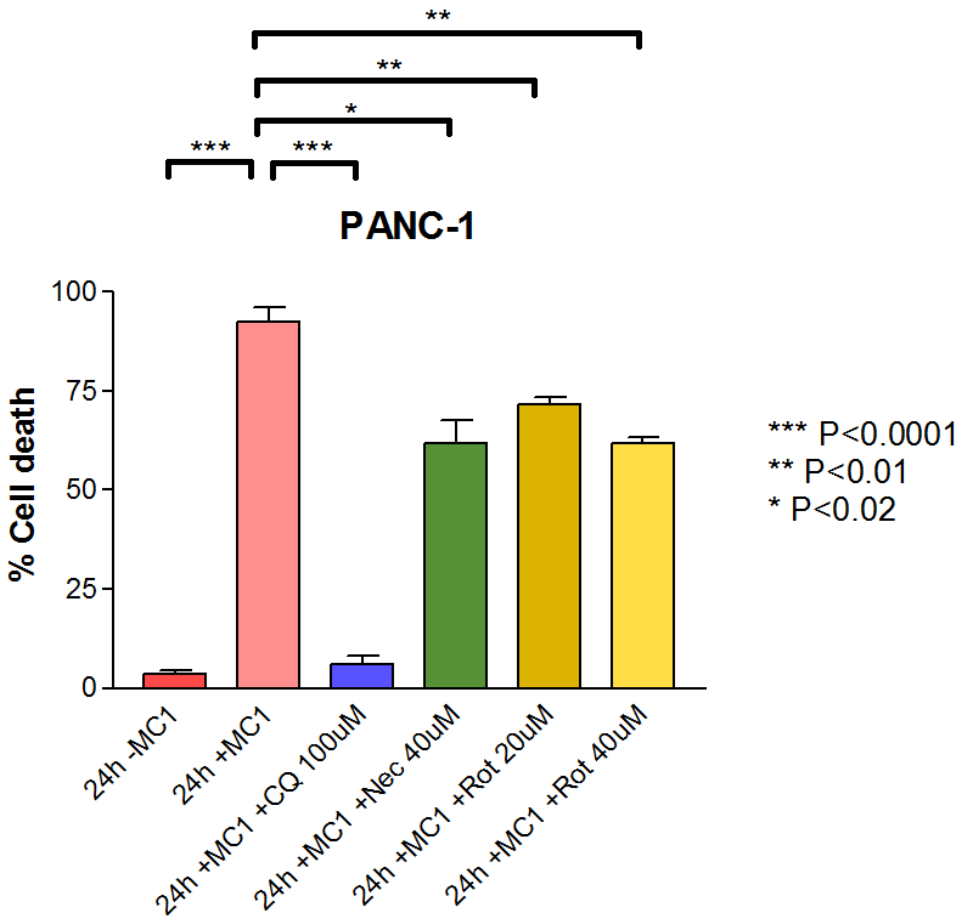

Figure 5.19: Effect of inhibitors on angelmarin treatment in PANC-1 cells. Cell death of PANC-1 cells was monitored using the trypan blue stain. Trypan blue selectively stains cells which have lost their membrane integrity while leaving healthy cells unstained. Following washing in PBS cells were incubated for 24 hours in PBS containing vitamins in the presence and absence of angelmarin and several inhibitors. MC-1 – angelmarin (7.5 µM), CQ – Chloroquine (100 µM), Nec – Necrostatin-1 (20 µM), Rot – Rottlerin (20 µM or 40 µM). Results expressed are the mean ± SEM of three replicate experiments.

5.10 Mitochondrial involvement in response to angelmarin

5.10.1 Monitoring mitochondrial morphology using Mitotracker

Mitochondrial morphology was examined to provide insight in the involvement of mitochondria in the response to angelmarin. Mitotracker was used to stain mitochondria, and over the 24 hour time course of angelmarin treatment mitochondrial morphology changed from distinct puncta at 0 hours to diffuse fluorescence at 24 hours (Figure 5.20). The change in mitochondrial morphology was first observable at 8 hours post treatment with angelmarin.

5.10.2 Monitoring ROS generation using MitoSOX

Monitoring the generation of mitochondrial superoxide using the MitoSox stain and fluorescence microscopy showed distinct bodies within the cell (open arrows) showing high levels of staining (Figures 5.21a and 5.21b). These fluorescing bodies became much more pronounced beginning at 8 hours post angelmarin treatment (closed arrows) in cells grown in PBS containing vitamins (Figures 5.21c and 5.21d). This shows that mitochondrial superoxide was being generated in response to angelmarin.

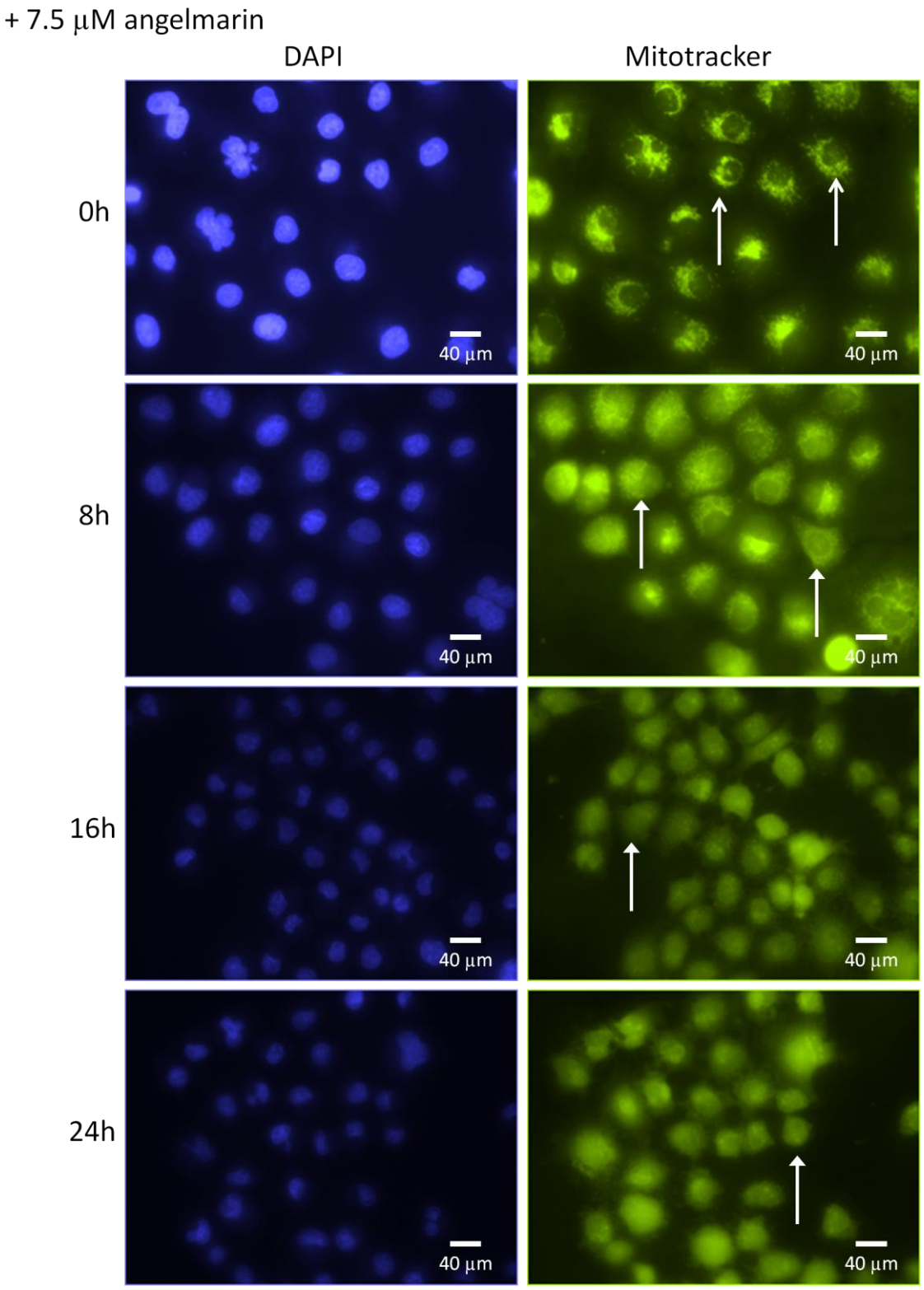

Figure 5.20: Morphology of cell nuclei and mitochondria in response to angelmarin (7.5µM). PANC-1 cells were grown in PBS containing vitamins for the times indicated (0-24 hours) and stained with DAPI and mitotracker. Open arrows show distinct punctate mitochondrial fluorescence. Closed arrow show diffuse fluorescence of mitochondria. Cells were viewed at 200x magnification on a Nikon Eclipse E800 fluorescence microscope. Results expressed are representative of three replicate experiments.

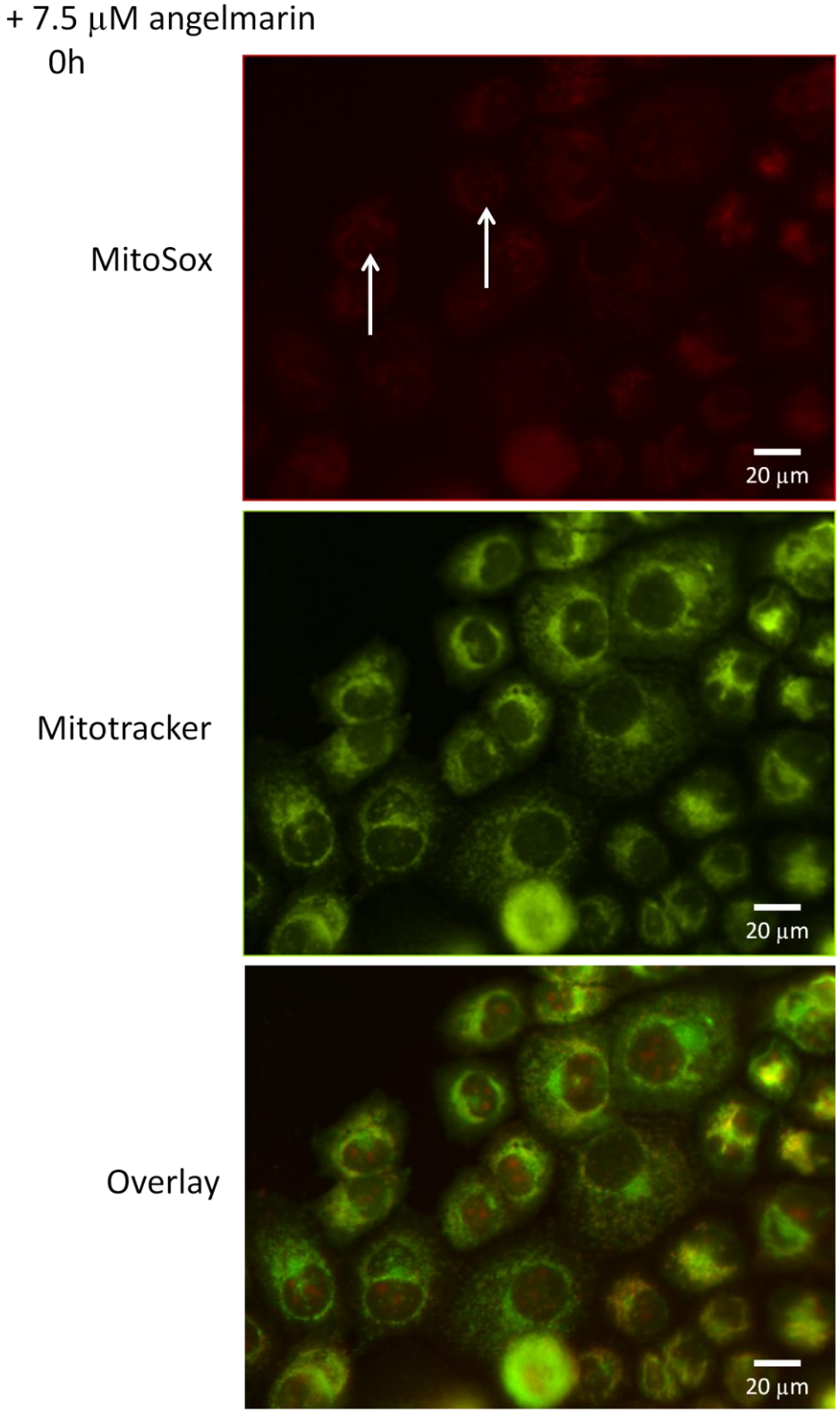

Figure 5.21a: Monitoring of ROS production using MitoSox in PANC-1 cells at 0h. PANC-1 cells were grown in PBS containing vitamins and the addition of 7.5 μM angelmarin and viewed at 0h post treatment. Arrows show brightly stained dots of unknown identity. The cells were stained using the mitochondria marker mitotracker (green) and the live cell mitochondrial superoxide stain MitoSox (red). The cells were viewed at 400x magnification on a Nikon Eclipse E800 fluorescence microscope. Results expressed are representative of two replicate experiments.

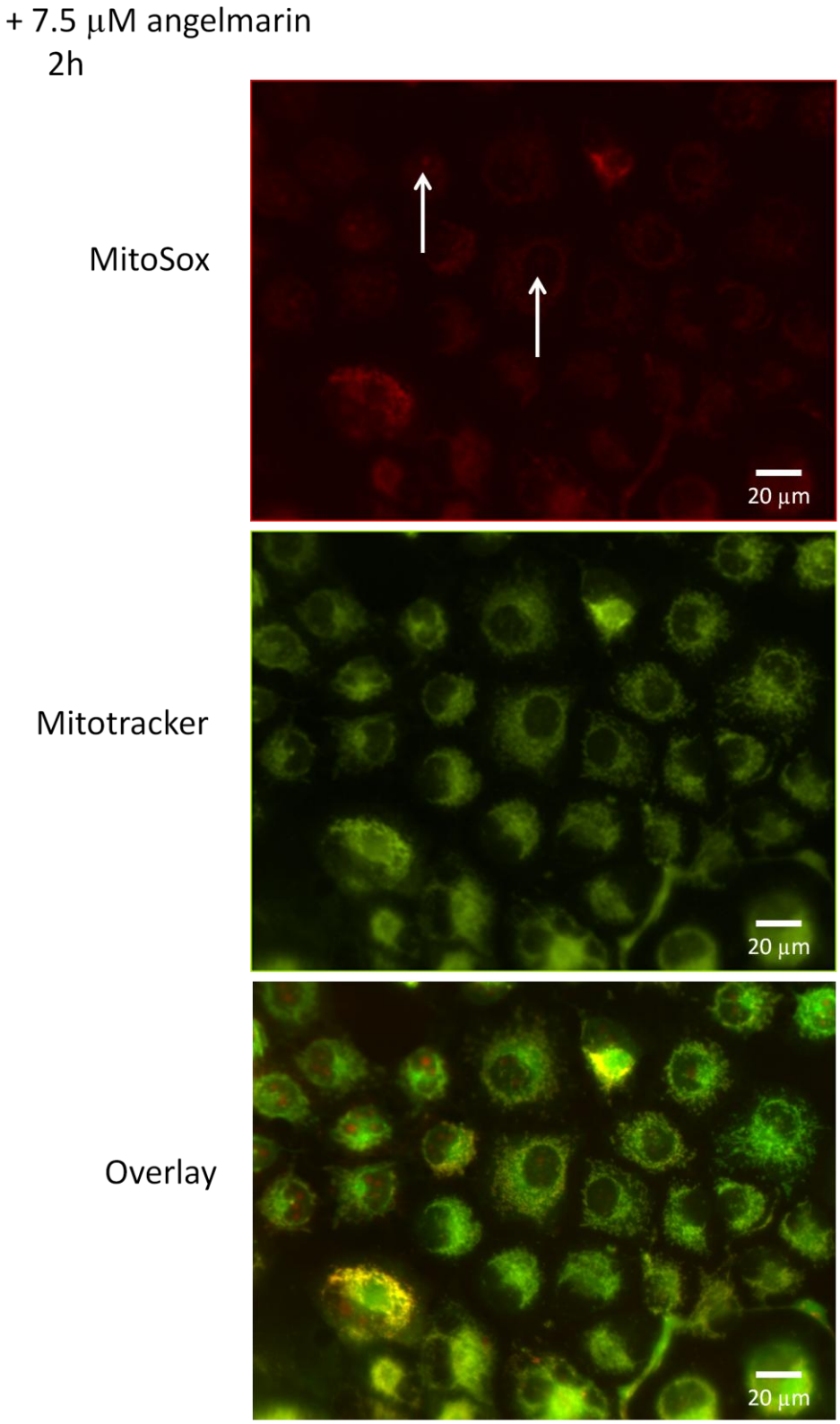

Figure 5.21b: Monitoring of ROS production using MitoSox in PANC-1 cells at 2h. PANC-1 cells were grown in PBS containing vitamins and the addition of 7.5 μM angelmarin and viewed at 2h post treatment. Arrows show brightly stained dots of unknown identity. The cells were stained using the mitochondria marker mitotracker (green) and the live cell mitochondrial superoxide stain MitoSox (red). The cells were viewed at 400x magnification on a Nikon Eclipse E800 fluorescence microscope. Results expressed are representative of two replicate experiments.

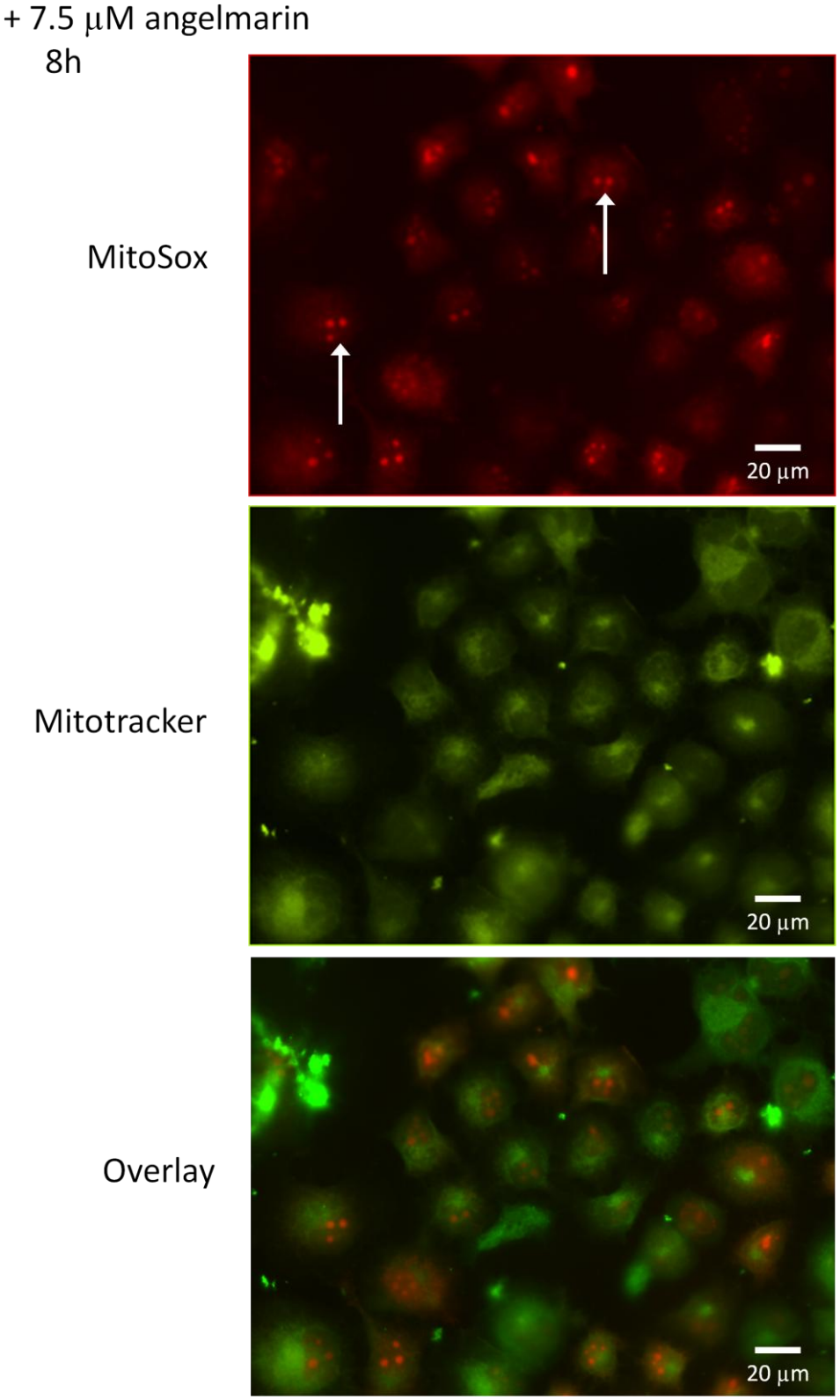

Figure 5.21c: Monitoring of ROS production using MitoSox in PANC-1 cells at 8h. PANC-1 cells were grown in PBS containing vitamins and the addition of 7.5 μM angelmarin and viewed at 8h post treatment. Arrows show brightly stained dots of unknown identity. The cells were stained using the mitochondria marker mitotracker (green) and the live cell mitochondrial superoxide stain MitoSox (red). The cells were viewed at 400x magnification on a Nikon Eclipse E800 fluorescence microscope. Results expressed are representative of two replicate experiments.

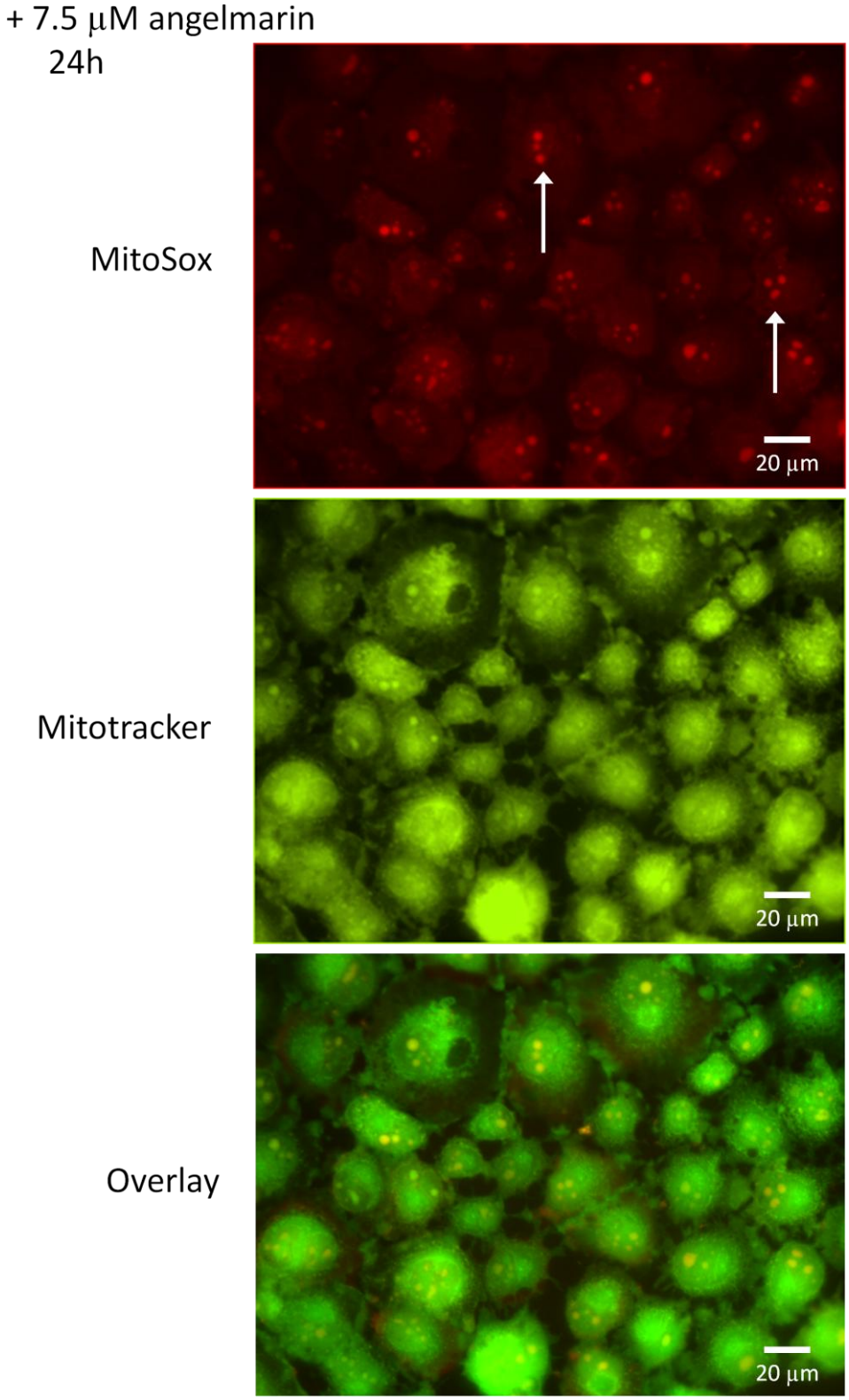

Figure 5.21d: Monitoring of ROS production using MitoSox in PANC-1 cells at 24h. PANC-1 cells were grown in PBS containing vitamins and the addition of 7.5 μM angelmarin and viewed at 24h post treatment. Arrows show brightly stained dots of unknown identity. The cells were stained using the mitochondria marker mitotracker (green) and the live cell mitochondrial superoxide stain MitoSox (red). The cells were viewed at 400x magnification on a Nikon Eclipse E800 fluorescence microscope. Results expressed are representative of two replicate experiments.

5.11 Preliminary investigation of combined treatment with angelmarin and gemcitabine

To examine the potential of angelmarin in combination therapy a preliminary experiment was conducted combining treatment of angelmarin and gemcitabine in PANC-1 cells. Figure 5.22 shows a concentration curve of gemcitabine in PANC-1 cells after 24 hours of incubation and a concentration curve of gemcitabine when paired with 7.5 μM angelmarin. However, no difference was observable between the two treatments indicating that this treatment combination will likely be ineffective. Nevertheless, further examination of angelmarin in other combination treatments should be investigated in future studies.

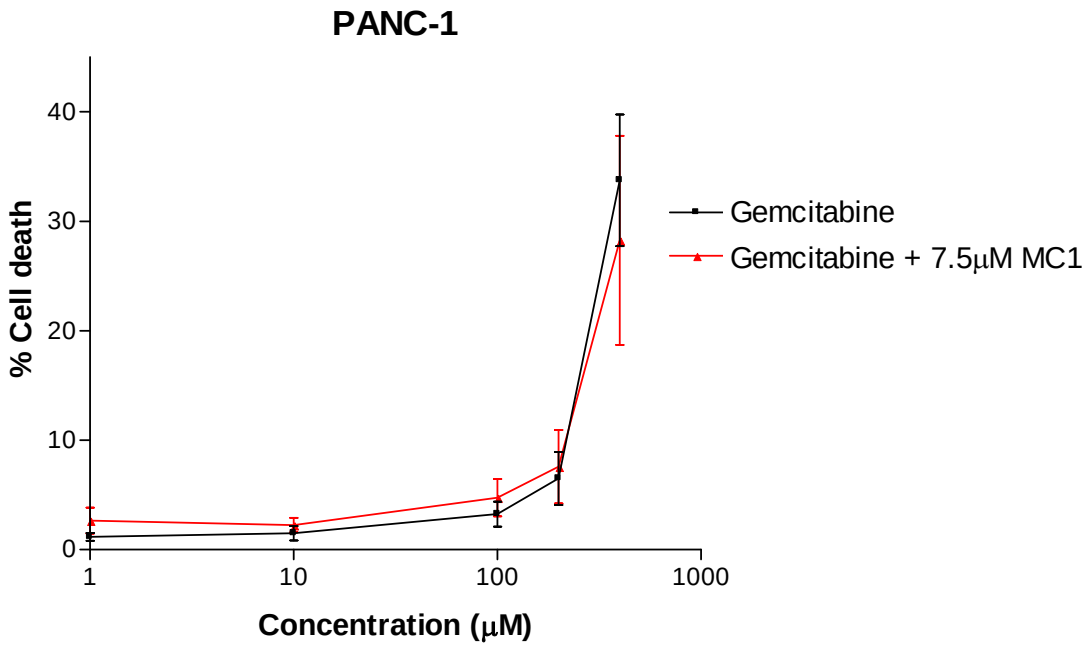

Figure 5.22: Combined treatment of angelmarin and gemcitabine in PANC-1 cells. The graph shows a concentration curve for gemcitabine in PANC-1 cells and a concentration curve for gemcitabine in combination with angelmarin. Cells were grown in DMEM supplemented with 10% FBS for 24 hours with gemcitabine (0.1 μM, 1 μM, 10 μM, 100 μM 200 μM and 400 μM) or gemcitabine plus 7.5 μM angelmarin (MC1) and then cell death was assessed using trypan blue staining. Treatment with 7.5 μM angelmarin (MC1) in nutrient deprived medium was also conducted to confirm angelmarin activity (data not shown). Results expressed are the mean ±SEM of three replicate experiments.

5.12 Discussion

There is currently no effective treatment for pancreatic cancer. New treatments must be investigated to combat this disease, especially targeted therapies based on molecular phenotype. Pancreatic cancers are not only resistant to treatments, but are also resistant to deficits in nutrient availability. PANC-1 pancreatic cancer cells exhibit extremely high tolerance to the absence of nutrients. PANC-1 cells grown in PBS supplemented with vitamins showed less than 25% cell death after 96 hours (Figure 5.1) and supplementation with glucose appeared to increase this survival. Slightly higher levels of cell death were observed in PANC-1 cells at 24 and 48 hours than levels in cells without glucose (Figure 5.1). A possible explanation for the slightly higher levels of cell death at 24 and 48 hours when grown with glucose compared to cells grown without glucose is that a large amount of glycolysis is occurring thus causing higher levels of lactic acid (Munoz-Pinedo, El Mjiyad et al. 2012; Blum and Kloog 2014) which results in a small decrease in cell survival. This effect seems to be abolished once the nutrient deficiency becomes too severe at 96 hours (Figure 5.1).

Angelmarin has been shown to selectively induce cell death under nutrient deprivation conditions in PANC-1 pancreatic cancer cells with a PC_{50} in PBS supplemented with vitamins of approximately 7.5 µM after 24 hours (Figure 5.3). Supplementation of the medium with glucose at 4.5g/L reduced the cell death response to angelmarin and changed the 24 hour PC_{50} to approximately 10 µM under these growth conditions. This indicates that glucose has a protective effect against angelmarin. These findings are similar to those regarding the anti-austerity compounds kigamicin D, arctigenin and pyrvinium pamoate which were all shown to selectively induce necrosis in nutrient starved medium (Lu, Kunimoto et al. 2004). Furthermore, both arctigenin and pyrvinium pamoate induced necrosis in glucose starved conditions (Esumi, Lu et al. 2004; Gu, Qi et al. 2012). Additionally, the toxicity of angelmarin under nutrient rich conditions appears to be very low. PANC-1 cells grown in complete medium failed to show a cell death response (Figures 5.2 and 5.3). Even upon treatment with the

extremely high concentration of 75 µM angelmarin, no effect was observable (Figure 5.4). Again, the lack of toxicity of angelmarin under nutrient rich conditions is consistent with findings regarding other anti-austerity compounds (Esumi, Lu et al. 2004; Lu, Kunimoto et al. 2004; Gu, Qi et al. 2012). These findings demonstrate the potential of angelmarin as a new treatment for pancreatic cancer, at least in pancreatic cancers with the same molecular phenotype as PANC-1. Angelmarin seems to kill selectively in cells grown in a deficit of nutrients – a condition very rare in healthy tissues, and thus could potentially be used to target solid tumour masses. Additionally, the butyl ester derivative of angelmarin shows higher activity with a PC_{50} in the conditions tested of 0.2 µM (Figure 5.5).

Anti-austerity drugs have been shown to activate necroptosis (Lu, Kunimoto et al. 2004; Gu, Qi et al. 2012), apoptosis (Dibwe, Awale et al. 2013; Kim, Yim et al. 2013), autophagy (Chang, Yan et al. 2013; Ueda, Athikomkulchai et al. 2013) or even multiple death types (Torricelli, Salvadori et al. 2012; Kim, Yim et al. 2013). In an effort to determine how angelmarin acts, autophagy was examined. Immunofluorescence of LC3b, a marker of autophagy revealed a small increase in autophagy in cells grown in the absence of nutrients with angelmarin (Figure 5.6a). PANC-1 cells treated with angelmarin and grown in PBS supplemented with vitamins showed autophagic puncta upon LC3b staining. However fewer puncta were observable in cells treated with angelmarin and grown in PBS supplemented with glucose, glutamine or 10% FBS. Regardless, the observed increase in autophagosomes did not account for the level of cell death observed by 24 hours in PANC-1 cells. Beclin-1 is involved in the elongation of the autophagic membrane (Kang, Zeh et al. 2011). Western blotting of Beclin-1 levels showed decreased expression at 24 hours post angelmarin treatment under nutrient deprivation conditions as compared to the 0 hour time point. However, expression of Beclin-1 did not change in the samples from deprivation media supplemented with glucose, glutamine or 10% FBS (Figure 5.8), all of which did not show increased cell death. This result provides evidence that autophagy is down-regulated by 24 hours and does not act as the cell death mechanism as Beclin-1 would be up-regulated to increase autophagy levels. This finding is the opposite of what

would be expected if autophagic cell death was being up-regulated. Indeed, the papers reporting autophagy in response to the anti-austerity compounds samsoeum, honokiol and grandifloracin all show large increases in LC3b expression. These papers also report increases in Beclin-1 expression with the exception of Ueda and colleagues work on grandifloracin which did not examine Beclin-1 expression (Chang, Yan et al. 2013; Kim, Yim et al. 2013; Ueda, Athikomkulchai et al. 2013). These results provide evidence that autophagy is not the cell death type activated in response to angelmarin, however autophagy may have been activated in low levels in this context as a survival mechanism.

Apoptosis was considered as an inducer of cell death to account for the large amount of observable cell death. However, monitoring of cell nuclei revealed that the nuclei remained intact throughout the time course of angelmarin treatment (Figure 5.7). Intact nuclei with normal morphology were observed in cells with and without angelmarin treatment in PBS supplemented with vitamins, or PBS supplemented with vitamins and either glucose, glutamine or 10% FBS (Figure 5.7). If apoptosis were the cell death type activated, nuclear fragmentation or chromatin condensation would have been observed, as was the case with samsoeum (Kim, Yim et al. 2013). This finding provides evidence that apoptosis is not the cell death type involved, as nuclear fragmentation and chromatin condensation are both hallmarks of apoptotic morphology. Initiator caspases - involved in cell death in not only the apoptotic pathways, appeared largely uninvolved in execution of cell death in response to angelmarin. Caspase-9 showed no change in expression of full length forms and cleavage fragments were entirely undetectable (Figure 5.14). Full length caspase-8 expression was initially high, however decreased at 2 hours and was absent at 24 hours (Figure 5.13). This result provided weak evidence of the involvement of caspase-8 however no cleavage fragments were detected which seemingly points away from caspase-8. Indeed caspase activity assays failed to show marked activation of caspases-8, -9 or -3 upon angelmarin treatment (Figure 5.14). Furthermore, inhibition of caspase-8, caspase-9 or caspase-3 activation was ineffective at preventing cell death

(Figure 5.16). These findings taken together provide evidence that apoptosis is not the cell death type activated by angelmarin.

Another candidate for the cell death type in response to angelmarin is programmed necrosis. RIP-1 can not only activate apoptosis, but also programmed necrosis or even promote cell survival (Bertrand and Vandenabeele 2011; Oberst and Green 2011). RIP-1 was expressed at high levels when assessed by Western blotting at 0 hours up to 4 hours in the time points tested, however was absent in the 24 hour time point (Figure 5.17). Evidence from the RIP-1 inhibitor necrostatin-1 also points to the involvement of RIP-1 as necrostatin-1 reduced the cell death response to angelmarin under nutrient deprivation (Figures 5.18 and 5.19). As mentioned earlier however necrostatin-1 does also have inhibitory effects on HSP70 and IDO (Kaiser, Kuhnl et al. 2011; Leu, Pimkina et al. 2011; Vandenabeele, Grootjans et al. 2013). To further explore programmed necrosis as the cell death type, mitochondrial morphology was monitored using fluorescence microscopy and the mitotracker stain. In contrast to autophagy and apoptosis, necroptotic cell death causes mitochondria to swell and lose their membrane integrity (Kroemer, Galluzzi et al. 2009; Fuchs and Steller 2015; Karch and Molkentin 2015). At the 0 hour time point mitochondrial fluorescence was quite defined showing distinct puncta, but this fluorescence became more diffuse over time (Figure 5.20). This indicates that permeabilisation of mitochondria was occurring in the execution of cell death or a by-product of the cell death process. This provides further evidence that necroptosis was occurring in response to angelmarin. Gu and colleagues demonstrated that arctigenin induced necrosis and also showed swollen mitochondria as assessed by transmission electron microscopy (Gu, Qi et al. 2012). In addition to disruption of mitochondria arctigenin elevated production of ROS. The anti-austerity compound pyrvinium pamoate also caused necrotic cell death in PANC-1 cells (Esumi, Lu et al. 2004).

Reactive oxygen species production is often linked to cell death as well as mitochondria therefore ROS production was examined. Glucose deprivation has been shown to induce ROS generation through a positive feedback loop involving inhibition of protein tyrosine phosphatises by oxidation and NADPH oxidase (Graham, Tahmasian et al. 2012). Staining using mitoSOX revealed large bodies containing ROS which were observed in all samples (open arrows), but beginning at 8 hours post treatment the fluorescence became much greater (closed arrows) (Figure 5.21). This provided evidence that ROS were being up-regulated in response to angelmarin. It should be noted however that the fluorescence did not co-localise with the mitochondria, indicating that ROS were either being produced or sequestered in another cellular compartment. It should also be noted that inhibition of mitochondrial activity under glucose deprivation conditions has been demonstrated to cause preferential cytotoxicity in PANC-1 cells (Momose, Ohba et al. 2010). Indeed, arctigenin caused elevation of ROS and necrosis under glucose starved conditions (Gu, Qi et al. 2012). Lu and colleagues also demonstrated the selective induction of necrosis under nutrient starved conditions but in response to kigamicin D (Lu, Kunimoto et al. 2004). Unfortunately the study did not examine which nutrients were required for the cell death response.

Inhibition of other pathways provided evidence against p38 MAPK or ERK/MAPK signalling pathway involvement (Figure 5.18). Pifithrin-μ, which acts on p53 interactions at mitochondria, provided marginal protection against cell death, implicating the mitochondria in the cell death response (Figure 5.18).However pifithrin-μ also interacts with HSP70 from the heat shock family of proteins (Kaiser, Kuhnl et al. 2011; Leu, Pimkina et al. 2011). Rottlerin is known to be an uncoupler of mitochondrial oxidative phosphorylation (Soltoff 2001), and to down-regulate survivin and XIAP (Kim, Kim et al. 2005). Rottlerin treatment provided marginal protection against cell death (Figure 5.19). This finding highlights the need for future investigations of survivin XIAP and mitochondrial oxidative phosphorylation. Chloroquine largely decreased the cell death response to angelmarin (Figure 5.18). Chloroquine can act by inhibiting autophagy (Kimura, Takabatake et al. 2013), amino

acid synthesis (Lefler, Lilja et al. 1973) or lysosomes (Seglen, Grinde et al. 1979). Complete lysosomal permeabilisation causes cell death via a necrosis like phenotype (Boya and Kroemer 2008). The protective effect of chloroquine could suggest that release of lysosomal contents causing acidification of the cytosol is a factor in the cell death response.

Analysis of more upstream signalling pathways show that phosphorylation of p90RSK is decreased as early as 2 hours post angelmarin treatment (Figure 5.10). A decrease in phosphorylation of p90RSK should lead to increased autophagy as phospho p90RSK activates RAPTOR which is needed for mTORC1 activation (Zhou and Huang 2010). However markers for autophagy did not show large increases in autophagy as discussed earlier. Additionally, p38 MAPK phosphorylation and phospho S6 ribosomal protein responded in a similar manner with decreases to undetectable levels at 2 hours (Figure 5.10). Decreases in the phosphorylation of p38MAPK and S6RP would both be expected if apoptosis was being down-regulated. S6 RP phosphorylation should reflect Bad phosphorylation, which leads to apoptosis (Adams and Cory 2007). Phosphorylation of p53 was high at 0 hours, however decreased at 2-4 hours and was undetectable at 24 hours (Figure 5.10). p53 transcriptional activity was monitored through expression of Bax – a p53 transcriptional target. Bax levels were decreased at 2 hours post angelmarin treatment, providing further evidence that p53 is down-regulated in response to angelmarin (Figure 5.11). These findings indicate that p53 is inhibited in response to angelmarin and that p53 may be protective against angelmarin induced cell death under these conditions.

Although not observed in all anti-austerity compounds, interaction with Akt is a reoccurring theme throughout anti-austerity compounds including kigamicin D, samsoeum and grandifloracin and pyrvinium pamoate (Esumi, Lu et al. 2004; Lu, Kunimoto et al. 2004; Torricelli, Salvadori et al. 2012; Kim, Yim et al. 2013; Ueda, Athikomkulchai et al. 2013). Akt phosphorylation at Ser473 was increased by 24 hours after addition of angelmarin under nutrient deprivation (Figure 5.12). However, recent

evidence has shown differences in the effects of phosphorylation of Akt at Ser473 compared to Thr308 in response to glucose deprivation (Gao, Liang et al. 2014). They demonstrate that prolonged glucose deprivation induces selective Akt Thr308 phosphorylation mediated by a complex containing Akt, phosphoinositide dependent kinase 1 (PDK1) and GRP78 (Gao, Liang et al. 2014). Additionally, Akt is able to inhibit autophagy through the phosphorylation of Beclin-1 (Wang, Wei et al. 2012). Because the levels of activation of Akt, as assessed by Akt Ser473 phosphorylation, rose (Figure 5.12) and Beclin-1 levels decreased in response to angelmarin treatment (Figure 5.8), Akt mediated Beclin-1 inhibition is a possibility (Wang, Wei et al. 2012). Phosphorylation of Akt at Thr308 only induces a partial activation of Akt, whereas phosphorylation of Akt at Ser473 induces full activation (Chan, Jo et al. 2014). It is worth noting that two additional Akt phosphorylation sites have recently been discovered (Chan, Jo et al. 2014; Liu, Begley et al. 2014). Future studies should be conducted on the phosphorylation status of Akt in response to angelmarin under nutrient deprivation conditions, and the investigation of a relationship between Akt473 phosphorylation and Beclin-1 levels should also be continued.

This study has explored the effects of angelmarin on PANC-1 pancreatic cancer cells and provided evidence that the cell death type induced is not apoptotic. The lack of nuclear fragmentation observed, as well as the low levels of caspase-8, caspase-9 and caspase-3 activity and lack of changes in expression levels or observable caspase cleavage fragments all support the conclusion that apoptosis is not the cell death type in response to angelmarin. The results on autophagy as the cell death are still inconclusive as autophagic puncta of LC3b staining did show a marginal increase in response to angelmarin, however this increase was small in comparison to other studies of autophagic induction. The effectiveness of chloroquine on preventing cell death in response to angelmarin would also seem to support an autophagic cell death type as chloroquine is a known inhibitor of lysosomal activity and autophagy is reliant on lysosomes for autophagosome formation. However a complete permeabilisation of lysosomes mediated by angelmarin would cause a necrotic phenotype. The finding that Beclin-1 is down-regulated in response to angelmarin provides evidence against a

link to the involvement of autophagy. Additionally, down-regulation of p90RSK expression highlights the regulation of mTOR and MAP kinase signalling pathways by angelmarin.

The high levels of expression of RIP-1 in the initial stages of treatment of angelmarin do seem to point to its involvement in the cell death response, as well as the finding that necrostatin-1 decreased the levels of cell death observed. The observation of mitochondria by fluorescence microscopy showing less distinct mitochondrial staining over time in response to angelmarin provided evidence that mitochondria are losing their membrane integrity, again pointing away from an apoptotic phenotype and more toward a necrosis like phenotype. Staining with MitoSox which monitors superoxide levels showed a difference between angelmarin treated and untreated cells beginning as early as 8 hours post treatment providing preliminary evidence that reactive oxygen species may be involved in cell death associated with angelmarin treatment. Reactive oxygen species are commonly seen in necrosis like cell death types. These findings seem to indicate that a necrosis like phenotype is triggered in response to angelmarin with the involvement of RIP1 in PANC-1 cells.

At this point the most likely cell death pathway activated in response to angelmarin would be necroptosis. However another possible cell death type involved which could fit the data is called paraptosis. In paraptosis insulin like growth receptor 1 expression is the initiating step (Sperandio, de Belle et al. 2000; Kroemer, Galluzzi et al. 2009). The cell death morphology is characterised by extensive vacuolisation in the cytoplasm and mitochondrial swelling without other morphological hallmarks of apoptosis (Kroemer, Galluzzi et al. 2009). Furthermore paraptosis is unable to be prevented by inhibition of caspases or Bcl-2 family members (Sperandio, de Belle et al. 2000). Paraptosis is thought to be activated by a signalling cascade involving proteins from the mitogen-activated protein kinase family (Sperandio, de Belle et al. 2000; Sperandio, Poksay et al. 2004; Kroemer, Galluzzi et al. 2009). Evidence found in this study supporting paraptosis as the cell death type in response to angelmarin include the lack of nuclear fragmentation associated with apoptosis and mitochondrial staining

becoming more diffuse over time consistent with the expansion of mitochondria. However these findings are also consistent with programmed necrosis, and the results regarding RIP1 make necroptosis a more likely candidate.

Angelmarin shows promise as a new therapeutic for pancreatic cancer. It has been demonstrated to kill PANC-1 cells in the absence of nutrients while having limited toxicity in cells grown under normal nutrient levels. Furthermore, the butyl ester derivative shows even more potent activity and further optimisation may lead to even greater effectiveness. However, despite the promising initial results, the dependence of angelmarin on a near complete lack of nutrient availability may lead to ineffectiveness in clinical trials as a complete nutrient absence is an unusual occurrence in biological systems. Monitoring the size of tumours in clinical trials could provide insight as to whether angelmarin is viable with the nutrient availability in a whole organism, however much more data should be gathered before this stage is reached. Data on the effect of angelmarin in non-cancerous Human Pancreatic Duct Epithelial (HPDE) cells is yet to be obtained. The application of angelmarin in tandem with another treatment may also prove useful in combating pancreatic cancer. Combination treatment of angelmarin and gemcitabine was briefly investigated (Figure 5.22), however this combination was found to be ineffective at improving the efficacy of angelmarin. Although the combination of angelmarin and gemcitabine did not successfully increase the effectiveness of angelmarin in killing PANC-1 cells combination therapy of angelmarin with other anti-cancer drugs should still be investigated in future studies as drug interactions are often complex and difficult to predict.

Triggering necrosis to treat cancer has not yet been thoroughly explored. Many anti-cancer drugs have also been reported to activate programmed necrosis. A major problem in oncology is the resistance of cancers to current anti-cancer drugs which trigger cell death. The investigation of triggering necrosis opens other avenues of killing cancers which are resistant to induction of cell death by apoptosis induction (Cho and Park 2014; Fulda 2014). It has also been postulated that the pro-

inflammatory nature of necroptosis may cause the activation of the immune system to help in elimination of tumours (Guerriero, Ditsworth et al. 2008; Cuadrado-Castano, Sanchez-Aparicio et al. 2015). Few studies have explored the potential of triggering necrosis to treat cancer. Exploration into angelmarin may lead to selectively inducing necrosis in pancreatic cancer as a new therapy.

Chapter 6

Thesis Summary and Future Directions

6.1 Thesis Summary and Future Directions

This thesis focused the pathways of cell death in Burkitt's lymphoma as well as the use of the anti-austerity compound angelmarin and its potential as a treatment for pancreatic cancer. The BL30A and BL30K cell lines were chosen because of preliminary data indicating an unusual pathway of apoptosis induction and a mechanism of resistance to induction by this pathway. In Chapter 3, pathways and proteins involved in apoptosis induction in BL30A were explored in order to elucidate the mechanisms of apoptosis induction. The chapter focused on the involvement and activation of caspases and also explored the involvement of death receptors and mitochondrial amplification or activation of apoptosis. The pathway of apoptosis observed required caspase-8 but not caspase-9 as indicated by caspase activity, inhibition and trapping experiments. Caspase-2 was also activated in BL30A cells, but at a later time than caspase-8 and caspase-9 indicating that it is not an initiating step which is necessary for apoptosis to proceed. It was also found that mitochondrial permeabilisation was not detectable until 3 hours post DNA damage – after apoptosis was already observable, indicating that mitochondrial amplification of apoptosis was activated but not essential for apoptosis induction. The findings of caspase-8 as the initiator caspase in response to DNA damage, while unusual are not contrary to the literature. Some of the publications indicating caspase-8 in response to DNA damage include activation of caspase-8 in response to IR in glioma cells (Afshar, Jelluma et al. 2006), activation of a RIP1 containing complex and caspase-8 in acute lymphoblastic leukaemia in response to chemotherapy (Loder, Fakler et al. 2012), and caspase-8 activation in response to etoposide in HT1080 and MDA-MB-231 cells (Tenev, Bianchi et al. 2011).

Depletion of ROS also appeared to have no effect on cell death induced by DNA damage in BL30A cells indicating that regulation of cell death by ROS is not a factor in DNA damage induced cell death in BL30A. p53 expression and inhibitor assays revealed a possible role for p53 in apoptosis signalling at the mitochondria however further experimentation is required to determine the mechanisms of how p53

influences the apoptotic response. However, transcriptional activity of p53 is likely not involved in the regulation of apoptosis as indicated by the pifithrin-α data and Western blotting of Bax. The data also indicates that ERK/MAPK signalling may modulate the apoptotic response to etoposide. Inhibition of MEK in the ERK/MAPK pathway reduced the levels of apoptosis observed, however p38 MAPK inhibition did not. The mechanism by which ERK signalling modulates apoptosis is yet to be elucidated. The involvement of cell surface death receptors including Fas is very likely not involved in response to DNA damage. Experiments monitoring the expression of Fas both externally and internally showed limited expression upon comparison to the control cell line used. Furthermore, depletion of cholesterol failed to influence the cell death response, and immunoprecipitation of the DISC was unsuccessful, again pointing away from surface receptor involvement. Activation of apoptosis by use of the Fas activating antibody was also not observed. Indeed, activation of caspase-8 independently of cell surface receptors has been demonstrated by several groups (Boesen-de Cock, de Vries et al. 1998; Tenev, Bianchi et al. 2011). However the data suggests that a high molecular weight complex is involved in the activation of caspase-8, and taken with the cholesterol depletion experiment data suggest that the complex resides within the cell. This complex likely contains caspase-8, FADD, and several proteins which remain to be identified. However, RIP1 interaction with FADD and caspase-8 should be further investigated. The RIP1 result must be re-assessed using a different antibody owing to the detection of bands at incorrect molecular weight which could be due to non-specific binding. These data taken together highlight an unusual mode of activation of apoptosis in the BL30A Burkitt's lymphoma cell line which is dependent on caspase-8 but not the conventional activation platform of caspase-8. This unusual pathway of caspase-8 dependent apoptosis in response to DNA damage is first described here in BL30A cells, however a similar pathway has been described in other cell lines (Tenev, Bianchi et al. 2011).

Tenev and colleagues described the formation of a 2 MDa complex - as determined through gel filtration techniques - which formed in the cytoplasm in response to genotoxic stress (Tenev, Bianchi et al. 2011). Formation of this complex was observed in MDA-MB-231, HT1080 and BE cell lines. The complex, called the RIPoptosome, was shown to contain RIP1, FADD and caspase-8, as determined through IP techniques. They have also indicated that the complex forms upon depletion of IAPs. Furthermore, the involvement of cell surface death receptors including Fas and TNF were not involved in activation of the complex. The RIPoptosome was shown to trigger caspase-8 dependent apoptosis or necrosis. Negative regulation of the RIPoptosome by cFLIP, and the IAPs - cIAP1, cIAP2 and XIAP were demonstrated. Addition of the RIP1 inhibitor necrostatin-1 blocked both RIPoptosome formation and apoptosis. Finally, the cytotoxic activity of the RIPoptosome was determined to be upstream of the mitochondria and independent of caspase-2 or PIDD activity (Tenev, Bianchi et al. 2011).

Feoktistova and colleagues also describe RIPoptosome formation in response to IAP depletion in HaCaT and HeLa cells (Feoktistova, Geserick et al. 2011). They characterise the complex as being 2 MDa and containing RIP1, FADD and caspase-8, however indicate caspase-10 and cFLIP to also be in the complex. They demonstrate that cIAP inhibits RIPoptosome formation by ubiquitinylation and degradation of RIP1. Genetic knockdown of TNFR did not stop formation of the RIPoptosome indicating it is death receptor independent. Also, in the absence of caspase activity the complex was shown to induce necrotic cell death. Finally, they provide evidence that cIAP levels are controlled by lysosomes, a finding corroborated by those of Vince and colleagues (Vince, Chau et al. 2008; Feoktistova, Geserick et al. 2011).

Basit and colleagues demonstrate synergistic treatment of lexatumumab and IAP inhibitors induced formation of a cytosolic complex containing RIP1, caspase-8 and FADD in rhabdomyosarcoma cells (Basit, Humphreys et al. 2012). They also provide evidence that the kinase activity of RIP1 is dispensable for apoptosis orchestrated by

this complex however protein expression of RIP1 was required. Furthermore, blockage of TNF receptors had no effect on formation of the complex. Upon formation the complex activation of caspases-3, -8 and -9 was induced, mitochondrial permeabilisation occurred and cell death via apoptosis resulted (Basit, Humphreys et al. 2012).

The findings from this research indicate a large molecular weight complex containing FADD and caspase-8 in response to DNA damage caused by etoposide in BL30A cells. This finding is consistent with publications about the RIPoptosome assembling in response to genotoxic stress or depletion of IAPs (Feoktistova, Geserick et al. 2011; Tenev, Bianchi et al. 2011; Basit, Humphreys et al. 2012). It is also worth noting that etoposide has been documented to reduce levels of IAPs in thymocytes (Yang, Fang et al. 2000), and this may be a contributing factor to etoposide inducing apoptosis in BL30 cells. The data also demonstrates that cell death by this pathway is dependent on caspase-8, consistent with the above studies. It was shown that Fas and cell surface death receptors are likely not involved in the execution of apoptosis in response to DNA damage, also consistent with the findings that neither Fas nor TNF is involved in RIPoptosome formation (Tenev, Bianchi et al. 2011). Independence of RIPoptosome formation from TNF was also demonstrated in HaCaT and HeLa cells (Feoktistova, Geserick et al. 2011). Interestingly, formation of a caspase-8, FADD and RIP1 containing complex was shown to be independent from TNF, however linked to sensitisation of TRAIL-R2 (Basit, Humphreys et al. 2012). This data has also shown increased expression of RIP1 in the apoptosis sensitive BL30A cell line compared to the apoptosis resistant BL30K cell line. This finding is consistent with reports that RIP1 expression is needed for RIP1 dependent apoptosis (Basit, Humphreys et al. 2012). Reports regarding the requirement of RIP1 kinase activity in RIP1 dependent apoptosis vary. RIP1 dependent apoptosis was found to be independent of RIP1 kinase activity in rhabdomyosarcoma (Basit, Humphreys et al. 2012) but require RIP1 kinase activity in HT1080, MDA-MB-231 and HeCaT cells (Geserick, Hupe et al. 2009; Tenev, Bianchi et al. 2011). These findings would seem to support RIP1 kinase activity being required for apoptosis. Mitochondrial permeabilisation in apoptosis occurs later in the apoptotic

process, consistent with the findings of Tenev regarding RIPoptosome mediated apoptosis (Tenev, Bianchi et al. 2011). Investigations of p53 have shown that transcriptional regulation of apoptosis in BL30A is unlikely, however pifithrin-μ did inhibit apoptosis. Additionally, phosphorylation of p53 was increased in response to DNA damage. These findings may indicate a role for p53 in the cytoplasm in regulation of apoptosis, however interactions of pifithrin-μ with HSP70 proteins should also be considered. Contrary to this, Tenev and colleages postulated that p53 was uninvolved in regulation of apoptosis by the RIPoptosome complex owing to the differences in p53 status in the cell lines they examined and the formation of the complex regardless of the cell lines p53 status, however no investigation of p53 was actually conducted (Tenev, Bianchi et al. 2011). Furthermore, no investigations into the activity of ERK/MAPK signalling were conducted regarding the RIPoptosome (Feoktistova, Geserick et al. 2011; Tenev, Bianchi et al. 2011), however the findings of phosphorylation of p38 MAPK and inhibition of the ERK/MAPK pathway by MEK inhibition in response to DNA damage demonstrate the need to explore ERK/MAPK signalling in the regulation of apoptosis by the RIPoptosome. Additionally, confirmation of formation of the RIPoptosome complex in BL30A cells through column filtration and IP techniques should be conducted. Finally, a thorough examination of the interactions of both cFLIP isoforms and IAP proteins should be conducted in BL30A cells to examine their effects on DNA damage induced apoptosis. The exploration of this unusual pathway of apoptosis induction could lead to development of new drugs targeting this apoptosis pathway to counteract the evasion of cell death prevalent in cancers.

In Chapter 4, the resistance to induction of apoptosis in response to DNA damage in the BL30K cell line was explored. The resistance to apoptosis induction manifested as a delay in apoptosis induction. The apoptosis sensitive BL30A cell line began apoptosis within 2 hours of treatment with etoposide however the BL30K cell line showed first signs of apoptosis at 12 hours post treatment, to a lesser extent than BL30A. Inhibition of caspase-8 and not caspase-9 inhibited apoptosis induction in BL30K, the same effect of caspase inhibition observed in BL30A cells. Fas expression was similarly low as

compared with the BL30A cell line. Expression of the phosphorylated form of p53 was increased in the BL30K cell line and should be noted that phospho p53 was observed even pre-treatment with etoposide. Monitoring of p53 transcription through Bax expression levels did not reveal any differences in expression indicating that p53 transcription is not active in apoptosis signalling in BL30K. Phosphorylation of p38 MAPK was observed at times coinciding with apoptosis induction in both BL30A and BL30K cells. As p38 MAPK has been shown to interact with caspases and phosphorylation of p38 MAPK times observed in response to etoposide coincide with cell death times, p38 MAPK should be further investigated for apoptosis regulation. Additionally, levels of phospho S6 ribosomal protein were comparatively lower in the BL30K cells than BL30A cells. Phospho S6 RP indicates the activity of several proteins such as mTOR and p70 S6K which is known to prevent mitochondrial outer membrane permeabilisation. As higher levels of phospho S6 RP are observed in BL30A than BL30K, intrinsic pathway amplification of apoptosis is more likely in BL30K cells. RIP1, involved in cell death signalling in both apoptosis and necroptosis showed decreased expression in the BL30K cell line. Decreased RIP1 expression could provide at least a partial cause of the resistance to apoptosis observed in BL30K. However the RIP1 activity should be examined with the expression of different FLIP isoforms. Additionally, GRP78 should be further investigated as a preliminary experiment indicated it interacts with caspase-8 in both cell lines (Table 4.1). Also, GRP78 has been indicated to modulate cell death signalling (Rao, Peel et al. 2002; Kong, Zhang et al. 2013), and has been shown to modulate caspase-8 mRNA expression (Liu, Yang et al. 2014), however investigations of GRP78 have not been thoroughly explored in this study. Lastly, HSP7C was found to only bind caspase-8 in BL30K samples and not BL30A. These finding points to HSP7C as a protective protein from DNA damage induced apoptosis in BL30K cells, however further investigation must be conducted as this is only a preliminary experiment. HSP7C is a chaperone protein and the sequestering of pro-apoptotic proteins could explain the delayed apoptosis in BL30K cells compared to BL30A cells.

The mechanisms of resistance to this pathway of apoptosis induction have not been explored in detail. cFLIP and IAP have however been conclusively demonstrated to negatively regulate apoptosis dependent on the RIPoptosome (Feoktistova, Geserick et al. 2011; Tenev, Bianchi et al. 2011; Basit, Humphreys et al. 2012). Here we have examined several as yet unexplored proteins and signalling pathways as alternative regulatory mechanisms of apoptosis in the BL30K cell line. Regulation of apoptotic death in response to genotoxic stress by p53 remains a possibility. Despite the findings that Bax is not transcriptionally up-regulated and that inhibition of p53 by pifithrin-α did not prevent apoptosis, p53 may regulate apoptosis through non transcriptional activity. Indeed p53 regulation of cell death at the mitochondria has been observed in MCF-7 breast cancer cells (Ahn, Trinh et al. 2010). Inhibition of the cytoplasmic activity of p53 by pifithrin-μ effectively prevented apoptosis in response to DNA damage. However as mentioned previously pifithrin-μ has also been shown to block HSP70 activity. Additionally, increased phosphorylation of p53 upon treatment with etoposide was observed which suggests p53 plays a role in response to DNA damage. These findings are contradictory to Khanna and colleagues findings that p53 was mutated in BL30A and BL30K cells (Khanna, Wie et al. 1996). p53 phosphorylation in BL30A acts as expected for normal p53, and BL30K despite possessing high initial levels of p53 phosphorylation also showed increased levels upon treatment with etoposide. However phosphorylation does not necessarily mean activation as active sites may be compromised in mutated p53 with the phosphorylation sites unaffected (Nguyen, Menendez et al. 2014). ERK/MAPK signalling has also been implicated in the apoptotic response to DNA damage. Phosphorylation of p38 MAPK was observed following treatment with etoposide. Inhibition of p38 MAPK however did not prevent the apoptotic response. This finding concurs with findings that MAPK signalling is defective in BL30A and BL30K by (Michael-Robinson, Spring et al. 2001). They also found that ERK activity decreased in the apoptosis sensitive BL30A cell line but did not in the resistant BL30K cell line. Interestingly, inhibition of MEK in the ERK/MAPK pathway did reduce the levels of apoptosis observed. The effects of the ERK/MAPK signalling pathway on apoptosis induction should therefore be explored further. Another finding of note was that RIP1 expression levels were lower in BL30K cells than BL30A cells. Quantification revealed approximately 2-3 times the expression of RIP1 in

BL30A than BL30K. As mentioned previously it has been suggested that RIP1 expression levels correlate with apoptosis induction (Basit, Humphreys et al. 2012). These results seem to agree with this finding as apoptosis occurs far quicker in BL30A where expression of RIP1 is high than in BL30K where expression of RIP1 is low by comparison. Finally, use of immunoprecipitation techniques were paired with mass spectrometry and revealed a protein of note: HSP7C. The preliminary findings indicated that HSP7C interacted with caspase-8 only in the BL30K cell line. Inhibition of HSP7C combined with inhibition of HSP72 led to extensive apoptosis in HCT116 human colon cancer cells (Powers, Clarke et al. 2008). These results indicate a protective role of HSP7C against apoptosis and are in agreement with findings of Powers and colleagues which found inhibition of HSP7C caused apoptosis. However these findings still remain to be confirmed by IP of HSP7C and caspase-8. Understanding the mechanisms of resistance to this apoptosis pathway will be important in the development of drugs to induce apoptosis through this new pathway.

In Chapter 5, the anti-austerity compound angelmarin was examined for its potential as a therapy for pancreatic cancer. The PANC-1 cell line was selected because several other studies on anti-austerity compounds have used this cell line, and because it shows incredible tolerance to nutrient deprivation (Izuishi, Kato et al. 2000; Awale, Nakashima et al. 2006). Some key genetic features of the PANC-1 cell line include two missense variants in the TP53 gene at exons 4 and 8, heterozygous missense mutation in codon 12 of KRAS, homozygous deletion of exons 1, 2 and 3 of the CDKN2A/p16 gene, but no mutations in the SMAD4/DPC4 gene (Deer, Gonzalez-Hernandez et al. 2010; Gradiz, Silva et al. 2016). PANC-1 cells also show high cell motility and invasion (Deer, Gonzalez-Hernandez et al. 2010). Preferential cytotoxicity of angelmarin in nutrient deprived PANC-1 cells compared to cells grown with nutrients was observed. The toxicity of angelmarin in cells grown in complete culture medium was undetectable even to ten times the concentration used under nutrient deprivation. Additionally, supplementation of nutrient deprivation medium with glucose appeared to mitigate the effect of angelmarin, indicating glucose as a key nutrient in the tolerance of PANC-1 cells to angelmarin. Gu and colleagues have also demonstrated

the toxicity of the anti-austerity compound arctigenin in the absence of glucose (Gu, Qi et al. 2012) and pyrvinium pamoate was also shown to be dependent on glucose withdrawal (Esumi, Lu et al. 2004; Gu, Qi et al. 2012). However the reason for this effect is yet to be conclusively demonstrated.

The cell death type observed in PANC-1 cells in response to angelmarin is likely programmed necrosis (necroptosis). The data gathered thus far indicate that neither apoptosis nor autophagy are primarily responsible for induction of cell death. Low levels of activity of caspases-8, -9 and -3 were observed, inhibition of caspases was ineffective at preventing cell death in response to angelmarin treatment and cell nuclei remained intact without typical apoptotic fragmentation morphology. These findings indicated apoptosis was not the cell death type. Expression of Beclin-1 was decreased in response to angelmarin and LC3b fluorescent puncta were not increased to a large degree, both of which indicate autophagic cell death is not the primary cell death type. However, the increase in autophagic puncta upon LC3b staining could indicate the cells are attempting to use autophagy as a survival mechanism, however cell death is still occurring indicating that autophagy is dysregulated or being evaded. Expression of RIP1 at high levels between 1 and 4 hours and then completely absent at 24 hours along with the findings from inhibition of RIP1 using necrostatin-1 point to RIP1 involvement in the regulation of cell death signalling. RIP1 is not only responsible for induction of apoptosis but can also initiate programmed necrosis (Imre, Larisch et al. 2011). Additionally, loss of mitochondrial membrane potential is also consistent with a necrosis like phenotype. Therefore programmed necrosis is the likely candidate for cell death and further investigation in the mode of cell death in response to angelmarin.

A mechanism for necroptotic cell death resulting from anti-austerity treatment was outlined by Gu and colleages (Gu, Qi et al. 2012). Many cancers are reliant on glycolysis for ATP production for energy in a phenomenon called the Warburg effect (Dang 2012). Gu and colleagues demonstrated the potential of anti-austerity drugs combined with glycolysis inhibition by 2DG which showed the combined treatment had increased activity against cancer cells compared to normal cells (Gu, Qi et al. 2012). They postulated that the removal of glucose would stop glycolysis and if the anti-austerity compound prevented oxidative phosphorylation – the normal method of ATP production, these two factors would co-operatively deplete cellular ATP leading to necrotic cell death (Gu, Qi et al. 2012). Conflicting with this theory, mitochondrial oxidative phosphorylation is often dysfunctional in cancers, with a truncated TCA cycle or repurposed for biosynthesis (Wise and Thompson 2010; Dang 2012; Stine and Dang 2013; Blum and Kloog 2014). Therefore an alternative explanation must be explored. Depending on whether the mitochondria are able to produce ATP in PANC-1 cells, and if so in what quantities, the effect of angelmarin could simply be through inhibition of glycolysis leading to a deficit of ATP, and consequently cell death. Alternatively, angelmarin may interfere with mitochondrial shuttle activity or the production of NADH which are known to lead to cell death (Vanden Berghe, Kaiser et al. 2015). Experiments investigating glycolysis inhibition in PANC-1 cells or NADH levels could provide insight into the mechanisms of angelmarin activity.

Basit and colleagues explored a drug called obatoclax for its induction of necroptosis in rhabdomyosarcoma. Obatoclax is an inhibitor of Bcl-2 proteins which promotes autophagy. However they demonstrate necroptosis being caused by formation of the necrosome on the autophagosomal membrane. Caspase activity appeared uninvolved as zVAD-fmk inhibition did not affect the cell death outcome, however addition of necrostatin-1 blocked cell death, as did the knockdown of autophagy related ATG5 or ATG7 proteins (Basit, Cristofanon et al. 2013). This study has indicated that a necroptotic cell death is activated in response to angelmarin treatment. Additionally, the results have indicated a marginal increase in autophagy by detection of LC3b puncta. Furthermore, chloroquine – a known inhibitor of autophagy inhibited cell

death caused by angelmarin. This data would be consistent with regulation of necroptosis on the autophagosome, as was described by Basit and colleagues. Further exploration of why chloroquine mitigated the effectiveness of angelmarin must therefore be explored. Lysosomes in particular would be of interest as they may be essential in the execution or signalling leading to necrosis in response to angelmarin

Akt inhibition appears quite commonly in investigations of anti-austerity compounds. These findings suggest that phosphorylation of Akt at Ser473 is increased at 24 hours in response to angelmarin. This finding should be further explored with the possible relation to Beclin-1 levels (Wang, Wei et al. 2012). Additionally, phosphorylation of Akt at the newly discovered phosphorylation sites Ser477 and Thr479 (Chan, Jo et al. 2014; Liu, Begley et al. 2014) should be examined. Phospho p90RSK and phospho p38 MAPK should both be investigated further as they are both down-regulated in response to angelmarin to undetectable levels within the first 2 hours of treatment. Samsoeum was also found to induce phosphorylation of MAPK proteins including p38 MAPK (Kim, Yim et al. 2013). Sustained activation of MAPK has been shown to lead to autophagy (Wang, Whiteman et al. 2009) and the results have indicated a marginal increase in autophagy. Activation of p53 may also play a protective role against angelmarin treatment as pifithrin-μ decreased the toxicity of angelmarin and large decreases in phosphorylation of p53 were observed. Investigation of p53 in response to anti-austerity compounds has not been explored in any of the compounds mentioned. These findings highlight the need to explore the effect of p53 on anti-austerity treatments. Reactive oxygen species effect on the activity of angelmarin should also be examined as mitoSOX staining demonstrates the production of ROS in response to angelmarin and also that the ROS were sequestered into another cellular compartment. Indeed the production of ROS caused by an anti-austerity drug leading to a necrotic phenotype was demonstrated in arctigenin (Gu, Qi et al. 2012).

Additionally, angelmarin- butyl-ester should be further examined as the data indicate a far higher toxicity to PANC-1 cells under nutrient deprivation conditions when compared to cells grown in complete culture medium. Despite the promising initial results of angelmarin in treatment of pancreatic cancer, studies in more complex models should be pursued. 3D cell culture would be the next logical step in exploring angelmarin as a treatment for pancreatic cancer, along with studies in other pancreatic cancer cell lines. Although 3D cell culture adds a level of complexity, it is a more accurate model of tumours. This is because 3D cell culture spheroids more closely resemble tumour morphology than traditional 2D culture, for example the different exposures of cells on the surface compared to cells buried within the spheroid to drugs or oxygen levels (Yamada and Cukierman 2007). If the results from these experiments remain promising animal models should be investigated for possible side effects of angelmarin. The anti-austerity approach has been demonstrated viable in a nude mice model of the drug kigamicin D where addition of the drug suppressed tumour growth (Lu, Kunimoto et al. 2004). Owing to the nature of angelmarin's target – cells under nutrient deprivation, it is unlikely to cause severe side effects in normal tissues as they should have access to nutrients. Indeed, the data indicated extremely low toxicity of angelmarin in PANC-1 cells in the presence of nutrients (Figure 5.4). However, future studies should examine the effects of angelmarin on non-cancerous cells to provide a good starting indication of whether angelmarin is toxic to normal cells grown in the presence of nutrients. The complexities of drug interactions in whole organisms cannot be overstated, as well as how any given cell line will respond to a particular drug. Finally, the end goal of investigation of angelmarin is developing its use in human trials for the treatment of pancreatic cancer.

The findings of this chapter highlight the potential of angelmarin, or its derivatives as a treatment of pancreatic cancer. The strategy of anti-austerity drugs could be applied to several cancer types especially those with poor nutrient supply and cancers with a tendency to form tumours with a solid mass, such as PANC-1, MIA PaCa-2 or Capan-1 (Deer, Gonzalez-Hernandez et al. 2010). This approach has the advantage of not targeting a particular protein or pathway but rather tolerance to lack of nutrients as a

whole. The limited toxicity of angelmarin in cells grown in nutrient rich conditions is also promising for the development of angelmarin as a cancer treatment in vivo. Although the majority of the solid mass of a tumour is necrotic, the anti-austerity approach may still be viable. Owing to the extreme demand for nutrients in aggressive cancers and the poor vascularisation of some tumours due to lack of formation of adequate blood supply, tumour microenvironments are often lacking in nutrients (Hanahan and Weinberg 2011; Gu, Qi et al. 2012; Dibwe, Awale et al. 2013). Thus, an anti-austerity approach could selectively target tumours without nutrient supply without affecting normal tissues which are generally supplied with sufficient nutrients. Furthermore, the pairing of anti-austerity treatment with glycolysis inhibition may selectively target cancers (Gu, Qi et al. 2012). Induction of programmed necrosis is a relatively new field of study with potential in treating cancers which are resistant to current anti-cancer treatments. The resistance of cancers to current anti-cancer drugs which trigger cell death remains a major problem in oncology. Triggering necroptosis provides an untapped field of resources to kill cancers evading induction of cell death by apoptosis. As mentioned previously activation of the immune system to help in elimination of tumours as a side effect of necroptosis could actually help in elimination of cancer although debate regarding this effect is ongoing (Guerriero, Ditsworth et al. 2008; Cuadrado-Castano, Sanchez-Aparicio et al. 2015). A recent study has highlighted the susceptibility of a sub-population of pancreatic cancers to immune modulation (Bailey, Chang et al. 2016). Under certain circumstances necroptosis can trigger anti-tumour immunity and promote tumour phagocytosis (Meng, Wang et al. 2016). Necroptosis induction has been demonstrated to provoke an immune response to kill other nearby cancer cells (Obeid, Tesniere et al. 2007; Kang, Bang et al. 2015; Schmidt, Seibert et al. 2015; Takemura, Takaki et al. 2015; Aaes, Kaczmarek et al. 2016). Exploration of angelmarin and its derivatives may lead to selective induction of necrosis in pancreatic cancer as a much needed new therapy. The initial investigations of angelmarin as an anti-austerity compound in PANC-1 cells have shown promise. However, investigations of the compound in other pancreatic cancer cell lines must be conducted. Recent studies have highlighted the heterogeneity present in pancreatic cancer (Biankin, Waddell et al. 2012; Waddell, Pajic et al. 2015; Bailey, Chang et al. 2016), and as such these findings must be evaluated in other cell lines. The large

amount of genetic differences in genomes of pancreatic cancers cause difficulties in treatment of pancreatic cancer, as treatments which work for one cell line may not be effective in another.

Two different approaches to exploring anti-cancer treatments were examined in this thesis. The characterisation of the unusual pathway of cell death triggered by DNA damage in Burkitt's lymphoma was explored with the aim of clearly defining the process of cell death in order to trigger it in other cancers selectively. This investigation continued with the examination of resistance in BL30K cells to apoptosis triggered by this pathway. Additionally, the investigation of angelmarin as a potential anti-cancer drug in pancreatic cancers highlighted the possibilities of targeting tolerance to nutrient deprivation. A thorough understanding of strategies used by cancer cells to survive will prove invaluable to drug discovery teams and provide benefits for streamlining the process from drug discovery to therapeutic treatment. Conversely, beneficial effects of compounds either manufactured or from natural products could lead to targeted exploitation of known signalling pathways and potentially discovery of new pathways which can help in developing new therapy options. As our knowledge of how cancers evade cell death grows, more treatment targets should emerge as a result.

References

7.1 Reference List

Aaes, T. L., A. Kaczmarek, T. Delvaeye, B. De Craene, S. De Koker, L. Heyndrickx, I. Delrue, J. Taminau, B. Wiernicki, P. De Groote, et al. (2016). "Vaccination with Necroptotic Cancer Cells Induces Efficient Anti-tumor Immunity." Cell Rep **15**(2): 274-87.

Adams, J. M. and S. Cory (1998). "The Bcl-2 protein family: arbiters of cell survival." Science **281**(5381): 1322-6.

Adams, J. M. and S. Cory (2007). "The Bcl-2 apoptotic switch in cancer development and therapy." Oncogene **26**(9): 1324-37.

Adi-Harel, S., S. Erlich, E. Schmukler, S. Cohen-Kedar, O. Segev, L. Mizrachy, J. A. Hirsch and R. Pinkas-Kramarski (2010). "Beclin 1 self-association is independent of autophagy induction by amino acid deprivation and rapamycin treatment." J Cell Biochem **110**(5): 1262-71.

Afshar, G., N. Jelluma, X. Yang, D. Basila, N. D. Arvold, A. Karlsson, G. L. Yount, T. B. Dansen, E. Koller and D. A. Haas-Kogan (2006). "Radiation-induced caspase-8 mediates p53-independent apoptosis in glioma cells." Cancer Res **66**(8): 4223-32.

Ahn, B. Y., D. L. Trinh, L. D. Zajchowski, B. Lee, A. N. Elwi and S. W. Kim (2010). "Tid1 is a new regulator of p53 mitochondrial translocation and apoptosis in cancer." Oncogene **29**(8): 1155-66.

Aisner, J. and E. J. Lee (1991). "Etoposide. Current and future status." Cancer **67**(1 Suppl): 215-9.

Alexander, A., S. L. Cai, J. Kim, A. Nanez, M. Sahin, K. H. MacLean, K. Inoki, K. L. Guan, J. Shen, M. D. Person, et al. (2010). "ATM signals to TSC2 in the cytoplasm to regulate mTORC1 in response to ROS." Proc Natl Acad Sci U S A **107**(9): 4153-8.

Alnemri, E. S., D. J. Livingston, D. W. Nicholson, G. Salvesen, N. A. Thornberry, W. W. Wong and J. Yuan (1996). "Human ICE/CED-3 protease nomenclature." Cell **87**(2): 171.

Alvarado-Kristensson, M., F. Melander, K. Leandersson, L. Ronnstrand, C. Wernstedt and T. Andersson (2004). "p38-MAPK signals survival by phosphorylation of caspase-8 and caspase-3 in human neutrophils." J Exp Med **199**: 449-458.

Amar, N., G. Lustig, Y. Ichimura, Y. Ohsumi and Z. Elazar (2006). "Two newly identified sites in the ubiquitin-like protein Atg8 are essential for autophagy." EMBO Rep **7**(6): 635-42.

Annovazzi, L., M. Mellai, V. Caldera, G. Valente, L. Tessitore and D. Schiffer (2009). "mTOR, S6 and AKT expression in relation to proliferation and apoptosis/autophagy in glioma." Anticancer Res **29**(8): 3087-94.

Anthony, B., P. Carter and A. De Benedetti (1996). "Overexpression of the proto-oncogene/translation factor 4E in breast-carcinoma cell lines." Int J Cancer **65**(6): 858-63.

Arya, R. and K. White (2015). "Cell death in development: Signaling pathways and core mechanisms." Semin Cell Dev Biol.

Ashford, T. P. and K. R. Porter (1962). "Cytoplasmic components in hepatic cell lysosomes." J Cell Biol **12**: 198-202.

Aslan, J. E. and G. Thomas (2009). "Death by committee: organellar trafficking and communication in apoptosis." Traffic **10**(10): 1390-404.

Awale, S., E. M. Nakashima, S. K. Kalauni, Y. Tezuka, Y. Kurashima, J. Lu, H. Esumi and S. Kadota (2006). "Angelmarin, a novel anti-cancer agent able to eliminate the tolerance of cancer cells to nutrient starvation." Bioorg Med Chem Lett **16**(3): 581-3.

Awale, S., J. Y. Ueda, S. Athikomkulchai, S. Abdelhamed, S. Yokoyama, I. Saiki and R. Miyatake (2012). "Antiausterity agents from Uvaria dac and their preferential cytotoxic activity against human pancreatic cancer cell lines in a nutrient-deprived condition." J Nat Prod **75**(6): 1177-83.

Baig, S., I. Seevasant, J. Mohamad, A. Mukheem, H. Z. Huri and T. Kamarul (2016). "Potential of apoptotic pathway-targeted cancer therapeutic research: Where do we stand?" Cell Death Dis **7**: e2058.

Bailey, P., D. K. Chang, K. Nones, A. L. Johns, A. M. Patch, M. C. Gingras, D. K. Miller, A. N. Christ, T. J. Bruxner, M. C. Quinn, et al. (2016). "Genomic analyses identify molecular subtypes of pancreatic cancer." Nature **531**(7592): 47-52.

Bantel, H., I. H. Engels, W. Voelter, K. Schulze-Osthoff and S. Wesselborg (1999). "Mistletoe lectin activates caspase-8/FLICE independently of death receptor signaling and enhances anticancer drug-induced apoptosis." Cancer Res **59**(9): 2083-90.

Bao, Q. and Y. Shi (2007). "Apoptosome: a platform for the activation of initiator caspases." Cell Death Differ **14**(1): 56-65.

Barnhart, B. C., E. C. Alappat and M. E. Peter (2003). "The CD95 type I/type II model." Semin Immunol **15**(3): 185-93.

Basit, F., S. Cristofanon and S. Fulda (2013). "Obatoclax (GX15-070) triggers necroptosis by promoting the assembly of the necrosome on autophagosomal membranes." Cell Death Differ **20**(9): 1161-73.

Basit, F., R. Humphreys and S. Fulda (2012). "RIP1 protein-dependent assembly of a cytosolic cell death complex is required for inhibitor of apoptosis (IAP) inhibitor-mediated sensitization to lexatumumab-induced apoptosis." J Biol Chem **287**(46): 38767-77.

Beck, J. W., D. Saavedra, G. J. Antell and B. Tejeiro (1959). "The treatment of pinworm infections in humans (enterobiasis) with pyrvinium chloride and pyrvinium pamoate." Am J Trop Med Hyg **8**(3): 349-52.

Bell, B. D., S. Leverrier, B. M. Weist, R. H. Newton, A. F. Arechiga, K. A. Luhrs, N. S. Morrissette and C. M. Walsh (2008). "FADD and caspase-8 control the outcome of autophagic signaling in proliferating T cells." Proc Natl Acad Sci U S A **105**(43): 16677-82.

Benkova, B., V. Lozanov, I. P. Ivanov and V. Mitev (2009). "Evaluation of recombinant caspase specificity by competitive substrates." Anal Biochem **394**(1): 68-74.

Bertrand, M. J. and P. Vandenabeele (2011). "The Ripoptosome: death decision in the cytosol." Mol Cell **43**(3): 323-5.

Berube, C., L. M. Boucher, W. Ma, A. Wakeham, L. Salmena, R. Hakem, W. C. Yeh, T. W. Mak and S. Benchimol (2005). "Apoptosis caused by p53-induced protein with death domain (PIDD) depends on the death adapter protein RAIDD." Proc Natl Acad Sci U S A **102**(40): 14314-20.

Bhardwaj, V., N. Rizvi, M. B. Lai, J. C. Lai and A. Bhushan (2010). "Glycolytic enzyme inhibitors affect pancreatic cancer survival by modulating its signaling and energetics." Anticancer Res **30**(3): 743-9.

Biankin, A. V., N. Waddell, K. S. Kassahn, M. C. Gingras, L. B. Muthuswamy, A. L. Johns, D. K. Miller, P. J. Wilson, A. M. Patch, J. Wu, et al. (2012). "Pancreatic cancer genomes reveal aberrations in axon guidance pathway genes." Nature **491**(7424): 399-405.

Bionda, C., A. Athias, D. Poncet, G. Alphonse, A. Guezguez, P. Gambert, C. Rodriguez-Lafrasse and D. Ardail (2008). "Differential regulation of cell death in head and neck cell carcinoma through alteration of cholesterol levels in lipid rafts microdomains." Biochem Pharmacol **75**(3): 761-72.

Blasco, M. A. (2005). "Telomeres and human disease: ageing, cancer and beyond." Nat Rev Genet **6**(8): 611-22.

Blum, R. and Y. Kloog (2005). "Tailoring Ras-pathway--inhibitor combinations for cancer therapy." Drug Resist Updat **8**(6): 369-80.

Blum, R. and Y. Kloog (2014). "Metabolism addiction in pancreatic cancer." Cell Death Dis **5**: e1065.

Bodemann, B. O., A. Orvedahl, T. Cheng, R. R. Ram, Y. H. Ou, E. Formstecher, M. Maiti, C. C. Hazelett, E. M. Wauson, M. Balakireva, et al. (2011). "RalB and the exocyst mediate the

cellular starvation response by direct activation of autophagosome assembly." Cell **144**(2): 253-67.

Boesen-de Cock, J. G., E. de Vries, G. T. Williams and J. Borst (1998). "The anti-cancer drug etoposide can induce caspase-8 processing and apoptosis in the absence of CD95 receptor-ligand interaction." Apoptosis **3**(1): 17-25.

Borges, H. L., R. Linden and J. Y. Wang (2008). "DNA damage-induced cell death: lessons from the central nervous system." Cell Res **18**(1): 17-26.

Bortner, C. D., N. B. Oldenburg and J. A. Cidlowski (1995). "The role of DNA fragmentation in apoptosis." Trends Cell Biol **5**(1): 21-6.

Bouchier-Hayes, L., A. Oberst, G. P. McStay, S. Connell, S. W. Tait, C. P. Dillon, J. M. Flanagan, H. M. Beere and D. R. Green (2009). "Characterization of cytoplasmic caspase-2 activation by induced proximity." Mol Cell **35**(6): 830-40.

Boya, P. and G. Kroemer (2008). "Lysosomal membrane permeabilization in cell death." Oncogene **27**(50): 6434-51.

Brady, H. J., G. Gil-Gomez, J. Kirberg and A. J. Berns (1996). "Bax alpha perturbs T cell development and affects cell cycle entry of T cells." Embo J **15**(24): 6991-7001.

Brocheriou, V., A. A. Hagege, A. Oubenaissa, M. Lambert, V. O. Mallet, M. Duriez, M. Wassef, A. Kahn, P. Menasche and H. Gilgenkrantz (2000). "Cardiac functional improvement by a human Bcl-2 transgene in a mouse model of ischemia/reperfusion injury." J Gene Med **2**(5): 326-33.

Bueno, C., M. L. Villegas, S. G. Bertolotti, C. M. Previtali, M. G. Neumann and M. V. Encinas (2002). "The excited-state interaction of resazurin and resorufin with amines in aqueous solutions. Photophysics and photochemical reactions." Photochem Photobiol **76**(4): 385-90.

Caro-Maldonado, A. and C. Muñoz-Pinedo (2011). "Dying for Something to Eat: How Cells Respond to Starvation." The Open Cell Signaling Journal **3**: 42-51.

Cerretti, D. P., C. J. Kozlosky, B. Mosley, N. Nelson, K. Van Ness, T. A. Greenstreet, C. J. March, S. R. Kronheim, T. Druck, L. A. Cannizzaro, et al. (1992). "Molecular cloning of the interleukin-1 beta converting enzyme." Science **256**(5053): 97-100.

Chan, C. H., U. Jo, A. Kohrman, A. H. Rezaeian, P. C. Chou, C. Logothetis and H. K. Lin (2014). "Posttranslational regulation of Akt in human cancer." Cell Biosci **4**(1): 59.

Chandra, D., G. Choy, X. Deng, B. Bhatia, P. Daniel and D. G. Tang (2004). "Association of active caspase 8 with the mitochondrial membrane during apoptosis: potential roles in cleaving BAP31 and caspase 3 and mediating mitochondrion-endoplasmic reticulum cross talk in etoposide-induced cell death." Mol Cell Biol **24**(15): 6592-607.

Chang, K. H., M. D. Yan, C. J. Yao, P. C. Lin and G. M. Lai (2013). "Honokiol-induced apoptosis and autophagy in glioblastoma multiforme cells." Oncol Lett **6**(5): 1435-1438.

Chen, M., A. Orozco, D. M. Spencer and J. Wang (2002). "Activation of initiator caspases through a stable dimeric intermediate." J Biol Chem **277**(52): 50761-7.

Chen, T. Y., K. H. Chi, J. S. Wang, C. L. Chien and W. W. Lin (2009). "Reactive oxygen species are involved in FasL-induced caspase-independent cell death and inflammatory responses." Free Radic Biol Med **46**(5): 643-55.

Chen, Y., E. McMillan-Ward, J. Kong, S. J. Israels and S. B. Gibson (2007). "Mitochondrial electron-transport-chain inhibitors of complexes I and II induce autophagic cell death mediated by reactive oxygen species." J Cell Sci **120**(Pt 23): 4155-66.

Chiba, T., S. Takahashi, N. Sato, S. Ishii and K. Kikuchi (1996). "Fas-mediated apoptosis is modulated by intracellular glutathione in human T cells." Eur J Immunol **26**(5): 1164-9.

Chikte, S., N. Panchal and G. Warnes (2013). "Use of LysoTracker dyes: a flow cytometric study of autophagy." Cytometry A **85**(2): 169-78.

Chinnaiyan, A. M., K. O'Rourke, M. Tewari and V. M. Dixit (1995). "FADD, a novel death domain-containing protein, interacts with the death domain of Fas and initiates apoptosis." Cell **81**(4): 505-12.

Chipuk, J. E., J. C. Fisher, C. P. Dillon, R. W. Kriwacki, T. Kuwana and D. R. Green (2008). "Mechanism of apoptosis induction by inhibition of the anti-apoptotic BCL-2 proteins." Proc Natl Acad Sci U S A **105**(51): 20327-32.

Chipuk, J. E., T. Kuwana, L. Bouchier-Hayes, N. M. Droin, D. D. Newmeyer, M. Schuler and D. R. Green (2004). "Direct activation of Bax by p53 mediates mitochondrial membrane permeabilization and apoptosis." Science **303**(5660): 1010-4.

Chittenden, T., C. Flemington, A. B. Houghton, R. G. Ebb, G. J. Gallo, B. Elangovan, G. Chinnadurai and R. J. Lutz (1995). "A conserved domain in Bak, distinct from BH1 and BH2, mediates cell death and protein binding functions." Embo J **14**(22): 5589-96.

Cho, Y. S. and S. Y. Park (2014). "Harnessing of Programmed Necrosis for Fighting against Cancers." Biomol Ther (Seoul) **22**(3): 167-75.

Choi, A. M., S. W. Ryter and B. Levine (2013). "Autophagy in human health and disease." N Engl J Med **368**(7): 651-62.

Chowdhury, I., B. Tharakan and G. K. Bhat (2006). "Current concepts in apoptosis: the physiological suicide program revisited." Cell Mol Biol Lett **11**(4): 506-25.

Clements, R. T., B. Cordeiro, J. Feng, C. Bianchi and F. W. Sellke (2011). "Rottlerin increases cardiac contractile performance and coronary perfusion through BKCa++ channel activation after cold cardioplegic arrest in isolated hearts." Circulation **124**(11 Suppl): S55-61.

Conradt, B. and H. R. Horvitz (1998). "The C. elegans protein EGL-1 is required for programmed cell death and interacts with the Bcl-2-like protein CED-9." Cell **93**(4): 519-29.

Corbett, A. H. and N. Osheroff (1993). "When good enzymes go bad: conversion of topoisomerase II to a cellular toxin by antineoplastic drugs." Chem Res Toxicol **6**(5): 585-97.

Corcoran, R. B., K. A. Cheng, A. N. Hata, A. C. Faber, H. Ebi, E. M. Coffee, P. Greninger, R. D. Brown, J. T. Godfrey, T. J. Cohoon, et al. (2013). "Synthetic lethal interaction of combined BCL-XL and MEK inhibition promotes tumor regressions in KRAS mutant cancer models." Cancer Cell **23**(1): 121-8.

Coutts, A. S., C. J. Adams and N. B. La Thangue (2009). "p53 ubiquitination by Mdm2: a never ending tail?" DNA Repair (Amst) **8**(4): 483-90.

Crighton, D., S. Wilkinson, J. O'Prey, N. Syed, P. Smith, P. R. Harrison, M. Gasco, O. Garrone, T. Crook and K. M. Ryan (2006). "DRAM, a p53-induced modulator of autophagy, is critical for apoptosis." Cell **126**(1): 121-34.

Cuadrado-Castano, S., M. T. Sanchez-Aparicio, A. Garcia-Sastre and E. Villar (2015). "The therapeutic effect of death: Newcastle disease virus and its antitumor potential." Virus Res **209**: 56-66.

Dai, C. and W. Gu (2010). "p53 post-translational modification: deregulated in tumorigenesis." Trends Mol Med **16**(11): 528-36.

Dai, Z. J., J. Gao, X. B. Ma, H. F. Kang, B. F. Wang, W. F. Lu, S. Lin, X. J. Wang and W. Y. Wu (2013). "Antitumor effects of rapamycin in pancreatic cancer cells by inducing apoptosis and autophagy." Int J Mol Sci **14**(1): 273-85.

Dang, C. V. (2012). "Links between metabolism and cancer." Genes Dev **26**(9): 877-90.

Danial, N. N. and S. J. Korsmeyer (2004). "Cell death: critical control points." Cell **116**: 205-219.

Debatin, K. M. (2004). "Apoptosis pathways in cancer and cancer therapy." Cancer Immunol Immunother **53**(3): 153-9.

Deer, E. L., J. Gonzalez-Hernandez, J. D. Coursen, J. E. Shea, J. Ngatia, C. L. Scaife, M. A. Firpo and S. J. Mulvihill (2010). "Phenotype and genotype of pancreatic cancer cell lines." Pancreas **39**(4): 425-35.

Degenhardt, K., R. Mathew, B. Beaudoin, K. Bray, D. Anderson, G. Chen, C. Mukherjee, Y. Shi, C. Gelinas, Y. Fan, et al. (2006). "Autophagy promotes tumor cell survival and restricts necrosis, inflammation, and tumorigenesis." Cancer Cell **10**(1): 51-64.

Degterev, A., J. Hitomi, M. Germscheid, I. L. Ch'en, O. Korkina, X. Teng, D. Abbott, G. D. Cuny, C. Yuan, G. Wagner, et al. (2008). "Identification of RIP1 kinase as a specific cellular target of necrostatins." Nat Chem Biol **4**(5): 313-21.

Degterev, A., Z. Huang, M. Boyce, Y. Li, P. Jagtap, N. Mizushima, G. D. Cuny, T. J. Mitchison, M. A. Moskowitz and J. Yuan (2005). "Chemical inhibitor of nonapoptotic cell death with therapeutic potential for ischemic brain injury." Nat Chem Biol **1**(2): 112-9.

Delbridge, A. R. and A. Strasser (2015). "The BCL-2 protein family, BH3-mimetics and cancer therapy." Cell Death Differ **22**(7): 1071-80.

DeLeo, A. B., G. Jay, E. Appella, G. C. Dubois, L. W. Law and L. J. Old (1979). "Detection of a transformation-related antigen in chemically induced sarcomas and other transformed cells of the mouse." Proc Natl Acad Sci U S A **76**(5): 2420-4.

Demchenko, A. P. and P. R. Callis (2010). Kim, Eunha; Park, Seung Bum (2010). "Discovery of New Synthetic Dyes: Targeted Synthesis or Combinatorial Approach?". In "Advanced fluorescence reporters in chemistry and biology I : fundamentals and molecular design". Heidelberg ; New York, Springer.

Dibwe, D. F., S. Awale, S. Kadota, H. Morita and Y. Tezuka (2013). "Heptaoxygenated xanthones as anti-austerity agents from Securidaca longepedunculata." Bioorg Med Chem **21**(24): 7663-8.

Dickens, L. S., I. R. Powley, M. A. Hughes and M. MacFarlane (2012). "The 'complexities' of life and death: death receptor signalling platforms." Exp Cell Res **318**(11): 1269-77.

Djavaheri-Mergny, M., M. C. Maiuri and G. Kroemer (2010). "Cross talk between apoptosis and autophagy by caspase-mediated cleavage of Beclin 1." Oncogene **29**(12): 1717-9.

Dodson, M., V. Darley-Usmar and J. Zhang (2013). "Cellular metabolic and autophagic pathways: traffic control by redox signaling." Free Radic Biol Med **63**: 207-21.

Donehower, L. A. (1996). "The p53-deficient mouse: a model for basic and applied cancer studies." Semin Cancer Biol **7**(5): 269-78.

Donepudi, M., A. Mac Sweeney, C. Briand and M. G. Grutter (2003). "Insights into the regulatory mechanism for caspase-8 activation." Mol Cell **11**(2): 543-9.

Downey, A. S., C. R. Chong, T. K. Graczyk and D. J. Sullivan (2008). "Efficacy of pyrvinium pamoate against Cryptosporidium parvum infection in vitro and in a neonatal mouse model." Antimicrob Agents Chemother **52**(9): 3106-12.

Du, C., M. Fang, Y. Li, L. Li and X. Wang (2000). "Smac, a mitochondrial protein that promotes cytochrome c-dependent caspase activation by eliminating IAP inhibition." Cell **102**(1): 33-42.

Du, H., J. Wolf, B. Schafer, T. Moldoveanu, J. E. Chipuk and T. Kuwana (2011). "BH3 domains other than Bim and Bid can directly activate Bax/Bak." J Biol Chem **286**(1): 491-501.

Dunlop, E. A. and A. R. Tee (2013). "The kinase triad, AMPK, mTORC1 and ULK1, maintains energy and nutrient homoeostasis." Biochem Soc Trans **41**(4): 939-43.

Duprez, L., E. Wirawan, T. Vanden Berghe and P. Vandenabeele (2009). "Major cell death pathways at a glance." Microbes Infect **11**(13): 1050-62.

Eckhart, L., C. Ballaun, M. Hermann, J. L. VandeBerg, W. Sipos, A. Uthman, H. Fischer and E. Tschachler (2008). "Identification of novel mammalian caspases reveals an important role of gene loss in shaping the human caspase repertoire." Mol Biol Evol **25**(5): 831-41.

Eckhart, L., C. Ballaun, A. Uthman, C. Kittel, M. Stichenwirth, M. Buchberger, H. Fischer, W. Sipos and E. Tschachler (2005). "Identification and characterization of a novel mammalian caspase with proapoptotic activity." J Biol Chem **280**(42): 35077-80.

Eckhart, L., W. Declercq, J. Ban, M. Rendl, B. Lengauer, C. Mayer, S. Lippens, P. Vandenabeele and E. Tschachler (2000). "Terminal differentiation of human keratinocytes and stratum corneum formation is associated with caspase-14 activation." J Invest Dermatol **115**(6): 1148-51.

Edinger, A. L. and C. B. Thompson (2004). "Death by design: apoptosis, necrosis and autophagy." Curr Opin Cell Biol **16**(6): 663-9.

Eguchi, Y., S. Shimizu and Y. Tsujimoto (1997). "Intracellular ATP levels determine cell death fate by apoptosis or necrosis." Cancer Res **57**(10): 1835-40.

Elmore, S. (2007). "Apoptosis: a review of programmed cell death." Toxicol Pathol **35**(4): 495-516.

Erster, S., M. Mihara, R. H. Kim, O. Petrenko and U. M. Moll (2004). "In vivo mitochondrial p53 translocation triggers a rapid first wave of cell death in response to DNA damage that can precede p53 target gene activation." Mol Cell Biol **24**(15): 6728-41.

Estornes, Y., F. Toscano, F. Virard, G. Jacquemin, A. Pierrot, B. Vanbervliet, M. Bonnin, N. Lalaoui, P. Mercier-Gouy, Y. Pacheco, et al. (2012). "dsRNA induces apoptosis through an atypical death complex associating TLR3 to caspase-8." Cell Death Differ **19**(9): 1482-94.

Esumi, H., K. Izuishi, K. Kato, K. Hashimoto, Y. Kurashima, A. Kishimoto, T. Ogura and T. Ozawa (2002). "Hypoxia and nitric oxide treatment confer tolerance to glucose starvation in a 5'-AMP-activated protein kinase-dependent manner." J Biol Chem **277**(36): 32791-8.

Esumi, H., J. Lu, Y. Kurashima and T. Hanaoka (2004). "Antitumor activity of pyrvinium pamoate, 6-(dimethylamino)-2-[2-(2,5-dimethyl-1-phenyl-1H-pyrrol-3-yl)ethenyl]-1-methyl-qu inolinium pamoate salt, showing preferential cytotoxicity during glucose starvation." Cancer Sci **95**(8): 685-90.

Faraco, P. R., E. C. Ledgerwood, P. Vandenabeele, J. B. Prins and J. R. Bradley (1999). "Tumor necrosis factor induces distinct patterns of caspase activation in WEHI-164 cells associated with apoptosis or necrosis depending on cell cycle stage." Biochem Biophys Res Commun **261**(2): 385-92.

Farrell, P. J., G. J. Allan, F. Shanahan, K. H. Vousden and T. Crook (1991). "p53 is frequently mutated in Burkitt's lymphoma cell lines." Embo J **10**(10): 2879-87.

Felix, C. A. (2001). "Leukemias related to treatment with DNA topoisomerase II inhibitors." Med Pediatr Oncol **36**(5): 525-35.

Feng, Y., D. He, Z. Yao and D. J. Klionsky (2014). "The machinery of macroautophagy." Cell Res **24**(1): 24-41.

Feoktistova, M., P. Geserick, B. Kellert, D. P. Dimitrova, C. Langlais, M. Hupe, K. Cain, M. MacFarlane, G. Hacker and M. Leverkus (2011). "cIAPs block Ripoptosome formation, a RIP1/caspase-8 containing intracellular cell death complex differentially regulated by cFLIP isoforms." Mol Cell **43**(3): 449-63.

Feoktistova, M., P. Geserick, D. Panayotova-Dimitrova and M. Leverkus (2011). "Pick your poison: the Ripoptosome, a cell death platform regulating apoptosis and necroptosis." Cell Cycle **11**(3): 460-7.

Ferecatu, I., M. Bergeaud, A. Rodriguez-Enfedaque, N. Le Floch, L. Oliver, V. Rincheval, F. Renaud, F. M. Vallette, B. Mignotte and J. L. Vayssiere (2009). "Mitochondrial localization of the low level p53 protein in proliferative cells." Biochem Biophys Res Commun **387**(4): 772-7.

Fernandes-Alnemri, T., J. Wu, J. W. Yu, P. Datta, B. Miller, W. Jankowski, S. Rosenberg, J. Zhang and E. S. Alnemri (2007). "The pyroptosome: a supramolecular assembly of ASC dimers mediating inflammatory cell death via caspase-1 activation." Cell Death Differ **14**(9): 1590-604.

Ferrari, D., A. Stepczynska, M. Los, S. Wesselborg and K. Schulze-Osthoff (1998). "Differential regulation and ATP requirement for caspase-8 and caspase-3 activation during CD95- and anticancer drug-induced apoptosis." J Exp Med **188**(5): 979-84.

Ferry, J. A. (2006). "Burkitt's lymphoma: clinicopathologic features and differential diagnosis." Oncologist **11**(4): 375-83.

Fischer, U., R. U. Janicke and K. Schulze-Osthoff (2003). "Many cuts to ruin: a comprehensive update of caspase substrates." Cell Death Differ **10**(1): 76-100.

Fiskum, G., S. W. Craig, G. L. Decker and A. L. Lehninger (1980). "The cytoskeleton of digitonin-treated rat hepatocytes." Proc Natl Acad Sci U S A **77**(6): 3430-4.

Foucher, A. L., B. Papadopoulou and M. Ouellette (2006). "Prefractionation by digitonin extraction increases representation of the cytosolic and intracellular proteome of Leishmania infantum." J Proteome Res **5**(7): 1741-50.

Fuchs, Y. and H. Steller (2015). "Live to die another way: modes of programmed cell death and the signals emanating from dying cells." Nat Rev Mol Cell Biol **16**(6): 329-44.

Fuentes-Prior, P. and G. S. Salvesen (2004). "The protein structures that shape caspase activity, specificity, activation and inhibition." Biochem J **384**(Pt 2): 201-32.

Fukuyama, H., S. Ndiaye, J. Hoffmann, J. Rossier, S. Liuu, J. Vinh and Y. Verdier (2012). "On-bead tryptic proteolysis: an attractive procedure for LC-MS/MS analysis of the Drosophila caspase 8 protein complex during immune response against bacteria." J Proteomics **75**(15): 4610-9.

Fulda, S. (2009). "Caspase-8 in cancer biology and therapy." Cancer Lett **281**(2): 128-33.

Fulda, S. (2014). "Therapeutic exploitation of necroptosis for cancer therapy." Semin Cell Dev Biol **35**: 51-6.

Gajate, C., F. Gonzalez-Camacho and F. Mollinedo (2009). "Involvement of raft aggregates enriched in Fas/CD95 death-inducing signaling complex in the antileukemic action of edelfosine in Jurkat cells." PLoS ONE **4**(4): e5044.

Galluzzi, L., C. Brenner, E. Morselli, Z. Touat and G. Kroemer (2008). "Viral control of mitochondrial apoptosis." PLoS Pathog **4**(5): e1000018.

Galluzzi, L., M. C. Maiuri, I. Vitale, H. Zischka, M. Castedo, L. Zitvogel and G. Kroemer (2007). "Cell death modalities: classification and pathophysiological implications." Cell Death Differ **14**(7): 1237-43.

Gao, M., J. Liang, Y. Lu, H. Guo, P. German, S. Bai, E. Jonasch, X. Yang, G. B. Mills and Z. Ding (2014). "Site-specific activation of AKT protects cells from death induced by glucose deprivation." Oncogene **33**(6): 745-55.

George, M. D., M. Baba, S. V. Scott, N. Mizushima, B. S. Garrison, Y. Ohsumi and D. J. Klionsky (2000). "Apg5p functions in the sequestration step in the cytoplasm-to-vacuole targeting and macroautophagy pathways." Mol Biol Cell **11**(3): 969-82.

Geserick, P., M. Hupe, M. Moulin, W. W. Wong, M. Feoktistova, B. Kellert, H. Gollnick, J. Silke and M. Leverkus (2009). "Cellular IAPs inhibit a cryptic CD95-induced cell death by limiting RIP1 kinase recruitment." J Cell Biol **187**(7): 1037-54.

Good, M., M. Lavin, P. Chen and C. Kidson (1978). "Dependence on cloning method of survival of human melanoma cells after ultraviolet and ionizing radiation." Cancer Res **38**(12): 4671-5.

Gradiz, R., H. C. Silva, L. Carvalho, M. F. Botelho and A. Mota-Pinto (2016). "MIA PaCa-2 and PANC-1 - pancreas ductal adenocarcinoma cell lines with neuroendocrine differentiation and somatostatin receptors." Sci Rep **6**: 21648.

Graham, N. A., M. Tahmasian, B. Kohli, E. Komisopoulou, M. Zhu, I. Vivanco, M. A. Teitell, H. Wu, A. Ribas, R. S. Lo, et al. (2012). "Glucose deprivation activates a metabolic and signaling amplification loop leading to cell death." Mol Syst Biol **8**: 589.

Greaves, M. and C. C. Maley (2012). "Clonal evolution in cancer." Nature **481**(7381): 306-13.

Green, D. R. and G. I. Evan (2002). "A matter of life and death." Cancer Cell **1**(1): 19-30.

Green, D. R. and G. Kroemer (2009). "Cytoplasmic functions of the tumour suppressor p53." Nature **458**(7242): 1127-30.

Grimm, S., B. Z. Stanger and P. Leder (1996). "RIP and FADD: two "death domain"-containing proteins can induce apoptosis by convergent, but dissociable, pathways." Proc Natl Acad Sci U S A **93**(20): 10923-7.

Gu, Y., C. Qi, X. Sun, X. Ma, H. Zhang, L. Hu, J. Yuan and Q. Yu (2012). "Arctigenin preferentially induces tumor cell death under glucose deprivation by inhibiting cellular energy metabolism." Biochem Pharmacol **84**(4): 468-76.

Guerriero, J. L., D. Ditsworth, Y. Fan, F. Zhao, H. C. Crawford and W. X. Zong (2008). "Chemotherapy induces tumor clearance independent of apoptosis." Cancer Res **68**(23): 9595-600.

Guo, Y., S. M. Srinivasula, A. Druilhe, T. Fernandes-Alnemri and E. S. Alnemri (2002). "Caspase-2 induces apoptosis by releasing proapoptotic proteins from mitochondria." J Biol Chem **277**(16): 13430-7.

Gyrd-Hansen, M., T. Farkas, N. Fehrenbacher, L. Bastholm, M. Hoyer-Hansen, F. Elling, D. Wallach, R. Flavell, G. Kroemer, J. Nylandsted, et al. (2006). "Apoptosome-independent activation of the lysosomal cell death pathway by caspase-9." Mol Cell Biol **26**(21): 7880-91.

Hacker, G. (2000). "The morphology of apoptosis." Cell Tissue Res **301**(1): 5-17.

Hagn, F., C. Klein, O. Demmer, N. Marchenko, A. Vaseva, U. M. Moll and H. Kessler (2009). "BclxL changes conformation upon binding to wild-type but not mutant p53 DNA binding domain." J Biol Chem **285**(5): 3439-50.

Han, J., P. Sabbatini, D. Perez, L. Rao, D. Modha and E. White (1996). "The E1B 19K protein blocks apoptosis by interacting with and inhibiting the p53-inducible and death-promoting Bax protein." Genes Dev **10**(4): 461-77.

Hanahan, D. and R. A. Weinberg (2011). "Hallmarks of cancer: the next generation." Cell **144**(5): 646-74.

Harada, H., J. S. Andersen, M. Mann, N. Terada and S. J. Korsmeyer (2001). "p70S6 kinase signals cell survival as well as growth, inactivating the pro-apoptotic molecule BAD." Proc Natl Acad Sci U S A **98**(17): 9666-70.

Hata, A. N., J. A. Engelman and A. C. Faber (2015). "The BCL2 Family: Key Mediators of the Apoptotic Response to Targeted Anticancer Therapeutics." Cancer Discov **5**(5): 475-87.

Haynes, A. P., I. Daniels, A. M. Abhulayha, G. I. Carter, R. Metheringham, C. D. Gregory and B. J. Thomson (2002). "CD95 (Fas) expression is regulated by sequestration in the Golgi complex in B-cell lymphoma." Br J Haematol **118**(2): 488-94.

He, M. X. and Y. W. He (2013). "A role for c-FLIP(L) in the regulation of apoptosis, autophagy, and necroptosis in T lymphocytes." Cell Death Differ **20**(2): 188-97.

Hengartner, M. O. and H. R. Horvitz (1994). "C. elegans cell survival gene ced-9 encodes a functional homolog of the mammalian proto-oncogene bcl-2." Cell **76**(4): 665-76.

Hickman, E. S., M. C. Moroni and K. Helin (2002). "The role of p53 and pRB in apoptosis and cancer." Curr Opin Genet Dev **12**(1): 60-6.

Hide, M., A. S. Ritleng, J. P. Brizard, A. Monte-Allegre and D. Sereno (2008). "Leishmania infantum: tuning digitonin fractionation for comparative proteomic of the mitochondrial protein content." Parasitol Res **103**(4): 989-92.

Holler, N., R. Zaru, O. Micheau, M. Thome, A. Attinger, S. Valitutti, J. L. Bodmer, P. Schneider, B. Seed and J. Tschopp (2000). "Fas triggers an alternative, caspase-8-independent cell death pathway using the kinase RIP as effector molecule." Nat Immunol **1**(6): 489-95.

Horvitz, H. R. (2003). "Worms, life, and death (Nobel lecture)." Chembiochem **4**(8): 697-711.

Hosokawa, N., T. Hara, T. Kaizuka, C. Kishi, A. Takamura, Y. Miura, S. Iemura, T. Natsume, K. Takehana, N. Yamada, et al. (2009). "Nutrient-dependent mTORC1 association with the ULK1-Atg13-FIP200 complex required for autophagy." Mol Biol Cell **20**(7): 1981-91.

Hrstka, R., P. J. Coates and B. Vojtesek (2009). "Polymorphisms in p53 and the p53 pathway: roles in cancer susceptibility and response to treatment." J Cell Mol Med **13**(3): 440-53.

Hsu, Y. T., K. G. Wolter and R. J. Youle (1997). "Cytosol-to-membrane redistribution of Bax and Bcl-X(L) during apoptosis." Proc Natl Acad Sci U S A **94**(8): 3668-72.

Huang, D. C., J. M. Adams and S. Cory (1998). "The conserved N-terminal BH4 domain of Bcl-2 homologues is essential for inhibition of apoptosis and interaction with CED-4." Embo J **17**(4): 1029-39.

Huang, H. L., L. W. Fang, S. P. Lu, C. K. Chou, T. Y. Luh and M. Z. Lai (2003). "DNA-damaging reagents induce apoptosis through reactive oxygen species-dependent Fas aggregation." Oncogene **22**(50): 8168-77.

Imre, G., S. Larisch and K. Rajalingam (2011). "Ripoptosome: a novel IAP-regulated cell death-signalling platform." J Mol Cell Biol **3**(6): 324-6.

Itoh, N., S. Yonehara, A. Ishii, M. Yonehara, S. Mizushima, M. Sameshima, A. Hase, Y. Seto and S. Nagata (1991). "The polypeptide encoded by the cDNA for human cell surface antigen Fas can mediate apoptosis." Cell **66**(2): 233-43.

Iwamaru, A., E. Iwado, S. Kondo, R. A. Newman, B. Vera, A. D. Rodriguez and Y. Kondo (2007). "Eupalmerin acetate, a novel anticancer agent from Caribbean gorgonian octocorals, induces apoptosis in malignant glioma cells via the c-Jun NH2-terminal kinase pathway." Mol Cancer Ther **6**(1): 184-92.

Izuishi, K., K. Kato, T. Ogura, T. Kinoshita and H. Esumi (2000). "Remarkable tolerance of tumor cells to nutrient deprivation: possible new biochemical target for cancer therapy." Cancer Res **60**(21): 6201-7.

Jamil, S., I. Lam, M. Majd, S. H. Tsai and V. Duronio (2015). "Etoposide induces cell death via mitochondrial-dependent actions of p53." Cancer Cell Int **15**: 79.

Jiang, P., W. Du, K. Heese and M. Wu (2006). "The Bad guy cooperates with good cop p53: Bad is transcriptionally up-regulated by p53 and forms a Bad/p53 complex at the mitochondria to induce apoptosis." Mol Cell Biol **26**(23): 9071-82.

Jin, Z. and W. S. El-Deiry (2005). "Overview of cell death signaling pathways." Cancer Biol Ther **4**(2): 139-63.

Jin, Z. and W. S. El-Deiry (2006). "Distinct signaling pathways in TRAIL- versus tumor necrosis factor-induced apoptosis." Mol Cell Biol **26**(21): 8136-48.

Jones, D. T., K. Ganeshaguru, A. E. Virchis, N. I. Folarin, M. W. Lowdell, A. B. Mehta, H. G. Prentice, A. V. Hoffbrand and R. G. Wickremasinghe (2001). "Caspase 8 activation independent of Fas (CD95/APO-1) signaling may mediate killing of B-chronic lymphocytic leukemia cells by cytotoxic drugs or gamma radiation." Blood **98**(9): 2800-7.

Kaiser, M., A. Kuhnl, J. Reins, S. Fischer, J. Ortiz-Tanchez, C. Schlee, L. H. Mochmann, S. Heesch, O. Benlasfer, W. K. Hofmann, et al. (2011). "Antileukemic activity of the HSP70 inhibitor pifithrin-mu in acute leukemia." Blood Cancer J **1**(7): e28.

Kalliolias, G. D. and L. B. Ivashkiv (2016). "TNF biology, pathogenic mechanisms and emerging therapeutic strategies." Nat Rev Rheumatol **12**(1): 49-62.

Kang, R., H. J. Zeh, M. T. Lotze and D. Tang (2011). "The Beclin 1 network regulates autophagy and apoptosis." Cell Death Differ **18**(4): 571-80.

Kang, Y. J., B. R. Bang, K. H. Han, L. Hong, E. J. Shim, J. Ma, R. A. Lerner and M. Otsuka (2015). "Regulation of NKT cell-mediated immune responses to tumours and liver inflammation by mitochondrial PGAM5-Drp1 signalling." Nat Commun **6**: 8371.

Karch, J. and J. D. Molkentin (2015). "Regulated necrotic cell death: the passive aggressive side of Bax and Bak." Circ Res **116**(11): 1800-9.

Kaufmann, S. H. and M. O. Hengartner (2001). "Programmed cell death: alive and well in the new millennium." Trends Cell Biol **11**(12): 526-34.

Kerr, J. F., B. Harmon and J. Searle (1974). "An electron-microscope study of cell deletion in the anuran tadpole tail during spontaneous metamorphosis with special reference to apoptosis of striated muscle fibers." J Cell Sci **14**(3): 571-85.

Kerr, J. F., A. H. Wyllie and A. R. Currie (1972). "Apoptosis: a basic biological phenomenon with wide-ranging implications in tissue kinetics." Br J Cancer **26**(4): 239-57.

Khanna, K. K., T. Wie, Q. Song, S. R. Burrows, D. J. Moss, S. Krajewski, J. C. Reed and M. F. Lavin (1996). "Expression of p53, bcl-2, bax, bcl-x2 and c-myc in radiation-induced apoptosis in Burkitt's lymphoma cells." Cell Death Differ **3**(3): 315-22.

Kikuchi, M., S. Kuroki, M. Kayama, S. Sakaguchi, K. K. Lee and S. Yonehara (2012). "Protease activity of procaspase-8 is essential for cell survival by inhibiting both apoptotic and nonapoptotic cell death dependent on receptor-interacting protein kinase 1 (RIP1) and RIP3." J Biol Chem **287**(49): 41165-73.

Kim, A., N. H. Yim and J. Y. Ma (2013). "Samsoeum, a traditional herbal medicine, elicits apoptotic and autophagic cell death by inhibiting Akt/mTOR and activating the JNK pathway in cancer cells." BMC Complement Altern Med **13**: 233.

Kim, E. H., S. U. Kim and K. S. Choi (2005). "Rottlerin sensitizes glioma cells to TRAIL-induced apoptosis by inhibition of Cdc2 and the subsequent downregulation of survivin and XIAP." Oncogene **24**(5): 838-49.

Kim, Y. S., M. J. Morgan, S. Choksi and Z. G. Liu (2007). "TNF-induced activation of the Nox1 NADPH oxidase and its role in the induction of necrotic cell death." Mol Cell **26**(5): 675-87.

Kimura, T., Y. Takabatake, A. Takahashi and Y. Isaka (2013). "Chloroquine in cancer therapy: a double-edged sword of autophagy." Cancer Res **73**(1): 3-7.

King, K. L. and J. A. Cidlowski (1998). "Cell cycle regulation and apoptosis." Annu Rev Physiol **60**: 601-17.

Kischkel, F. C., S. Hellbardt, I. Behrmann, M. Germer, M. Pawlita, P. H. Krammer and M. E. Peter (1995). "Cytotoxicity-dependent APO-1 (Fas/CD95)-associated proteins form a death-inducing signaling complex (DISC) with the receptor." Embo J **14**(22): 5579-88.

Klionsky, D. J., J. M. Cregg, W. A. Dunn, Jr., S. D. Emr, Y. Sakai, I. V. Sandoval, A. Sibirny, S. Subramani, M. Thumm, M. Veenhuis, et al. (2003). "A unified nomenclature for yeast autophagy-related genes." Dev Cell **5**(4): 539-45.

Klionsky, D. J. and S. D. Emr (2000). "Autophagy as a regulated pathway of cellular degradation." Science **290**(5497): 1717-21.

Kluck, R. M., E. Bossy-Wetzel, D. R. Green and D. D. Newmeyer (1997). "The release of cytochrome c from mitochondria: a primary site for Bcl-2 regulation of apoptosis." Science **275**(5303): 1132-6.

Kobashigawa, S., G. Kashino, K. Suzuki, S. Yamashita and H. Mori (2015). "Ionizing radiation-induced cell death is partly caused by increase of mitochondrial reactive oxygen species in normal human fibroblast cells." Radiat Res **183**(4): 455-64.

Koenig, U., L. Eckhart and E. Tschachler (2001). "Evidence that caspase-13 is not a human but a bovine gene." Biochem Biophys Res Commun **285**(5): 1150-4.

Kohler, B., S. Anguissola, C. G. Concannon, M. Rehm, D. Kogel and J. H. Prehn (2008). "Bid participates in genotoxic drug-induced apoptosis of HeLa cells and is essential for death receptor ligands' apoptotic and synergistic effects." PLoS ONE **3**(7): e2844.

Kohli, V., J. F. Madden, R. C. Bentley and P. A. Clavien (1999). "Calpain mediates ischemic injury of the liver through modulation of apoptosis and necrosis." Gastroenterology **116**(1): 168-78.

Komarov, P. G., E. A. Komarova, R. V. Kondratov, K. Christov-Tselkov, J. S. Coon, M. V. Chernov and A. V. Gudkov (1999). "A chemical inhibitor of p53 that protects mice from the side effects of cancer therapy." Science **285**(5434): 1733-7.

Kong, D. H., Q. Zhang, X. Meng, Z. H. Zong, C. Li, B. Q. Liu, Y. Guan and H. Q. Wang (2013). "BAG3 sensitizes cancer cells exposed to DNA damaging agents via direct interaction with GRP78." Biochim Biophys Acta **1833**(12): 3245-53.

Kreuzaler, P. and C. J. Watson (2012). "Killing a cancer: what are the alternatives?" Nat Rev Cancer **12**(6): 411-24.

Kroemer, G., L. Galluzzi, P. Vandenabeele, J. Abrams, E. S. Alnemri, E. H. Baehrecke, M. V. Blagosklonny, W. S. El-Deiry, P. Golstein, D. R. Green, et al. (2009). "Classification of cell death: recommendations of the Nomenclature Committee on Cell Death 2009." Cell Death Differ **16**(1): 3-11.

Kruse, J. P. and W. Gu (2009). "Modes of p53 regulation." Cell **137**(4): 609-22.

Krysko, D. V., T. Vanden Berghe, K. D'Herde and P. Vandenabeele (2008). "Apoptosis and necrosis: detection, discrimination and phagocytosis." Methods **44**(3): 205-21.

Kuwana, T., M. R. Mackey, G. Perkins, M. H. Ellisman, M. Latterich, R. Schneiter, D. R. Green and D. D. Newmeyer (2002). "Bid, Bax, and lipids cooperate to form supramolecular openings in the outer mitochondrial membrane." Cell **111**(3): 331-42.

Kuwana, T., N. H. Olson, W. B. Kiosses, B. Peters and D. D. Newmeyer (2016). "Pro-apoptotic Bax molecules densely populate the edges of membrane pores." Sci Rep **6**: 27299.

Laemmli, U. K. (1970). "Cleavage of structural proteins during the assembly of the head of bacteriophage T4." Nature **227**(5259): 680-5.

Lakin, N. D. and S. P. Jackson (1999). "Regulation of p53 in response to DNA damage." Oncogene **18**(53): 7644-55.

Lamkanfi, M. and T. D. Kanneganti (2010). "Caspase-7: a protease involved in apoptosis and inflammation." Int J Biochem Cell Biol **42**(1): 21-4.

Landowski, T. H., M. C. Gleason-Guzman and W. S. Dalton (1997). "Selection for drug resistance results in resistance to Fas-mediated apoptosis." Blood **89**(6): 1854-61.

Lavin, M. F. and N. Gueven (2006). "The complexity of p53 stabilization and activation." Cell Death Differ **13**(6): 941-50.

Lee, J. S., Q. Li, J. Y. Lee, S. H. Lee, J. H. Jeong, H. R. Lee, H. Chang, F. C. Zhou, S. J. Gao, C. Liang, et al. (2009). "FLIP-mediated autophagy regulation in cell death control." Nat Cell Biol **11**(11): 1355-62.

Lee, Y. J. and E. Shacter (1999). "Oxidative stress inhibits apoptosis in human lymphoma cells." J Biol Chem **274**(28): 19792-8.

Lefler, C. F., H. S. Lilja and D. J. Holbrook, Jr. (1973). "Inhibition of aminoacylation and polypeptide synthesis by chloroquine and primaquine in rat liver in vitro." Biochem Pharmacol **22**(6): 715-28.

Leu, J. I., P. Dumont, M. Hafey, M. E. Murphy and D. L. George (2004). "Mitochondrial p53 activates Bak and causes disruption of a Bak-Mcl1 complex." Nat Cell Biol **6**(5): 443-50.

Leu, J. I., J. Pimkina, P. Pandey, M. E. Murphy and D. L. George (2011). "HSP70 inhibition by the small-molecule 2-phenylethynesulfonamide impairs protein clearance pathways in tumor cells." Mol Cancer Res **9**(7): 936-47.

Levine, B. and D. J. Klionsky (2004). "Development by self-digestion: molecular mechanisms and biological functions of autophagy." Dev Cell **6**(4): 463-77.

Levy, A. G., P. E. Zage, L. J. Akers, M. L. Ghisoli, Z. Chen, W. Fang, S. Kannan, T. Graham, L. Zeng, A. R. Franklin, et al. (2012). "The combination of the novel glycolysis inhibitor 3-BrOP and rapamycin is effective against neuroblastoma." Invest New Drugs **30**(1): 191-9.

Li, H., P. Wang, Q. Sun, W. X. Ding, X. M. Yin, R. W. Sobol, D. B. Stolz, J. Yu and L. Zhang (2011). "Following cytochrome c release, autophagy is inhibited during chemotherapy-induced apoptosis by caspase 8-mediated cleavage of Beclin 1." Cancer Res **71**(10): 3625-34.

Li, H., P. Wang, J. Yu and L. Zhang (2011). "Cleaving Beclin 1 to suppress autophagy in chemotherapy-induced apoptosis." Autophagy **7**(10): 1239-41.

Li, H., H. Zhu, C. J. Xu and J. Yuan (1998). "Cleavage of BID by caspase 8 mediates the mitochondrial damage in the Fas pathway of apoptosis." Cell **94**(4): 491-501.

Li, J. and J. Yuan (2008). "Caspases in apoptosis and beyond." Oncogene **27**(48): 6194-206.

Li, X., J. Yan, L. Wang, F. Xiao, Y. Yang, X. Guo and H. Wang (2013). "Beclin1 inhibition promotes autophagy and decreases gemcitabine-induced apoptosis in Miapaca2 pancreatic cancer cells." Cancer Cell Int **13**(1): 26.

Lin, C. F., C. L. Chen, W. T. Chang, M. S. Jan, L. J. Hsu, R. H. Wu, M. J. Tang, W. C. Chang and Y. S. Lin (2004). "Sequential caspase-2 and caspase-8 activation upstream of mitochondria during ceramideand etoposide-induced apoptosis." J Biol Chem **279**(39): 40755-61.

Lin, Y., A. Devin, Y. Rodriguez and Z. G. Liu (1999). "Cleavage of the death domain kinase RIP by caspase-8 prompts TNF-induced apoptosis." Genes Dev **13**(19): 2514-26.

Linderoth, N. A., P. Model and M. Russel (1996). "Essential role of a sodium dodecyl sulfate-resistant protein IV multimer in assembly-export of filamentous phage." J Bacteriol **178**(7): 1962-70.

Lindsten, T., A. J. Ross, A. King, W. X. Zong, J. C. Rathmell, H. A. Shiels, E. Ulrich, K. G. Waymire, P. Mahar, K. Frauwirth, et al. (2000). "The combined functions of proapoptotic Bcl-2 family members bak and bax are essential for normal development of multiple tissues." Mol Cell **6**(6): 1389-99.

Liu, P., M. Begley, W. Michowski, H. Inuzuka, M. Ginzberg, D. Gao, P. Tsou, W. Gan, A. Papa, B. M. Kim, et al. (2014). "Cell-cycle-regulated activation of Akt kinase by phosphorylation at its carboxyl terminus." Nature **508**(7497): 541-5.

Liu, Y., L. Yang, K. L. Chen, B. Zhou, H. Yan, Z. G. Zhou and Y. Li (2014). "Knockdown of GRP78 promotes apoptosis in pancreatic acinar cells and attenuates the severity of cerulein and LPS induced pancreatic inflammation." PLoS ONE **9**(3): e92389.

Lockshin, R. A. and C. M. Williams (1965). "Programmed Cell Death--I. Cytology of Degeneration in the Intersegmental Muscles of the Pernyi Silkmoth." J Insect Physiol **11**: 123-33.

Lockshin, R. A. and Z. Zakeri (2004). "Apoptosis, autophagy, and more." Int J Biochem Cell Biol **36**(12): 2405-19.

Loder, S., M. Fakler, H. Schoeneberger, S. Cristofanon, J. Leibacher, N. Vanlangenakker, M. J. Bertrand, P. Vandenabeele, I. Jeremias, K. M. Debatin, et al. (2012). "RIP1 is required for IAP inhibitor-mediated sensitization of childhood acute leukemia cells to chemotherapy-induced apoptosis." Leukemia **26**(5): 1020-9.

Lorsch, J. (2007). Translation Initiation: Cell Biology, High-throughput and Chemical-based Approaches, Elsevier Science.

Lowe, S. W. and A. W. Lin (2000). "Apoptosis in cancer." Carcinogenesis **21**(3): 485-95.

Lu, J., S. Kunimoto, Y. Yamazaki, M. Kaminishi and H. Esumi (2004). "Kigamicin D, a novel anticancer agent based on a new anti-austerity strategy targeting cancer cells' tolerance to nutrient starvation." Cancer Sci **95**(6): 547-52.

Luo, S. and D. C. Rubinsztein (2013). "BCL2L11/BIM: a novel molecular link between autophagy and apoptosis." Autophagy **9**(1): 104-5.

Luo, X., I. Budihardjo, H. Zou, C. Slaughter and X. Wang (1998). "Bid, a Bcl2 interacting protein, mediates cytochrome c release from mitochondria in response to activation of cell surface death receptors." Cell **94**(4): 481-90.

Luthi, A. U. and S. J. Martin (2007). "The CASBAH: a searchable database of caspase substrates." Cell Death Differ **14**(4): 641-50.

Magolan, J., N. B. Adams, H. Onozuka, N. L. Hungerford, H. Esumi and M. J. Coster (2011). "Synthesis and evaluation of anticancer natural product analogues based on angelmarin: targeting the tolerance towards nutrient deprivation." ChemMedChem **7**(5): 766-70.

Magolan, J. and M. J. Coster (2010). "Targeting the resistance of pancreatic cancer cells to nutrient deprivation: anti-austerity compounds." Curr Drug Deliv **7**(5): 355-69.

Malins, D. C., K. E. Hellstrom, K. M. Anderson, P. M. Johnson and M. A. Vinson (2002). "Antioxidant-induced changes in oxidized DNA." Proc Natl Acad Sci U S A **99**(9): 5937-41.

Malorni, W. and G. Donelli (1992). "Cell death. General features and morphological aspects." Ann N Y Acad Sci **663**: 218-33.

Mantwill, K., U. Naumann, J. Seznec, V. Girbinger, H. Lage, P. Surowiak, D. Beier, M. Mittelbronn, J. Schlegel and P. S. Holm (2013). "YB-1 dependent oncolytic adenovirus efficiently inhibits tumor growth of glioma cancer stem like cells." J Transl Med **11**: 216.

Marchenko, N. D. and U. M. Moll (2014). "Mitochondrial death functions of p53." Mol Cell Oncol **1**(2): e955995.

Matissek, K. J., A. Okal, M. Mossalam and C. S. Lim (2014). "Delivery of a monomeric p53 subdomain with mitochondrial targeting signals from pro-apoptotic Bak or Bax." Pharm Res **31**(9): 2503-15.

Matsuoka, S., B. A. Ballif, A. Smogorzewska, E. R. McDonald, 3rd, K. E. Hurov, J. Luo, C. E. Bakalarski, Z. Zhao, N. Solimini, Y. Lerenthal, et al. (2007). "ATM and ATR substrate analysis reveals extensive protein networks responsive to DNA damage." Science **316**(5828): 1160-6.

McDonnell, M. A., D. Wang, S. M. Khan, M. G. Vander Heiden and A. Kelekar (2003). "Caspase-9 is activated in a cytochrome c-independent manner early during TNFalpha-induced apoptosis in murine cells." Cell Death Differ **10**(9): 1005-15.

Meng, M. B., H. H. Wang, Y. L. Cui, Z. Q. Wu, Y. Y. Shi, N. G. Zaorsky, L. Deng, Z. Y. Yuan, Y. Lu and P. Wang (2016). "Necroptosis in tumorigenesis, activation of anti-tumor immunity, and cancer therapy." Oncotarget.

Mercado-Feliciano, M., I. U. Pharmacology and Toxicology (2008). Estrogenic Activity of the Polybrominated Diphenyl Ether Flame Retardant Mixture DE-71, Indiana University.

Michael-Robinson, J., K. Spring, M. Lavin and D. Watters (2001). "Radioresistant Burkitt's lymphoma cells exhibit defective Mapk signalling " Drug Develop Res **52**(4): 534-541.

Michael, J. M., M. F. Lavin and D. J. Watters (1997). "Resistance to radiation-induced apoptosis in Burkitt's lymphoma cells is associated with defective ceramide signaling." Cancer Res **57**(16): 3600-5.

Micheau, O., E. Solary, A. Hammann and M. T. Dimanche-Boitrel (1999). "Fas ligand-independent, FADD-mediated activation of the Fas death pathway by anticancer drugs." J Biol Chem **274**(12): 7987-92.

Micheau, O. and J. Tschopp (2003). "Induction of TNF receptor I-mediated apoptosis via two sequential signaling complexes." Cell **114**(2): 181-90.

Mihara, M., S. Erster, A. Zaika, O. Petrenko, T. Chittenden, P. Pancoska and U. M. Moll (2003). "p53 has a direct apoptogenic role at the mitochondria." Mol Cell **11**(3): 577-90.

Milella, M., Z. Estrov, S. M. Kornblau, B. Z. Carter, M. Konopleva, A. Tari, W. D. Schober, D. Harris, C. E. Leysath, G. Lopez-Berestein, et al. (2002). "Synergistic induction of apoptosis by simultaneous disruption of the Bcl-2 and MEK/MAPK pathways in acute myelogenous leukemia." Blood **99**(9): 3461-4.

Mitra, A., J. I. Luna, A. I. Marusina, A. Merleev, S. Kundu-Raychaudhuri, D. Fiorentino, S. P. Raychaudhuri and E. Maverakis (2015). "Dual mTOR Inhibition Is Required to Prevent TGF-beta-Mediated Fibrosis: Implications for Scleroderma." J Invest Dermatol **135**(11): 2873-6.

Miura, T., M. Tanno and T. Sato (2010). "Mitochondrial kinase signalling pathways in myocardial protection from ischaemia/reperfusion-induced necrosis." Cardiovasc Res **88**(1): 7-15.

Mizushima, N., T. Noda, T. Yoshimori, Y. Tanaka, T. Ishii, M. D. George, D. J. Klionsky, M. Ohsumi and Y. Ohsumi (1998). "A protein conjugation system essential for autophagy." Nature **395**(6700): 395-8.

Mizushima, N., T. Yoshimori and Y. Ohsumi (2011). "The role of Atg proteins in autophagosome formation." Annu Rev Cell Dev Biol **27**: 107-32.

Mohr, A. and R. M. Zwacka (2007). "In situ trapping of initiator caspases reveals intermediate surprises." Cell Biol Int **31**(5): 526-30.

Molejon, M. I., A. Ropolo, A. L. Re, V. Boggio and M. I. Vaccaro (2012). "The VMP1-Beclin 1 interaction regulates autophagy induction." Sci Rep **3**: 1055.

Momose, I., S. Ohba, D. Tatsuda, M. Kawada, T. Masuda, G. Tsujiuchi, T. Yamori, H. Esumi and D. Ikeda (2010). "Mitochondrial inhibitors show preferential cytotoxicity to human pancreatic cancer PANC-1 cells under glucose-deprived conditions." Biochem Biophys Res Commun **392**(3): 460-6.

Monian, P. and X. Jiang (2012). "Clearing the final hurdles to mitochondrial apoptosis: regulation post cytochrome C release." Exp Oncol **34**(3): 185-91.

Monma, H., N. Harashima, T. Inao, S. Okano, Y. Tajima and M. Harada (2013). "The HSP70 and autophagy inhibitor pifithrin-mu enhances the antitumor effects of TRAIL on human pancreatic cancer." Mol Cancer Ther **12**(4): 341-51.

Moquin, D. and F. K. Chan (2010). "The molecular regulation of programmed necrotic cell injury." Trends Biochem Sci.

Mossalam, M., K. J. Matissek, A. Okal, J. E. Constance and C. S. Lim (2012). "Direct induction of apoptosis using an optimal mitochondrially targeted p53." Mol Pharm **9**(5): 1449-58.

Moubarak, R. S., V. J. Yuste, C. Artus, A. Bouharrour, P. A. Greer, J. Menissier-de Murcia and S. A. Susin (2007). "Sequential activation of poly(ADP-ribose) polymerase 1, calpains, and Bax is essential in apoptosis-inducing factor-mediated programmed necrosis." Mol Cell Biol **27**(13): 4844-62.

Muchmore, S. W., M. Sattler, H. Liang, R. P. Meadows, J. E. Harlan, H. S. Yoon, D. Nettesheim, B. S. Chang, C. B. Thompson, S. L. Wong, et al. (1996). "X-ray and NMR structure of human Bcl-xL, an inhibitor of programmed cell death." Nature **381**(6580): 335-41.

Munoz-Pinedo, C., N. El Mjiyad and J. E. Ricci (2012). "Cancer metabolism: current perspectives and future directions." Cell Death Dis **3**: e248.

Muzio, M., A. M. Chinnaiyan, F. C. Kischkel, K. O'Rourke, A. Shevchenko, J. Ni, C. Scaffidi, J. D. Bretz, M. Zhang, R. Gentz, et al. (1996). "FLICE, a novel FADD-homologous ICE/CED-3-like protease, is recruited to the CD95 (Fas/APO-1) death--inducing signaling complex." Cell **85**(6): 817-27.

Muzio, M., B. R. Stockwell, H. R. Stennicke, G. S. Salvesen and V. M. Dixit (1998). "An induced proximity model for caspase-8 activation." J Biol Chem **273**(5): 2926-30.

Nakagawa, T., H. Zhu, N. Morishima, E. Li, J. Xu, B. A. Yankner and J. Yuan (2000). "Caspase-12 mediates endoplasmic-reticulum-specific apoptosis and cytotoxicity by amyloid-beta." Nature **403**(6765): 98-103.

Nguyen, T. A., D. Menendez, M. A. Resnick and C. W. Anderson (2014). "Mutant TP53 posttranslational modifications: challenges and opportunities." Hum Mutat **35**(6): 738-55.

Nicholson, D. W. (1999). "Caspase structure, proteolytic substrates, and function during apoptotic cell death." Cell Death Differ **6**(11): 1028-42.

Nylandsted, J., M. Gyrd-Hansen, A. Danielewicz, N. Fehrenbacher, U. Lademann, M. Hoyer-Hansen, E. Weber, G. Multhoff, M. Rohde and M. Jaattela (2004). "Heat shock protein 70 promotes cell survival by inhibiting lysosomal membrane permeabilization." J Exp Med **200**(4): 425-35.

Obeid, M., A. Tesniere, F. Ghiringhelli, G. M. Fimia, L. Apetoh, J. L. Perfettini, M. Castedo, G. Mignot, T. Panaretakis, N. Casares, et al. (2007). "Calreticulin exposure dictates the immunogenicity of cancer cell death." Nat Med **13**(1): 54-61.

Oberst, A. and D. R. Green (2011). "It cuts both ways: reconciling the dual roles of caspase 8 in cell death and survival." Nat Rev Mol Cell Biol **12**(11): 757-63.

Ohnishi, T. (2005). "The role of the p53 molecule in cancer therapies with radiation and/or hyperthermia." J Cancer Res Ther **1**(3): 147-50.

Olsson, M., H. Vakifahmetoglu, P. M. Abruzzo, K. Hogstrand, A. Grandien and B. Zhivotovsky (2009). "DISC-mediated activation of caspase-2 in DNA damage-induced apoptosis." Oncogene **28**(18): 1949-59.

Oltvai, Z. N., C. L. Milliman and S. J. Korsmeyer (1993). "Bcl-2 heterodimerizes in vivo with a conserved homolog, Bax, that accelerates programmed cell death." Cell **74**(4): 609-19.

Oppenheim, R. W. (1981). "Cell death of motoneurons in the chick embryo spinal cord. V. Evidence on the role of cell death and neuromuscular function in the formation of specific peripheral connections." J Neurosci **1**(2): 141-51.

Oral, O., D. Oz-Arslan, Z. Itah, A. Naghavi, R. Deveci, S. Karacali and D. Gozuacik (2012). "Cleavage of Atg3 protein by caspase-8 regulates autophagy during receptor-activated cell death." Apoptosis **17**(8): 810-20.

Ozben, T. (2007). "Oxidative stress and apoptosis: impact on cancer therapy." J Pharm Sci **96**(9): 2181-96.

Pandey, M. K., S. Prasad, A. K. Tyagi, L. Deb, J. Huang, D. N. Karelia, S. G. Amin and B. B. Aggarwal (2016). "Targeting Cell Survival Proteins for Cancer Cell Death." Pharmaceuticals (Basel) **9**(1).

Pankiv, S., T. H. Clausen, T. Lamark, A. Brech, J. A. Bruun, H. Outzen, A. Overvatn, G. Bjorkoy and T. Johansen (2007). "p62/SQSTM1 binds directly to Atg8/LC3 to facilitate degradation of ubiquitinated protein aggregates by autophagy." J Biol Chem **282**(33): 24131-45.

Papadimitrakopoulou, V. (2012). "Development of PI3K/AKT/mTOR pathway inhibitors and their application in personalized therapy for non-small-cell lung cancer." J Thorac Oncol **7**(8): 1315-26.

Park, H. H. (2012). "Structural features of caspase-activating complexes." Int J Mol Sci **13**(4): 4807-18.

Park, M. T., J. A. Choi, M. J. Kim, H. D. Um, S. Bae and C. M. Kang (2003). "Suppression of extracellular signal-related kinase and activation of p38 MAPK are two critical events leading to caspase-8- and mitochondria-mediated cell death in phytosphingosine-treated human cancer cells." J Biol Chem **278**: 50624-50634.

Pennarun, B., A. Meijer, E. G. de Vries, J. H. Kleibeuker, F. Kruyt and S. de Jong (2009). "Playing the DISC: turning on TRAIL death receptor-mediated apoptosis in cancer." Biochim Biophys Acta **1805**(2): 123-40.

Peterson, T. R., M. Laplante, C. C. Thoreen, Y. Sancak, S. A. Kang, W. M. Kuehl, N. S. Gray and D. M. Sabatini (2009). "DEPTOR is an mTOR inhibitor frequently overexpressed in multiple myeloma cells and required for their survival." Cell **137**(5): 873-86.

Pike, L. J. (2004). "Lipid rafts: heterogeneity on the high seas." Biochem J **378**(Pt 2): 281-92.

Pop, C., G. S. Salvesen and F. L. Scott (2008). "Caspase assays: identifying caspase activity and substrates in vitro and in vivo." Methods Enzymol **446**: 351-67.

Poreba, M., A. Strozyk, G. S. Salvesen and M. Drag (2013). "Caspase substrates and inhibitors." Cold Spring Harb Perspect Biol **5**(8): a008680.

Powers, M. V., P. A. Clarke and P. Workman (2008). "Dual targeting of HSC70 and HSP72 inhibits HSP90 function and induces tumor-specific apoptosis." Cancer Cell **14**(3): 250-62.

Proskuryakov, S. Y. and V. L. Gabai (2010). "Mechanisms of tumor cell necrosis." Curr Pharm Des **16**(1): 56-68.

Puzio-Kuter, A. M. (2011). "The Role of p53 in Metabolic Regulation." Genes Cancer **2**(4): 385-91.

Rao, R. V., A. Peel, A. Logvinova, G. del Rio, E. Hermel, T. Yokota, P. C. Goldsmith, L. M. Ellerby, H. M. Ellerby and D. E. Bredesen (2002). "Coupling endoplasmic reticulum stress to the cell death program: role of the ER chaperone GRP78." FEBS Lett **514**(2-3): 122-8.

Rath, A., M. Glibowicka, V. G. Nadeau, G. Chen and C. M. Deber (2009). "Detergent binding explains anomalous SDS-PAGE migration of membrane proteins." Proc Natl Acad Sci U S A **106**(6): 1760-5.

Ravikumar, B., S. Sarkar, J. E. Davies, M. Futter, M. Garcia-Arencibia, Z. W. Green-Thompson, M. Jimenez-Sanchez, V. I. Korolchuk, M. Lichtenberg, S. Luo, et al. (2010). "Regulation of mammalian autophagy in physiology and pathophysiology." Physiol Rev **90**(4): 1383-435.

Reed, J. C. (2006). "Drug insight: cancer therapy strategies based on restoration of endogenous cell death mechanisms." Nat Clin Pract Oncol **3**(7): 388-98.

Renehan, A. G., C. Booth and C. S. Potten (2001). "What is apoptosis, and why is it important?" BMJ **322**(7301): 1536-8.

Riedl, S. J. and Y. Shi (2004). "Molecular mechanisms of caspase regulation during apoptosis." Nat Rev Mol Cell Biol **5**(11): 897-907.

Riganti, C., E. Gazzano, M. Polimeni, E. Aldieri and D. Ghigo (2012). "The pentose phosphate pathway: an antioxidant defense and a crossroad in tumor cell fate." Free Radic Biol Med **53**(3): 421-36.

Robertson, J. D., M. Enoksson, M. Suomela, B. Zhivotovsky and S. Orrenius (2002). "Caspase-2 acts upstream of mitochondria to promote cytochrome c release during etoposide-induced apoptosis." J Biol Chem **277**(33): 29803-9.

Rock, K. L. and H. Kono (2008). "The inflammatory response to cell death." Annu Rev Pathol **3**: 99-126.

Roos, W. P. and B. Kaina (2006). "DNA damage-induced cell death by apoptosis." Trends Mol Med **12**(9): 440-50.

Rooswinkel, R. (2013). "SOURCE (OR PART OF THE FOLLOWING SOURCE): Type PhD thesis Title Targeting anti-apoptotic BCL-2 proteins in cancer: the importance of intermolecular interactions and protein turnover."

Ryter, S. W., S. M. Cloonan and A. M. Choi (2013). "Autophagy: a critical regulator of cellular metabolism and homeostasis." Mol Cells **36**(1): 7-16.

Ryter, S. W., K. Mizumura and A. M. Choi (2014). "The impact of autophagy on cell death modalities." Int J Cell Biol **2014**: 502676.

Sagulenko, V., S. J. Thygesen, D. P. Sester, A. Idris, J. A. Cridland, P. R. Vajjhala, T. L. Roberts, K. Schroder, J. E. Vince, J. M. Hill, et al. (2013). "AIM2 and NLRP3 inflammasomes activate both apoptotic and pyroptotic death pathways via ASC." Cell Death Differ **20**(9): 1149-60.

Salvesen, G. S. and V. M. Dixit (1999). "Caspase activation: the induced-proximity model." Proc Natl Acad Sci U S A **96**(20): 10964-7.

Sancak, Y., C. C. Thoreen, T. R. Peterson, R. A. Lindquist, S. A. Kang, E. Spooner, S. A. Carr and D. M. Sabatini (2007). "PRAS40 is an insulin-regulated inhibitor of the mTORC1 protein kinase." Mol Cell **25**(6): 903-15.

Savill, J. and V. Fadok (2000). "Corpse clearance defines the meaning of cell death." Nature **407**(6805): 784-8.

Scaffidi, C., S. Fulda, A. Srinivasan, C. Friesen, F. Li, K. J. Tomaselli, K. M. Debatin, P. H. Krammer and M. E. Peter (1998). "Two CD95 (APO-1/Fas) signaling pathways." Embo J **17**(6): 1675-87.

Scaffidi, C., J. P. Medema, P. H. Krammer and M. E. Peter (1997). "FLICE is predominantly expressed as two functionally active isoforms, caspase-8/a and caspase-8/b." J Biol Chem **272**(43): 26953-8.

Schmidt, S. V., S. Seibert, B. Walch-Ruckheim, B. Vicinus, E. M. Kamionka, J. Pahne-Zeppenfeld, E. F. Solomayer, Y. J. Kim, R. M. Bohle and S. Smola (2015). "RIPK3 expression in cervical cancer cells is required for PolyIC-induced necroptosis, IL-1alpha release, and efficient paracrine dendritic cell activation." Oncotarget **6**(11): 8635-47.

Schuler, M., E. Bossy-Wetzel, J. C. Goldstein, P. Fitzgerald and D. R. Green (2000). "p53 induces apoptosis by caspase activation through mitochondrial cytochrome c release." J Biol Chem **275**(10): 7337-42.

Seglen, P. O., B. Grinde and A. E. Solheim (1979). "Inhibition of the lysosomal pathway of protein degradation in isolated rat hepatocytes by ammonia, methylamine, chloroquine and leupeptin." Eur J Biochem **95**(2): 215-25.

Seth, R., C. Yang, V. Kaushal, S. V. Shah and G. P. Kaushal (2005). "p53-dependent caspase-2 activation in mitochondrial release of apoptosis-inducing factor and its role in renal tubular epithelial cell injury." J Biol Chem **280**(35): 31230-9.

Shi, Y. (2002). "Mechanisms of caspase activation and inhibition during apoptosis." Mol Cell **9**(3): 459-70.

Shimizu, S., Y. Eguchi, W. Kamiike, S. Waguri, Y. Uchiyama, H. Matsuda and Y. Tsujimoto (1996). "Retardation of chemical hypoxia-induced necrotic cell death by Bcl-2 and ICE inhibitors: possible involvement of common mediators in apoptotic and necrotic signal transductions." Oncogene **12**(10): 2045-50.

Shore, S., D. Vimalachandran, M. G. Raraty and P. Ghaneh (2004). "Cancer in the elderly: pancreatic cancer." Surg Oncol **13**(4): 201-10.

Short, D. M., I. D. Heron, J. L. Birse-Archbold, L. E. Kerr, J. Sharkey and J. McCulloch (2007). "Apoptosis induced by staurosporine alters chaperone and endoplasmic reticulum proteins: Identification by quantitative proteomics." Proteomics **7**(17): 3085-96.

Siddiqui, M. A., S. Mukherjee, P. Manivannan and K. Malathi (2015). "RNase L Cleavage Products Promote Switch from Autophagy to Apoptosis by Caspase-Mediated Cleavage of Beclin-1." Int J Mol Sci **16**(8): 17611-36.

Simoes Magluta, E. P., F. C. Vasconcelos, R. C. Maia and C. E. Klumb (2009). "Insights into apoptosis mechanisms induced by DNA-damaging agents in Burkitt's lymphoma cells." Cancer Invest **27**(8): 830-5.

Slee, E. A., S. A. Keogh and S. J. Martin (2000). "Cleavage of BID during cytotoxic drug and UV radiation-induced apoptosis occurs downstream of the point of Bcl-2 action and is catalysed by caspase-3: a potential feedback loop for amplification of apoptosis-associated mitochondrial cytochrome c release." Cell Death Differ **7**(6): 556-65.

Slevin, M. L. (1991). "The clinical pharmacology of etoposide." Cancer **67**(1 Suppl): 319-29.

Soltoff, S. P. (2001). "Rottlerin is a mitochondrial uncoupler that decreases cellular ATP levels and indirectly blocks protein kinase Cdelta tyrosine phosphorylation." J Biol Chem **276**(41): 37986-92.

Soulie, S., J. V. Moller, P. Falson and M. le Maire (1996). "Urea reduces the aggregation of membrane proteins on sodium dodecyl sulfate-polyacrylamide gel electrophoresis." Anal Biochem **236**(2): 363-4.

Sperandio, S., I. de Belle and D. E. Bredesen (2000). "An alternative, nonapoptotic form of programmed cell death." Proc Natl Acad Sci U S A **97**(26): 14376-81.

Sperandio, S., K. Poksay, I. de Belle, M. J. Lafuente, B. Liu, J. Nasir and D. E. Bredesen (2004). "Paraptosis: mediation by MAP kinases and inhibition by AIP-1/Alix." Cell Death Differ **11**(10): 1066-75.

Spinozzi, F., I. Nicoletti, E. Agea, S. Belia, R. Moraca, G. Migliorati, C. Riccardi, F. Grignani and A. Bertotto (1995). "IL-4 is able to reverse the CD2-mediated negative apoptotic signal to CD4-CD8- alpha beta and/or gamma delta T lymphocytes." Immunology **86**(3): 379-84.

Srinivasula, S. M., M. Ahmad, T. Fernandes-Alnemri, G. Litwack and E. S. Alnemri (1996). "Molecular ordering of the Fas-apoptotic pathway: the Fas/APO-1 protease Mch5 is a CrmA-inhibitable protease that activates multiple Ced-3/ICE-like cysteine proteases." Proc Natl Acad Sci U S A **93**(25): 14486-91.

Steinbach, J. P., H. Wolburg, A. Klumpp, H. Probst and M. Weller (2003). "Hypoxia-induced cell death in human malignant glioma cells: energy deprivation promotes decoupling of mitochondrial cytochrome c release from caspase processing and necrotic cell death." Cell Death Differ **10**(7): 823-32.

Stine, Z. E. and C. V. Dang (2013). "Stress eating and tuning out: cancer cells re-wire metabolism to counter stress." Crit Rev Biochem Mol Biol **48**(6): 609-19.

Strom, E., S. Sathe, P. G. Komarov, O. B. Chernova, I. Pavlovska, I. Shyshynova, D. A. Bosykh, L. G. Burdelya, R. M. Macklis, R. Skaliter, et al. (2006). "Small-molecule inhibitor of p53 binding to mitochondria protects mice from gamma radiation." Nat Chem Biol **2**(9): 474-9.

Su, Z., Z. Yang, L. Xie, J. P. DeWitt and Y. Chen (2016). "Cancer therapy in the necroptosis era." Cell Death Differ **23**(5): 748-56.

Sui, X., R. Chen, Z. Wang, Z. Huang, N. Kong, M. Zhang, W. Han, F. Lou, J. Yang, Q. Zhang, et al. (2013). "Autophagy and chemotherapy resistance: a promising therapeutic target for cancer treatment." Cell Death Dis **4**: e838.

Suk, F. M., S. Y. Lin, R. J. Lin, Y. H. Hsine, Y. J. Liao, S. U. Fang and Y. C. Liang (2015). "Bortezomib inhibits Burkitt's lymphoma cell proliferation by downregulating sumoylated hnRNP K and c-Myc expression." Oncotarget **6**(28): 25988-6001.

Suzuki, A., G. Kusakai, A. Kishimoto, J. Lu, T. Ogura, M. F. Lavin and H. Esumi (2003). "Identification of a novel protein kinase mediating Akt survival signaling to the ATM protein." J Biol Chem **278**(1): 48-53.

Suzuki, Y., Y. Imai, H. Nakayama, K. Takahashi, K. Takio and R. Takahashi (2001). "A serine protease, HtrA2, is released from the mitochondria and interacts with XIAP, inducing cell death." Mol Cell **8**(3): 613-21.

Sweadner, K. J. (1991). "Trypsin inhibitor paradoxically stabilizes trypsin activity in sodium dodecyl sulfate, facilitating proteolytic fingerprinting." Anal Biochem **194**(1): 130-5.

Taatjes, D. J., B. E. Sobel and R. C. Budd (2008). "Morphological and cytochemical determination of cell death by apoptosis." Histochem Cell Biol **129**(1): 33-43.

Tait, S. W. and D. R. Green (2010). "Mitochondria and cell death: outer membrane permeabilization and beyond." Nat Rev Mol Cell Biol **11**(9): 621-32.

Takemura, R., H. Takaki, S. Okada, H. Shime, T. Akazawa, H. Oshiumi, M. Matsumoto, T. Teshima and T. Seya (2015). "PolyI:C-Induced, TLR3/RIP3-Dependent Necroptosis Backs Up Immune Effector-Mediated Tumor Elimination In Vivo." Cancer Immunol Res **3**(8): 902-14.

Tamm, I., Y. Wang, E. Sausville, D. A. Scudiero, N. Vigna, T. Oltersdorf and J. C. Reed (1998). "IAP-family protein survivin inhibits caspase activity and apoptosis induced by Fas (CD95), Bax, caspases, and anticancer drugs." Cancer Res **58**(23): 5315-20.

Tang, D., R. Kang, K. M. Livesey, C. W. Cheh, A. Farkas, P. Loughran, G. Hoppe, M. E. Bianchi, K. J. Tracey, H. J. Zeh, 3rd, et al. (2010). "Endogenous HMGB1 regulates autophagy." J Cell Biol **190**(5): 881-92.

Tang, D., J. M. Lahti and V. J. Kidd (2000). "Caspase-8 activation and bid cleavage contribute to MCF7 cellular execution in a caspase-3-dependent manner during staurosporine-mediated apoptosis." J Biol Chem **275**(13): 9303-7.

Tang, D., H. Okada, J. Ruland, L. Liu, V. Stambolic, T. W. Mak and A. J. Ingram (2001). "Akt is activated in response to an apoptotic signal." J Biol Chem **276**(32): 30461-6.

Taylor, R. C., S. P. Cullen and S. J. Martin (2008). "Apoptosis: controlled demolition at the cellular level." Nat Rev Mol Cell Biol **9**(3): 231-41.

Tenev, T., K. Bianchi, M. Darding, M. Broemer, C. Langlais, F. Wallberg, A. Zachariou, J. Lopez, M. MacFarlane, K. Cain, et al. (2011). "The Ripoptosome, a signaling platform that assembles in response to genotoxic stress and loss of IAPs." Mol Cell **43**(3): 432-48.

Thon, L., H. Mohlig, S. Mathieu, A. Lange, E. Bulanova, S. Winoto-Morbach, S. Schutze, S. Bulfone-Paus and D. Adam (2005). "Ceramide mediates caspase-independent programmed cell death." FASEB J **19**(14): 1945-56.

Thornberry, N. A., T. A. Rano, E. P. Peterson, D. M. Rasper, T. Timkey, M. Garcia-Calvo, V. M. Houtzager, P. A. Nordstrom, S. Roy, J. P. Vaillancourt, et al. (1997). "A combinatorial approach defines specificities of members of the caspase family and granzyme B. Functional relationships established for key mediators of apoptosis." J Biol Chem **272**(29): 17907-11.

Tichy, E. D., Z. A. Stephan, A. Osterburg, G. Noel and P. J. Stambrook (2013). "Mouse embryonic stem cells undergo charontosis, a novel programmed cell death pathway dependent upon cathepsins, p53, and EndoG, in response to etoposide treatment." Stem Cell Res **10**(3): 428-41.

Tinel, A. and J. Tschopp (2004). "The PIDDosome, a protein complex implicated in activation of caspase-2 in response to genotoxic stress." Science **304**(5672): 843-6.

Torricelli, C., S. Salvadori, G. Valacchi, K. Soucek, E. Slabakova, M. Muscettola, N. Volpi and E. Maioli (2012). "Alternative Pathways of Cancer Cell Death by Rottlerin: Apoptosis versus Autophagy." Evid Based Complement Alternat Med **2012**: 980658.

Trauth, B. C., C. Klas, A. M. Peters, S. Matzku, P. Moller, W. Falk, K. M. Debatin and P. H. Krammer (1989). "Monoclonal antibody-mediated tumor regression by induction of apoptosis." Science **245**(4915): 301-5.

Tsujimoto, T., I. A. Lisukov, N. Huang, M. S. Mahmoud and M. M. Kawano (1996). "Plasma cells induce apoptosis of pre-B cells by interacting with bone marrow stromal cells." Blood **87**(8): 3375-83.

Tu, S., G. P. McStay, L. M. Boucher, T. Mak, H. M. Beere and D. R. Green (2006). "In situ trapping of activated initiator caspases reveals a role for caspase-2 in heat shock-induced apoptosis." Nat Cell Biol **8**(1): 72-7.

Tulumello, D. V. and C. M. Deber (2009). "SDS micelles as a membrane-mimetic environment for transmembrane segments." Biochemistry **48**(51): 12096-103.

Ueda, J. Y., S. Athikomkulchai, R. Miyatake, I. Saiki, H. Esumi and S. Awale (2013). "(+)-Grandifloracin, an antiausterity agent, induces autophagic PANC-1 pancreatic cancer cell death." Drug Des Devel Ther **8**: 39-47.

Van Cruchten, S. and W. Van Den Broeck (2002). "Morphological and biochemical aspects of apoptosis, oncosis and necrosis." Anat Histol Embryol **31**(4): 214-23.

van Houdt, I. S., J. J. Muris, A. T. Hesselink, D. Kramer, S. A. Cillessen, L. M. Moesbergen, W. Vos, E. Hooijberg, C. J. Meijer, J. A. Kummer, et al. (2007). "Expression of c-FLIP is primarily detected in diffuse large B-cell lymphoma and Hodgkin's lymphoma and correlates with lack of caspase 8 activation." Histopathology **51**(6): 778-84.

Vande Velde, C., J. Cizeau, D. Dubik, J. Alimonti, T. Brown, S. Israels, R. Hakem and A. H. Greenberg (2000). "BNIP3 and genetic control of necrosis-like cell death through the mitochondrial permeability transition pore." Mol Cell Biol **20**(15): 5454-68.

Vanden Berghe, T., W. J. Kaiser, M. J. Bertrand and P. Vandenabeele (2015). "Molecular crosstalk between apoptosis, necroptosis, and survival signaling." Mol Cell Oncol **2**(4): e975093.

Vandenabeele, P., S. Grootjans, N. Callewaert and N. Takahashi (2013). "Necrostatin-1 blocks both RIPK1 and IDO: consequences for the study of cell death in experimental disease models." Cell Death Differ **20**(2): 185-7.

Vaseva, A. V., N. D. Marchenko and U. M. Moll (2009). "The transcription-independent mitochondrial p53 program is a major contributor to nutlin-induced apoptosis in tumor cells." Cell Cycle **8**(11): 1711-9.

Vaupel, P., F. Kallinowski and P. Okunieff (1989). "Blood flow, oxygen and nutrient supply, and metabolic microenvironment of human tumors: a review." Cancer Res **49**(23): 6449-65.

Vaux, D. L., I. L. Weissman and S. K. Kim (1992). "Prevention of programmed cell death in Caenorhabditis elegans by human bcl-2." Science **258**(5090): 1955-7.

Vazquez, A., E. E. Bond, A. J. Levine and G. L. Bond (2008). "The genetics of the p53 pathway, apoptosis and cancer therapy." Nat Rev Drug Discov **7**(12): 979-87.

Vince, J. E., D. Chau, B. Callus, W. W. Wong, C. J. Hawkins, P. Schneider, M. McKinlay, C. A. Benetatos, S. M. Condon, S. K. Chunduru, et al. (2008). "TWEAK-FN14 signaling induces lysosomal degradation of a cIAP1-TRAF2 complex to sensitize tumor cells to TNFalpha." J Cell Biol **182**(1): 171-84.

Vogelstein, B. and K. W. Kinzler (1992). "p53 function and dysfunction." Cell **70**(4): 523-6.

Vrana, J. A., C. K. Bieszczad, E. S. Cleaveland, Y. Ma, J. P. Park, T. K. Mohandas and R. W. Craig (2002). "An MCL1-overexpressing Burkitt lymphoma subline exhibits enhanced survival on exposure to serum deprivation, topoisomerase inhibitors, or staurosporine but remains sensitive to 1-beta-D-arabinofuranosylcytosine." Cancer Res **62**(3): 892-900.

Waddell, N., M. Pajic, A. M. Patch, D. K. Chang, K. S. Kassahn, P. Bailey, A. L. Johns, D. Miller, K. Nones, K. Quek, et al. (2015). "Whole genomes redefine the mutational landscape of pancreatic cancer." Nature **518**(7540): 495-501.

Wajant, H. (2002). "The Fas signaling pathway: more than a paradigm." Science **296**(5573): 1635-6.

Walczak, H., R. E. Miller, K. Ariail, B. Gliniak, T. S. Griffith, M. Kubin, W. Chin, J. Jones, A. Woodward, T. Le, et al. (1999). "Tumoricidal activity of tumor necrosis factor-related apoptosis-inducing ligand in vivo." Nat Med **5**(2): 157-63.

Wang, J., M. W. Whiteman, H. Lian, G. Wang, A. Singh, D. Huang and T. Denmark (2009). "A non-canonical MEK/ERK signaling pathway regulates autophagy via regulating Beclin 1." J Biol Chem **284**(32): 21412-24.

Wang, R. C., Y. Wei, Z. An, Z. Zou, G. Xiao, G. Bhagat, M. White, J. Reichelt and B. Levine (2012). "Akt-mediated regulation of autophagy and tumorigenesis through Beclin 1 phosphorylation." Science **338**(6109): 956-9.

Ward, P. S. and C. B. Thompson (2012). "Metabolic reprogramming: a cancer hallmark even warburg did not anticipate." Cancer Cell **21**(3): 297-308.

Waterhouse, N., S. Kumar, Q. Song, P. Strike, L. Sparrow, G. Dreyfuss, E. S. Alnemri, G. Litwack, M. Lavin and D. Watters (1996). "Heteronuclear ribonucleoproteins C1 and C2, components of the spliceosome, are specific targets of interleukin 1beta-converting enzyme-like proteases in apoptosis." J Biol Chem **271**(46): 29335-41.

Wei, M. C., T. Lindsten, V. K. Mootha, S. Weiler, A. Gross, M. Ashiya, C. B. Thompson and S. J. Korsmeyer (2000). "tBID, a membrane-targeted death ligand, oligomerizes BAK to release cytochrome c." Genes Dev **14**(16): 2060-71.

Wei, M. C., W. X. Zong, E. H. Cheng, T. Lindsten, V. Panoutsakopoulou, A. J. Ross, K. A. Roth, G. R. MacGregor, C. B. Thompson and S. J. Korsmeyer (2001). "Proapoptotic BAX and BAK: a requisite gateway to mitochondrial dysfunction and death." Science **292**(5517): 727-30.

Wei, Y., S. Pattingre, S. Sinha, M. Bassik and B. Levine (2008). "JNK1-mediated phosphorylation of Bcl-2 regulates starvation-induced autophagy." Mol Cell **30**(6): 678-88.

Weinkauf, M., Y. Zimmermann, E. Hartmann, A. Rosenwald, M. Rieken, A. Pastore, G. Hutter, W. Hiddemann and M. Dreyling (2009). "2-D PAGE-based comparison of proteasome inhibitor bortezomib in sensitive and resistant mantle cell lymphoma." Electrophoresis **30**(6): 974-86.

Weinstein, I. B. (2000). "Disorders in cell circuitry during multistage carcinogenesis: the role of homeostasis." Carcinogenesis **21**(5): 857-64.

Weinstein, I. B. and A. K. Joe (2006). "Mechanisms of disease: Oncogene addiction--a rationale for molecular targeting in cancer therapy." Nat Clin Pract Oncol **3**(8): 448-57.

Westphal, D., G. Dewson, P. E. Czabotar and R. M. Kluck (2011). "Molecular biology of Bax and Bak activation and action." Biochim Biophys Acta.

Westphal, D., G. Dewson, M. Menard, P. Frederick, S. Iyer, R. Bartolo, L. Gibson, P. E. Czabotar, B. J. Smith, J. M. Adams, et al. (2014). "Apoptotic pore formation is associated with in-plane insertion of Bak or Bax central helices into the mitochondrial outer membrane." Proc Natl Acad Sci U S A **111**(39): E4076-85.

Willingham, S. B., D. T. Bergstralh, W. O'Connor, A. C. Morrison, D. J. Taxman, J. A. Duncan, S. Barnoy, M. M. Venkatesan, R. A. Flavell, M. Deshmukh, et al. (2007). "Microbial pathogen-induced necrotic cell death mediated by the inflammasome components CIAS1/cryopyrin/NLRP3 and ASC." Cell Host Microbe **2**(3): 147-59.

Willis, S. N., L. Chen, G. Dewson, A. Wei, E. Naik and J. I. Fletcher (2005). "Proapoptotic Bak is sequestered by Mcl-1 and Bcl-xL, but not Bcl-2, until displaced by BH3-only proteins." Genes Dev **19**: 1294-1305.

Wilson, T. R., K. M. McLaughlin, M. McEwan, H. Sakai, K. M. Rogers, K. M. Redmond, P. G. Johnston and D. B. Longley (2007). "c-FLIP: a key regulator of colorectal cancer cell death." Cancer Res **67**(12): 5754-62.

Wise, D. R. and C. B. Thompson (2010). "Glutamine addiction: a new therapeutic target in cancer." Trends Biochem Sci **35**(8): 427-33.

Wittig, I. and H. Schagger (2005). "Advantages and limitations of clear-native PAGE." Proteomics **5**(17): 4338-46.

Wolter, K. G., Y. T. Hsu, C. L. Smith, A. Nechushtan, X. G. Xi and R. J. Youle (1997). "Movement of Bax from the cytosol to mitochondria during apoptosis." J Cell Biol **139**(5): 1281-92.

Wu, C. A., D. Y. Huang and W. W. Lin (2014). "Beclin-1-independent autophagy positively regulates internal ribosomal entry site-dependent translation of hypoxia-inducible factor 1alpha under nutrient deprivation." Oncotarget **5**(17): 7525-39.

Xie, X., E. P. White and J. M. Mehnert (2013). "Coordinate autophagy and mTOR pathway inhibition enhances cell death in melanoma." PLoS ONE **8**(1): e55096.

Xie, Z. G., Y. Xie and Q. R. Dong (2013). "Inhibition of the mammalian target of rapamycin leads to autophagy activation and cell death of MG63 osteosarcoma cells." Oncol Lett **6**(5): 1465-1469.

Xu, H. D., D. Wu, J. H. Gu, J. B. Ge, J. C. Wu, R. Han, Z. Q. Liang and Z. H. Qin (2013). "The pro-survival role of autophagy depends on Bcl-2 under nutrition stress conditions." PLoS ONE **8**(5): e63232.

Yamada, K. M. and E. Cukierman (2007). "Modeling tissue morphogenesis and cancer in 3D." Cell **130**(4): 601-10.

Yang, Y., S. Fang, J. P. Jensen, A. M. Weissman and J. D. Ashwell (2000). "Ubiquitin protein ligase activity of IAPs and their degradation in proteasomes in response to apoptotic stimuli." Science **288**(5467): 874-7.

Yang, Z. and D. J. Klionsky (2010). "Mammalian autophagy: core molecular machinery and signaling regulation." Curr Opin Cell Biol **22**(2): 124-31.

Yeh, W. C., A. Itie, A. J. Elia, M. Ng, H. B. Shu, A. Wakeham, C. Mirtsos, N. Suzuki, M. Bonnard, D. V. Goeddel, et al. (2000). "Requirement for Casper (c-FLIP) in regulation of death receptor-induced apoptosis and embryonic development." Immunity **12**(6): 633-42.

Yonehara, S., A. Ishii and M. Yonehara (1989). "A cell-killing monoclonal antibody (anti-Fas) to a cell surface antigen co-downregulated with the receptor of tumor necrosis factor." J Exp Med **169**(5): 1747-56.

Yoo, S. M., S. J. Cho and Y. Y. Cho (2015). "Molecular Targeting of ERKs/RSK2 Signaling Axis in Cancer Prevention." J Cancer Prev **20**(3): 165-71.

Young, M. M., Y. Takahashi, O. Khan, S. Park, T. Hori, J. Yun, A. K. Sharma, S. Amin, C. D. Hu, J. Zhang, et al. (2012). "Autophagosomal membrane serves as platform for intracellular death-inducing signaling complex (iDISC)-mediated caspase-8 activation and apoptosis." J Biol Chem **287**(15): 12455-68.

Yousefi, S., R. Perozzo, I. Schmid, A. Ziemiecki, T. Schaffner, L. Scapozza, T. Brunner and H. U. Simon (2006). "Calpain-mediated cleavage of Atg5 switches autophagy to apoptosis." Nat Cell Biol **8**(10): 1124-32.

Zalckvar, E., H. Berissi, L. Mizrachy, Y. Idelchuk, I. Koren, M. Eisenstein, H. Sabanay, R. Pinkas-Kramarski and A. Kimchi (2009). "DAP-kinase-mediated phosphorylation on the BH3 domain of beclin 1 promotes dissociation of beclin 1 from Bcl-XL and induction of autophagy." EMBO Rep **10**(3): 285-92.

Zapata, J. M., R. Takahashi, G. S. Salvesen and J. C. Reed (1998). "Granzyme release and caspase activation in activated human T-lymphocytes." J Biol Chem **273**(12): 6916-20.

Zha, J., H. Harada, E. Yang, J. Jockel and S. J. Korsmeyer (1996). "Serine phosphorylation of death agonist BAD in response to survival factor results in binding to 14-3-3 not BCL-X(L)." Cell **87**(4): 619-28.

Zhang, J., D. N. Tripathi, J. Jing, A. Alexander, J. Kim, R. T. Powell, R. Dere, J. Tait-Mulder, J. H. Lee, T. T. Paull, et al. (2015). "ATM functions at the peroxisome to induce pexophagy in response to ROS." Nat Cell Biol **17**(10): 1259-69.

Zhang, Y., D. Xing and L. Liu (2009). "PUMA promotes Bax translocation by both directly interacting with Bax and by competitive binding to Bcl-X L during UV-induced apoptosis." Mol Biol Cell **20**(13): 3077-87.

Zhao, E. G., Q. Song, S. Cross, I. Misko, S. P. Lees-Miller and M. F. Lavin (1998). "Resistance to etoposide-induced apoptosis in a Burkitt's lymphoma cell line." Int J Cancer **77**(5): 755-62.

Zhivotovsky, B. and S. Orrenius (2005). "Caspase-2 function in response to DNA damage." Biochem Biophys Res Commun **331**(3): 859-67.

Zhou, H. and S. Huang (2010). "The complexes of mammalian target of rapamycin." Curr Protein Pept Sci **11**(6): 409-24.

Zhou, H. and S. Huang (2010). "Role of mTOR signaling in tumor cell motility, invasion and metastasis." Curr Protein Pept Sci **12**(1): 30-42.

Zidovetzki, R. and I. Levitan (2007). "Use of cyclodextrins to manipulate plasma membrane cholesterol content: evidence, misconceptions and control strategies." Biochim Biophys Acta **1768**(6): 1311-24.